2012

Out of Site but Not Out of Mind: Submerged Prehistoric Landscapes on the Northwestern Gulf of Mexico Outer Continental Shelf

Amanda M. Evans
Louisiana State University and Agricultural and Mechanical College

OUT OF SITE BUT NOT OUT OF MIND: SUBMERGED PREHISTORIC LANDSCAPES ON THE NORTHWESTERN GULF OF MEXICO OUTER CONTINENTAL SHELF

A Dissertation

Submitted to the Graduate Faculty of the
Louisiana State University and
Agricultural and Mechanical College
in partial fulfillment of the
requirements for the degree of
Doctor of Philosophy

in

The Department of Geography and Anthropology

by
Amanda M. Evans
B.A., Indiana University, 1998
M.A., Florida State University, 2005
May 2013

Matt Keith, for your limitless support.

ACKNOWLEDGEMENTS

Funding for this dissertation was provided through a Coastal Marine Institute cooperative agreement, No. M07AC13373, provided by the Bureau of Ocean Energy Management (BOEM). Patrick Hesp served as the PI for this grant, and also as the dissertation committee chair. Thanks to the dissertation committee, Heather McKillop, Brooks Ellwood, and Barry Keim, for their guidance and assistance with this dissertation. Thanks also to the Dean's Representative Daniel Sheey for his participation in the dissertation process and comments during the defense.

The following individuals gave their time, effort, and expertise towards the overall grant project, and allowed their work to be referenced in this dissertation: Barun Sen Gupta, Graziela da Silva, Brooks Ellwood, Laurie Anderson, Sophie Warny, and Linda Cummings. Graduate research assistants Jennifer Gardner and Elizabeth Cory Sills provided field and laboratory assistance. Radiocarbon dates were processed under contract to Beta Analytic.

It would not have been possible to conduct this research without the assistance of Nedda Taylor and Linda Strain with the Department of Geography and Anthropology, for their assistance and expertise in grant management and administration.

The following individuals provided technical assistance, expertise, and support for this dissertation: Alan Craig and Gary Sayers with Survey Equipment Services; Joe Marlbrough, Van Domangue, Carl Sevin, and Cindy Sevin with the R/V *Acadiana* and the Louisiana Universities Marine Consortium (LUMCON); Nancy DeWitt with the United States Geological Survey (USGS); Tim Dellapenna with Texas A&M University, Galveston; James Brooks with TDI Brooks; Vaught Bryant with Texas A&M University; Dave Conlin with the National Park Service Submerged Resources Center; Charlie Pearson and Rich Weinsten with Coastal Environments Inc.; Melanie Stright with the Minerals Management Service; Rob Floyd with Sylvetti; Glen Doran with Florida State University; Michael Faught with Panamerican Consultants Inc.; Sean Kemnuir, Mike Wenger, Mike Bureau, John Windhaus, Mike Leavitt, Wesley Schneider and Nathan Lozano with the M/V *Thunderforce* and American Vibracore Services; Tom Oliver, Jerry Cook, Steve Garrett, Greg Schexnider, Chris Chaney, Ryan Newchurch, Curtis Chaney, Anthony Hidalgo, Mike Tripp, Matt Keith, Rick Clemmons, Donald Spicer, CD Schempf, Randy Bergeron, Teresa Bowman, and Dana Montgomery with Tesla Offshore; and Dave Ball, Melanie Damour, Jack Irion, Chris Horrell, Olivia Adrian, Deborah Epperson, and Ron Brinkman with the Bureau of Ocean Energy Management and the Bureau of Safety and Environmental Enforcement.

PREFACE

This dissertation is related to a larger, regional study titled *Testing and Examining Potential Prehistoric Archaeological Features on the Gulf of Mexico Outer Continental Shelf*. Funding for this regional project was awarded to Principal Investigator Patrick Hesp through Coastal Marine Institute (CMI) cooperative agreement, No. M07AC13373, provided by the Bureau of Ocean Energy Management (BOEM). The purpose of this study was to conduct geophysical survey and physical sampling at six high probability features in the Gulf of Mexico identified for their prehistoric archaeological potential. Two of these features, located in Galveston 356 and High Island 160, were required for inclusion in the study by the funding agency. The remaining sites were selected as part of the study, and included Eugene Island 224, High Island 178, Galveston 356 and Galveston A40.

BOEM requires oil and gas operators to conduct pre-disturbance archaeological assessments of geophysical data in compliance with Section 106 of the National Historic Preservation Act. Amanda Evans reviewed 204 reports that had subbottom acoustic data and selected the four additional sites included in the CMI study. Following selection of the study sites, additional geophysical surveys were conducted to better image the sites using tighter intervals. Amanda Evans designed the survey grids used at each location, arranged for vessel and equipment rental and directed the geophysical survey acquisition on board the R/V *Acadiana*, with the assistance of Graziela da Silva and Jennifer Gardner. Amanda Evans interpreted all of the geophysical data and prepared all of the data samples and maps in the CMI report and this dissertation. Due to data quality issues, Amanda Evans designed additional survey lines over the four most promising sites (High Island 160 and 178, and Galveston 356 and 426) and arranged for acquisition of supplemental data that was used in illustrating the CMI report and this dissertation. Amanda Evans identified preliminary coring sites based on the interpreted geophysical data; final coring sites were selected and prioritized by Patrick Hesp, Graziela da Silva, and Amanda Evans. Patrick Hesp arranged for the coring contractor, and Amanda Evans directed coring operations on board with M/V *Thunderforce* with the assistance of Jennifer Gardner. Evans, with assistance from Gardner, inventoried all cores on the vessel, and Evans was responsible for selecting alternate coring sites when field conditions precluded the acquisition of previously planned cores. A total of 30 cores were acquired as part of the CMI study, from High Island 178, High Island 160, Galveston 426, and Galveston 356. Fifteen of these cores are included in this dissertation.

Patrick Hesp arranged for all cores to be processed through a core logger at the School of Coast and the Environment. Jennifer Gardner ran all of the calibrations and conducted all core logging under the direction of Floyd DeMars. Amanda Evans opened all of the cores obtained as part of the CMI study and prepared intial core lithologies, with assistance from Jennifer Gardner, Cory Sills, and Matt Keith. Patrick Hesp and Brooks Ellwood provided assistance with lithologies and recommendations for laboratory sampling strategies. Amanda Evans prepared all of the final core logs in LogPlot 7 for the CMI study and this dissertation. Amanda Evans with assistance from Jennifer Gardner, Cory Sills, and Matt Keith, prepared all of the grain size, mass-specific magnetic susceptibility, and radiocarbon samples. All radiocarbon samples were submitted to Beta Analytic for testing. Patrick Hesp arranged for all grain size samples to be measured with a laser particle counter at LUMCON. Cory Sills ran all of the grain size samples and prepared

initial S-curves of each sample; Amanda Evans calculated graphic mean and median grain sizes for all samples. Amanda Evans, with assistance from Jennifer Gardner, ran all of the mass-based magnetic susceptibility samples under the direction of Brooks Ellwood. Graziela da Silva and Barun Sen Gupta sampled Core No. 1, High Island 178 for foraminifera and conducted the analysis. Sophie Warny and Patick Hesp selected pollen samples from Core No. 1, High Island 178. Sophie Warny, with assistance from David Jarzen, analyzed the pollen samples. Amanda Evans and Patrick Hesp selected additional samples from High Island 178 and Galveston 426, which were submitted to PaleoResearch Institute for pollen and FTIR analysis. Patrick Hesp coordinated with Laurie Anderson for preliminary shell species identification, and Amanda Evans conducted research on the identified species. Amanda Evans analyzed all of the recorded core logger data, including p-wave velocity and magnetic susceptibility (volume-based).

For this dissertation, Amanda Evans developed a hypothesis that tested the ability to identify elements of the real environment through the use of geophysical data. She incorporated the results from two of the CMI study sites, High Island 178 and Galveston 426, into the dissertation. The results from all sites are included in the CMI final report, which includes comparisons of geophysical line spacing intervals, recommendations for improved data collection, and interpretation relevant to protecting submerged prehistoric landscapes against development pressures.

TABLE OF CONTENTS

LIST OF TABLES

LIST OF FIGURES

ABSTRACT

Archaeological sites are more important than simply the artifacts they contain. Locations of human occupation and activity form a pattern that can provide information about perceptions of the landscape, decisions about resources, or preferences. Explaining this "perceived" environment is one of archaeology's goals in explaining past human behavior. In order to address these goals, archaeologists must first identify elements of the "real" landscape, including the geographical environment, its resources, and evidence of human modification. Only after these real elements have been identified can the perceived environment be explored. On the outer continental shelf of the northwestern Gulf of Mexico, formerly subaerial geographical environments are now submerged offshore of Texas and Louisiana. These areas could have been occupied by Paleoindian or Early Archaic populations prior to final inundation related to sea-level rise following the last glacial maximum. Due to sediment accretion related to transgression, as well as active sedimentation in the marine environment, the formerly subaerial surface is now buried below the seafloor. This dissertation discusses the use of geophysical data in identifying environments, resources, and evidence of environmental modification at areas that are currently buried below the seafloor on the outer continental shelf. The use of methods and data grounded in physical geography can ultimately add to patterns of past human behavior.

CHAPTER 1. SUBMERGED PREHISTORIC LANDSCAPES AS CONTEXTUAL ARCHAEOLOGY

The search for submerged prehistoric landscapes is an intricate endeavor requiring use of physical scientific methods to address a question rooted in the social sciences. Archaeology is the study of past human behavior using evidence from discrete sites to build patterns, and is generally classified as a social science. However, archaeology's objectives are rooted in the natural sciences (Butzer 1982:7).

The seafloor underneath the waters of the Gulf of Mexico hides evidence of prehistoric landscapes and resources important for the economic development of the United States. Oil and gas reserves created through geological processes and fish and shellfish resources are all extracted or harvested from the waters offshore of Texas and Louisiana, in the northwestern Gulf of Mexico (GOM). Competing economic interests for GOM resources are regulated by the federal government, which has jurisdiction over waters extending from three (Louisiana) to nine (Texas) nautical miles offshore to the edge of the Exclusive Economic Zone, located 200 nm offshore (NOAA CSC 2009). The densest area of offshore development and resource extraction in the northwestern GOM is on the outer continental shelf (OCS), which is defined as those portions of the seabed and submarine sediments adjacent to the shoreline and extending out to a depth of 200 m (656 ft) BSL (UNESCO 1958). The OCS is a high probability area for submerged prehistoric landscapes. In order to protect prehistoric landscapes against damage related to resource extraction it is necessary to identify where preserved elements of the prehistoric landscape exists.

1.1 Submerged Landscapes and Middle-Range Theory

The search for buried and submerged sites is based on contextual archaeology, which as defined by Butzer (1982:7), relies less on the discovery of artifacts than with examining sites as an expression of human agency, or decision-making. In the northwestern GOM contextual archaeology is an important analytical tool used to delineate areas where submerged prehistoric landscapes are most likely to be found on the OCS, which includes the entire continental shelf in

water depths less than 200 m (656 ft). When examined as part of a network within the human ecosystem, site location becomes somewhat predictable, based on the presence of various factors required to sustain a given population. In the northwestern GOM, a contextual approach to submerged prehistoric archaeology is necessary because the formerly exposed surfaces on which sites were created were buried prior to final inundation by rising sea-levels, making the recovery of artifacts unlikely. Using a predictive model for human preferences within the landscape, contextual archaeology relies on empirical methods of physical geography applied to middle-range theory.

Middle-range theory was first developed for use in sociology following World War II as a way to conceive of social systems and societal functions (Raab and Goodyear 1984:256). As used by R.K. Merton in the 1940s (Herbert 1996), the goal of middle-range theory was to allow empirical testing of theories based on abstract human behavior that otherwise would be untestable. According to Raab and Goodyear (1984:258), there is little direct discussion of the sociological origins of middle-range theory in the archaeological literature, despite its prevalence and association with the New Archaeology. Instead, they argue that middle-range theory's goals of linking empirical data with higher order theoretical constructs have been usurped by an emphasis on site formation process modeling (Raab and Goodyear 1984:258). Raab and Goodyear (1984:258-259) are correct in asserting that some studies over-emphasize site formation processes without relating the evidence back to social constructs of human behavior. However, middle-range theory should not be categorically dismissed as a viable tool in archaeology.

Two of the most influential works using middle-range theory in archaeology were conducted by Lewis Binford (1978, 1981) in which empirical data were tied to hypotheses of past human behavior through observations of modern human behavior. From the sociological and archaeological perspectives, middle-range theory is used to bridge empirical data with theories concerning past cultural patterns of behavior, which may be too abstract or generalized to be testable. Binford's (1978) initial use of middle-range theory applied knowledge of modern human technologies and their effects on faunal materials to models of past technologies and evidence of prehistoric butchering. Binford moved from the known across time to the unknown, to develop hypotheses relevant to cultures in the past with similar technologies.

In one of the first studies to explicitly address use of middle-range theory in underwater archaeology, Rik Anuskiewicz (1992:92) stated that geophysical signatures and their correlation with archaeological sites form empirical data consistent with middle-range theory building. Data produced through geophysical prospection are then tested against models of human behavior, which are intended to provide meaning to the empirical observations represented by the data (Anuskiewicz 1992:92). Anuskiewicz (1992) was writing about magnetometer data to locate submerged nautical sites (e.g., shipwrecks, ballast piles), but demonstrated that the empirical data led to the identification of sites which provided information about the local maritime culture. Middle-range theory, he wrote, was useful in explaining how the past is perceived by researchers rather than how it is explained (Anuskiewicz 1992:92).

Normally used in temporal studies, middle-range theory is applied here spatially to translate what is known about site patterns and interactions, the basis of contextual archaeology, from a given time period on land to the offshore environment as a way to model where sites would have been located. Perceived archaeological indices have been identified through previous research on prehistoric landscape occupation and exploitation patterns, resulting in indices for landscape identification that can be observed through geophysical survey. In other words, by identifying locations that prehistoric people preferred to occupy, and resources that were selectively exploited on land, archaeologists can extend those patterns spatially to areas that are now underwater.

1.2 Contextual Archaeology and the 'Real' Environment

Archaeologists study past human behavior. They build patterns by scaling-up data observed at the micro-scale, or site, to the regional, cultural, or temporal scales. An archaeological site is defined differently depending on the purpose, but generally is defined as a spatially-delimited accumulation of cultural material that has sufficient quantity and quality to allow inferences to be made about behavior occurring at that location (Butzer 1982:259). Sites are critical to reconstructing past human behavior. However, nonsites or data occurrences may still provide information needed to inform patterns of available resources (Butzer 1982:260).

In geography, environments may have both a real and a perceived character. Real environments are comprised of three elements: the geographical environment; the operational environment; and the modified environment (Butzer 1982:253). The macro-scale geographical environment, or the physical landscape, is that which is available for occupation and exploitation by a human population (Butzer 1982:253). The operational environment consists of the resources available for subsistence within the overall geographical environment (Butzer 1982:253). The modified environment is defined by Butzer (1982:253) as the space where "frequent or effective activity results in tangible modification" of the landscape. Only after these elements of the real, or objective, environment have been identified can the human dimensions be explored, including motives, preferences, and traditions (Butzer 1982:254). The perceived environment consists of elements from the geographical and operational environments of which a human population may or may not be aware, and which influence decisions. Real and perceived environments are not diametrically opposed. Nor do they completely overlap. Inferences about the perceived environment cannot be made without knowledge of the real environment.

In this dissertation, the geographical, operational, and modified environments are identified in buried and submerged contexts through a spatial application of middle-range theory using geophysical data.

1.3 Federal Requirements for Offshore Archaeology

Geophysical survey data is routinely collected on the OCS in relation to resource extraction surveys. Beginning in the 1960s, federal legislation was drafted to balance the protection of the nation's cultural and natural heritage against development pressures. Specifically, the National Historic Preservation Act (NHPA) was passed in 1966 and requires that all federal undertakings consider the effects of the activity on potential historic cultural resources within the area of proposed effect (NPS 2006). Federal undertakings are those activities which occur on federal land, require a federal permit, or involve the use of federal funding (NPS 2006). Due to other legislative acts, the NHPA is the only mechanism that requires consideration of archaeological resources on the OCS (Evans [n.d]). Following passage of the NHPA, the responsibility for archaeological resources on the OCS was vested with the Bureau of Land Management (BLM),

who at the time managed all offshore oil and gas leases. In 1982, the Minerals Management Service (MMS), a new agency within the Department of the Interior, was created with the specific purpose of managing offshore oil and gas permitting, leasing, and revenue (US Congress 1983). The MMS was superseded by the formation of the temporary Bureau of Ocean Energy Management, Regulation, and Enforcement in 2010, followed by the permanent split into two agencies, the Bureau of Ocean Energy Management (BOEM) and the Bureau of Safety and Environmental Enforcement (BSEE) in 2011.

To fulfill its NHPA responsibilities, BOEM/BSEE (and all preceding agencies) issue Notices to Lessees (NTL) that provide oil and gas industry operators with the guidelines and reporting requirements necessary for federal permit applications. Specific to archaeology, NTL 2005-G07 outlines the current requirements for surveys and reports used to identify the two types of resources most likely to be encountered on the OCS, which are historic sites (i.e., shipwrecks, lighthouses, and ballast piles), and drowned sites associated with prehistoric occupation or exploitation dating from the Late Pleistocene, when sea-levels were lower than at present (BOEM 2005). Previous studies conducted on behalf of BOEM, and its predecessors, were commissioned to determine the highest probability areas for the presence and occurrence of archaeological resources (CEI 1977; Garrison et al. 1989; Pearson et al. 2003). Despite the use of studies to delineate areas requiring archaeological survey, requirements remain vague. Survey guidelines published in NTL 2005-G07 Appendix I, Section III do not provide a maximum water depth for areas in which prehistoric archaeological survey assessments are required. In fact, NTL 2005-G07 states that surveys may be conducted for prehistoric archaeological resource identification in areas where water depths exceed 200 m (656 ft) utilizing acoustic profiles. This fact means that prehistoric archaeological surveys and assessments are required along the entire outer continental shelf (Figure 1.1).

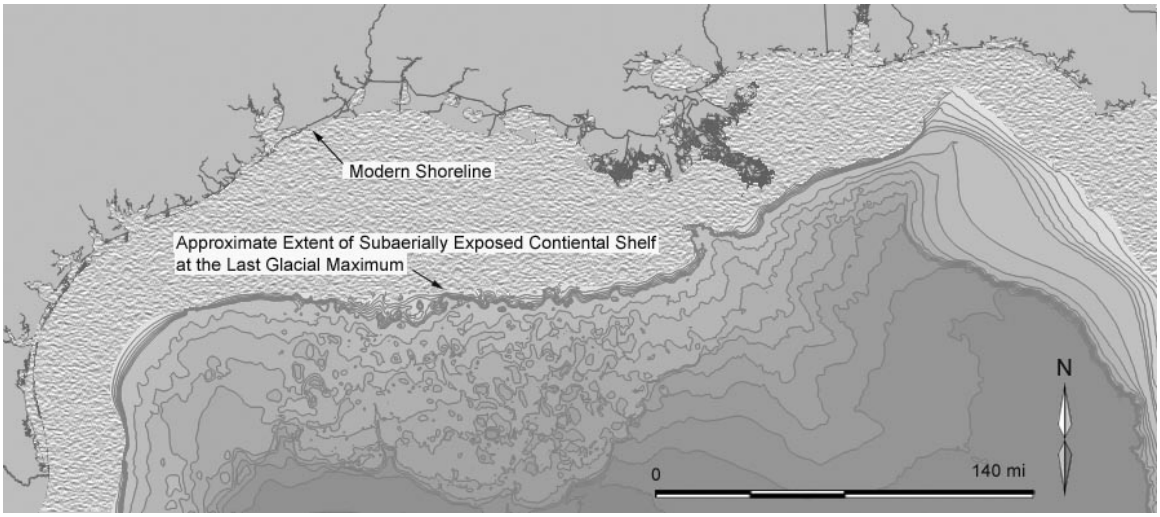

Figure 1.1 Gulf of Mexico Region with the Modern Shoreline and Approximate Extent of the Subaerially Exposed Continental Shelf at Approximately 200 m Isobath (Evans and Keith 2011a:167).

1.4 'Real' Environments on the OCS

The physical landscape of the OCS has experienced significant change over the last 18,000 years. In this study, geophysical data are used to identify three specific types of environments that are presently submerged on the OCS, as they relate to prehistoric archaeological sites. The geographical environment that was subaerially exposed during the last glacial maximum is a large area that could have been used by prehistoric populations. The identification of operational and modified environments allows archaeologists to narrow down possible areas of human occupation within the context of the OCS. The geophysical data record the entire subseafloor profile, and not just the areas of interest. Chapter 2 includes a discussion of the modern marine environment, and the recent history of sea-level changes that inundated the formerly subaerial landscape, which formed the geographical environment during prehistoric times. Sea-level transgression is a source of landscape modification; however, these modifications must be differentiated from anthropogenic, or human-induced, changes. Chapter 3 includes a discussion of the known patterns of human behavior from the Paleoindian and Early Archaic in the southeastern United States, which are the cultural-chronological periods that coincide with subaerial exposure of the OCS. Elements of the operational environment expected on the OCS are identified from contemporaneous sites located in modern terrestrial settings, and are outlined as indices for middle-range theory building. Chapter 4 includes a discussion of previous investigations of submerged prehistoric landscapes in general. More specifically, Chapter 4

includes a review of a series of previous studies from the GOM region that provide information on indices useful in identifying modified landscapes on the OCS. Chapter 5 includes a detailed discussion of the methodology used in this study, which focuses on the use of geophysical data in the identification of modified landscapes. Results of this investigation are presented in Chapters 6 (acoustic survey) and 7 (coring and sediment analyses). Chapter 8 includes a discussion of the results as they apply to middle-range theory and the identification of geographical, operational, and modified environments. A summary of the utility of geophysical data in a spatial application of middle-range theory used to identify elements of the real environment is presented in Chapter 9, along with considerations for future research. Several appendices are included, providing detailed information on sea-level curves used in this study (Appendix A), individual logs for each core (Appendix B), and supplemental reports utilized in the discussion of real environments (pollen analysis; Appendix C).

CHAPTER 2. PHYSICAL LANDSCAPE: SETTING AND RECONSTRUCTION

The search for submerged and buried prehistoric archaeological landscapes is predicated on an accurate assessment of the landscape from the point in time the landscape could have been occupied to the present. The synchronic reconstruction of the landscape, or reconstruction of place at a given point in time, provides information about exploitable resources that would have been necessary to support populations, and discrete areas within the landscape where evidence of past occupation is most likely to be found. Diachronic reconstruction of that same place provides information about changes to the site over time that influence preservation of any archaeological materials from their time of deposition, and influence secondary site formation processes. Reconstruction of geologic and climatic events from the time of occupation through to the present is necessary to interpret the stratigraphy under analysis. Although geologists tend to examine strata from the bottom up, archaeologists address stratigraphy from a top-down perspective, starting with the present surface and moving backwards through time with depth. Geologic formations and processes on the northwestern Gulf of Mexico (GOM) Outer Continental Shelf (OCS) are interpreted in this study from the top down. Sediment stratigraphy in the Gulf of Mexico, from the Jurassic to the Holocene, can be up to 20 km thick (Galloway 2011:33). Coleman et al. (1991:325) estimate Late Quaternary sediment thickness at approximately 3,600 m on the Texas and Louisiana shelf, where the areas under investigation are located. Core samples acquired as part of this study, and discussed in subsequent chapters, measure approximately 6 m long, and therefore capture only a fraction of the Gulf's Late Quaternary stratigraphic profile. The top-down approach is conducive for the types of analyses used in this study, which begins with the identification of known modern marine sediment at the seafloor and works backwards through time with depth.

The sites selected for inclusion in this study are located in the northwestern portion of the OCS offshore of south-central Texas and western Louisiana. The only other published study conducted in the Western Gulf on submerged archaeological landscapes focused on the Sabine River Valley, and examined areas where current water depths are up to 15 m BSL (Pearson et al. 1986). Despite this limited testing, conservative estimates suggest that prehistoric landscapes may exist on the shelf at areas where current water depths exceed 50 m BSL (Gagliano 1984:14);

however archaeological surveys must consider prehistoric landscapes in water depths that exceed 200 m BSL (BOEM 2005). The current study sites are located in the High Island and Galveston federal lease protraction areas, and represent current water depths ranging from 15 m to 40 m BSL. These sites are located within and between the relict Sabine, relict Trinity/San Jacinto, and relict Brazos river valleys (Figure 2.1).

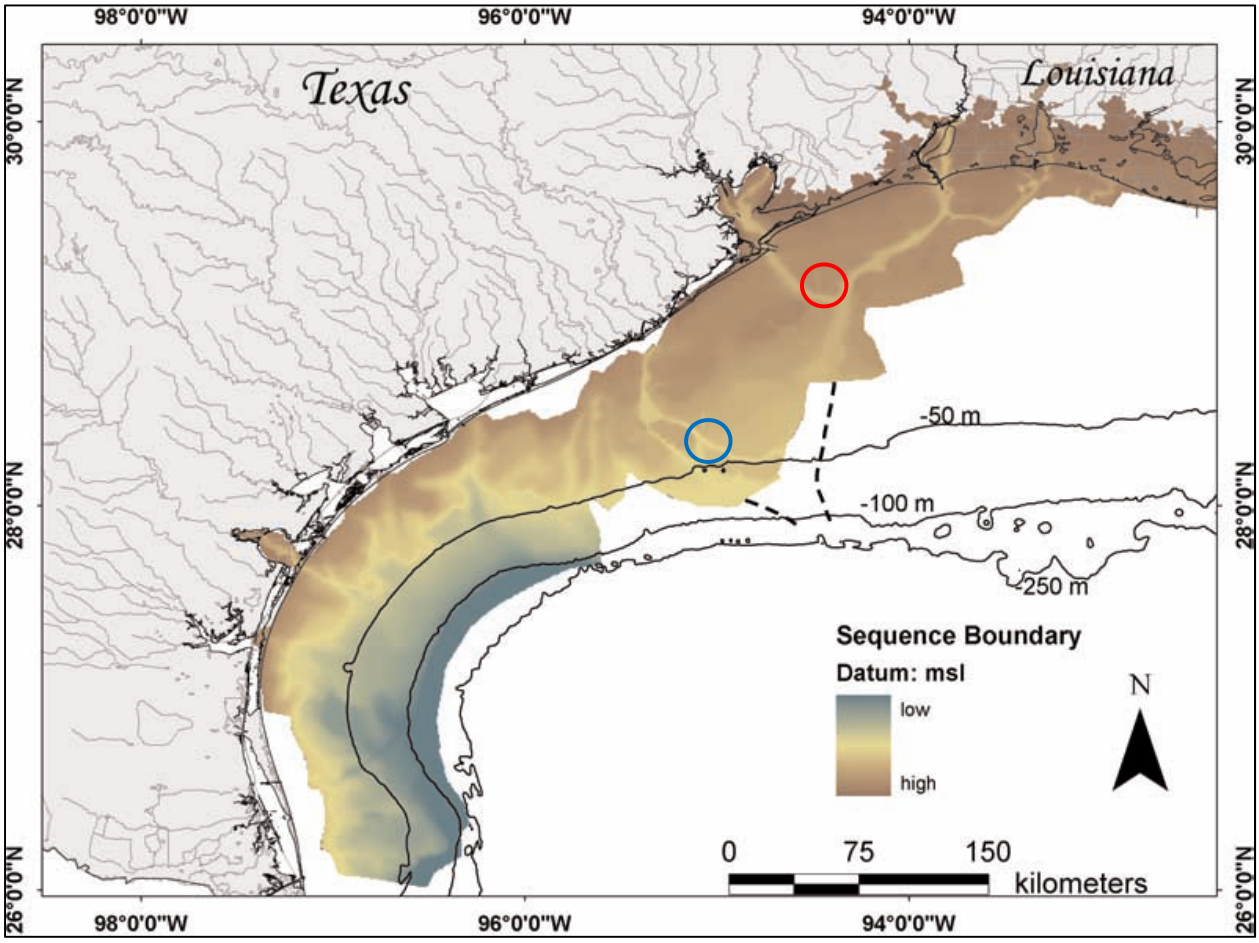

Figure 2.1 Map showing study areas in relation to relict river channels; HI 178 is outlined in red; GA 426 is outlined in blue (modified from Simms et al. 2008).

2.1 Sediment Stratigraphy

The Gulf of Mexico is a small ocean basin that developed through the opening of the North and South American tectonic plates (Galloway 2011:33). Formation of the Gulf basin was complete by approximately 140 million years ago (Bird et al. 2011:14). Since that time, the basin has

experienced multiple episodes of uplift, erosion, and sedimentation, resulting in the present stratigraphic sequence (Galloway 2011:47). Relevant to this study, the northwestern and northeastern Gulf of Mexico represent two distinct geologic zones. The northeastern Gulf is characterized by an underlying carbonate platform and the Mississippi-Alabama-Florida sand sheet (Coleman et al. 1991). The northwestern Gulf is completely different, characterized by alluvial sediments built up along the wide, shallow continental shelf (Coleman et al. 1991). High rates of sedimentation in the northwest during the Pleistocene are attributed to Quaternary glacial epochs that controlled sediment transport systems, ultimately forming the stratigraphic sequences observed in data collected as part of this scope of work. During the Holocene, sediment accretion has been most pronounced at the Mississippi river deltas, with limited to no appreciable sediment accretion on the western flank of the OCS (Curray 1960; Bernard 1970).

Due to the presence of recoverable oil and gas reserves in the northern Gulf of Mexico, significant efforts have been made to map geologic formations and develop sedimentary models in this region (Holmes 2011:195). Curray's 1960 analysis of Holocene sediments resulted in the identification of four distinct surficial sediment zones in the present northwestern Gulf of Mexico (ranging across Texas and Louisiana). The zones were created by assessing heavy mineral assemblages and correlating surficial deposits with their source; Mississippi River sediments were found in greatest concentration near the modern delta, but were distributed within all of the identified zones (Curray 1960:235). Curray's findings illustrate that the Mississippi River has had the most significant impact on shelf sedimentation rates and patterns since the Late Quaternary. Mississippi and weathered Mississippi River sediments are found in greatest abundance in the central and central Louisiana regions (as identified by Curray). In contrast, the western area consists of a mix of primarily Mississippi, weathered Mississippi, and Colorado river sediments with smaller amounts of Brazos, Trinity, and Neches river sediments in the western extent of the western area (Curray 1960:247).

Subsequent studies of Holocene sediment structures and thicknesses support Curray's earlier assessment that the thickest zone of recent sediment deposition is located around the mouth of the modern Mississippi River. Bernard (1970:Plate 17) estimates approximately 45 to 90 meters of Recent (or post-glacial) sediment close to the modern Balize delta, with sediments thinning to

less than 8 meters on portions of the shelf located west of the Atchafalaya Basin. Areas offshore of Texas are shown to have little to no recent sediment, with some exposed areas of Beaumont, or late Pleistocene, sediment (Bernard 1970:Plates 17, 18; Berryhill 1984). Soil borings analyzed by McClelland Engineers (1979) identified a similar pattern, with the majority of recent sedimentation located closest to the modern Balize delta, and little to no active sediment deposition along the northwestern margins of the Gulf of Mexico. The modern Mississippi River drainage basin, which includes the Atchafalaya basin, deposits approximately $2.34x10^{12}$ kg (230 million tons) of sediment annually (Holmes 2011:198). These sediments are deposited preferentially along the Louisiana coast. The Brazos and Colorado Rivers deposit approximately $1.12x10^{10}$ kg (11 million tons) along the south-central Texas portions of the modern continental shelf (Holmes 2011:198). Due to the low gradient of the offshore OCS, sediments are distributed over a wide area in the northwest, resulting in low levels of gross accumulation.

The GOM OCS is relatively wide and shallow, measuring approximately 54 statute miles wide at the Rio Grande and a maximum 130 miles wide at the Texas-Louisiana border (Curray 1960:223). Average seafloor gradients become shallower from southwest to northeast; average gradient is 2.2 meters (7.3 ft) per statute mile at the Rio Grande, 1.8 meters (6 ft) per mile at the Brazos River Delta, 1 meter (3.2 ft) per statute mile at the Texas-Louisiana border, and less than 0.3 meter (1 ft) per mile at the Recent Mississippi delta (Curray 1960:223; Bernard and LeBlanc 1965:137).

The modern seafloor in the GOM is comprised of a mixture of sand, silts, and clays deposited along a gradual slope. Significant bed forms are virtually non-existent. A few areas of naturally occurring topographic relief are located on the shallow shelf; features such as salt outcrops, pinnacles, and mud mounds are located closer to the shelf/slope break. There is little indication from seafloor morphology that significant portions of the shallow OCS were part of a fluvial plain during lower sea-level periods in the recent past (Nelson and Bray 1970:55). All evidence of these channels and their related features have been buried by sediment accretion following the most recent marine regression. Investigations of formerly subaerial landscapes therefore require the ability to image and examine subseafloor sediments, which is most commonly achieved through acoustic profiling.

Acoustic profiling, as discussed in more detail in Chapter 5, provides a top-down image that represents strata of varying acoustic impedance. Depending on the strength of the acoustic returns, a profile is generated that depicts strata of varying thicknesses and signal strength, represented visually by dark and light horizons (Figure 2.2). Features such as channels, levees, and inset terraces can be identified from the acoustic profile. In addition, interpretations can be made of sediment types and consistencies, including water-logged sediments, sands, biogenic gas, and peat deposits (e.g., Whelan et al. 1977; Plets et al. 2007).

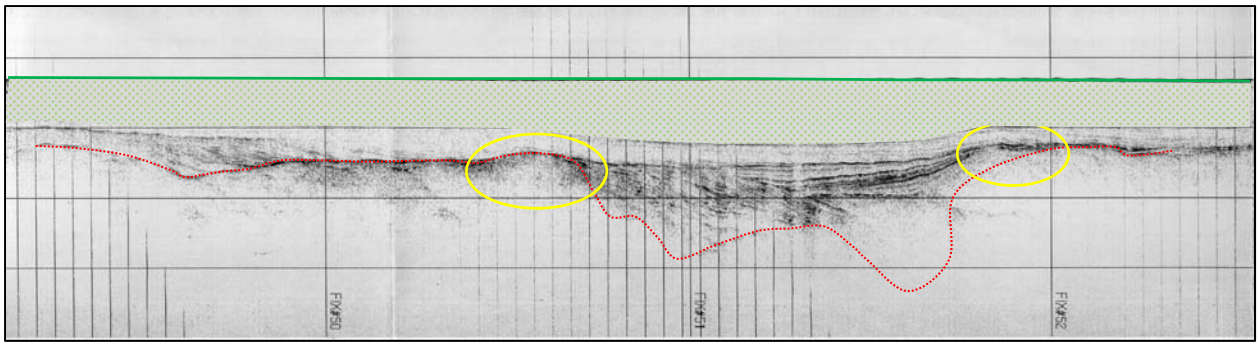

Figure 2.2 Sub-bottom profiler sample of acoustic data depicting a preserved river channel (outlined in red) and levees (circled in yellow) underneath modern marine sediment (shaded in green) (data courtesy Tesla Offshore).

Acoustic profiling as used in this study is the first step in identifying potential prehistoric landscapes. The study sites are located in proximity to the relict Sabine, Trinity/San Jacinto, and Brazos rivers. During the last glacial maximum, these rivers extended across the newly exposed OCS, carving channels and creating a fluvial landscape that included inset terraces and natural levees. As sea-level began to rise, the river systems backed up the shelf, depositing sediments and filling the most recently entrenched channels. Sediments deposited during the Holocene and Late Pleistocene represent distinct depositional events and episodes attributable to changes in sea-level and regional climate (Frazier 1974). These episodes are visible on the acoustic profiling data, and form the basis of the depositional sequence paradigm, in which subaerial erosion surfaces are interpreted as sequence boundaries because of the strong influence of glacio-eustasy (Galloway 2011:38).

Offshore entrenched river valley fill typically consists of alluvial and deltaic sediments overlain by marine, deltaic, or coastal interdeltaic deposits (Bernard and LeBlanc 1965:138). Offshore sedimentary sequences are uncomformably deposited on eroded and/or subaerially weathered sufaces correlating with major glacial stages (Bernard and LeBlanc 1965:138). Fisk observed that each Quaternary depositional sequence consisted of gravelly basal sands fining upwards to sands, silts, and clays, followed by an erosiosal surface, on which the sequence was again repeated (Bernard and LeBlanc 1965:141). Glacial stages include net lowering and lower-than-modern sea-level substages, and interglacials include net rising, and high-standing sea-level substages (Bernard and LeBlanc 1965:139).

Sea-level change has altered the extent and shape of the outer continental shelf repeatedly during the Pleistocene. The geographical environment available to prehistoric human populations was expanded and minimized by these progradations and transgressions; it also was altered and reworked by these same mechanisms. Sea-level position is useful in determining areas of potential prehistoric landscapes. Since people did not live underwater, sea-level curve data are used to estimate the possible time period of exposure for a given sediment horizon. Final inundation, or the most recent inundation as sea-level approached the present high-stand, marks the last possible date for potential occupation by prehistoric populations before the landscape became part of a submerged environment.

2.2 Sea-level Change

Some of the first scientific observations and hypotheses regarding sea-level changes were made in the mid-1700s (Pirazzoli 1991:1). Early explanations for the rise and fall of sea-levels were attributed to diminishing global water supplies, evaporation, and crustal movement on earth's surface (Pirazolli 1991:1). In 1885, Suess developed the concept of eustatic sea-level change, or uniform vertical displacement of the ocean surface on a global scale, which influenced sea-level change studies well into the twentieth century (Pirazolli 1991:1-2). The concept of glacio-isostatic changes in sea-level was introduced by Daly (1934) and correlated sea-level change to glacial melt and land subsidence (Pirazolli 1991:2). Early sea-level studies were characterized by an assumption that the interconnectedness of the earth's oceans would result in uniform

eustatic sea-level change, and that data from any tectonically stable region was representative of global sea-level at that point in time (Pirazzolli 1991:4). Current understanding is that sea-level is geographically and temporally dynamic. Factors that influence eustatic sea-level at any given time may include changes in ocean volume, water mass, and water density (Pirazolli 1991:6). Overall global patterns are influenced locally by relative changes associated with regional land uplift or subsidence, meteorological or atmospheric events, gravity, and eccentricity (Pirazolli 1991:6).

Sea-level change can be assessed by identifying evidence of former shoreline stands and related environments, and by absolute dating of samples taken from sediment and ice. Sea-level indicators include naturally occurring features such as sediment deposits, erosion features, corals, fossils, shells, or plant remains, as well as anthropogenic materials such as archaeological artifacts (Pirazolli 1991:10-16). These indicators will only provide evidence of possible shoreline positions and translations, or patterns of change. In and of themselves they do not provide dates of shoreline positions. Isotope analysis is a commonly accepted method for determining ages, or age ranges, for specific samples. Radiocarbon dating is one of the more common isotopic analyses used to determine absolute date ranges, and has been in use since the 1950s (Pirazolli 1991:19). More recently, the marine oxygen isotope record has been used by scientists to date global climate change, as well as correlate eustatic sea-level changes (Chappell et al. 1996; Thacker and Ellwood 2007). Despite the seeming reliability of absolute dates, caution must be exercised when using and comparing sea-level curve data. As stated by Pirazolli (1991:21), many sea curves are created by extrapolating change among discrete data points, without regard to estimates of error. Line graphs of age/depth below modern sea-level represent an oversimplified interpretation of sea-level change. Error ranges for individual data points allow for a more comprehensive, although more complex, visualization of sea-level change within a given data set (e.g., Balsille and Donoghue 2004). Furthermore, oscillations and reversals become exaggerated at smaller time intervals. Positive and negative alternations of sea-level observed at a time scale on the order of a thousand years are likely to become insignificant within the overall pattern of sea-level change when viewed on a scale of tens of thousands of years (Pirazolli 1991:21). The issue of scale becomes pertinent when sea-level

curves are applied to archaeology in the Western Hemisphere, where the record of human habitation is about 15,000 years (Figure 2.3).

At the local or site level, researchers rely on sediment data to correlate climate conditions with a relative site age. Geochemical properties and physical assemblages within the sediment matrix can be tested at the local level and correlated over regions. This process is essential to determining a successful age range since sea-level curve data and even marine oxygen isotope records are determined at the regional scale or larger, without accommodating for local variations.

Global rates of sea-level change can be assessed using a variety of data sets and correlative methods. Chappell et al. (1996) modeled global sea-levels by cross-referencing $^{230}Th/^{234}U$ dating of coral reef terraces in Papua New Guinea with $\delta^{18}O$ curves from deepwater marine sediment cores. Toscano and Macintyre (2003) produced a sea-level curve specific to the western Atlantic region using calibrated ^{14}C and U-Th absolute dates derived from coral reefs and mangrove peat samples. While rates of change vary among data sets, most eustatic sea-level models indicate that sea levels were approximately 140 to 125 meters lower than present mean sea level at the end of the last glacial maximum (Bailey and Flemming 2008; Bird 1993:14).

Changes in the relative position of a given shoreline involve complicated processes. A discussion of sea-level change at the end of the last glacial maximum should address more than the increasing amount of water introduced to global basins by melting glaciers. Sea-level rise can be attributed to either eustatic or isostatic change (Lewis 2000). Eustatic change refers specifically to a rising sea-level in relation to a stable land surface, and is most often attributed to changes in climate (Lewis 2000). Isostatic sea-level change is measured on a more localized scale, and is given as the vertical displacement between stable sea-level and the elevation of the land surface (Lewis 2000:526). Isostatic changes can be attributed to sediment load compaction, fluid extraction, and other localized changes in conditions, and are generally associated with subsidence (Lewis 2000). Oscillations and differences in early global sea-level curves may be attributed to data that were obtained from areas now characterized as subsiding coasts, rather than resulting from faulty data (Pirazolli 1991:4).

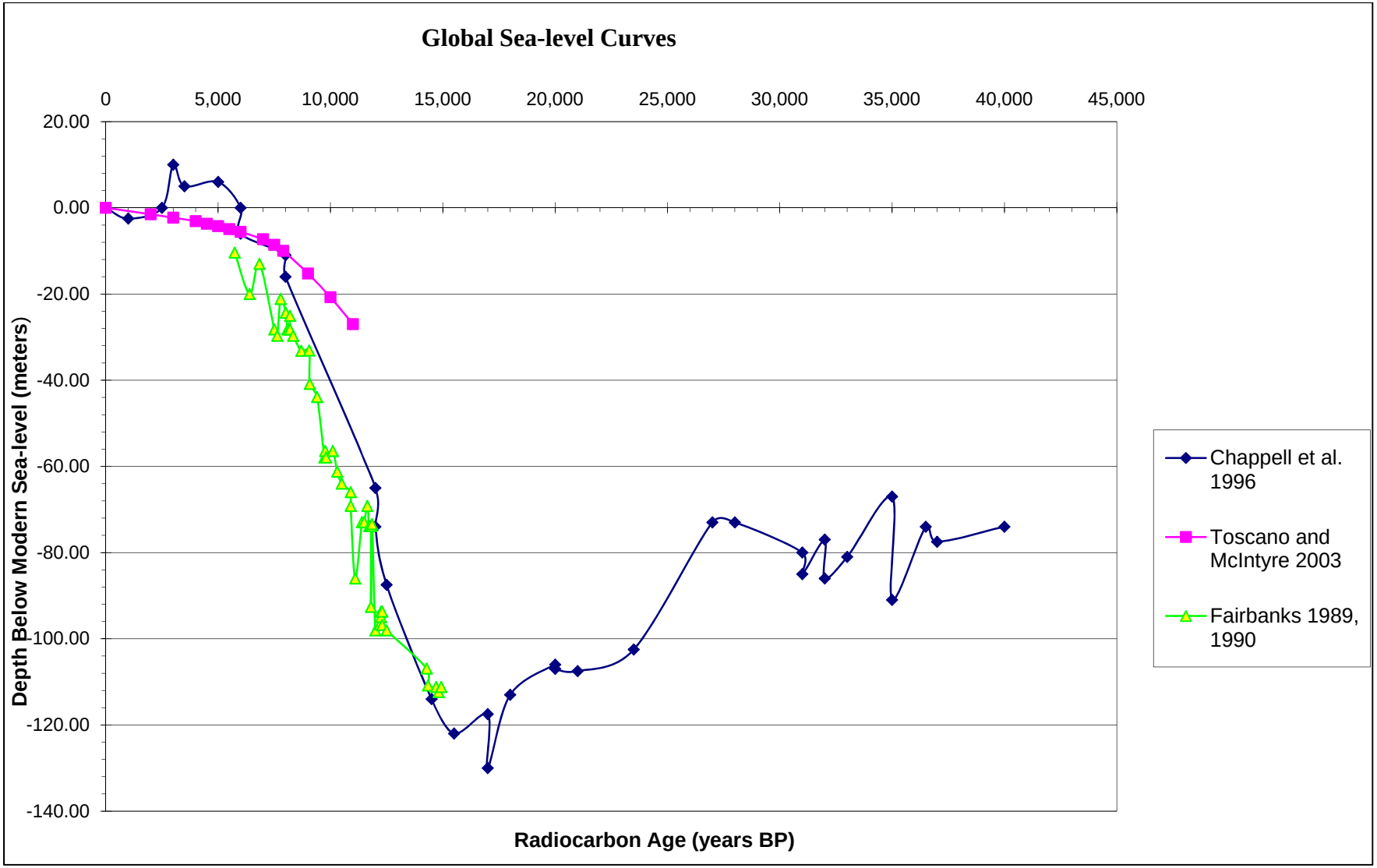

Figure 2.3 Global sea-level curves demonstrate the variability within the record at different positions on the earth in the recent past.

2.2.1 Sea-level Change and Archaeology

Eustatic sea-level rise has significantly impacted the archaeological record of early coastal cultures. Archaeological sites related to the earliest inhabitants of the Gulf coast area likely are located on the now submerged continental shelf (Lewis 2000). According to Lewis (2000:531), no true coastal sites associated with these populations have been identified, because the location of the coastal zone relative to those cultural periods is on now-inundated portions of the continental shelf.

The majority of researchers agree that sea-level change is a locally specific phenomenon. Therefore, reconstructions must include some measure of local variability within trends that would otherwise suggest uniform rates of global sea-level change (Lewis 2000). As early as 1965, Bernard and LeBlanc (1965:140) cited factors that complicate the construction of sea-level curves based on radiocarbon dates. Complications may arise from, but are not limited to, sediment compaction and local subsidence, recognition of marsh and swamp peats, range of peat formation relative to water depth, and habitat extent within the water column (Bernard and LeBlanc 1965:140). Awareness of these complications has led to re-evaluations of regions once considered to reflect homogenous rates of sea-level rise, and have demonstrated high rates of local variability (Lewis 2000). Global patterns of sea-level change are insufficient for a study of localized impacts to archaeological sites related to rates of sea-level rise. According to Dott (1992:2):

> … we have come to realize that the problem of isolating an unambiguous eustatic signal is even more complex than prior generations could imagine. This is because there are so many complex feedbacks among glacial isostasy and glacial eustasy, hydro-isostasy affecting the entire world ocean through changing water volume, tectonic eustatic effects, erosional and sedimentational isostasy, compaction and decompaction of sediments, and even changing evaporative potential over the oceans.

Estimates for sea-level position during the last glacial maximum indicate a difference of -140 meters from the modern sea-level stand, whereas estimates of sea-level rise indicate a change of approximately 1 meter per century between 18 and 6 kya (Bird 1993:14). Sea-level rise is commonly described as oscillating. Regressions or pauses interrupt periods of continual rise. However, some argue that oscillations are the result of statistical aberrations within the data

(Bird 1993:14). The rate and timing of sea-level rise are complicated by many factors including tectonic uplift or localized subsidence (Bird 1993:14). Subsidence and or downwarping commonly occur along coastal deltas due to the accretion of fluvial sediment (Bird 1993:17). Downwarping also may occur as a result of hydro-isostaic subsidence, especially along low-lying shallow continental shelves, as the weight of deepening water compresses soft sediments such as peat (Bird 1993:17-18).

The variability in different sea-level curves results in great difficulty for archaeologists attempting to reconstruct shoreline changes within time periods of several hundred, or even several thousand years. To be useful in archaeological settings, rates of sea-level rise must be accurate at the site-specific level.

2.2.2 Late Quaternary Sea-level Change in the Gulf of Mexico

Archaeologists have argued for the construction of regional sea-level curves (Ricklis 2004). Global curves, such as those proposed by Chappell et al. 1996, can accurately demonstrate general climate trends. However, global models can overwhelm or mask distinct regional patterns (Ricklis 2004:183). The importance of a regionally-accurate curve was demonstrated by archaeologists working at a 10,700 yr BP site in Florida. Attempts to reconstruct the shoreline position at the time the site (8JE1004) was occupied using global curves resulted in estimates of sea-levels 10 to 70 meters below present mean sea-level (Balsillie and Donoghue 2004). In this case, the scale of the global data resulted in sea-level positions too gross to make finite assessments of a short interval in the recent past.

The sequence of sea-level change in the northwestern Gulf of Mexico was summarized by Simms et al. (2008) as follows. Approximately 120,000 years ago, during oxygen isotope stage 5E (OIS 5E), sea-level was 5m above present mean sea level. Regionally in the Gulf of Mexico, this time period was known as the Peorian Interglacial. Shoreline progradation occurred between 120 kya and 60 kya (OIS 4) reaching levels of approximately 80 meters below present mean sea level during the initial phase of the Late Wisconsinan. This progradation was followed by a rapid transgression, coinciding with OIS 3, during which time sea-level rose to 15m below present mean sea-level. The end of Late Wisconsin glacial conditions, referred to as the Last

Glacial Maximum (OIS2), occurred approximately 22 kya to 17 kya and resulted in shoreline progradation to approximately 90m – 120m below present mean sea-level. Shoreline transgression began again approximately 17 kya, rising rapidly until approximately 6 kya. Although most researchers agree on this basic pattern of sea-level change, the rates and details of change are debated.

A review of sea-level curve data produced by Ricklis (2004) for the northern Gulf of Mexico region suggests that sea-level rise over the last 20,000 years consists of a discontinuous pattern of change. The curve hypothesized by Ricklis (2004) consists of sequential periods of rapid sea-level rise, consisting of glacial meltwater pulses, interrupted by periods of slow sea-level rise, stillstands, or slight regressions. This revised model does not exhibit the same sea-level oscillations that appear in earlier works, which differ from Ricklis' sequence and each other (i.e., Curray 1960; Frazier 1974; Morton et al. 2000; Figure 2.4). Individual sea-level curves are provided in Appendix A.

In 2004, the Florida Geological Survey published a comprehensive survey report that compared high resolution data on sea-level change since the Late Pleistocene for the northeastern Gulf of Mexico region (Balsillie and Donoghue 2004). The study included 22 data sets specific to the region (Balsillie and Donoghue 2004), and compared a statistical analysis of the regional data with the eustatic global curve developed by Siddall et al. (2003) from $\delta^{18}O$ analyses of foraminifera from Red Sea sediment cores. The researchers found that the regional data sets were consistent with trends illustrated in the global eustatic curve from approximately 18,000 years BP until approximately 6,000 years BP (Balsillie and Donoghue 2004). In the northeastern Gulf of Mexico data sets, two trends emerged, both of which differed from the eustatic global curve. The global eustatic curve since 6,000 yr BP resembles the sea-level oscillations reported by Frazier (1974). The Gulf of Mexico data depict pulses of sea-level rise more on par with those hypothesized by Ricklis (2004). This assessment is specific to the northeastern Gulf of Mexico, where the carbonate platform and seafloor sands are less susceptible to isostatic change than the alluvial sediments characteristic of the northwestern Gulf.

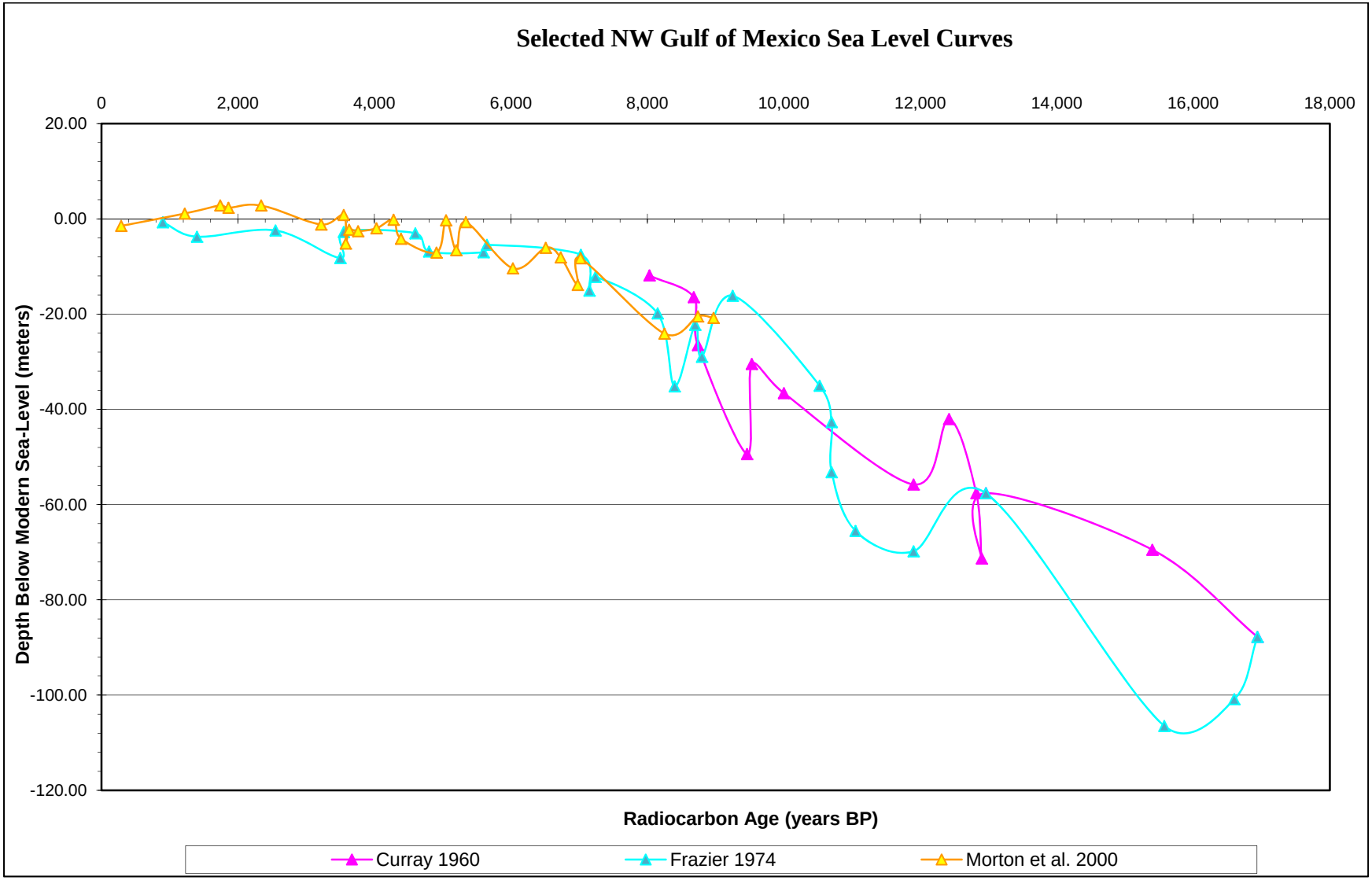

Figure 2.4 Comparison between selected published sea-level curves constructed from data specific to the northwestern GOM.

A review of sea-level curve data published by Milliken, Anderson, and Rodriguez (2008) argues for rapid, possibly episodic, rates of sea-level rise in the Northern Gulf of Mexico region during the early Holocene, followed by slower, nearly continuous, rates of rise during the middle to late Holocene. Specifically, the authors identified several Holocene-era flooding events: ca. 9800 – 9500 cal yr BP; ca. 8900 – 8500 cal yr BP; ca. 8400 – 8000 cal yr BP; and ca. 7400 – 6800 cal yr BP. These flooding events are generally correlated with climate events, such as an 8200 cal yr BP event associated with a glacial meltwater pulse related to mass wasting of the Laurentide ice sheet (Milliken, Anderson, and Rodriguez 2008). Correlated data from peat samples and *Donax* species suggests that sea-level ranged from 3 – 10 m below present mean sea-level from 8000 cal yr BP to 4000 cal yr BP (Milliken, Anderson, and Rodriguez 2008). Based on evidence from their study, Milliken, Anderson, and Rodriguez (2008) argue that sea-level rise was rapid in the middle Holocene, but did not reach present levels until after 4000 cal yr BP. Sea-level rise from the late Holocene occurred at an approximate rate of 0.4 – 0.6 mm/yr, and was variably influenced along the Gulf coast by localized subsidence (Milliken, Anderson, and Rodriguez 2008).

The most notable area of disagreement in regional curves is within the last 10,000 years of sea-level change. Unlike the previously discussed models, Blum et al. (2008) argue that landforms along the Gulf coast, including samples from Texas and Alabama, indicate that present mean sea-level was reached by approximately 6.7 kya. This model contradicts most other sea-level curves, which indicate that sea-level was rapidly rising until approximately 2,000 – 5,000 years ago (Blum et al. 2008).

One explanation for the difference in rates of sea-level rise within the Gulf of Mexico is the local expression of both eustatic and isostatic change resulting in simultaneously different patterns of transgression (Simms et al. 2008). Subsidence rates for the Gulf region are estimated to increase from several centimeters per thousand years onshore to approximately one meter per thousand years at the shelf edge (Simms et al. 2008). This isostatic change occurs in tandem with eustatic sea-level rise. Rates of subsidence and compaction have been studied along the deltaic plains of the Mississippi River. However, the impacts of both isostatic and eustatic sea-level rise serve to demonstrate the difficulty in calculating local rates of sea-level rise from global, and even

regional, data sets. Even within regionally discrete areas, sea-level curve data are not always consistent. Nelson and Bray (1970:66) compared radiocarbon dates from brackish shells, marine shells, and wood and peat samples to create a sea-level curve specific to the Sabine-High Island Area. They developed a primary sequence of events (Table 2.1), but noted the existence of numerous outliers within their data set.

Table 2.1 Sea-Level Sequence for Sabine-High Island Areas

Date Range (yrs BP)		Description	Minimum Depth Below Modern Sea-Level
18,200	10,200	Subaerial exposure along portions of the OCS, freshwater entrenchment of the Sabine River along a wide, flat plain	35 m (117 ft)
10,200	9,400	Rapidly rising sea-level; brackish waters intrude upstream but remain contained within river channels	22 m (73 ft)
9,400	8.660	Rising sea-level, brackish waters breach channels but remain within river valley	19 m (62 ft)
8,660	7,800	Falling sea-level, re-entrenchment of river channels	22 m (72 ft)
7,800	6,660	Stable sea-level; sedimentation remains confined within the river valley, which now forms a brackish, estuarine lagoon	22 m (72 ft)
6,600	5,650	Rapidly rising sea-level (approx. 1.6 m/century)	15 m (50 ft)
5,650	3,600	Slower rate of sea-level rise	1.8 m (6 ft)
3,600	2,800	Slowest rate of sea-level rise (approx. 0.27 m/century)	--
Source: Nelson and Bray (1970:67-70)			

Although the work of Nelson and Bray (1970) represents a detailed account of sea-level rise, their research is restricted in area to the Sabine River valley. It also represents an area in which numerous data points were collected within one locality and is therefore anomalous among other sea-level data sets for the northwestern Gulf. Despite the detailed nature of Nelson and Bray's sea-level sequence, it varies significantly from other regional reconstructions. Milliken, Anderson, and Rodriguez (2008) suggested sea-levels were 3 to 10 meters below present from 8,000 to 4,000 BP, the same time during which Nelson and Bray estimated sea-levels were 2 to

22 meters below present. Sea-level curves are generally consulted by archaeologists to determine when a given location on the outer continental shelf was last exposed to subaerial weathering, and if that time coincides with likely periods of human occupation. Given the complexity of sea-level rise patterns, and the need to address landscapes in areas with variable data sets, a single pre-existing sea-level curve was not selected for use in this study. Instead, locally- and regionally-specific curves were deconstructed, and their data points combined into a cumulative data set along an X-Y axis, where the X axis represents time and the Y axis represents depth below modern sea-level (Figure 2.5; Curray 1960; Shepard 1960; Nelson and Bray 1970; Frazier 1974; Morton et al. 2000; Blum et al. 2001; Tornqvist et al. 2006; Blum et al. 2008). A 4-point polynomial average was plotted along the sea-level curve, depicting the general trend of sea-level rise within the region. The calculated average depicts a generalized pattern of sea-level rise, but does not account for outliers within the data set. Minimum and maximum lines were created for the composite curve because the original data sets for many of the locally-specific sea-level curves could not be obtained, and therefore the necessary error distributions (as used by Balsillie and Donoghue 2004 and advocated by Pirazolli 1991) were not available. From an archaeological perspective, the minimum and maximum dates provide an objective range for correlating the age of an identified landscape feature with the potential for human occupation since site specific issues such as sediment compaction or regional subsidence will affect the feature's age relative to any pre-existing sea-level curve. The minimum and maximum lines allow the archaeologist to correlate a feature's depth with times of potential subaerial exposure and final inundation relative to cultural chronological periods and dates of known human habitation in the region. This date range can be refined through physical sampling of the feature and absolute dating of samples.

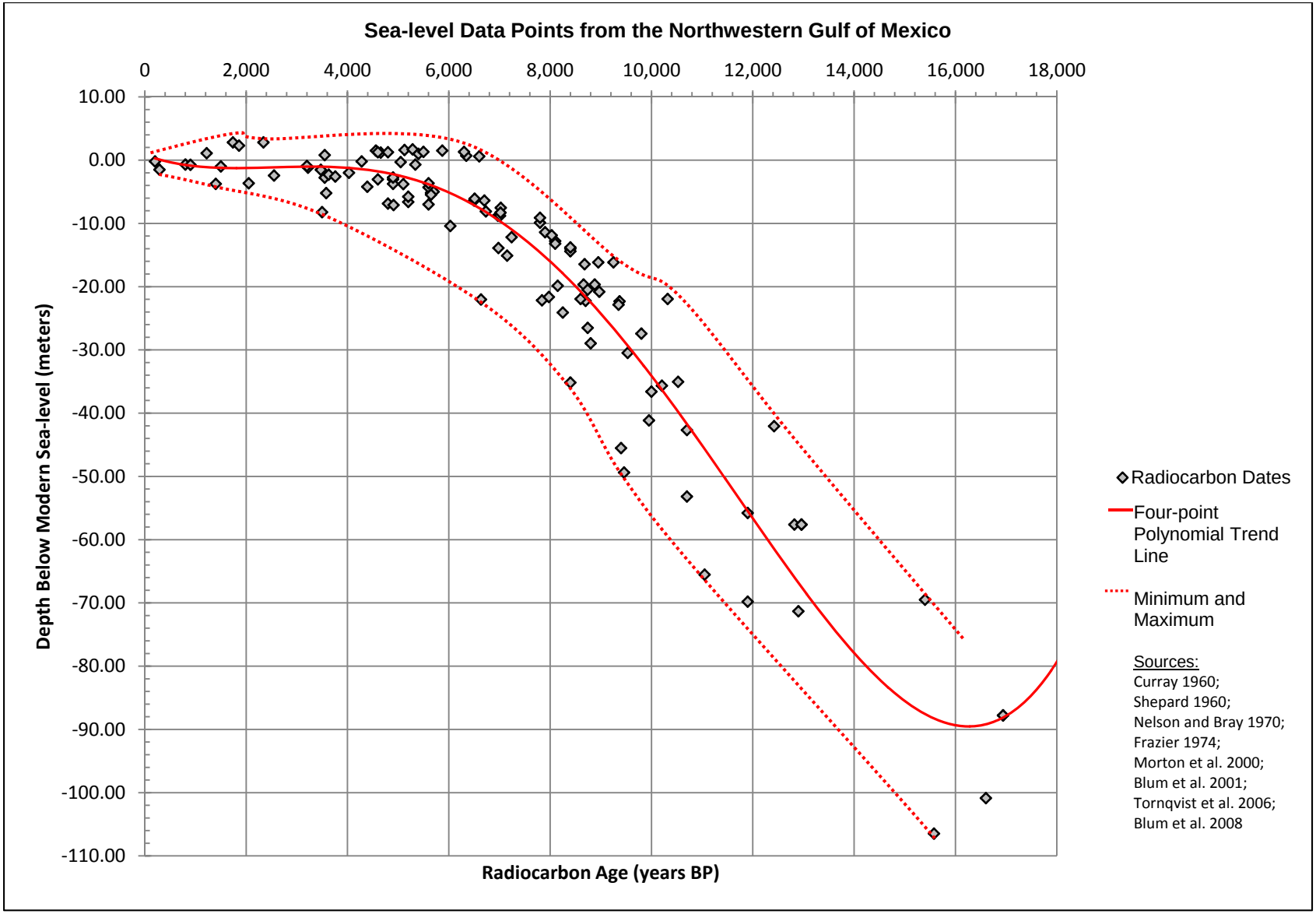

Figure 2.5 Composite sea-level curve for the northwestern Gulf of Mexico.

2.3 Diachronic Reconstruction and Site Preservation Potential

The northwestern Gulf of Mexico is considered a high probability area for the preservation of prehistoric archaeological sites due to the presence of the various river valleys that were entrenched on the subaerial OCS (CEI 1977; BOEM 2005). One cannot argue for evidence of prehistoric occupation simply because the geographical environment was available for human exploitation. A study of submerged landscapes requires that any evidence of occupation or exploitation be preserved *in situ*. Preservation begins with the creation of the archaeological site, and continues through inundation and eventual transformation into an open water marine environment.

Studies on site preservation potential specific to the northwestern Gulf of Mexico (CEI 1977; Pearson et al. 1986; Waters 1992) have demonstrated that relict river channels represent the optimum place for site preservation. As demonstrated in Nelson and Bray's sea-level rise sequence, river channels and ultimately river valleys, fill with brackish water, becoming low-energy estuaries or lagoons during the initial stages of sea-level rise. Archaeological sites located within these river valleys become buried underneath newly deposited estuarine sediments, which eventually fill the channels and valley so that they are topographically indistinguishable from the surrounding seafloor. Localized subsidence into estuarine peats also would have encouraged the preservation of archaeological materials, as they would have been below the immediate seafloor sediments at the time of final inundation (Lewis 2000; Weinstein et al. 2012). As the shoreline begins to translate over the site, the high energy surf zone impacts the newly deposited sediments and surrounding paleosols, leaving those landscape features underneath the estuarine transgressive zone (defined here as the maximum depth to which sediments were scoured and eroded during sea-level rise) protected from erosion. The Nelson and Bray (1970), Blum et al. (2008), and Milliken, Anderson, and Rodriguez (2008) studies demonstrate the various rates of sea-level rise at any given time. All sea-level curves imply the movement of the shoreline. In terms of site preservation potential, shoreline change includes the movement of the high energy surf zone across the continental shelf. For any given location on the OCS, estimates of time during which that portion of the shelf was undergoing active erosion as part of the high energy surf zone will vary from hundreds to thousands of years depending upon the sea-level curve being used. Following stabilization of the shoreline, and depending on

the depth of the buried feature, its long-term preservation is dependent upon oceanographic processes impacting the marine environment, especially scour and erosion.

The Gulf of Mexico OCS is characterized as a micro-tidal, low energy environment (Curray 1960:231-234). Diurnal and mixed diurnal tidal fluctuations in the Gulf of Mexico typically average less than 0.3 meters (1 foot). However, tidal ranges are highly variable during meteorological events; hurricane-induced tides in the Gulf often exceed 3 meters (10 feet) (Curray 1960:233). Wave conditions are normally low to moderate; average deepwater wave periods range from 3 to 8 seconds, and waves rarely exceed 1 meter (3 feet) in height (Curray 1960:231). These small-size waves generally are only capable of moving sediment in the shallow surf-zone (Curray 1960:231). Shallow water sediments are principally sands and coarser-grained material than that found on the continental shelf, since sands fall out of suspension before silts and clays and are therefore preferentially deposited along the coast (Masselink and Hughes 2003). Under bed stress and flow conditions, cohesionless sands "behave individually". In contrast, silts and clays (grain size less than 63 μm) are electro-statically charged and therefore cohesive (Masselink and Hughes 2003:124). According to Masselink and Hughes (2003:124), "the dynamic behavior of cohesive sediment depends less on single-grain properties and more on bulk-sediment properties (e.g., floc size and water content)."

Sediments on the OCS are generally considered to be at equilibrium. Fine-grained sediments correspond to areas with weaker currents (Whitehouse 1998:62). Hurricane waves and tidal currents disrupt this equilibrium and are responsible for reworking and modifying sediments on the shelf (Curray 1960:234). According to Curray (1960:233), "a velocity of 35cm/second is … the approximate mean velocity at 1 meter above the bottom which is required to pick up and move fine quartz sand," although actual net transport also requires unidirectional flow and a velocity gradient that extends to the seafloor. Using hindcast wind/wave data for normal wave conditions in the Gulf of Mexico, Curray estimated that areas in water depths less than 10 fathoms (18.3 m or 60 ft) experienced bottom velocities greater than or equal to 35 cm/second for more than 500 hours per year, or approximately 5% of the time (1960:233).

Due to the relatively minor impact of normal current and tidal conditions, the majority of pronounced episodes of erosion and scour recorded in the uppermost sedimentary record stem from discrete or punctuated events, such as extreme storms, or anthropogenic impacts, such as dredging. Anthropogenic activities such as trawling, construction, and dredging have occurred on the GOM OCS with increasing regularity for the last hundred years (Evans et al. 2009; Evans and Keith 2011a, 2011b). Trawling has resulted in the occasional isolated find of archaeological materials. Otter trawl nets and their associated equipment typically only disrupt the uppermost 0.2 meter of sediment (FAO 2005). Dredging and construction can have a much deeper impact, but are more likely to be regulated on the OCS. No finds of prehistoric artifacts have been reported from either of these activities offshore in the northwestern Gulf. Extreme storm events impact the OCS with some regularity. When applied to actual hurricane wave statistics, Curray's (1960:233) calculations for sediment transport velocities indicated that areas in water depths between 10 and 15 fathoms (18.3 to 27.5 m; 60 to 90 ft) experienced storm induced scour less than once every 18 months. All of the areas included within this study are located in depths that, according to Curray's estimates, experience bottom current velocities sufficient to result in transport and scour of fine, cohesionless, sands at least once every 18 months.

To accurately assess the potential for sediment scour and erosion of seafloor sediments resulting from extreme storm events, computer modeling of sediment transport was conducted under contract by Deltares for each of the study areas (Galveston and High Island), at water depths of 15.5 and 31.0 m (50.8 and 101.7 ft) below sea level (BSL) (Rego et al. 2011). The modeling incorporated H*WIND data for recent hurricanes and simulated hydrodynamics and waves using proprietary Delft3D-FLOW and Delft3D-WAVE models in the Gulf of Mexico basin using a rectangular model of 10km resolution around the datum points. Smaller, curvilinear models of 50 meters (164 feet) maximum resolution were also created with Delft3D-FLOW and Delft3D-WAVE to simulate localized conditions. Curves for each site were created representing model results for both loose and consolidated sediment types. Hurricane surface wind speed data were prepared by the National Oceanic and Atmospheric Administration (NOAA) and are available as real-time analyses of tropical cyclone surface wind observations (H*WIND). Delft3D-FLOW is a three-dimensional hydrodynamic model that simulates horizontal and vertical water movement on the continental shelf. Delft3D-WAVE is designed to simulate the transformation and

propagation of "random, short-crested, wind-generated waves in coastal waters" (Rego et al. 2011).

Based on the results of the oceanographic modeling, each of the study areas experienced some degree of maximum scour during recent hurricane events (Table 2.2). Sediment porosity and plasticity were not measured for the datum sites; therefore, to provide a range of expected conditions, both a loose and consolidated bed scenario were modeled for the specific grain sizes found at each sample site located within the study areas. For loose bed scenarios, maximum scour was reduced by between 70% and 91% following sediment redeposition (calculated 7 days after each modeled storm and reported as "net" scour; Table 2.2).

Table 2.2 Scour Estimates Based on Oceanographic Modeling

Hurricane	Bed Scenario	Scour Type	Study Area	
			High Island	Galveston
Ike	Loose	Maximum	1.0 m	1.3 m
		Net	30 cm	30 cm
	Consolidated	Maximum	0.2 cm	0.24 cm
		Net	0.03 cm	--
Rita	Loose	Maximum	84 cm	60 cm
		Net	10 cm	+ 5 cm
	Consolidated	Maximum	0.2 cm	0.10 cm
		Net	~ 0 cm	--

At the Galveston datum, sediment redeposition resulted in net sediment accretion. This datum was the only site to display accretion following a hurricane event. Under consolidated bed scenarios, maximum scour was reduced by 85% to 99% following sediment redeposition (Rego et al. 2011). Hurricanes have the potential to cause seafloor scour above a potentially preserved landscape feature. In some cases, sediment resettles on the seabed, resulting in a reduced amount of net scour over the feature. Depending on the depth of burial of a specific feature below the

modern sea-floor the feature may be protected from both long-term processes and extreme punctuated scour events.

2.4 Summary

Lowered sea-levels during the Late Wisconsinan transformed the OCS from a marine environment to a subaerial plain entrenched by numerous river channels. As sea-level began to recede following maximum glacial conditions, these same rivers retreated backwards up the shelf, changing freshwater systems to brackish lagoons before finally reverting to open marine systems. Evidence of the former landscape was buried underneath these lagoons and estuaries, the overlying sediment serving as a protective sediment layer during shoreline transgression and, in some cases, subsequent storm events. Geologic studies suggest that Pleistocene surfaces exposed as dry land on the OCS are buried under thin veneers of recent sediment in the northwestern GOM. Investigations into sediment scour during extreme storm events indicate that storm-induced scour may be followed by redepositon of sediment, resulting in minimal net scour, or in some cases net sediment accretion. Geographical, operational, and modified environments may lie preserved on the OCS at depths accessible to researchers.

CHAPTER 3. MATERIAL CULTURE AND THE PHYSICAL LANDSCAPE

The formerly subaerial outer continental shelf defines the geographical as well as temporal setting for this study. Based on a range of sea-level curves, the modern shoreline position was reached by approximately 4,000 years BP at the latest, or as early as 6,800 years BP (as shown in Chapter 2, Figure 2.6), by which time the OCS had been completely transformed into an open marine environment. The establishment of the modern shoreline serves as a *terminus post quem* for occupation of the OCS, which correlates with the Archaic cultural period. Sea-level lowering during the most recent glaciation, the Late Wisconsin, started as early as 35,200 years BP (Frazier 1974:10), predating any known occupation of North America. Previous estimates for the arrival of humans into North America adopted a terminus ante quem of 11,500 years BP. However, increasing numbers of older sites are being identified that preclude a precise *terminus ante quem* (e.g., Erlandson et al. 2011; Waters et al. 2011).

3.1 Defining the Temporal Period of Interest

In searching for archaeological landscapes on the OCS the dates of subaerial exposure, and therefore the potential for human landscape exploitation, must be correlated with the dates of known occupations within the region. A fundamental question in archaeology is the timing of the arrival of North America's first inhabitants and their route of entry into and across the landscape.

The peopling of the New World is a complicated topic in which hypotheses have been tested and, in some cases, revised in light of new evidence. As a science, archaeology is restricted to the data that have been found. Researchers must be ready to account for newly discovered data that can, and have, challenged the dominant paradigm. As discussed in the previous chapter (Chapter 2. Physical Landscape), the landscape of the present-day northwestern Gulf of Mexico region has changed significantly since the last glacial maximum. The coastal margins and modern shorelines are very different than when the first inhabitants entered North America. Current models of early prehistoric population density, subsistence, and interaction are based on evidence found from inland terrestrial settings, where artifact preservation rates have in many cases restricted the archaeological record to discussions of stone tools. Keeping in mind the

diachronic landscape, significant portions of the coast have been altered by sea-level rise and associated landscape changes have contributed to a potentially biased archaeological record. What is known is that while modern humans have been in the Gulf of Mexico region since approximately 11,000 BP (Ricklis 2004; Rees 2011), new discoveries continue to push back the dates for potential occupation (e.g., Waters et al. 2011).

3.2 Migration Routes and Dates

One of the most prevalent hypotheses, and for a time the only accepted theory, for the peopling of the New World argued that the first Americans walked across the Beringea land bridge during the last glacial maximum, and populated the New World at approximately 11,000 years BP (Bonnichsen and Lepper 2005; Meltzer 2009:3). Consensus could not be reached in explaining how those early inhabitants spread from what is now mainland Alaska throughout the remainder of the western hemisphere (e.g., Wendorf 1966; Fladmark 1979; Dixon 1999). Further complicating the question of modern human's first arrival in the New World are the increasing numbers of archaeological sites that pre-date 11,000 BP.

Early archaeological sites (older than 11,500 BP) were once considered to be anomalous. Absolute dates, stratigraphy, and site integrity were, and continue to be closely scrutinized. In the case of Monte Verde, Chile, one of the first sites to return anomalously early dates, the occupation dates were highly disputed, and subjected to intensive scrutiny by a multi-disciplinary panel of over 40 specialists in 1997 (Bonnichsen 2005:15). The findings of the panel, which included several staunch critics of the site, validated some of the dates for Monte Verde and were cited as evidence that the hypothesis of the Bering land bridge as the first and only migration route was inaccurate (Bonnichsen and Lepper 2005:15).

Archaeological sites such as Meadowcroft Rockshelter (Pennsylvania), Monte Verde (Chile), the Debra L. Friedkin site (Texas), and the Channel Islands of California have produced absolute dates that indicate the presence of modern humans much earlier than 11,000 years BP (Table 3.1; Bonnichsen et al. 2005; Goebel, Waters, and O'Rourke 2008; Erlandson et al. 2011; Waters et al. 2011). Evidence from these and other recently published sites continues to push back the date range for possible occupation of the western hemisphere before 12,000 years BP. Despite

uncertainly over the origin and location of the first Americans, evidence to date demonstrates that humans occupied the Gulf of Mexico's present coastal areas by approximately 11,500 BP (Gagliano 1967; Aten 1983; Neuman 1984). Identified as Paleoindians, these early inhabitants left minimal evidence of their presence and culture.

Table 3.1 Chronology of Archaeological Sites with Absolute Dates Greater than 12,000 BP.

Site	Location	Method	Dates	Source
CA-SRI-512	California	N/A	11,200 – 12,200	Erlandson et al. 2011:1181
Daisy Cave	California	C^{14}	11,950 – 12,780 cal BP	Rick, Erlandson, and Vellanoweth 2001:598
Paisley Caves	Oregon	C^{14}	12,300 RCYBP	Gilbert et al. 2008:786
Page-Ladson	Florida	C^{14}	12,480 BP	Faught 2008:675
Monte Verde II	Chile	C^{14}	12,500 BP	Bonnichsen and Lepper 2005:14
Meadowcroft Rockshelter	Pennsylvania	C^{14}	12,000 – 15,000 BP	Adovasio and Pedler 2005:26
Miles Point (18TA365)	Maryland	C^{14}/ OSL	13,200	Lowery et al. 2010:1472
Debra L. Friedkin (41BL1239)	Texas	OSL	13,200 – 15,500	Waters et al. 2011:1599
Topper (8AL23)	South Carolina	OSL	15,200 +/- 1,500 cal BP	Goodyear 2005:107
Cactus Hill (44SX202)	Virginia	C^{14}/ OSL	15,000 – 17,000 RCYBP	Goodyear 2005:107

3.3 Material Culture and Paleoindian Subsistence

Projectile points and other lithic tools often are used as proxy indicators of subsistence strategies. Subsistence strategies are a complete cultural package, incorporating environmental variables such as climate and available natural resources, or the operational environment, to create a culture's unique way of life, or more specifically the foods that prehistoric people ate, the tools and techniques used to acquire those resources and manipulate them into edible food (Price and

Feinman 2008:26). Paleoindians were the first cultural group to occupy North America. They are routinely described as nomadic hunter gatherers who subsisted on large herbivore game animals, or megafauna (Milanich 1994:38). The early Paleoindian diet probably consisted of a variety of terrestrial game animals such as mammoth, bison, caribou, and elk, and gathered foods such as berries, nuts, seeds, roots, smaller game animals, and fish (Kelly and Todd 1988:233). Kelly and Todd (1988) have referred to early Paleoindian populations as "high technology foragers" who relied primarily on faunal food sources. Based on archaeological evidence recovered to date, early Paleoindian groups were sparsely located within North America. They probably lacked local knowledge of new floral food resources during migration, suggesting a primary dependence on hunting. Early Paleoindian subsistence lacked geographical specialization, since low population densities allowed groups to utilize large hunting ranges (Anderson 1996; Kelly and Todd 1988; Milanich 1994).

In the southeastern United States, Anderson (1996:32-34) states that Paleoindians initially utilized a generalized foraging strategy with a preference for hunting and frequent changes in hunting radii. Therefore, Paleoindians did not stay in any given place for extended periods of time. This subsistence system resulted in scattered sites of low density. He further argues that this pattern was likely true of earlier initial occupations. The mobile lifestyle associated with this type of subsistence is supported by the Paleoindian archaeological record. As noted by Kelly and Todd (1988:235), the artifact assemblage of early Paleoindians included several similar artifact types, such as scrapers, beaked gravers, and bifaces with little regional variation. This lack of regional types led Kelly and Todd (1998:235) to suggest that Paleoindians across different environments lived a relatively similar lifestyle. Similar Paleoindian artifacts have been identified from areas across the United States, spanning various ecosystems. According to Milanich (1994:48), many of these stone tools were unifacial, and likely served multiple purposes. People may have found travel easier with a smaller number of general purpose tools as opposed to a greater number of highly specialized tools.

According to Anderson (1996:50) bands of Paleoindians became "place-oriented" once they found resource rich areas where they could stage hunting trips from, creating a locus for their subsistence range. The establishment and use of large staging areas contributed to the

development of regional traditions observed within later Paleoindian assemblages (Anderson 1996:50). Subregional specializations likely developed due to differences in resource base, local climate, and physiography (Anderson 1996:51).

In the Gulf coast region, archaeologists have found evidence of subregional adaptations in later Paleoindian subsistence strategies, probably necessitated by local climate fluctuations (Milanich 1994:40). One such example is the oasis model (Dunbar and Waller 1983; Dunbar 1983, 1991), which shows an adaptation to specific fresh water sources such as tertiary karst sinkholes and shallow lakes in the dry, arid Florida interior. Paleoindians exploited the sinkholes and lakes, not only as their own freshwater source, but also as hunting sites, since game animals utilized the same water sources (Milanich 1994:41). As of 1994, Milanich reported that 92% of all diagnostic Paleoindian artifacts found in Florida were recovered from the tertiary karst regions. This finding has profound implications for the Paleoindian archaeological record in Louisiana and Texas, where freshwater sources, such as rivers, have experienced significant alteration. Modern shoreline positions were reached approximately 6,800 to 4,000 years ago, based on the sea-level curve presented in Chapter 2 (Figure 2.6). Given that prehistoric peoples were known to have been in the Gulf region since at least 11,500 years BP, areas of the now-submerged OCS may have been inhabited by Paleoindian and even Archaic period peoples.

Paleoindians did not live within modern political boundaries. Since much of the information in the archaeological record is generated through state-permitted activities and NHPA-compliant surveys, the data needed to address this time period often are organized by, and classified within state boundaries (Table 3.2). Typologies and cultural chronologies may be developed on a state or micro-regional basis. In reality, these early inhabitants were located across modern geographical boundaries.

Table 3.2 Comparison of Early Cultural Periods in the Northwestern Gulf of Mexico Region

Louisiana		Southeast Texas	
Middle Archaic [a]	7950 – 3950 BP	Archaic Coastal [b]	5000 – 2200 BP
Early Archaic [a]	9950 – 7950 BP	Archaic Inland [b]	8000 – 1500 BP
Late Paleoindian [a]	10750 – 9950 BP		
Middle Paleoindian [a]	11450 – 10750 BP		
Early Paleoindian [a]	13450 – 11450 BP	Paleoindian [b]	11,500 – 8000 BP
Sources: (a) adapted from Rees 2010; (b) Ricklis 2004			

3.3.1 Louisiana

Compared to other southeastern states, southern Louisiana has few Paleoindian archaeological sites. According to Rees (2010:40), the most well documented Paleoindian and early Archaic sites are located on Tertiary uplands. Landscapes in the west-central and northwestern portions of the state account for over half of all known Paleoindian sites in Louisiana. Paleoindian sites in southern Louisiana have been identified on Pleistocene surfaces. These sites include the remains of megafauna in the assemblage, such as the Salt Mine Valley site (16IB23), the Tapir site (16IB66), Côte Blanche Island (16SMY79), Trappey Mastodon (16LY63), and Above the Mastodon (16WF63) (Rees 2010:37).

The archaeological site at Avery Island (16IB23) has produced evidence of the earliest known occupation in coastal Louisiana. Avery Island (16IB23) is a large salt piercement dome located in present day Iberia Parish, in south-central Louisiana (Gagliano 1967:iii). As opposed to an island that is surrounded by water, the distinct vegetation and relative relief of the salt piercement domes creates a distinct boundary, separate from the surrounding swampy landscape (Gagliano 1964:1). Underlying salt deposits have uplifted localized areas of sediment, creating topographic highs with a maximum elevation of 46 m (152 ft) above the surrounding landscape (Gagliano 1964:1). The earliest evidence for human occupation at Avery Island dates to what was defined locally as the Early Recent Stage, 18,000 – 5,000 years BP, by Gagliano (1967:101). This period includes the entire Paleoindian period and part of the Archaic period as defined by Louisiana's cultural chronology (Table 3.2). Radiocarbon dates from excavations in 1968 provided absolute dates of 12,000 (+/- 400) BP and 10,900 (+/- 300) BP (Neuman 1984:63).

Fossils of Pleistocene megafauna, such as mastodon and giant bison were recovered from Avery Island deposits, suggesting an abundance of game animals utilizing the surrounding environment (Gagliano 1967:39). The interpreted hunter-gatherer populations present at Avery Island are believed to have visited the site seasonally. Artifacts include a small number of sharp-edged scrapers and cutters (1967:102).

Avery Island is one of few sites in Louisiana that links early Paleoindians with Pleistocene megafauna. At the Trappey Mastodon site, mastodon faunal remains including teeth and fragments of a mandible, scapula, and tibia were recorded *in situ* (Neuman 1984:65). Two corner-notched projectile points were also recorded at this site. However, there is no direct evidence that the projectile points were used to hunt, kill, or butcher the animal (Neuman 1984:65). Early Paleoindians in Louisiana, like most Paleoindians in North America, are described as hunter gatherers. There is limited evidence for Louisiana-specific subsistence systems. However, analogies with other early Paleoindian populations suggest that hunter gatherers exploited mastodon and *Bison antiques* (Rees 2010:37). Later Paleoindians in Louisiana became adept at hunting mammals such as deer (Neuman 1984:69). Despite the lack of direct evidence of Paleoindian and Early Archaic subsistence systems, archaeologists have created models of subsistence based on landscape reconstructions which detail the available fauna and flora, and correlating that information with archaeologically excavated tools that were used in food procurement and processing. This type of modeling can produce an accurate interpretation of subsistence systems because of the relationship between available resources and the technologies required to utilize and process them. As summarized by Gagliano (1984:26):

> … it is conceivable that a coastal system could have high biological productivity and produce a great annual yield of biomass, but this biomass may not be readily accessible to people living in the area there if their technology is inadequate to harvest or to utilize key species, or both.

Artifacts such as stone tools are commonly used to identify and differentiate prehistoric cultures due to their abundance in the archaeological record. Organic materials such as textiles, clothing, and food remains which could have identified specific populations often are not preserved within terrestrial settings, and are therefore unavailable as direct evidence. The Paleoindian and Early

Archaic cultural periods in Louisiana are therefore defined by their tool assemblages, which include projectile points such as Clovis, San Patrice, untyped lanceolate, Folsom, Plainview, Dalton, Pelican, and Scottsbluff. Tools were made from both exotic and local materials such as chert, petrified wood, and sandstone (Rees 2010:43-51). In prehistoric archaeology, an emphasis on stone tools, specifically projectile points, exists because these materials do not deteriorate significantly over time. In many cases, they are the only surviving artifacts at sites from early archaeological contexts (Young et al. 1994:209). Unfortunately, projectile points can and have been disarticulated from their archaeological context by any number of processes including erosion, fluvial migration and associated reworking, and human modification of the landscape (Schiffer 1987; Gagliano 1984). Due to significant modification of the southern Louisiana landscape by river channel migration, the geographical density of Louisiana's Paleoindian sites is more likely attributed to site preservation conditions in the north than occupation densities in the south (Rees 2010:51; Gagliano 1984:40).

Based on existing archaeological evidence, the Late Paleoindian period is characterized by a decrease in population mobility coupled with an increase in total population (Rees 2010:53). In the archaeological record, this increase in regionalization is demonstrated through the abundance of regional projectile point types, including bifurcate and stemmed points, and a decrease in the use of exotic materials in tool production (Rees 2010:54). The projectile points of the Late Paleoindian and Early Archaic periods generally were smaller, more complex technologies than those used by Paleoindians to hunt megafauna. The change in lithic technologies is generally attributed to climatic shifts from the last glacial maximum, which resulted in an abundance of smaller animals such as deer and fish that replaced megafauna as the primary subsistence (Rees 2010:54). Another reason for the diversification of projectile point types during the Early Archaic period, according to Rees (2010:57) was related to the manner in which projectile points were hafted, or fastened to spears, and used. The *atl atl*, or spear thrower, was first used in Louisiana during the Early or Middle Archaic periods (Rees 2010:67). Continuing through the Middle Archaic period, increasingly sedentary populations exploited more diverse resources such as aquatic resources and wild plants that could be gathered (Rees 2010:60). Middle Archaic subsistence adaptations appear in the archaeological record in the form of increased types of stone tools, including manos, metates, abraders, and mortar and pestles used to process plant

foods. Other significant adaptations include the development of intensive middens and human burials (Rees 2010:59-60).

3.3.2 Texas

As is the case in Louisiana, few Paleoindian sites have been identified along the coastal regions of southeast Texas. Most of the early Paleoindian sites in this region are found within or associated with stream drainage areas (Stright 1986; Ricklis 2004:184). According to Ricklis (2004:184), the majority of recovered Paleoindian points were created from high-quality lithic materials that are exotic to southeast Texas, suggesting that early populations introduced these materials to the coastal region through migration or trade.

One of the earliest sites in southeastern Texas, McFadden Beach (41JF50), contains a large quantity of early Paleoindian projectile points. McFadden Beach is a 32-kilometer area along the modern Texas coast in Jefferson County, located west of Sabine Pass (Stright 1999:2). Eustatic sea-level rise and a lack of modern sediment have resulted in beach erosion revealing artifacts that date from the Paleoindian period through to the historic era (Stright 1999:5). Although the primary depositional sites are gone, the artifacts and their secondary context have been studied by amateur and professional archaeologists since the 1970s (Stright 1999:10). According to Stright (1999:15) the area surrounding McFadden Beach was an upland ridge above the now-relict Sabine River valley during lower sea-level stands, approximately 11,500 years BP.

Analysis of 880 artifacts recovered from the McFadden Beach site indicated that the largest single percentage of the assemblage, 43% of the total artifacts, dated to the Paleoindian period, 11,500 – 8,000 BP (Stright 1999:112). According to Stright (1999:112), the next time period most represented in the assemblage dated to the Middle Archaic, 4,500 – 1,300 BP. The majority of the artifacts recovered from the McFadden Beach site were identified as projectile points (Stright 1999:115). McFaddin Beach is an impressive, but unusual, assemblage. The majority of Paleoindian sites in southeastern Texas, particularly along the modern coast, consist of isolated finds or scatters, such as site 41GV101. This site is located off the coast of Bolivar Peninsula near Crystal Beach and consisted of a single Clovis point (Texas Historical Commission [THC] 1988). Archaeologists have historically placed great emphasis on the

correlation between projectile point types and game animals when modeling prehistoric subsistence strategies. Early models showed a continuum within the Paleoindian period in which Clovis mega-fauna hunters transitioned to Folsom bison-hunters, becoming generalized hunter gatherers in the Archaic period (Bousman et al. 2004:75). In this same vein, lanceolate projective points were universally attributed to big game hunting (Bousman et al. 2004:75).

Supplemental evidence from faunal remains suggests that the correlation between game size and projectile point type is oversimplified. Faunal evidence from Texas sites such as Aubrey, Lubbock Lake, and Lewisville suggests a broader range of game animals that included megafauna, such as mammoth, camel, horse, bison, and giant armadillo, and smaller vertebrates and invertebrates, including fish, turtle, alligator, deer, and rabbit (Bousman, Baker, and Kerr 2004:75). As is the case in Louisiana, stone tools provide evidence of subsistence systems, and offer insight into specific activities. Due to the abundance of lithic tools, Paleoindian sites in Texas have been subdivided into three types: food procurement or consumption sites; butchering or processing sites; and campsites (Bousman, Baker, and Kerr 2004:76-78). Contrary to the idea of Paleoindians as exclusively big game hunters, some archaeologists hypothesize that prehistoric populations that occupied what is now classified as the modern coastal zone exploited estuarine resources (Evans and Keith 2011a:166-167). According to Newcomb (1961:329), Paleoindian and Early Archaic populations exhibited some maritime adaptations, but maintained ties with inland populations rather than adopt a completely maritime subsistence. Aten (1983:11) developed a similar interpretation of coastal Texas' prehistoric populations, stating:

> … to suggest that the peoples of the upper coast were adapted to maritime life is to substantially stretch the point; a much more appropriate descriptor is strandlooper, as South African coastal scavenger-hunter-gatherer-collectors are commonly called.

3.4 Modified Environments as Evidence of Human Occupation

The Pleistocene landscapes on the OCS were created through episodic changes in environmental conditions at both the regional and local scales, beginning in the late Quaternary and extending into the Recent and Holocene periods (Hill 2007:13). Humans, however, do not merely live on a landscape. Humans actively modify their landscape, matching their subsistence objectives with

available resources, and modifying natural processes to better meet their needs (Butzer 1982:32). As previously discussed, the lithic record of Paleoindians and Early Archaic populations demonstrates a growing specialization within the form of projectile points. This pattern has been interpreted as a change in hunting patterns from megafauna to smaller game animals coupled with increasing resource diversification. Environmental evidence from this same time period indicates a changing climate, suggesting that early inhabitants adapted their subsistence systems to take advantage of the changing conditions.

The climate of North America at the end of the last glacial maximum (LGM) was largely controlled by the presence of the Cordilleran and Laurentide ice sheets, which altered prevailing weather patterns by shifting circulation patterns to the south, causing a southward shift of climate zones (Burroughs 2005:78-79). The Gulf of Mexico experienced less of a decrease in temperature than waters closer to the ice sheets, resulting in an exaggerated temperature gradient from north to south across the United States (Burroughs 2005:79,99). Northern Florida and the Gulf coast experienced conditions more commonly found across modern southern New England; faunal evidence indicates average July temperatures in southern Missouri during the Heinrich 2 event were 10 – 12 degrees C lower than at present (Burroughs 2005:99).

According to Burroughs (2005:82), temperature fluctuations related to the last glacial maximum had a significant impact on local populations, especially cooling temperatures associated with Heinrich events that likely rendered large portions of the northern landmass inhospitable to human habitation. Warming occurred between 10,000 and 8,200 years ago, resulting in increased precipitation out of the Gulf of Mexico during summer (Burroughs 2005:183). Conditions in the Gulf coastal regions of Mexico were conducive to wild plant use and land clearance (Pohl et al. 2007). Human adaptation to climate shifts at this time period include nascent plant cultivation and domestication, with the earliest dates for domesticaton of maize (*Zea mays*) by 9,100 years BP (Pohl et al. 2007:6870); other cultigens such as squash (*Cucurbita pepo*) developed between 9,000 and 7,000 years BP (Story 1985:37-38; Galinat 1985:247). Evidence of cultivation is found in preserved pollen grains, but these are not the only ecological evidence of human landscape manipulation. Anthropogenic fires have been studied through analyses of charcoal and pollen (Fowler and Konopik 2007:165).

Fire was used for several purposes in the Gulf coast during the Paleoindian and Early Archaic periods. While it can be difficult to differentiate lightning-induced fires from anthropogenic, fire is associated with Paleoindian game hunting, during which fires were used to create barriers, forcing game animals into areas more conducive for capture (Fowler and Konopik 2007:166). Fire also was used to clear landscapes in the fall and winter, encouraging pioneer plant species or species associated with secondary succession. Collection of nuts was facilitated by landscape clearance (Fowler and Koponik 2007:166). During the Early Archaic period, fire was still used in hunting, but was applied in indirect ways. Rather than creating barriers to trap game animals, Early Archaic populations used fire to burn areas within the landscape, maintaining habitats that were attractive to specific game animals (Fowler and Koponik 2007:166-167). Landscape clearance through burning, occurring most often in the fall and winter months, created larger areas for seasonal gatherings of several small bands (Fowler and Koponik 2007:166).

Conclusive evidence of human habitation does not rely solely on the presence of anthropogenic artifacts. Evidence of anthropogenic landscape manipulation in the form of species selection or landscape clearance may be found within sedimentary strata (Thomas 1989:314-315; Hill 2007:6-7). A 1982 study by researchers with Coastal Environments, Inc., conducted on behalf of the National Park Service, examined sedimentary signatures of anthropogenic activity within terrestrial sites along the northwestern Gulf of Mexico. In some cases macro-sedimentary characteristics can be identified from physical samples, such as the presence of exotic shell in a non-natural habitat, or an abundance of worked shell, or unnaturally large percentages of a specific shell type or size (CEI 1982:53). Signatures of fire can be identified beyond the presence of charcoal. Chemical alteration of sediments, such as oxidation of clays, or particularly the presence of baked clay, have been cited as indicators of human activities (CEI 1982:90). Areas of crushed shell, or mechanically packed sediment may indicate an intensive activity area (CEI 1982:90). Depending on the type of sampling conducted, artifacts may not be collected from formerly subaerial landscapes on the OCS. However, their absence does not preclude the ability to identify areas of potential human occupation or activities.

3.5 Prehistoric Occupation Potential in the Coastal Zone

Subsistence strategies are intrinsically linked to site location; the variables incorporated into a specific subsistence strategy can be used to delineate areas of probable site location or interaction. McFadden Beach and Avery Island are located along and near the present-day shoreline. Reconstructions of the shoreline position 11,000 years ago indicate that McFadden Beach was located in a woodland environment. Avery Island was at the boundary between the woodland and coastal zones (Aten 1983:145). This distinction is important because models of prehistoric populations in the northwestern Gulf coast area have stated that the highest population densities are located in the deltaic and littoral zones (CEI 1977:314-324; Aten 1983:138). If population densities are greatest near the shoreline, then a larger density of sites should be expected where the deltaic and littoral zones occurred during lower shoreline positions, areas that are presently underwater.

Reviews of prehistoric settlement patterns indicate a prehistoric preference for the coastal zone (Aten 1983; Westley and Dix 2006). In terms of locating Gulf coast Paleoindian or Early Archaic sites this finding is an important point. Any definition of "coastal zone" implies a temporally constrained period during which terrestrial and marine processes interact within a given area (Masselink and Hughes 2003). What was the coastal zone at the time of possible Paleoindian and Early Archaic occupation, is now located underwater, having been submerged during sea-level transgression related to climate changes at the end of the last glacial maximum (CEI 1977; Faught and Donoghue 1997; Pearson et al. 1986; Stright 1986). According to Aten (1983), prehistoric population density increases from the woodland, into the prairie setting, and is highest in the coastal zone. This finding would suggest that a search for evidence of Paleoindian culture would be most successful in the areas with the highest density at the time of occupation.

As discussed in Chapter 2, geographical environments, and potentially prehistoric archaeological sites, may have survived sea-level transgression. Previous studies have demonstrated the potential for offshore submerged archaeological site preservation in the northwestern Gulf of Mexico region (CEI 1977; Pearson et al. 1986). Investigations in other parts of the world have

identified prehistoric sites in submerged offshore contexts (Masters and Flemming 1983; Benjamin et al. 2011; Evans et al. [n.d.]).

CHAPTER 4. SUBMERGED PREHISTORIC ARCHAEOLOGY AND THE GOM

Interest in the geology of continental shelves often is inter-related with economic development. In the Gulf of Mexico, recoverable oil and gas reserves located offshore have instigated research in aid of energy extraction industries. Open water oil and gas drilling began in the 1890s, with drilling rigs built on piers extending from the shore (Evans and Keith 2011b; National Commission 2011). In 1937, the world's first freestanding drilling structure was built in the Gulf of Mexico (GOM). The structure was located one and a half miles from shore in approximately 14 feet (4.3 meters) of water (National Commission 2011). In 1947, the first successful well was drilled out of sight of land, approximately 10.5 miles (17 kilometers) offshore of Louisiana, in 20 feet (6 meters) of water (National Commission 2011). Geologic and geophysical studies were necessary to identify oil and gas fields, as well as to determine if near-seafloor sediments were stable enough to support installation of pipelines and placement of drilling rigs. While much of the GOM geologic and geophysical research has been published, more exists as grey literature reports, including studies conducted by oil and gas operators and studies funded by the US government in efforts to manage oil and gas operations.

In the United States, oil and gas industry activities on the outer continental shelf (OCS) are regulated by the US Department of the Interior's (USDOI) Bureau of Ocean Energy Management (BOEM) and Bureau of Safety and Environmental Enforcement (BSEE). As discussed in Chapter 1, BOEM/BSEE have a responsibility under the NHPA to consider the impacts of federal undertakings on cultural resources within the area of potential effect. From the first NTL in 1974, survey guidelines addressed both the presence of historic shipwrecks and submerged prehistoric sites on the continental shelf, requiring archaeological assessments prepared by a qualified marine archaeologist in order for an operator to obtain approval to drill a well, or install a pipeline.

4.1 Developing a Predictive Model for Submerged Site Location

To develop accurate survey guidelines and assessment requirements, the National Park Service (NPS) funded a study in the early 1970s to determine the archaeological potential of the GOM OCS. The final report divided the results between prehistoric potential for sites on the now-

submerged portions of the OCS (Vol. 1), and the potential for historic shipwrecks (Vol. 2) (CEI 1977). The goals of the study included development of a predictive model for the identification of the most likely resources to be found on the OCS, and the highest probability areas for the occurrence of these resources. The methodology outlined by the authors was one of the earliest publications specific to submerged archaeological landscape research, and their recommendations still serve as the basis for methodologies used in modern studies.

The predictive model developed by researchers with Coastal Environments Inc., or CEI, (1977) began with the identification of distinct geologic systems and features found within each discrete region of the GOM, from the Rio Grande to the Florida Keys, with a focus on Late Quaternary formations. Sea-level position, including fluctuations, climate changes, and geologic history were then correlated with each type of geologic feature in order to determine the likelihood of preservation through to the modern period. Landforms with the highest rates of predicted preservation were then correlated with similar landforms in modern terrestrial settings to determine any association with archaeological sites or prehistoric human habitation. According to the study's authors, prehistoric cultural resources do not occur randomly, and their results argued for correlations between specific landform types and artifacts or other evidence of past human behavior (Table 4.1; CEI 1977:331). The authors then made correlations between types of landforms and the effectiveness of different survey techniques in identifying these same features in submerged contexts.

Table 4.1 Correlation of Terrestrial Landforms, Cultural Period, and Effectiveness of Survey Techniques

Landform	Cultural Period		Survey Effectiveness	
	Early Archaic	Paleoindian	Subbottom Profiler	Piston Corer
Quarry Sites	V	V	Low	Not effective
Salt Dome Sites	V	V	High	Medium
Spring/Sinkhole Sites	V	V	High	Medium
Valley Margin Sites	V	P	Low	Not effective – Low
Natural Levee Sites	V	V	High	Not effective – Low
Point Bar Sites	V	V	High	Not effective – Low

(Table 4.1 continued)

Landform	Cultural Period Early Archaic	Survey Effectiveness Paleoindian	Landform	Cultural Period Early Archaic
Bay Margin Sites	V	V	Low	Not effective – Low
Coastal Dune Lake Sites	V	V	High	Medium
Shell Middens	U	U	High	Not effective
Key: V (verified or known correlation); P (probable correlation); U (unknown)				
Source: CEI 1977:333,340				

The CEI (1977) study examined geographical environment across the entire GOM. However, not all of the recommendations are applicable to all environments. The authors suggested that any investigation of submerged prehistoric resources take a three-step approach beginning with remote sensing of the area through either small-scale bathymetry or subbottom profiling to resolve the upper 9 m (30 feet) of sediment coupled with acquisition of a grab or drag sample of seafloor sediments (CEI 1977:341). If a probable site was indicated by the data acquired in Step 1, then subsequent data should be collected, either in the form of side scan sonar imagery of the area, bottom cores, and or additional grab or drag samples (CEI 1977:341). The final step, if warranted, was recommended as underwater photography/videography, box core sampling, and or diver investigation (CEI 1977:341). The majority of the recommendations, such as bathymetric survey or diver photography, assume that the landform is exposed at the seafloor, which is appropriate for the northeastern GOM, where, for example, sinkholes and river channels are readily apparent on bathymetry and side scan sonar data due to the underlying karst formations (Faught and Donoghue 1997; Adovasio and Hemmings 2011). Based on geologic reconstructions of sea-level rise at the end of the last glacial maximum (Chapter 2) methodologies used in the northwestern GOM must assume that relict landforms such as those specified by CEI (1977) will be buried below the modern sediment and not readily apparent at the seafloor.

The methodologies created as a result of this study were developed for use on landforms identified as correlating with archaeological sites through construction of a predictive model for

site occurrence. While the predictive model isolated landforms and general areas for research, the cultural groups included within this model were highly-mobile hunter gatherers with scant material culture (Aten 1983; Neuman 1984; Ricklis 2004). The predictive model included geological reconstruction and landscape change modeling, but recognized that a paucity of artifacts would likely exist at submerged sites. Cultural signatures of human occupation were therefore identified that went beyond artifacts, such as potsherds and lithics, to include signatures more likely to be recovered in core samples, such as shells, faunal fragments, black earth, burned rock, charcoal, and pollen (CEI 1977:172).

In the thirty years since the creation of the dominant archaeological site prediction and preservation model used in the GOM (CEI 1977), subsequent studies have been conducted worldwide that add to the theory and methodology of investigating submerged prehistoric sites.

4.2 Thirty Years of Submerged Prehistoric Archaeology

In 1981, in recognition of advances in paleocoastline reconstruction, archaeologists, anthropologists, geologists, and oceanographers were invited to participate in a symposium addressing Quaternary coastlines and prehistoric archaeology; the resulting papers were published in one of the first edited volumes on the subject (Masters and Flemming 1983). The participants in this symposium noted that, at that time, the majority of submerged prehistoric artifacts were the result of chance finds by recreational SCUBA divers, fishermen, or activities related to offshore construction (Masters and Flemming 1983:611). Site discovery, they maintained, depended on both physical preservation of the site and ease of detection (Masters and Flemming 1983:622). The participants presented diverse case studies ranging in location from Siberia to Australia, but concluded that several methodologies could be universally applied to site prediction and detection. At minimum, local geomorphology has to be modeled to identify areas of probable feature preservation, recognizable features (such as shell middens) must exist, and an operational environment including basic requirements such as access to fresh water, protection from environmental exposure, and or availability of food (Masters and Flemming 1983:623). Recommendations for survey and identification of prehistoric features were similar to those outlined by CEI (1977): chiefly, bathymetric or subseafloor survey conducted at tight intervals (no greater than 150 m). The authors stressed, however, that this

type of survey cannot prove without doubt the existence of prehistoric sites, it can only identify the most probable areas in which sites could be preserved (Masters and Flemming 1983:624).

In 1982, Gagliano et al. published the results of a study that analyzed terrestrial analogues for potential offshore deposits. The results, developed under contract for the National Park Service, analyzed core samples from verified terrestrial prehistoric sites along the Gulf coast. Lab analyses of sediment core data indicated that the following variables were credible indicators of modified environment: grain size, pollen content, geochemical composition, point-counts, foraminifera species identification, and radiocarbon dating of appropriate samples (Gagliano et al. 1982). Recognizing that site identification could not be dependent upon the presence of man-made artifacts, the terrestrial corollaries were developed so that landforms could be tested for indicators of prehistoric archaeological site occurrence without the presence of obvious anthropogenic artifacts such as projectile points (Gagliano et al. 1982:115).

To test the effectiveness of the predictive model and recommended methodology proposed by the CEI (1977, 1982) reports, the MMS funded a study in the early 1980s, concentrated in the relict Sabine River Valley on the GOM OCS (Pearson et al. 1986). This area was identified as an ideal test area because of a wealth of pre-existing geologic data (e.g., Nelson and Bray 1970) and existing subseafloor surveys conducted on behalf of oil and gas operators and available to the researchers through the funding agency (Pearson et al. 1986:xix). Eight (8) targeted areas were selected for inclusion in the project based on a review of existing shallow high resolution seismic data, and then subjected to tight interval seismic survey over the areas of interest to both relocate and further delineate the features of interest (Pearson et al. 1986:53-76). Survey grids were located in the Sabine Pass, High Island, and Galveston federal lease areas; current water depths in these areas range from approximately 8 m (27 ft) to 16 m (54 ft) and are referenced to MLLW (NOAA 2006). Vibracores were acquired from five (5) of the surveyed areas, including Sabine Pass blocks 3, 6, and 9, and High Island Area blocks 18 and 49; cores measured 12 m (40 ft) in length. The cored areas ranged in water depth from approximately 8 m (27 ft) to 12 m (40 ft) in depth (NOAA 2006). Vibracores were planned for additional areas but adverse weather conditions precluded further coring operations. The collected cores, 76 in total, were subjected to a series of laboratory analyses in efforts to identify potential signatures of anthropogenic

activity (Pearson et al. 1986:76-80), as identified by the Gagliano et al. (1982) study. No artifacts, or distinctly man-made materials were recovered within the cores, however two cored features included sediments exhibiting characteristics of archaeological deposits. One was interpreted as a possible shell midden, dating to approximately 8,055 +/- 90 BP and the second was interpreted as an area of burnt bone dating to approximately 8,500 BP (Pearson et al. 1986:xxiii,127-162). The study's authors were hesitant to identify the features as concrete evidence of human occupation, but stated "that they more closely resemble archaeological deposits than known natural deposits" (Pearson et al. 1986:162).

The results of the Sabine River Valley study supported the theories behind the predictive model created for use in the GOM, and demonstrated the complicated task of identifying discrete archaeological features from buried contexts offshore. The northwestern GOM is unique from other submerged prehistoric contexts in that archaeological data are not simply submerged, but also buried underneath a seafloor which gives little to no indication of the underlying features. Despite the identification of potential archaeological features in cores from Sabine Pass 6, no further sampling was conducted offshore for prehistoric archaeology in the northwestern GOM prior to the start of the current project.

The Sabine River Valley was not the only study to investigate submerged prehistoric resources. Numerous studies have been conducted around the world, but are distinct from the Sabine River Valley study in that these other sites are exposed at the seafloor, located in relatively shallow water depths, or some combination thereof (Johnson and Stright 1992; Browne 1994; Faught and Donoghue 1997; Momber 2000; Dix et al. 2004; Benjamin et al. 2011; Evans et al. [2013]). Some research projects have avoided the complications of working in submerged environments by using evidence from terrestrial contexts to address changes in human subsistence and coastal settlement patterns instigated by changing climate conditions (Bailey and Parkington 1988). Despite systematic studies and surveys though, a significant amount of data have been uncovered accidently, such as the Cinmar site off of the US Atlantic coast, which was recovered by a commercial dredging operation (Stanford and Bradley 2012). Estimates suggest that approximately 550 submerged prehistoric archaeological sites have been identified globally, dating from the Lower Paleolithic/Early Pleistocene periods, or within the last approximately 2.5

million years (Dix et al. 2004:5). This is contrasted with approximately 10,834 prehistoric sites recorded in the state of Louisiana alone (*Rachel Watson, LA Division of Archaeology, pers. comm.*).

Despite 30 years of research in locations ranging from Beringea to Argentina, the methodology used in submerged prehistoric research has remained relatively unchanged from the CEI 1977 recommendations. As outlined by Gaffney and Thomson (2007:4) the most common techniques used in the investigation of submerged prehistoric contexts include high resolution 2-D seismic (subbottom) profiling, high resolution 3-D seismic profiling, high resolution bathymetric mapping, and seabed sampling and shallow coring. The acquired remote sensing data or sediment samples/cores are then put into a locally specific context. These paleolandscape reconstructions remain critically dependent upon accurate understandings of sea-level, including isostatic and eustatic changes, and rates of sedimentation or erosion (Dix et al. 2004:13-30).

4.3 Submerged GOM Landscapes Methodology

In the GOM, the existing predictive model for submerged prehistoric site occurrence was created by extrapolating observed terrestrial settlement patterns onto the formerly exposed continental shelf. Additional data acquired since creation of the first predictive model (CEI 1977) have supported the hypothesis that prehistoric sites in coastal Texas and Louisiana occur near fresh water sources, and that inhabitants occupied or exploited landforms associated with fluvial systems, including naturally occurring levees and inset river terraces (Pearson et al. 1986; Ricklis and Blum 1997). For example, a regional survey of 23 terrestrial archaeological sites along coastal Texas resulted in an observable pattern of site location (Ricklis and Blum 1997). Archaeological deposits were identified on landward channel margins in close proximity to shorelines, but at elevations above the effects of surf zone dynamics that could potentially bias the archaeological record by eroding, reworking, or destroying sites before they could be preserved (Ricklis and Blum 1997).

Archaeological data are used to reconstruct patterns of past human behavior. After data have been located and documented, site level observations can be correlated with environmental climate reconstructions on the local, regional, and global scales to accurately identify cultural

chronologies and subsistence patterns (Thacker and Ellwood 2007). Land and water are both active mechanisms impacting the coastal environment, and influence long-term coastal archaeological site distribution patterns (Lewis 2000). Paleoenvironmental reconstructions depend upon both synchronic and diachronic processes. As discussed in detail in Chapter 2, synchronic reconstructions are used to develop a static landscape at a given point in time, determine when a potential area may have been subaerially exposed, and correlate that time period with possible occupations in the Gulf coast region. Diachronic reconstructions determine how the landscape changed over time, illustrating the geomorphological processes related to site inundation, and identifying key processes impacting site preservation potential. Both of these models are essential for determining if a geographical environment may contain *in situ* archaeological deposits (Waters 1992).

Archaeologists have hypothesized that offshore sites are most likely to be preserved by sediment deposition related to a low energy environment that covers the site prior to transgression of the high energy surf zone. According to Pearson et al. (1986) prehistoric sites have the highest probability for preservation when they are located within, or underneath, the estuarine transgressive zone in channel features and channel fill (Figure 4.1). Prehistoric sites on the offshore continental shelf may also be preserved when they are buried by sediments in a low energy environment prior to sea level rise and subsequent marine inundation, such as sites located on floodplains and inset river terraces (Pearson et al. 1986; Stright 1986; Lewis 2000). According to Waters (1992:279), Quaternary archaeological deposits on the continental shelf are most likely to be preserved within drowned river channels below the ravinement surface (Figure 4.2). For use in this archaeological study, the "ravinement surface" is defined as the erosional unconformity that marks the maximum depth of transgression-related disturbance (Waters 1992:277).

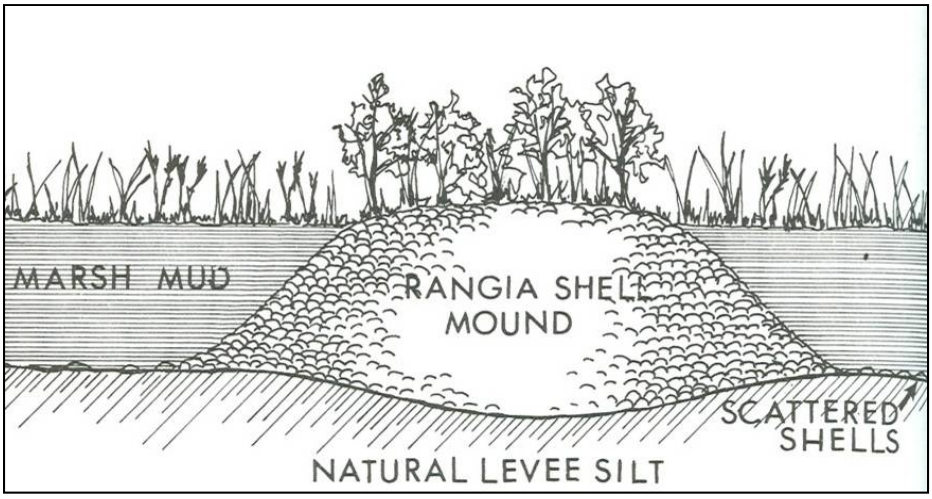

Figure 4.1 Archaeological site buried by and preserved within estuarine sediments (CEI 1977).

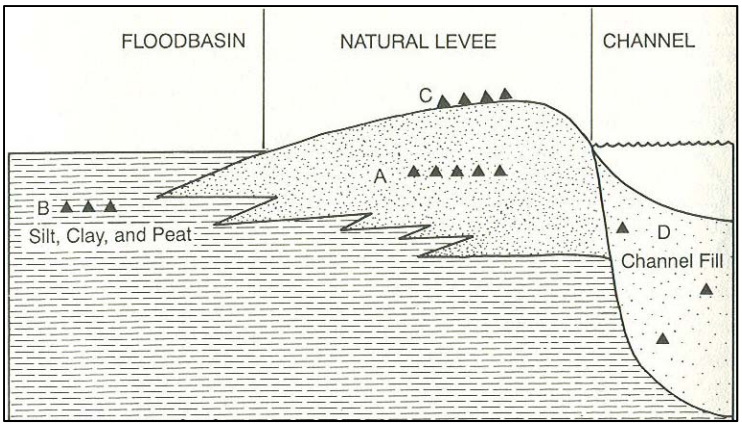

Figure 4.2 Hypothetical model of prehistoric archaeological sites associated with a channel feature. Sites are located (A) interbedded in levee sediments, (B) within floodplain sediments, (C) on the natural levee surface, and (D) within the channel fill (Waters 1992:142).

The typical method for determining site preservation potential for submerged prehistoric sites calculates the maximum depth of erosion and scour in relation to the depth of the potential feature below the seafloor and the thickness of any protective sediment overburden. Archaeological site formation processes are well documented for different terrestrial landforms (e.g., Schiffer 1987), but few quantitative studies have been published for submerged archaeological sites (Muckelroy 1976; Quinn 2006; Evans et al. 2012). Notable exceptions include studies conducted in areas dominated by sand and gravel, which do not compare with the

behavior of silts and clays like those found on the northwestern GOM OCS (Quinn et al. 1997; Quinn 2006). In the submerged environment, hydrodynamic and physical site formation processes have been quantitatively modeled as they pertain to historic shipwreck sites (McNinch, Wells, and Trembanis 2006; Foecke et al. 2010). McNinch, Wells, and Trembanis modeled the environmental characteristics and geomorphology of the Beaufort tidal inlet in North Carolina, site of the 18th-century shipwreck interpreted as Blackbeard's flagship, *Queen Anne's Revenge*. They modeled wave height and direction, wave-driven and mean current, and sediment transport in order to determine effective rates and depth of scour (McNinch, Wells, and Trembanis 2006). The goal of this project was to determine effective management strategies for the wreck site, and to assess the potential for artifact movement within the site matrix. The lack of quantitative studies for submerged prehistoric site formation processes is likely attributed to the lower number of confirmed sites as compared to shipwrecks.

The study conducted at Beaufort Inlet highlights a fundamental challenge for archaeologists attempting to study submerged prehistoric site formation. In the Gulf of Mexico region, prehistoric sites would have been in place and impacted by any combination of physical processes during sea-level rise including, but not limited to: deposition of sediment overburden; erosion by lateral migration or channel avulsion; scour within the high energy surf zone; and storm surge (Waters 1992). Essentially, submerged prehistoric sites form from the bottom up; the sites are already in place and the water rises over the top of them. This is fundamentally different from historic shipwreck sites, which form from the top down as the materials are introduced to the seabed and become incorporated into the site matrix (McNinch, Wells, and Trembanis 2006; Muckelroy 1978; Stewart 1999; Stanbury 2003). An understanding of submerged prehistoric site formation processes in the GOM region depends upon an explicitly geomorphological and geoarchaeological approach. Initial surveys for prehistoric sites offshore will predominantly rely on limited testing, such as the extraction of sediment cores; therefore sediment analyses must be utilized which can correlate offshore sediments with local climate changes, and potentially, absolute dates for sea-level rise (Pearson et al. 1986; Stright 1986).

It has been argued by CEI (1977), Gagliano et al. (1982), Pearson et al. (1986), Stright (1986, 1991), Waters (1992), and Faught and Donoghue (1997), among others, that more information

concerning the earliest Gulf coast inhabitants may be preserved on portions of the now submerged offshore continental shelf. The predictive model and methodology in use since the late 1970s appears to remain valid, with some minor adjustments based on new research.

4.4 Towards an Updated Predictive Model

> If submarine archaeological sites are to be found … we must be able to predict the approximate location of sites so as to minimize the search area, and the conditions must be known which will maximize the chance of survival of material (Flemming 1983:138).

The existing predictive model for prehistoric archaeological resources in the northwestern GOM is fundamentally a spatial application of middle range theory in archaeology. The model is built upon the assumption that a pattern of site locations, constructed from data at what would have been inland sites, can be translated accurately to what was the coastal zone at the time of occupation. To date, no evidence has been found of marine exploitation by either Paleoindian or Early Archaic peoples in the northwestern GOM. The lack of marine exploitation is likely due to the fact that the evidence simply has not been found yet. Almost all archaeological evidence from the northwestern GOM has been recovered from terrestrial settings which were inland at the time of occupation, and does not represent evidence from what would have been contemporary coastal occupations. According to Dix et al. (2004:199), a fundamental assumption of predictive models is that settlement patterns are strongly influenced by environmental factors. Generally, predictive models include the following types of variables: topography, hydrology, geomorphology, available resources (food, water, raw materials), and social processes (symbolic, political, or economic) (Dix et al. 2004:201-202).

Synchronic reconstructions of possible site locations and diachronic reconstructions of landscape change in the GOM are both driven by and dependent upon an accurate understanding of sea-level change. Dated sediments or deposits from high probability landforms must correlate with both the date ranges of subaerial exposure, and potential human occupation in order to be viable locations for site occurrence. Correlations are created by scaling up site level data from a specific location to compare with regional or even global models of sea-level change and climate

trends. It is necessary to make a critical assessment of the validity and applicability of any sea-level data set used, as errors are known to occur in almost all data sets (Dix et al. 2004:208). To address the inherent errors within a given data set, a new sea-level range was prepared for this study (presented in Chapter 2), incorporating several locally-specific northwestern GOM sea-level curves and focusing on the minimum and maximum times of probable exposure, rather than a single curve of inundation.

Diachronic landscape reconstruction is related to site formation process modeling (Schiffer 1987). Qualitative models of underwater site formation have been developed by Muckelroy (1978), Stewart (1999), and Stanbury (2003) and include both cultural and environmental factors that can affect the sea bed at or near an archaeological site. Environmental processes of site formation include bioturbation, gravity, tides and currents, waves, seismic activity, sedimentary movement (e.g. mud flows), and regional climate (Stewart 1999). Waters (1992:278) modeled underwater site formation processes specifically related to prehistoric sites, and identified variables that encourage site preservation, including: the energy level of coastal processes and the depth of effective erosion; the cohesiveness of site matrix sediments; the amount of subsidence prior to inundation; the gradient of the continental shelf; tidal range; and sediment import and export. Transgressive shorelines also impact upstream river valleys, causing a shift to the entire system. Diachronic landscape reconstructions must recognize all potential sources of site preservation or erosion, including lateral fluvial migration, avulsion stages, and river valley entrenchment. One of the driving mechanisms of diachronic change in the GOM since the Late Pleistocene is sea-level change, reinforcing the need for a locally-accurate sea-level change data set.

The existing model for submerged prehistoric site occurrence and preservation used in the northwestern Gulf of Mexico was originally developed in 1977. Subsequent research on submerged prehistoric landscapes worldwide demonstrates that the basis of the GOM model is still valid, and represents basic methodology. Additional research in sea-level rise and climate change data from the last thirty years complements, rather than contradicts this model. New sea-level curve data specific to the northwestern GOM is the most important recent contribution to synchronic modeling of the region, as it allows archaeologists to best determine the time span

associated with final inundation. Previous studies have used a single curve, which may not account for local variability caused by subsidence or isostatic uplift. The expanded curve used in this study is not intended to produce an absolute date of final inundation, but for the purposes of archaeological inquiry provides the most likely periods of subaerial exposure therefore allowing the archaeologist to determine if the area is suitable for continued investigation.

Sediment analyses, such as those identified by Gagliano et al. (1982), are useful in identifying sediments that have been altered by anthropogenic activity, such as those within a midden. At issue in submerged prehistoric landscape reconstruction, however, is that cores or physical samples may not be from anthropogenic features, but the geographical environment on which those features are located. The ability to identify the climate, environment, and age of a given landscape is necessary before in-depth archaeological research can be justified at a given location offshore. Additional geophysical techniques, not included in the 1977 predictive model, are included in this research as a means identifying climate proxy indicators, sediment ages, and evidence of diachronic landscape change necessary for prehistoric site preservation.

CHAPTER 5. METHODOLOGY

Late Pleistocene and early Holocene landscapes on the outer continental shelf (OCS) in the northwestern GOM have been inundated by rising sea levels, and buried in place by associated sediment accretion. These geographical environments may contain evidence of operational and even modified environments related to Paleoindian and Early Archaic populations. Unlike submerged prehistoric sites in other parts of the world (discussed in Chapter 4), the emphasis in the northwestern GOM is not on artifacts or even sites, but rather on the identification of the geographical environments in which archaeological sites would have been located prior to sea-level rise. The first step in identifying and verifying these features, and any subsequent sites, consists of geophysical remote sensing, especially acoustic profiling, to identify subseafloor horizons and depositional events.

5.1 Geophysical Remote Sensing

All of the studies reviewed as part of this research include unanimous recommendations that remote sensing survey of the seafloor, either plan view or profile, shoud be the first step in examining submerged prehistoric features. Geophysical instruments that are routinely used in the search for terrestrial and submerged archaeological sites include both passive and active sensors (e.g., Herz and Garrison 1998:147; Benjamin 2010; Evans and Voisin 2011). In the search for buried prehistoric features in terrestrial contexts, subsurface imaging through ground penetrating radar, and magnetic survey have been used to locate prehistoric sites or features that indicate human habitation or exploitation. Submerged archaeological features may also be identified through the use of geophysics, however the methods and tools are adapted to meet the specific challenges presented by the submerged environment. Marine geophysical data are often acquired during a towed survey; the geophysical sensor is towed behind a boat along a predefined survey grid, and positioned from the vessel. Offshore magnetic survey intervals are too great to reliably identify short duration or low intensity anomalies such as those caused by hearths or other anthropogenically altered sediments. Unlike terrestrial sites which may utilize sub-meter magnetometer sampling intervals, line intervals of 15 – 30 meters are considered high density for marine surveys (CEI 1977; Garrison et al. 1989; BOEM 2005; Enright et al. 2006; Camidge et al. 2010). The use of towed acoustic sensors, particularly subbottom profilers, is

therefore the preferred method for the identification of buried geographical environments offshore.

5.1.1 Acoustic Survey: Overview.

Acoustic sensors are used in offshore survey because of the superior ability of sound waves to propagate through both the water column and seafloor sediments. Sound waves are preferred over electromagnetic waves such as x-ray and ultra-violet rays, which have limited penetration of less than 1 meter in water, and visible light (Wille 2005:9). In contrast, sound waves of varying frequencies can travel through the water column to depths ranging from 100 meters to 10,000 km (Wille 2005:9). Acoustic sensors include side scan sonar, multibeam bathymetry fan echosounders, single beam bathymetry profilers, and subbottom profilers. All acoustic sensors operate by emitting a fixed or variable frequency signal and recording both the amount of time it takes the signal to return to the transceiver (known as the speed of sound in two-way time travel), and the strength and direction of the returned signal, also known as backscatter (Wille 2005:42-60; Blondel 2009:18-22). Acoustic data are used to reconstruct either 2D plan view images (e.g., multibeam or side scan sonar) or profiles of the seafloor and subseafloor structures (e.g., single beam bathymetry and subbottom profiler) (Wille 2005:42-60).

Geologic conditions in the northwestern Gulf of Mexico create a unique environment for submerged prehistoric archaeological sites. As discussed in Chapter 2, the influx of sediment from the Rio Grande to the Mississippi has filled in relict river channels that incised across the OCS during the last glacial maximum (Nelson and Bray 1970; Anderson 2007:20-46). Unlike river systems in other parts of the world, including the eastern Gulf, evidence of these relict channels is not visible at the seafloor, therefore side scan sonar and multibeam bathymetry are not useful tools for submerged prehistoric research in the northwestern Gulf. The identification of geographical environments offshore Texas and Louisiana is dependent upon careful interpretation of subseafloor sediment horizons (CEI 1977; Pearson et al. 1986; Stright 1986; Evans and Keith 2011a).

Imagery based on sound requires interpretation; although acoustic images may appear similar to photographs they represent data that must be interpreted (Evans and Voisin 2011). Sound

images are produced when an object has a different acoustic impedance than its surroundings; acoustic impedance is defined mathematically as the product of the speed of sound and density, where a change in either density or speed of sound will produce an acoustic echo (Wille 2005:29). The ability to measure depth from acoustic data is dependent upon the actual speed of sound in two way time travel that exists when the data are recorded, which is itself the product of temperature, density, and salinity levels within the water column. In the absence of a velocity cast that records the true speed of sound, data can be interpreted for marine environments by using the average speed of sound in salt water, which is 1,500 meters/second two-way time travel (Wille 2005:27). Recorded acoustic signals generate images but do not have a genuine color; typical sound images are black and white, with a large and dynamic gray scale, although a false color scale may be added in post-processing to assist with interpretation or presentation of data (Wille 2005:30); acoustic data samples provided in the following chapters are displayed in gray scale. Sediments of varying densities or acoustic impedance produce different echoes, which can be identified on the resulting images as layers of varying color. Variation in acoustic impedance may also indicate stratification and a relative record of deposition events. According to Wille (2005:30):

> … the seabed may have no echo producing layers during even thousands of years of continuous sedimentation. On the other hand the presence of a clearly discernible layer is an indication of an event of sedimentation, disrupting continuity. A difference of only one percent and even less in the impedance of adjacent layers may appear as a visible horizon.

Marine geophysical surveys for archaeological resources utilize acoustic data that have been collected line by line along a predefined survey grid (BOEM 2005; Wille 2005:49). Independent of cost, line spacing intervals used to construct the survey grid are dependent upon many factors such as the size of the anticipated feature, but are predominantly controlled by practical survey parameters such as water depth, the size of the survey vessel, and its ability to maintain survey course heading given prevailing weather conditions. Survey data quality can also be compromised due to physical factors that diminish the acoustic signal's strength or return trajectory such as lateral deviation of the towfish due to currents, heave or sea surface conditions, boat pitch and or roll, and towfish height above the seafloor (Edgetech 2003: 3-29; Wille 2005:38-39).

5.1.2 Subbottom Profilers.

Subbottom profilers are used to record the seafloor and underlying internal structures of subsurface sediments (Wille 2005:52). Typically, acoustic frequencies of between 3 kHz and 16 kHz are used to image the upper 100 meters of sediment (Wille 2005:53). Subbottom profiler data acquisition is a balance between high resolution of detail and depth of data penetration. Detailed, high resolution of near-seafloor stratigraphy is achieved by using higher frequencies, while penetration into deeper sediment structures is generally accomplished using lower frequency signals (Wille 2005:53).

Subbottom data quality is directly related to the type of sediment being imaged. Several things can severely compromise subbottom data quality, including underconsolidated sediments, the presence and amount of interstitial or dispersed biogenic gas, high percentages of sand grains within a horizon, or the presence of pore water (Fleischer et al. 2001:103; Whelan et al. 1977:157-158). Based on studies from the South Pass area in the northwestern GOM, Whelan (1977:158) found that when methane concentrations were greater than 30 ml/L within a sediment sample (or horizon) the acoustic signal was either completely absorbed or scattered laterally, decreasing the strength of the acoustic return. Acoustic data must be reflected back to the transducer/receiver to be recorded, therefore the survey medium must have sufficient density or consolidation to reflect the signal; dewatered and compacted clays typically produce high quality data. Sands, which are uncompressible, contain trapped pore water. Pore water and biogenic gas function similarly during acoustic profiling; neither reflects the acoustic signal well, and both contribute to signal scattering, resulting in an acoustic void or opacity on the resulting image (Figure 5.1.1).

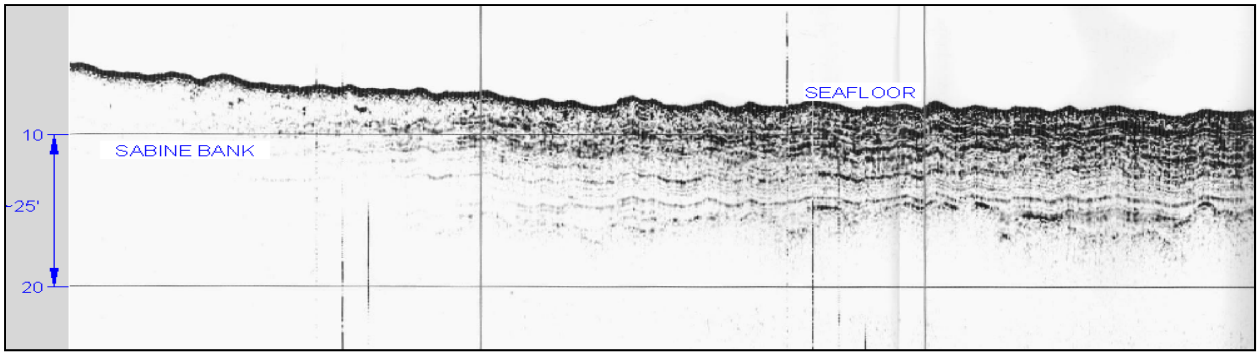

Figure 5.1 Subbottom profiler data (2 – 10 kHz) recorded over Sabine Bank, offshore Texas, illustrates the difference of acoustic reflectivity of sands (left) and compacted clays (right) (data courtesy Tesla Offshore, LLC).

5.1.3 Subbottom Interpretation

Subbottom interpretation for prehistoric archaeology is based on a contextual pattern of site preference, in which modified environments are best preserved in assocation relict river channels underneath the estuarine transgressive zone; the transgressive zone is defined here as the maximum depth to which sediments were scoured and eroded during sea-level rise (Pearson et al. 1986; Waters 1992:279). Depending upon the sediments within the survey area channels, channel margins, infilled sediments, levees, and inset terraces can be observed as significant depositional events based on their reflective properties. Channel margins and inset terraces may exhibit greater consolidation than surrounding sediments, appearing as more reflective horizons than under-, or over-lying sediments. Channel fill, however can be more difficult to identify, depending upon the degree of consolidation and grain sizes. Well-stratified channel fill, deposited slowly over time, and/or allowed to naturally dewater and compact, will appear as parallel to subparallel, distinct reflectors inside the channel margins. Channel fill that is deposited quickly, or contains a high degree of sand or deltaic material is less likely to reflect the acoustic signal and in some cases may appear as a distinct acoustic void within an otherwise stratified sediment profile (Edgetech 2003:1-10; Wille 2005:53). Once channel margins and thalwegs (the site of maximum depth of entrenchment within the channel) are identified along survey lines, the channels can be extrapolated across survey lines, delineating their horizontal extent. Related features such as levees and inset terraces are then identified within the overall channel pattern. Feature depths can be calculated as depth below the seafloor (BSF) and depth below sea level (BSL) using half of the average speed of sound, or 750 meters per second.

Depth below seafloor (BSF) is calculated as the product of time in milliseconds at the feature of interest multiplied by 0.75 meter. Depth below sea level (BSL) is calculated by adding the depth below seafloor (BSF) to the water depth at the interpreted feature. Approximate dates can be determined for an interpreted feature by plotting depth BSL on a sea-level curve appropriate to the survey area to determine the approximate time of exposure.

5.1.4 Survey Methodology.

According to Blondel (2009:201), the primary motivation for mapping of the OCS and its shallow geology is oil exploration. Study areas for this project were selected after reviewing a total of 204 shallow hazard and archaeological NTL-compliant surveys on file with the BOEM. The only other study to survey and physically sample sediments on the northwestern OCS for evidence of prehistoric exploitation was centered in the Sabine Pass, High Island, and Galveston Areas, in water depths ranging from 8 m (27 ft) to 12 m (40 ft) (Pearson et al. 1986). To complement the previous project, this survey review specifically targeted survey reports in which features were located at depths ranging from 15 m (50 ft) to 40 m (130 ft) BSL and located within the West Cameron, Sabine, High Island, or Galveston federal lease areas. The original maps, data samples, and geologic and archaeological interpretation were reviewed for each report. Existing surveys were searched in order to find subbottom features that resembled high probability areas for prehistoric site occurrence and preservation (as defined in Chapter 4); neither of the features selected for study as part of this dissertation were originally identified as potential prehistoric archaeological features. When possible, preference was given to features based on the availability of the original subbottom data. Finally, survey features of interest were ranked by their relative depth below the seafloor, with preference given to sites in the near-surface (less than 2 meters below the seafloor). This ranking was done to facilitate future excavation or data recovery in selected survey areas if physical sampling indicated a probable modified environment.

The selected study areas were initially identified from industry surveys that utilized either 150- or 300-meter survey line spacing for acquisition of subbottom data; supplemental tie lines were collected perpendicular to the primary survey lines at 900-meter intervals for correlation of geologic features, as required by NTL 2005-G07. New geophysical survey grids were designed

explicitly for research purposes using grid spacing of 25-meters. The centerline of each new survey was designed to reproduce the original survey line from which the feature was previously identified, with additional parallel lines to either side. Strike lines were designed perpendicular to the primary survey lines, and also utilized 25-meter line spacing. The 25-meter line spacing was deemed necessary for research purposes based on recommendations published in 1982. According to Gagliano et al. (1982) survey intervals should be designed with the relative size of the search target in mind. They demonstrated this necessity using the example of terrestrial analogues within an offshore survey grid. Magnolia Mound, one of the largest recorded shell midden sites in Louisiana, was superimposed onto a 150-meter subbottom profiler survey grid. It should be noted that the line spacing for this hypothetical grid is half the 300-meter line spacing maximum allowed for industry surveys. When placed on the 150-meter grid, the mound was intersected by one survey line only (Gagliano et al. 1982:113). The first objective of geophysical survey for this study was to relocate the originally reported feature; the second objective was to obtain more detailed information about the geographical environment by conducting close interval survey around the feature. Two discrete areas were selected for use in this study, one located in High Island (HI) 178 and the other in Galveston (GA) 426, based on the reports review.

Geophysical survey was conducted from the R/V *Acadiana*, an 18 meter survey vessel owned and operated by the Louisiana Universities Marine Consortium (LUMCON) and operating out of Cocodrie, Louisiana. The vessel is equipped with an A-frame on the back deck for deployment of the subbottom towfish (Figure 5.1.2). An Edgetech 3100 series SB2-16 subbottom profiler with variable chirp frequency settings was selected for this survey work. An independent Trimble unit provided DGPS via USCG WAAS signals to an EZNav navigation system for positioning of the towfish; setback from the antennae to the towfish was entered into EZNav and no cable changes were made during individual survey lines. Digital data was recorded using CODA for acquisition, post-processing, and interpretation. Equipment was dry-tested to ensure that the correct navigation string was input from the navigation system directly into the digital acquisition system, and that the chirp signal was emitting from the transducers before deployment. The subbottom was towed by a Kevlar-reinforced data cable, and deployed over the stern of the vessel using the survey vessel's A-frame and winch (Figure 5.1.3).

Recommended tow speeds vary from 3 – 5 knots for this model subbottom unit, and the *Acadiana* typically operated at 4 knots. All survey work was conducted between July 12 and 22, 2008.

Figure 5.2 The R/V *Acadiana* at the LUMCON dock.

Figure 5.3 Subbottom profiler being deployed from the stern of the vessel.

5.2 Physical Sampling

Geophysical survey has been used regularly for the last 40 years to identify subsurface features in marine environments (Blondel 2009; Wille 2005). Measurements of the speed of sound allow for accurate measuring of feature depths, but acoustic data, with the exception of sonar backscatter, is largely qualitative, or relative within a specific data set. Changes in acoustic impedance may result in the identification of sedimentary episodes, but this sequence of events is relative to the surrounding sediments and does not provide definitive sediment age or date of deposition. Physical samples are therefore required to provide additional data that can either refute or confirm an interpretation based on geophysical data.

Ocean cores are recognized for their potential to contribute to climate and geologic reconstruction studies. Historically, core acquisition was dependent upon development of a practical means of recovery, such as Kullenberg's invention of the piston corer in the 1940s (Catt 1986:16). Sediments captured stratigraphically within cores can be tested using a number of different methods to develop both relative dating chronologies and absolute dates. Relative chronologies are often tied to temperature or climatic fluctuations. An early method of determining climate fluctuation was to measure and plot the relative proportions of temperature-sensitive foraminfera species in the sediments (Catt 1986:16). Emiliani developed a technique for determining previous water temperatures from the oxygen isotope ratios ($^{18}O/^{16}O$) measured in fossil foraminifera recovered from core sediments (Catt 1986:17). Radiocarbon dating produces absolute dates that are used to anchor relative chronologies constructed using other methods within core samples for archaeological studies in the Gulf of Mexico region; radiocarbon dating is effective only until approximately 40,000 years BP, which far exceeds the known dates of human occupation in the region (Catt 1986:17).

There are two basic bottom sampling methods for the collection of cores. Cores may be obtained from a platform (such as piston cores or vibracores), or collected by divers (including push cores and box cores) (Mudroch and Azcue 1995:48). Sediments sampled by divers have been shown to retain greater integrity than those sampled remotely (Mudroch and Azcue 1995:54). As described by Mudroch and Azcue (1995:54), a comparison of sampling methods used in the

study of meiobenthos found greater numbers of specimens in the cores collected by divers due to disturbance of the sediments during gravity, or drop, core acquisition. According to Mudroch and Azcue (1995:54) gravity cores create downwash as they fall through the water column, which disperses a significant portion of the superficial sediments, resulting in a biased sample. It must be noted that there is no universal bottom sediment sampler; the coring method used must be selected with regard to the dominant type of sediment that will be sampled and the desired depth of core penetration (Mudroch and Azcue 1995:55).

Actions prior to and during sediment sampling can alter the physical composition of the sediments, which can skew results of the data analysis (Mudroch and Azcue 1995:56). Disturbances can stem from many actions. In shallow water, vessel movement can create a current that disturbs the uppermost sediment layer (Mudroch and Azcue 1995:56). Other sources of disturbance may include a pressure wave generated by placement of the coring device, a less than vertical coring sleeve that results in a skewed profile, washout of sediments, or sediment loss during core retrieval (Mudroch and Azcue 1995:56).

Previous physical sampling of the OCS for prehistoric resources included the use of 12 m (40 ft) cores deployed from a jack-up barge (Pearson et al. 1986). A total of 76 cores were collected, with the potential for maximum recovery of 921 m (3,040 ft) of sediment; actual vertical core penetration was 550 m (1,815 ft) (Pearson et al. 1986:79). Water content and sediment compaction were hypothesized to impact the total amount of sediment recovered within each core. Sediment content down the core from open ocean samples increases as the water content decreases; according to Mudroch and Azcue (1995:66) fine-grained sediments in the uppermost 20 cm contain 70-80% water, and sediments between 30 and 40 cm below seafloor contain 50-60% water. Sediments below 50 cm are typically more compacted and exhibit minimal changes in water content (Mudroch and Azcue 1995:66). Sediment recovery within the previous cores ranged from 34% to 78%; average recovery was 55% (Pearson et al. 1986:79).

The degree to which sediment disturbances caused by sampling procedures impact data interpretation depends upon the type of analysis being conducted (Mudroch and Azcue 1995:67). Contamination profiling or monitoring is dependent upon accurate sampling to the sub-

centimeter, and requires that the uppermost sediments be captured during the sampling process (Mudroch and Azcue 1995:67). Piston corers generally can recover cores ranging from 3 m to 20 m in length with minimal sediment disturbance within the sample (Mudroch and Azcue 1995:76). They are not appropriate for contaminant sampling, or other studies that require intact sediments from the uppermost sediments due to loss of material during the sampling procedure but are appropriate for landscape reconstruction that extends several meters below the seafloor (Mudroch and Azcue 1995:76).

When cores are required in areas with sandy unconsolidated sediments, vibracores are better able to penetrate the sediment and recover samples that are often used in geotechnical and structural assessments (Mudroch and Azcue 1995:76). Vibration is "the most popular and successful technique for increasing the penetration depth of a platform sampler" (Lee 1986:195). Vibration can be produced in a single direction by counter rotating pistons, hammers, or eccentric weights (Lee 1986:196). Disturbance is expected within vibracore sediment samples but has not been found to significantly affect stratigraphy, grain size, or Atterberg limits (Lee 1986:197). Additionally, vibracore sediment penetration rates may provide rough estimates of *in situ* soil strength (Lee 1986:197), which may be used to infer sediment type and water content.

Surface procedures further impact the quality of acquired core sediments. Collected cores need to be capped on both ends immediately during or following retrieval to the surface to prevent the loss of material (Mudroch and Azcue 1995:126). If the core liner is made of clear plastic, "the appearance of the sediment core should be recorded prior to subsampling, along with other features such as the length of the core; sediment color, texture, and structure; occurrence of fauna; etc. (Mudroch and Azcue 1995:126)." Long cores can be sectioned laterally into smaller pieces for ease of transportation and or storage (Mudroch and Azcue 1995:126). In the lab, cores that have been sectioned longitudinally and labeled can be wrapped to preserve sediment stratigraphy and moisture content, and stored for months (Mudroch and Azcue 1995:142-144).

5.2.1 Coring Methodology

A total of fifteen cores were collected for this research project from the two areas previously subjected to acoustic survey; HI 178 and GA 426. It was expected that cores would be acquired

from a matrix of sand, silt, and clay, therefore a vibracore platform was chosen for maximum penetration depth within these various sediment profiles. Given that previous cores for prehistoric archaeological research averaged just 54% sediment recovery within a 12 m (40 ft) core sleeve (Pearson et al. 1986:79) it was decided that a vessel-mounted coring rig with a 6 m (20 ft) core sleeve would be sufficient to capture the strata of interest, and be more cost-effective than coring from a jack-up barge. At each of the survey sites, at least one core was acquired from the originally interpreted feature; the remaining core locations were selected from the interpreted geophysical data (detailed in Chapter 6). The coring methodology was designed to be inherently flexible; the methodology had to be adaptable depending upon observed sediments or possible features identified in the field. If a shell midden was encountered, it was planned that additional cores would be acquired from that location in order to provide sufficient data to determine if the feature was natural or anthropogenic.

Coring operations were conducted from June 24th to July 3rd, 2009 on board the M/V *Thunderforce*, a dedicated coring vessel operated by American Vibracore Services (Figure 5.4). The M/V *Thunderforce* is a fully Coast Guard inspected 26 meter steel-hull vessel with twin 12-71 diesel engines, a removable stern rail, and a 10,000 lb stern-mounted A-frame. Coring site coordinates were prepared from DGPS digital subbottom data with integrated navigation data as NAD27 state plane coordinate system (SPCS) X/Y (easting and northing) pairs and converted to WGS84 Latitude and Longitude in decimal minutes for integration with the coring vessel's Nobeltec Pro software. The Nobeltec Pro system received differential signals provided via WAAS and USCG Reference Station Networks operated by the US Department of Defense (DOD).

The coring rig consisted of a pneumatic vibracore unit with a 6 m (20 ft) drill pipe, and 20-cm drill bit. Clear, plastic, 10-cm diameter core sleeves were inserted into the drill pipe. Following core acquisition the drill bit was removed from the pipe, and sediments from the drill bit were collected. The core sleeve was extruded from the drill pipe and cut into pre-determined lengths of 0.9 m or 1.2 m (3 ft or 4 ft) depending on if the core was to be frozen. Each core section was capped, labeled, and measured as soon as it was removed from the drill pipe.

Figure 5.4 M/V *Thunderforce* with stern mounted A-frame, as seen from starboard.

The vessel was positioned above each core location as a "live boat"; no anchors were set. The coring rig was lifted from the back deck of the vessel and lowered into position on the seafloor using the vessel's stern-mounted A-frame and winch (Figures 5.5 and 5.6). The pneumatic vibracore was powered by a surface-supplied air compressor. Core penetration depths and rate of penetration were monitored on the vessel using a penetrometer connected to a laptop computer and recorded when possible.

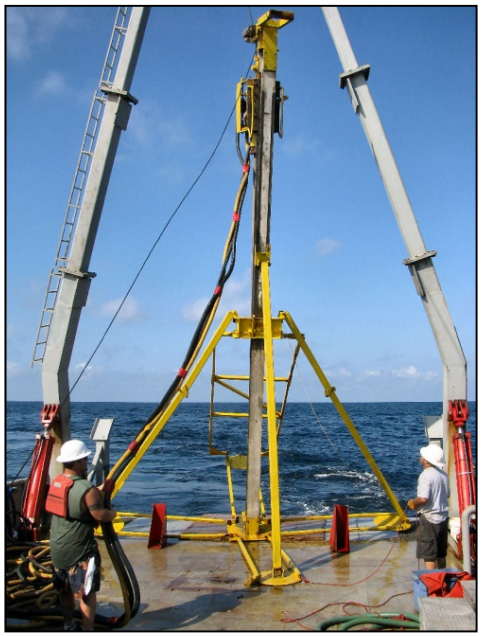

Figure 5.5 Pneumatic vibracore rig on the deck of the M/V *Thunderforce*.

Figure 5.6 Pneumatic vibracore rig being lifted on the deck of the M/V *Thunderforce*.

Coring operations were conducted in tandem with coring for a larger regional study which involved acquisition of thirty (30) cores, including the 15 used in this dissertation. On Sunday June 28th, a total of five (5) cores were acquired from features in HI 178 where water depths are approximately 12 to 15 meters BSL (Figure 5.7). One of the pre-planned core sites (core no. 4) was located approximately 412 meters inside the eastern boundary of a dedicated Fairway. Approval could not be obtained from the US Coast Guard and the Captain of the Port of Houston to conduct coring at this location. Core no. 4 was a low priority location and was therefore removed from the coring plan, and replaced with an alternate core location selected in the field.

On Tuesday June 30th and Wednesday July 1st, a total of ten (10) cores were acquired from features in GA 426 where water depths are approximately 27 to 31 meters BSL. Following acquisition of core no. 1, moderately-sized shell fragments were observed in the drill bit (Figure 5.8).

Figure 5.7 Sediment color variations are visible in High Island 178, Core no. 5, sections A – E.

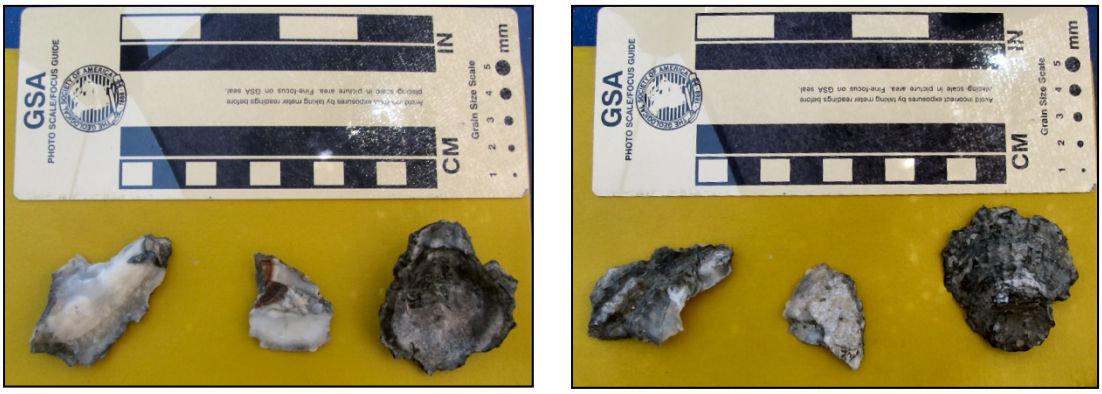

Figure 5.8. Shell fragments recovered in the drill bit from Core no. 1, GA 426.

Based on the identification of shell fragments in the drill bit section of Core no. 1, the decision was made in the field to acquire additional cores at that location. While attempting to core a second time at the location of Core no. 1 (labeled as Core no. 9) the crew experienced difficulty with the penetrometer cable. Failure of the penetrometer meant that field personnel were unable to verify core depths during drilling. Core no. 9 achieved a maximum penetration of 4.6 meters below the seafloor (BSF), missing the observed feature from core no. 1 which had a maximum

depth of 5.8 meters BSF. Various repairs were attempted on the penetrometer, and two additional cores were acquired at this same location (cores no. 10 and no. 11). The decision to acquire more samples from the shell feature was made to provide a sufficient sample size to determine if the observed shell deposit is natural or anthropogenic (Figure 5.9).

Figure 5.9 Shells observed in GA 426 Core no. 10, between sections D and E.

At the conclusion of coring operations at GA 426, all of the cores for both the dissertation and regional study had been acquired. The vessel returned to Port Fourchon, Louisiana and the cores were offloaded for immediate transport to the H.J. Walker Geomorphology Lab at LSU. Refrigerated cores were transported inside a separate vehicle and immediately placed in cold storage at LSU. The remaining cores were unloaded at the Walker Lab for sampling and analysis.

5.3 Sediment Analysis Methodologies

Before being opened, all core sections were run through a Geotek multi-sensor core logger (MSCL) by lab assistant Jennifer Gardner at the LSU School of Coast and the Environment. The MSCL recorded primary wave, or p-wave, velocity and magnetic susceptibility (as volume-specific values). P-wave velocity was recorded as µsec (seconds per foot) and processed to calculate the speed of sound through the various strata as meters per second. These data were used to correlate sediment strata with their measured depths as estimated from the acoustic profile data. Volume-specific measurements of magnetic susceptibility were recorded to identify

stratigraphic sequences within the sediment profile, and specifically any data irregularities (or spikes) that could indicate an erosional unconformity. The core logger is equipped with a 10 cm sensor for recording MS measurements. Following core logging, all cores were returned to the Walker lab, where they were sectioned longitudinally. One half was immediately wrapped in plastic core sleeves, labeled, and sealed as an archived sample. The other half was photographed in the lab, and logs were made describing each section's stratigraphy, Munsell color, sediment type (based on qualitative data), horizon thickness, and any observed inclusions. Cores were subsampled for additional analyses, including measurements for grain size and magnetic susceptibility, and carbon dating. Additional research was undertaken by specialists analyzing preserved pollen species.

5.3.1 Grain Size Analysis

The extensive literature regarding the sediment distribution on the OCS of the Gulf of Mexico indicates that the sediments between the Mississippi Delta and the Mexican border fall into one of two types; transgressive nearshore sands or shelf muds (Curray 1960; Balsam & Beeson 2003). More specifically, the outer continental shelf of Texas, Louisiana, Mississippi, Alabama, and north Florida is dominated by river transported terrigenous sediments. Major portions of the Texas and Louisiana shelf are covered with clay and with varying amounts of sand, silt and organics (Allison et al. 2000; Gordon et al. 2001; Balsam & Beeson 2003; Ellwood et al. 2006).

The areas investigated are located offshore Texas and Louisiana, and the most likely sediments to be analyzed are principally quartz sands and muds. The latter are modern, suspended and transported during river high flow stages and storms and hurricanes, and preferentially deposited during calm conditions. Sand layers are predominantly relict and deposited near the coastline by transgressive events (Curray 1960), or can be attributed to and/or reworked by storms or hurricanes. Limited sandy sediment is being supplied to the nearshore or shelf at the present time (Bentley et al. 2002). Grain size is an important indicator in reconstructing sedimentary structures and the controlling "hydrodynamics of deposition" (Wells 2001:157). Specific environments exhibit distinct sedimentary characteristics, which can be identified through grain size. Peat deposits exhibit high percentages of very-fine clay and silt; mudflats contain a

combination of clay, silt, and molluscan fauna; and marsh sediments contain highly organic sand to clay (Wells 2001:159-162).

Grain size samples were collected from units identified during core logging to refine the final core log. Samples were collected and placed into labeled whirl-pak bags. Grain size analysis was conducted by lab assistant Cory Sills using a laser particle counter at the Louisiana Universities Marine Consortium (LUMCON). Results were exported into excel; both median and mean grain sizes were calculated following procedures outlined by Folk (1980) and Shackley (1975).

5.3.2 Magnetic Susceptibility

Magnetic susceptibility (MS) measurements can be described generally as a measurement of the concentration of iron-containing grains within a sediment sample (Thacker and Ellwood 2007). Magnetic susceptibility should not be confused with remnant magnetization, which is used to determine polarity and measured in areas devoid of a magnetic field (Ellwood and Burkart 1996; Ellwood et al. 2004). According to Thacker and Ellwood (2007:164), geological studies of MS are possible because soil minerals, especially iron rich sediments, "are more easily magnetized in the presence of an inducing magnetic field." In archaeology, MS has been used to identify anthropogenic activities such as organic refuse disposal and repeated burning, as in hearths (Evans and O'Connor 1999). A different application of MS, however, may aid in linking local data from submerged contexts to regional data sets. Measurements of MS may be used to develop a proxy record of climate conditions within a sediment profile, facilitating relative dating of strata, and reconstruction of diachronic changes in a given area.

Soil forming processes, or pedogenesis, are controlled by five variables that include climate, the activities of organisms within the sediment profile, relief, parent material, and time (Goldberg and Macphail 2006). Chemical changes during pedogenesis can result in mineral oxidation and *in situ* development of magnetic grains and iron oxides including magnetite and maghemite (Ellwood et al. 2004; Ellwood and Burkhart 1996). There is a direct relationship between magnetic susceptibility and the amount of iron-containing grains in a given sediment sample;

generally, the higher the amount of iron-containing grains, the higher the measurement of MS (Ellwood and Burkart 1996).

Pedogenesis and eolian deposition are the two primary mechanisms controlling deposition of sediments resulting in an observable MS trend. MS levels can be impacted by other processes that can potentially alter the observed climate trend. These include deposition from other sources, such as alluvial systems, unconformities caused by nondeposition or erosion, or post-depositional mixing or alteration (Harrold et al. 2004).

Climate, as previously stated, is one of the five controlling factors for pedogenesis, with temperature and moisture playing important roles in determining rates of pedogenesis (Goldberg and Macphail 2006; Ellwood et al. 2004). Increases in temperature and moisture typically result in increased production of magnetite and maghemite (Ellwood et al. 2004). Variations in climate can therefore be inferred from sediment stratigraphy as variations in the amount of magnetic grains, and therefore the measure of magnetic susceptibility (Ellwood et al. 2004). The use of MS in archaeological projects has demonstrated the utility of correlating local site MS curves with global climate patterns (Ellwood et al. 2004; Thacker and Ellwood 2007).

Magnetic susceptibility has been used in archaeological studies, but it must be noted that MS data have inherent limitations; in and of itself the data will only result in a relative curve of conditions and change. Magnetic susceptibility data does not, by itself, indicate an age for the sampled sediments nor does it provide absolute temperature values (Thacker and Ellwood 2007). MS data can be used to create a general pattern of warmer versus cooler climate trends, creating a relative dating profile that must then be tied into the stratigraphic record using radiometric or biological absolute ages (Thacker and Ellwood 2007).

Climate correlation using MS data works in a variety of environmental settings. Measurements of magnetic susceptibility from Chinese loess deposits resulted in the creation of a data curve that was directly correlated with the marine oxygen isotope record developed by Imbrie et al. (Ellwood et al. 2004). In the Chinese loess data, higher MS levels correlated with a warmer and wetter climate, while lower values correlated with relatively colder and drier climate conditions

(Ellwood et al 2004). In this same example, pedogenesis was the main source of deposition within the warmer climate sediments, while eolian deposition accounted for sediments with the lower values deposited during colder climate periods (Ellwood et al 2004). In a separate application, sediment data from Hall's Cave, Texas demonstrated that MS data were a more accurate indicator of the end of full glacial climate conditions than sediment lithology (Ellwood and Gose 2006).

According to Holliday (2004), magnetic susceptibility is useful for determining buried soils, especially in areas with thick, stratified sequences. Although Holliday specifically refers to the utility of MS in correlating stratified soils within loess deposits, formerly exposed sediments on the OCS can exhibit well preserved stratified layers (Figure 5.10).

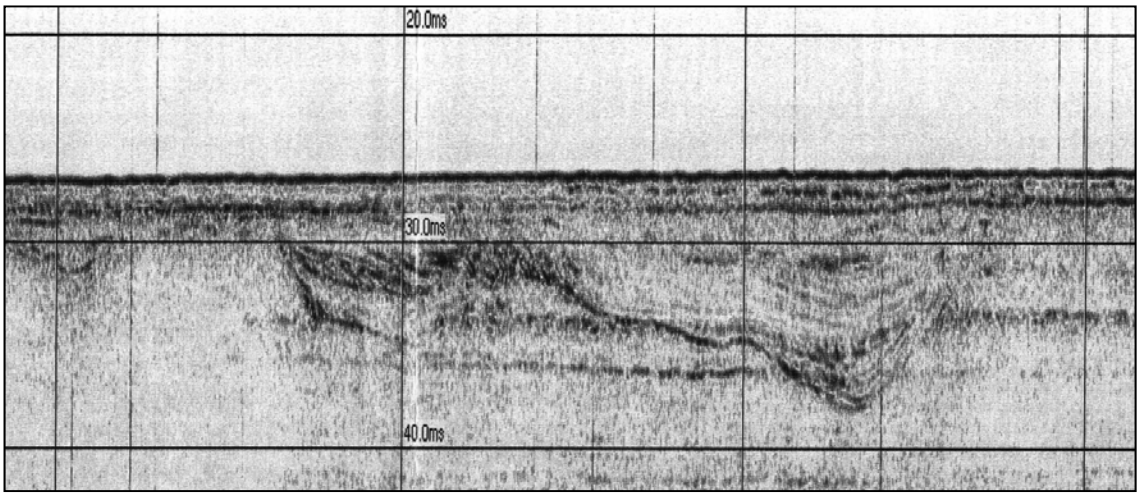

Figure 5.10 Subbottom profiler data sample of stratified sediments within a relict river channel offshore Galveston. Vertical scale lines are in 150m (492 ft) intervals; horizontal scales lines are in 10ms (25 ft) intervals (image courtesy Tesla Offshore, LLC).

Magnetic susceptibility data have proven effective in studies of offshore, marine sediments (Ellwood et al. 2006). A study of MS values measured from surface sediment samples throughout the Gulf of Mexico allowed researchers to model sediment flow and distribution in the offshore environment (Ellwood et al. 2006). Sediment profiles on the OCS consist of modern marine sediments overlying buried soils (Bernard 1970; Coleman and Roberts 1988; McClelland Engineers 1979). Existing estimates of middle to late Holocene sediment

overburden state that thickness ranges from less than 1 meter to approximately 8 meters along portions of the OCS near the Texas-Louisiana border (Bernard 1970; McClelland Engineers 1979; Berryhill 1984).

One of the limitations in using magnetic susceptibility data is the potential for disruption of observable climate trends (Harrold et al. 2004). According to Harrold et al. (2004) disruptions can be caused by unconformities within the sediment profile, post-depositional mixing, and deposition from fluvial systems. All of the potential sources for disruption are anticipated within a sediment profile of a fluvial landform that underwent shoreline transgression. Although these disruptions may restrict the ability to use the MS data to correlate climate change, it may be possible to correlate the expected unconformities or disruptions across multiple samples to determine the local expression of regional climate events.

Magnetic susceptibility is a cost-effective, but labor intensive laboratory analysis (Dearing 1994). Sediment samples, depending on the core, were collected either continuously or at regular intervals from a vertical sediment column in $2cm^3$ plastic sampling boxes. Materials such as limestone, bone, or calcium create mass within a sample but are non-magnetic and not related to climate change (Thacker and Ellwood 2007). Samples in this study were not screened prior to MS measurement, therefore samples that include these types of materials may produce artificially lower MS values (Thacker and Ellwood 2007). Samples were weighed and normalized for mass; mass-specific measurements were chosen as a supplemental analysis for this study because volume-specific measurements, such as those recorded during Geotek core logging, can introduce unnecessary error to the interpretation because of potential sediment compaction within samples (Thacker and Ellwood 2007). Prepared samples were measured using a balanced coil induction system, also referred to as a susceptibility bridge (Dearing 1994; Thacker and Ellwood 2007). The magnetic susceptibility bridge was calibrated before each project using values from the National Bureau of Standards or other conventional source (Ellwood and Burkhart 1996).

5.4 Presentation of Results

Site specific acoustic survey and coring and sediment analyses results are presented in the following chapters (Chapters 6 and 7). Results of these methods are supplemented with data provided by other researchers (Warny et al. 2012) and from samples sent to commercial labs for preparation and analysis. Following core logging, organic samples appropriate for radiocarbon, or ^{14}C dating, were selected from individual cores. Radiocarbon dates were obtained from shells, charcoal, and sediment samples. Samples were not collected from every core, but were collected at both sites. Samples were sent to Beta Analytic Inc. for radiocarbon dating and are detailed in the following chapters. Pollen samples were acquired from cores at each study location (HI 178 and GA 426) to provide additional detail about environments that were initially identified as possible operational environments.

CHAPTER 6. ACOUSTIC SURVEY RESULTS

Multiple data sets were available for review as part of this study. Industry surveys completed under BOEM survey guidelines were initially used to select locations for further study, and are cited here by the year in which the survey data were acquired. References are given for the industry survey on file with the BOEM, with the archaeologist's name given first (in the case of an archaeological and shallow hazards combined report).

6.1 High Island Area 178

Four separate data sets were available for use at this study location. The first data set was the industry block survey report that originally identified the channel system of interest (Keith and Pryor 2007). Acoustic profiling conducted as part of this scope of work was acquired in 2008. A separate industry pipeline survey was conducted in 2009 and overlapped the areas of interest identified in the 2007 industry block report; this data set was made available for use in this study (Keith and Evans 2009). Supplemental acoustic profiles were collected by Tesla Offshore in 2011 for use in this study.

A high probability feature for prehistoric archaeological site occurrence and preservation was recorded at High Island Area 178 (HI 178) during a BOEM-compliant shallow hazards and archaeological survey conducted in October 2007 (Keith and Pryor 2007). The grid utilized for data acquisition was designed with survey lines oriented parallel to the northern boundary of an existing fairway, or approximately northwest to southeast. Subbottom profiler survey lines were spaced 150 m apart. Four tie-lines were designed perpendicular to the primary lines and spaced 900 m apart (Keith and Pryor 2007). The subbottom interpretation identified up to 1.5 m (5 ft) of strongly to moderately reflective stratified sediment, which was interpreted as Holocene in age, overlying weakly reflective to acoustically opaque sediments (Keith and Pryor 2007). Paleochannels were observed within the lower sedimentary unit, with observed margins identified at depths of 1 m (3 ft) to 1.5 m (5 ft) below the seafloor; observed thalwegs were up to 16.6 m (55 ft) below the seafloor. A possible levee was identified along the margins of a large channel feature, and appeared to be intact below the interpreted modern sediment horizon (Figure 6.1.1). Based on a sea-level curve developed by CEI (1977), the feature was estimated to

have been exposed as dry land and available for occupation prior to 6,000 BP, after which it was inundated by rising sea-level (Keith and Pryor 2007). The feature was recommended for avoidance during future lease activities, and no further testing was required at that time.

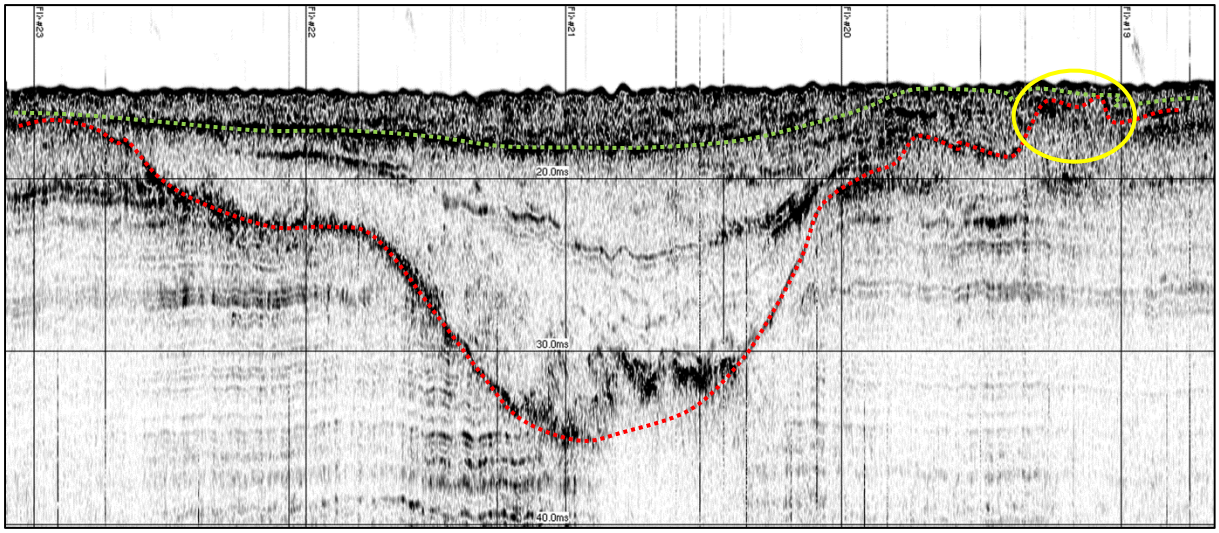

Figure 6.1.1 Annotated subbottom profiler image of survey line 4 shows the levee feature (circled in yellow) identified in 2007 with the channel horizon (red) and ravinement surface (green). Vertical scale lines are in 150 m intervals; horizontal scale lines are in 7.5 m intervals (modified from Keith and Pryor 2007).

The interpreted feature in HI 178 was selected for survey and testing because it is a shallow buried feature located at a depth of 17 m (51 ft) BSL, and represents a high probability feature for archaeological site occurrence and preservation as defined by CEI (1977) and Waters (1992). In order to collect high-density data around the interpreted feature of interest a new acoustic survey grid was created and centered on the interpreted feature, with a north-south and an east-west survey line serving as the central axes. Additional survey lines were created so that ten lines extended to each direction of the reported feature. All survey lines were 450 m (1,500 ft) in length, and spaced at 25 m (82 ft) intervals (Figure 6.1.2); survey was conducted on July 21, 2008. In addition to the 42 survey lines originally planned, an additional eight survey lines were added in the field to provide broader-scale imaging of the channels in the area and oriented diagonal to the primary survey lines (northwest to southeast, and southwest to northeast). The resulting data were interpreted digitally and contoured. Vessel stability issues resulted in

significant heave that could not be processed out of the survey data, creating image distortion. Supplemental survey lines (501-509) were created over the interpreted features of interest for use in illustrating the feature further. These lines were recorded by Tesla Offshore's survey vessel M//V *Nikola* in 2011 while in transit between regularly scheduled work.

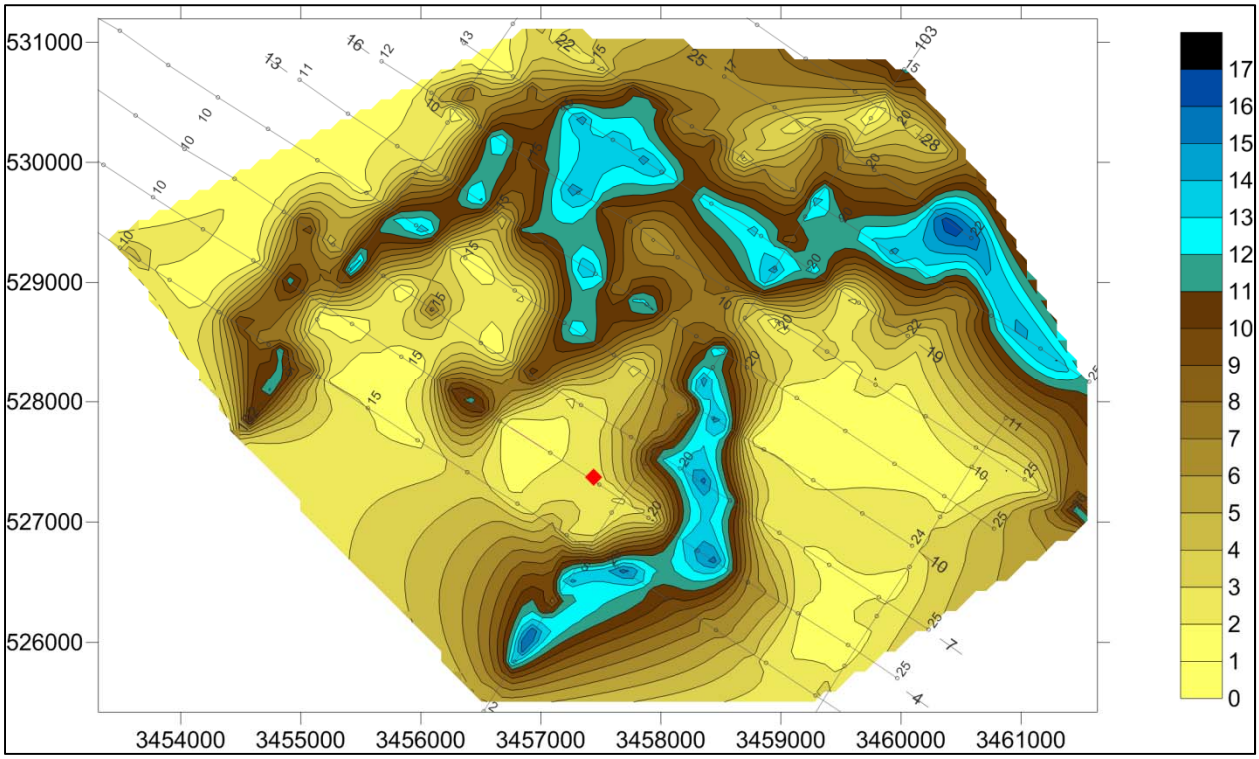

Figure 6.1.2 Contours depict the channel system as interpreted from the 2007 data set. The site of interest is indicated by the red diamond. The survey lines are superimposed over the channel system in black; primary survey lines are spaced 150 m (492 ft) apart. Depths are in meters below the seafloor.

The 2008 data set was designed to provide detailed coverage of the area immediately surrounding the potential levee and accurately delineate the feature's boundaries. Longer lines were added in the field to provide additional coverage over features observed during acquisition (represented by the 100 and 200 series lines). The higher density 2008 data reflect greater variability within the channel's margins, and depict the channel wrapping around the northern boundary of the survey area (Figure 6.1.3). The interpreted levee was relocated (Figure 6.1.4),

and an additional area of interest was observed to the northwest; this second area was interpreted as a possible levee or terrace (Figure 6.1.5).

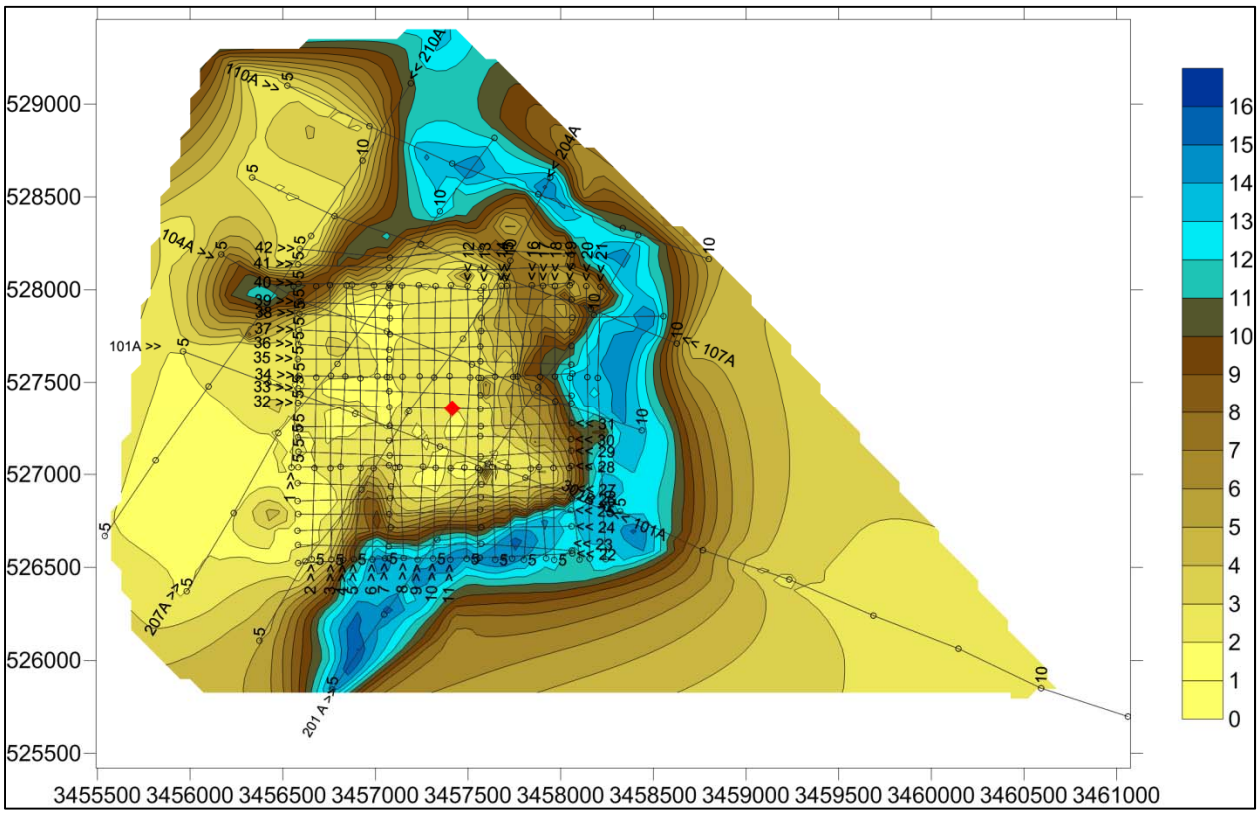

Figure 6.1.3 Contours depict the channel system as interpreted from the 2008 data sets. The site of interest is indicated by the red diamond. The survey lines are superimposed over the channel system in black; primary survey lines are spaced 25 m (82 ft) apart. Depths are in meters below the seafloor.

Following acquisition of the acoustic survey data a proposed pipeline survey was conducted between HI 154 and HI 178 in November 2009 (Keith and Evans 2009); those data were made available for inclusion in this study.

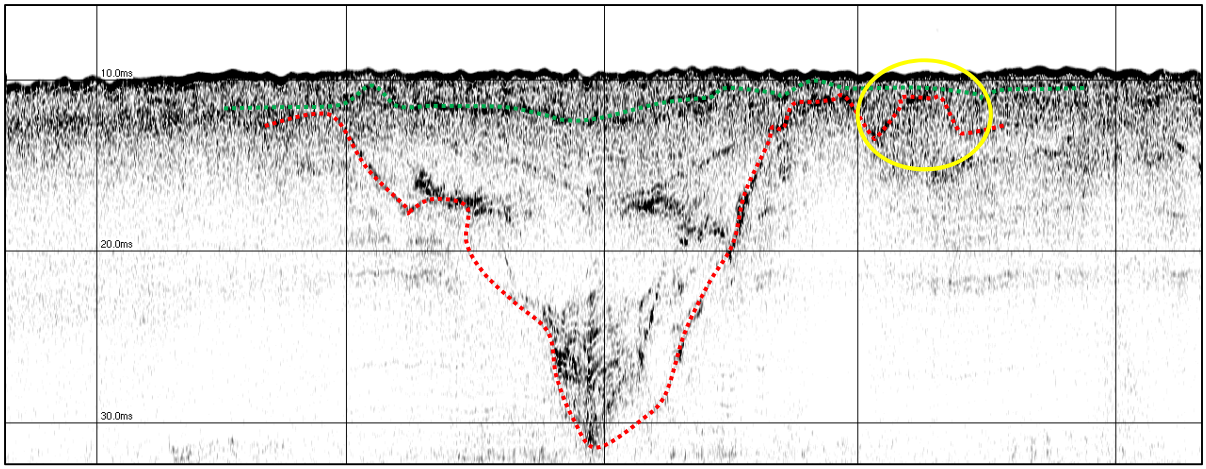

Figure 6.1.4 Annotated subbottom profiler from Iine 506A shows the levee feature (circled in yellow) previously identified in 2007 shows the channel horizon (red) and interpreted ravinement surface (green). Vertical scale lines are in 150 m intervals; horizontal scale lines are in 7.5 m intervals.

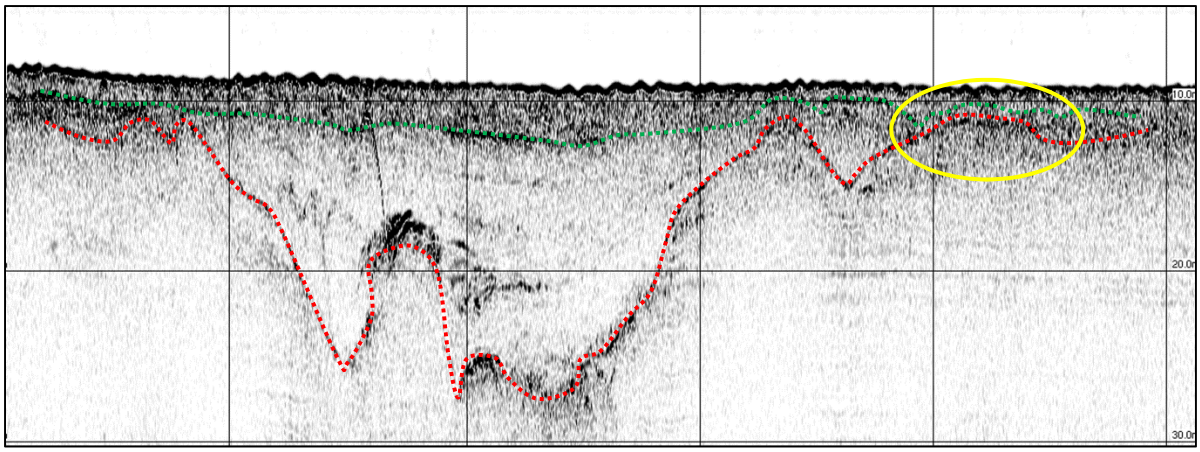

Figure 6.1.5 Annotated subbottom profiler image from line 508 of a second possible levee feature (circled in yellow) identified from the 2008 survey with the channel horizon (red) and interpreted ravinement surface (green). Vertical scale lines are in 150 m intervals; horizontal scale lines are in 7.5 m intervals.

The 2009 survey included the area over the high probability feature for prehistoric archaeological site occurrence and preservation identified in 2007 and correlated with the interpreted 2008 data (Keith and Evans 2009). The 2009 survey grid also included supplemental coverage over the secondary feature of interest identified from the 2008 data. The 2009 grid was designed with survey lines oriented parallel to a proposed pipeline route, approximately

northwest to southeast; survey line orientation was similar to the 2007 survey grid. Subbottom profiler survey lines were spaced 50 m (164 ft) apart, and eight tie lines were designed perpendicular to the primary survey lines and spaced 900 m apart (Keith and Evans 2009). The subbottom interpretation correlated strongly with the two previous data sets and identified a moderately to strongly reflective surficial unit approximately 0.6 m (2 ft) to 1.5 m (5 ft) thick overlying weakly reflective to acoustically opaque sediments. Buried paleochannels were observed in the eastern extent of the survey grid, correlating with the approximate area of buried paleochannels from the 2007 and 2008 surveys. Channel margins were observed within the upper 0.6 m (2 ft) to 1.8 m (6 ft) of sediment; entrenched thalwegs were observed to depths of 15 m (52 ft). Subbottom data from the southeastern portion of this survey grid were incorporated into the 2007 and 2008 contoured data, and provide a significant amount of additional detail (Figure 6.1.6).

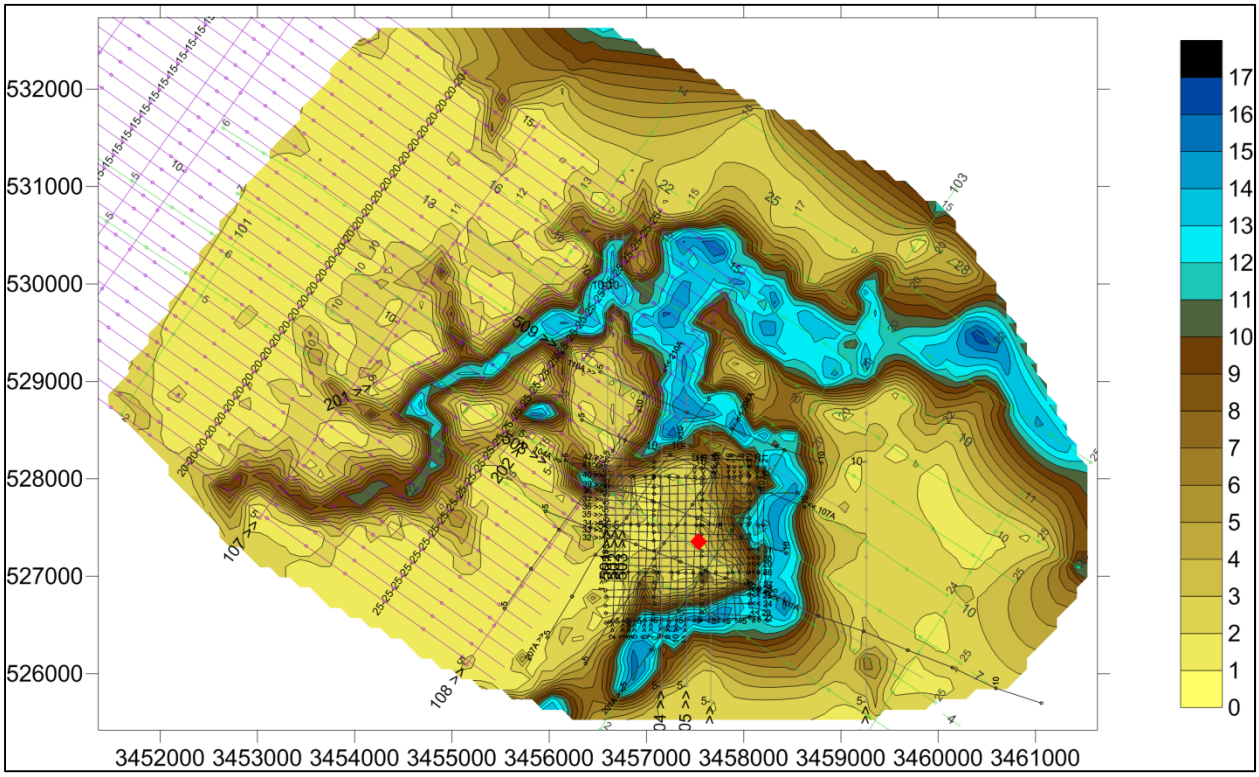

Figure 6.1.6 Contours depict the channel system as interpreted from all available data sets (2007, 2008, 2009, and 2011). Survey lines are superimposed in the following colors: 2007 in green, 2008 in black, 2009 in purple, and 2011 in gray. Depths are in meters below the seafloor.

6.2 Galveston Area 426

A high probability feature for prehistoric archaeological site occurrence and preservation was recorded at Galveston Area 426 (GA 426) during a BOEM-compliant shallow hazards and archaeological survey conducted in December 2007 (Keith and Geresi 2008). Water depths in this survey area were approximately 30.5 m BSL (101 ft BSL). The grid utilized for data acquisition was designed with survey lines oriented arbitrarily north-south. Subbottom profiler survey lines were spaced 300 m apart, and five tie-lines were designed perpendicular to the primary lines (oriented east-west) and spaced 900 m apart (Keith and Geresi 2008). The subbottom interpretation identified a very thin veneer of probable Holocene sediment immediately underlain by the probable Holocene-Pleistocene unconformity. East-west trending channels and channel fragments were identified in the survey area, with channel margins located at depths ranging from 1.5 m (5 ft) to 4.5 m (15 ft) below the seafloor; observed thalwegs were up to 8.8 m (29 ft) below the seafloor (Keith and Geresi 2008). Two distinct channels were identified in the central portion of the survey area, separated by a topographic rise, located at a depth of approximately 1.5 m (5 ft) below the seafloor. At least one inset terrace was identified on subbottom data within the southern margin of the northern channel approximately 3.8 m (12.5 ft) below the modern sea-floor, and below the interpreted ravinement surface (Figure 6.2.1). Based on a sea-level curve developed by CEI (1977), the topographic feature between channels was estimated to have been exposed as dry land and available for occupation prior to 10,500 years BP and the inset terrace prior to 11,000 years BP, after which these features were inundated by rising sea-level (Keith and Geresi 2008).

Geophysical data also recorded an outcropping diapir approximately 780 m (2,575 ft) south of the interpreted channel system (Keith and Geresi 2008). Uplifted sediments associated with the interpreted diapir were recorded on the processed 2-D seismic data to depths of 1.2 seconds (900 m) below sea-level before the signal was completely attenuated (Keith and Geresi 2008). The diapir, which likely represents upwardly mobile salt, was also observed on the sonar data and associated with outcropping features as recorded on the sonar, subbottom, and bathymetry data (Keith and Geresi 2008). The probable salt diapir was not identified as a high probability feature

for prehistoric archaeological site occurrence, but could have contributed to the local environment and served as an exploitable resource.

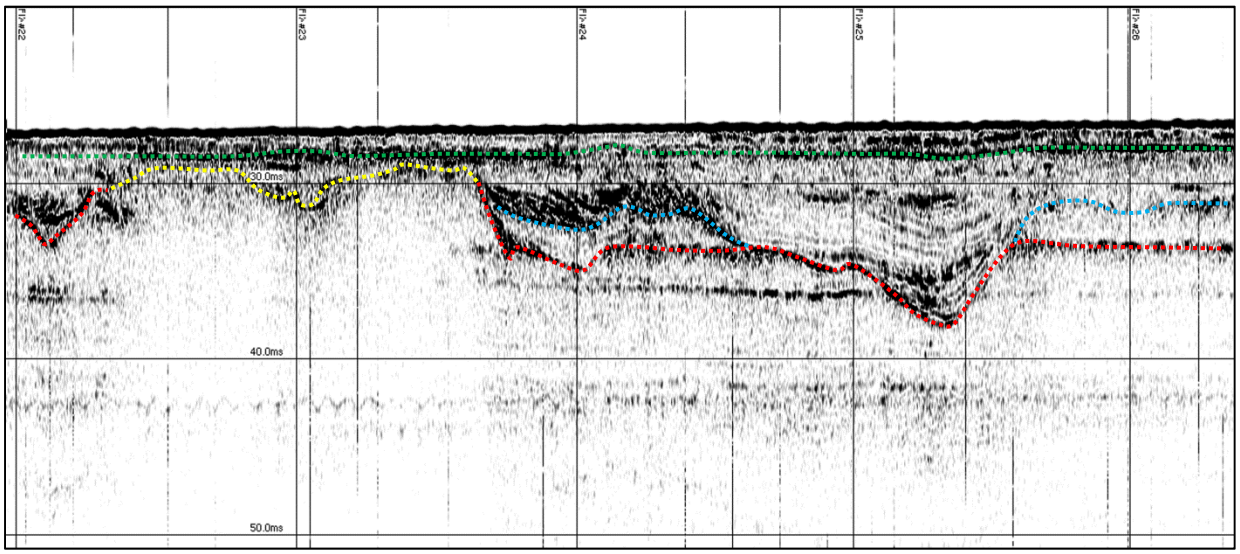

Figure 6.2.1 Annotated subbottom profiler image of survey line 6 depicts the topographic feature (yellow) and inset terrace (cyan) identified in the 2008 report with the channel horizon (red) and interpreted ravinement surface (green). Vertical scale lines are in 150 m intervals; horizontal scale lines are in 7.5 m intervals; north is at right (modified from Keith and Geresi 2008).

The interpreted features in GA 426 were selected for inclusion in this study because of their shallow depth and apparent similarity to high probability features for archaeological site occurrence and preservation as defined by CEI (1977) and Waters (1992). A new survey grid was created and centered on the topographic feature, with a north-south and an east-west survey line serving as the central axis. Additional survey lines were created so that twenty lines extended to the east and west of the interpreted feature, oriented north-south, and spaced at 25 m (82 ft) intervals. Due to the east-west orientation of the channels, tie lines were designed over the grid at approximately 150 m (500 ft) intervals. All survey lines were 900 m (1,500 ft) in length (Figure 6.2.2). Survey at GA 426 was conducted on July 19, 2008. The acquired data were interpreted digitally and contoured. Vessel stability issues resulted in significant heave that could not be processed out of the survey data, resulting in extremely distorted images. Additional survey lines were created over the interpreted features of interest for use in

illustrating the feature further (lines 501-511) and were acquired by Tesla Offshore's survey vessel M/V *Nikola* in 2011 while in transit between regularly scheduled work.

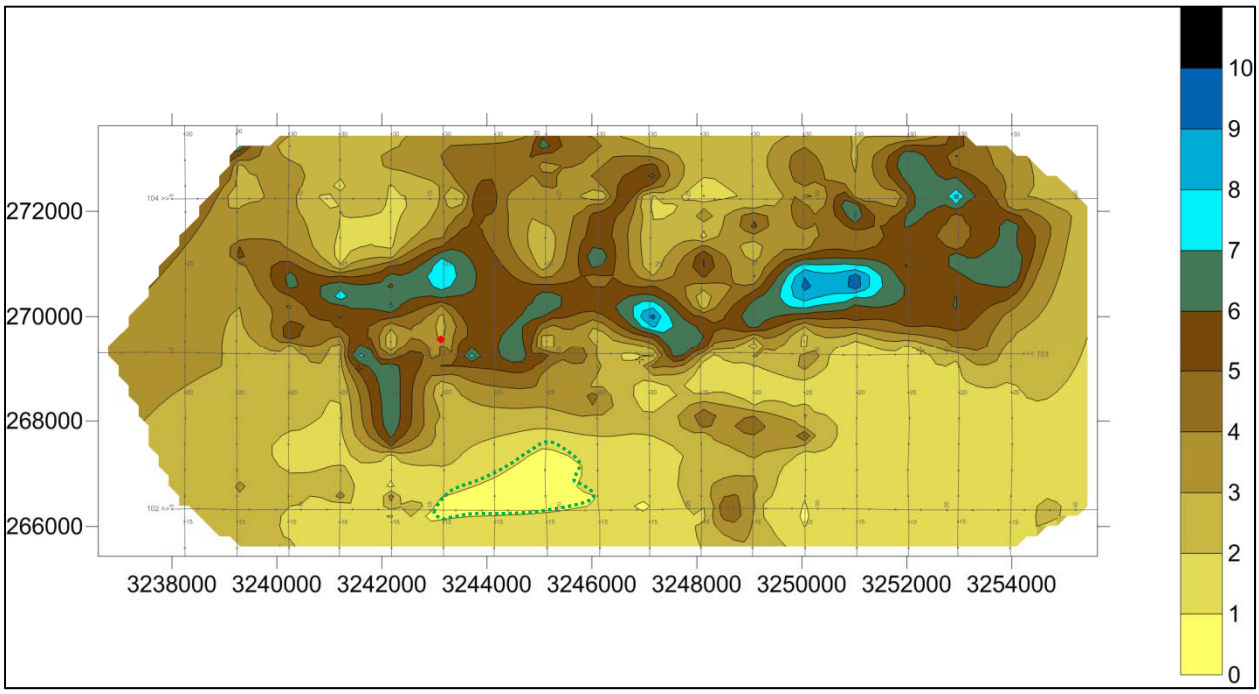

Figure 6.2.2 Contours depict the channel system as re-interpreted from the 2007 data set. The site of interest is indicated by the red diamond; the outcropping feature is outlined in green. The survey lines are superimposed over the channel system in black; primary survey lines are spaced 300 m (82 ft) apart. Depths are in meters below the seafloor.

The 2008 data set was designed to provide detailed coverage of the inset terraces observed to either side of the topographic feature, and more accurately delineate the features' boundaries. The 2008 data indicate greater variability within the channel's margins than was plotted from the 2007 data, which is not unexpected since the 2007 interpretation was based on data acquired at 300 m (984 ft) intervals. The 25 m (82 ft) interval data depict greater variability along the X, Y, and Z axes, although it is apparent that inset terraces are preserved to both sides of the topographic feature (Figure 6.2.3). Maximum channel entrenchment is variable, and it is likely that discontinuous contours may be the result of poor data reflection based on survey line orientation.

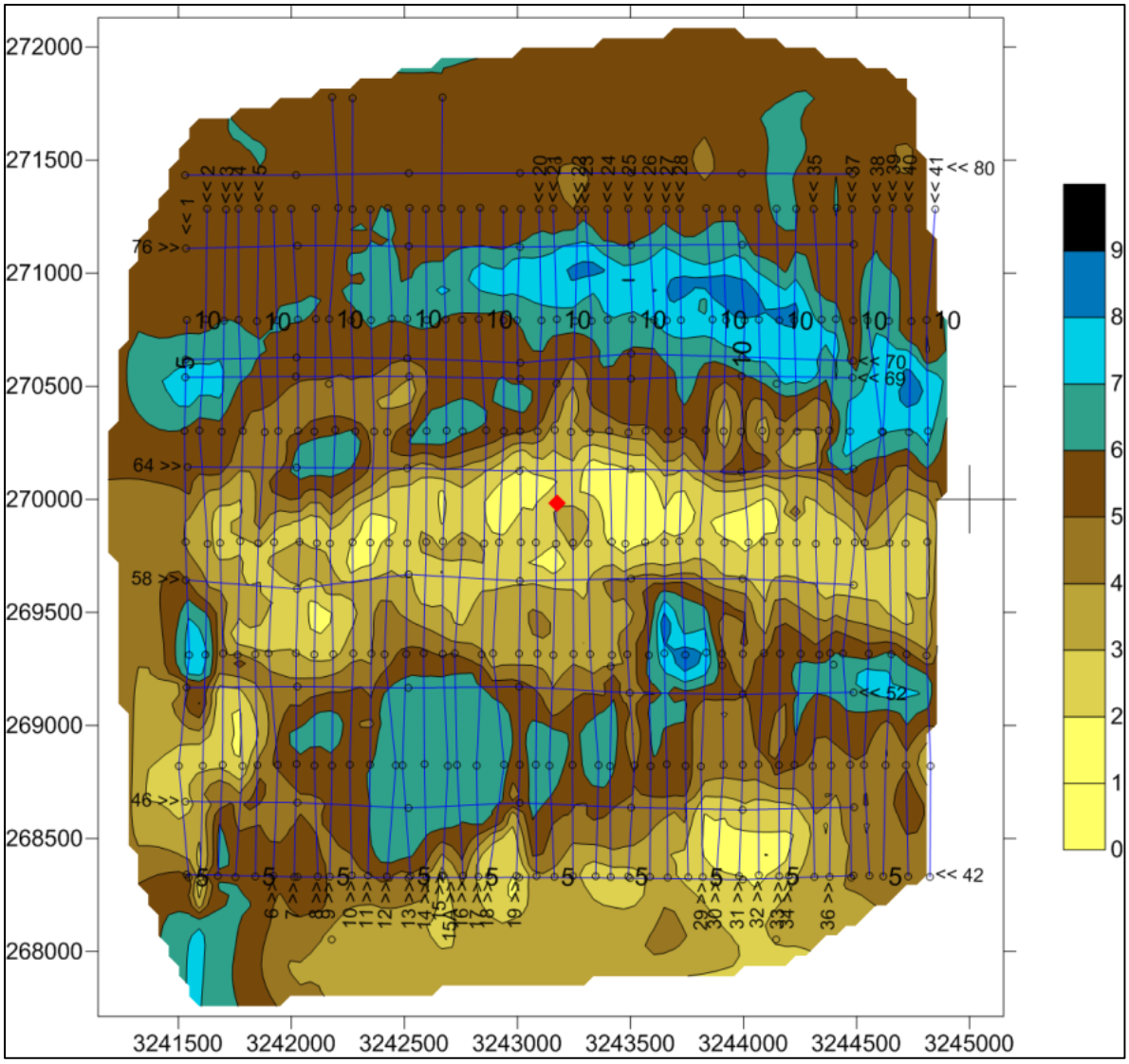

Figure 6.2.3 Contours depict the channel system as interpreted from the 2008 data set. The site of interest is indicated by the red diamond. The survey lines are superimposed over the channel system in black; primary survey lines are spaced 25 m (82 ft) apart. Depths are in meters below the seafloor.

The interpreted topographic feature and inset terrace associated with its northern margin were relocated during the survey (Figure 6.2.4). During data interpretation it became apparent that a highly reflective feature was associated with the inset terrace, representing a deposit with greater density than the surrounding sediments (Figure 6.2.5). This feature was hypothesized to represent either hard packed sediment or shell.

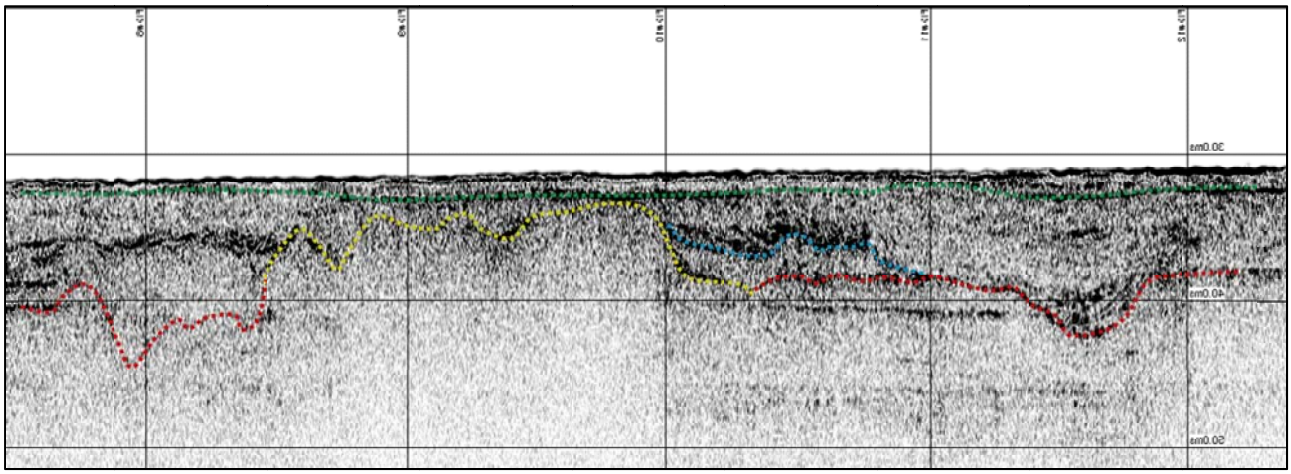

Figure 6.2.4 Annotated subbottom profiler image from survey line 504 illustrates the topographic feature (yellow) previously identified in 2007, as well as the inset terrace (blue), channel horizon (red), and ravinement surface (green). Data have been inverted to show the features in the same orientation as the 2007 image. Vertical scale lines are in 150 m intervals; horizontal scale lines are in 7.5 m intervals; north is at right.

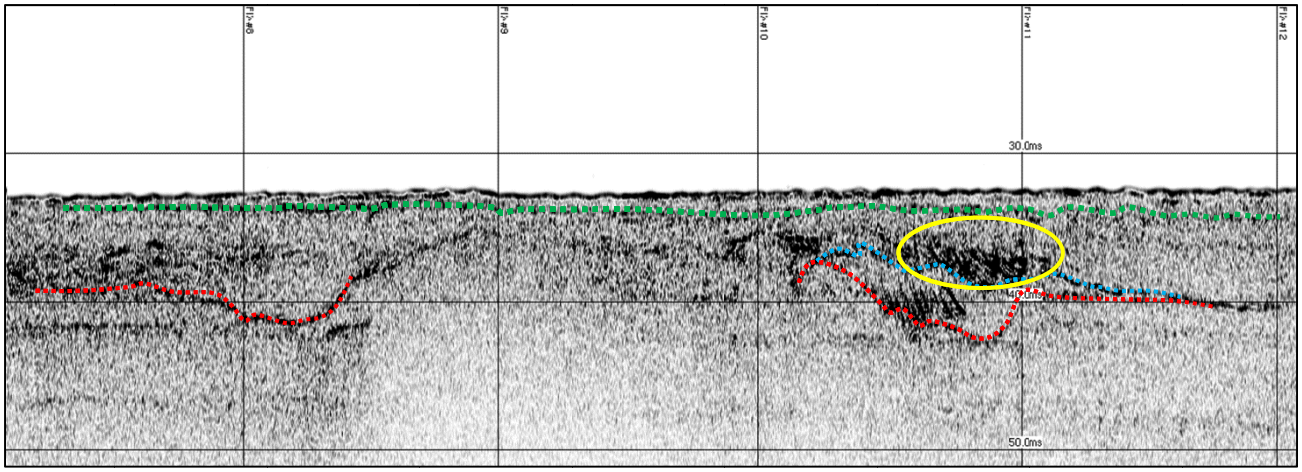

Figure 6.2.5 Annotated subbottom profiler image from survey line 502 of the extended inset terrace (cyan) with highly reflective feature (circled in yellow) identified from the 2008 survey, and also depicts the channel horizon (red) and ravinement surface (green). Vertical scale lines are in 150 m intervals; horizontal scale lines are in 7.5 m intervals; north is at right.

The interpreted features represent two distinct channels, but it is not possible to determine from the acoustic data alone whether or not the channels were active contemporaneously (Figure 6.2.6).

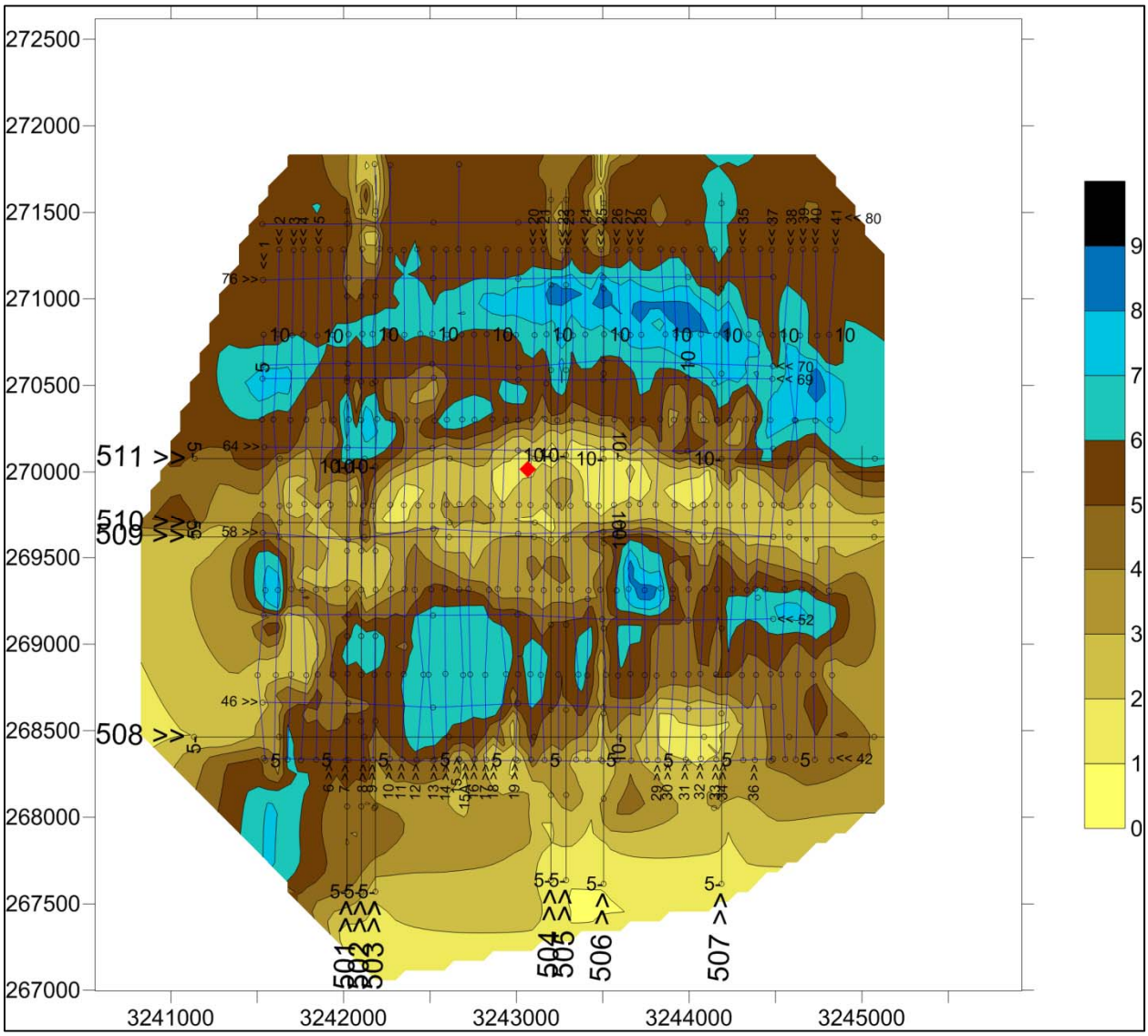

Figure 6.2.6 Contours depict the channel system as interpreted from the 2008 and 2011 supplemental data set. The site of interest is indicated by the red diamond. The survey lines are superimposed over the channel system in black; 2008 survey lines are spaced 25 m (82 ft) apart. Depths are in meters below the seafloor.

6.3 Discussion

The interpreted terraces and levees associated with the channel systems in HI 178 and GA 426 are located at depths ranging from 1.5 m to 6 m below the seafloor, respectively. Based on the sea-level curve created for this study, the landforms in HI 178 could have been exposed as dry

land until between 5,000 BP and 10,200 BP; the features in GA426 could have been available for occupation until final inundation between 7,800 BP and 11,800 BP (Figure 6.3.1). Contours based on the acoustic data have been used to generate plan view maps of the formerly exposed landscape, and indicate areas similar to high probability landforms for prehistoric site occurrence and preservation. These features appear to be buried by a thin veneer of sediment, but have not been truncated or significantly eroded by overlying sediment units. Sea-level curve data indicate that landforms in both of the survey areas would have been exposed and available for occupation and/or exploitation during the Paleoindian period; HI 178 may have remained exposed as late as the Archaic period. Without physical samples it is not possible to definitively ascertain the dates of these landscape features and their potential within prehistoric archaeology.

The geophysical survey represented just one phase of field work required to identify landforms, and more importantly, assess the potential for buried prehistoric sites in the northwestern GOM. Subbottom data are a relative data set and do not provide an accurate age of interpreted features therefore physical sampling is necessary to verify the interpretation of geophysical data. As stated by Wille (2005:56):

> Sediment acoustics needs verification by coring and probing regarding mineralogy, chemistry, and fossils. But it can reveal on its own even very weak reflecting horizons and is peerless in verifying whether a core stratification is only a local peculiarity or a symptomatic regularity over an extended ocean region.

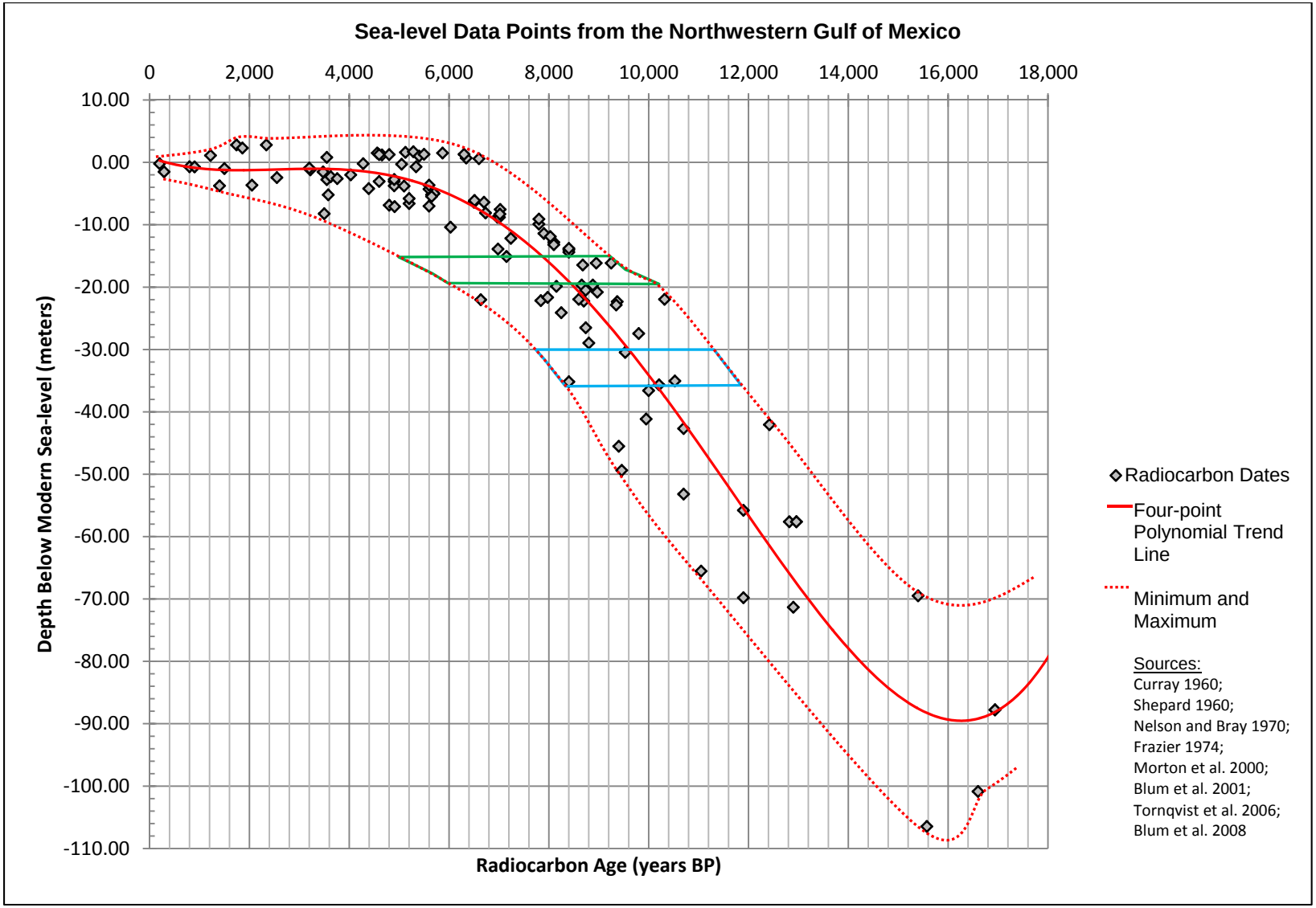

Figure 6.3.1 Landform depths from High Island 178 are plotted on the sea-level curved in green; Galveston 426 landform depths are plotted in blue. Both areas are at depths correlating with known occupations in the Gulf region.

CHAPTER 7. SEDIMENT CORING AND ANALYSES

Cores were acquired from the interpreted features identified from the acoustic survey profiles in HI 178 and GA 426. Coring locations were selected prior to the start of fieldwork. In some cases these cores had to be moved or cancelled in the field. Due to the presence of over-consolidated sediments, not all cores recovered the full 6 m (20 ft) maximum depth sample. A penetrometer was used to monitor coring depth and potential refusal on all cores, but malfunctioned during coring operations at GA 426. Once opened, the observed sediment stratigraphy within each core was correlated with the acoustic impedance observed on the profiles. Distinct landforms and features were evident within the sediment, while sediment subsampling allowed for the identification of discrete details, such as radiocarbon age and grain size.

7.1 High Island Area 178

Coring locations were selected from the combined geophysical data (Figure 7.1.1). Based on the interpreted subbottom data, core no. 1 was located over a terrace feature (Figures 7.1.2). Cores no. 2 (Figure 7.1.3) and 3 were located on top of a possible levee; core no. 3 was canceled in the field by the coring operator because of its proximity to an existing pipeline located approximately 75 m to the north. Core no. 4 was selected as an offsite control sample, but was canceled in the field because of its location within a designated shipping fairway. Core no. 5 was selected to core through stratified sediments as observed from the subbottom data (Figure 7.1.4). Cores no. 6 and 7 were selected in the field to substitute for the canceled cores no. 3 and 4. Core no. 6 was placed on a terrace (Figure 7.1.5), while core no. 7 was placed directly over top of the feature first identified as a levee from the 2007 survey (Figure 7.1.6).

All cores from the High Island 178 area were acquired on June 28, 2009. Core recovery ranged from 50% to 100% of the possible 6 meters maximum; sediment recovery within each core ranged from 72% to 97% (Table 7.1).

Table 7.1 Core Penetration and Sediment Recovery, High Island 178

Core No.	Maximum Core Depth (m)	Maximum Core Depth (%)	Sediment Recovery (m)	Sediment Recovery (%)
1	4.96	83	4.80	97
2	4.18	70	3.62	87
5	6.33	105	4.93	78
6	3.82	64	2.74	72
7	2.99	50	2.81	94

Once the cores were opened it became apparent that cores no. 2, 5, 6, and 7 reflected similar sedimentary units. Despite the similarity of the acoustic profiles, the observed sediment stratigraphy in Core no. 1 represents a unique area within the channel system (Figures 7.1.2 through 7.1.6), and is unlike any of the other cores from the HI 178 area. Cores no. 2, 5, 6, and 7 are located on opposing margins of the same channel feature (Figures 7.1.3 through 7.1.6). Cores no. 2, 6, and 7 are located on a probable naturally-occurring levee and associated terrace, and core no. 5 is on the opposite channel margin. Core no. 1 is interpreted as a separate inset terrace.

7.1.1 Interpreted Levee Feature

Cores 2, 7, and 6 represent an approximate west-east transect 170 m long across an interpreted levee bounded on three sides by a channel. Core no. 5 is located 625 m away, on the eastern side of the same channel, in-line with cores 2, 7, and 6 along a northwestern-southeastern axis. Core no. 5 was interpreted as having probable Holocene sediment to a depth of approximately 3 m (10 ft) BSF, where a horizon of increased reflectivity suggested the depth of the subaerially exposed Pleistocene surface. Cores 2, 7, and 6 were interpreted as having approximately 1 to 2 m (3 to 6 ft) BSF of Holocene sediment overlying the interpreted subaerially-exposed Pleistocene surface. Once opened, the cores reflect this general pattern of sedimentation. Beginning in the west with core no. 2, soft, cohesive, probable modern marine and estuarine sediments occur from the top of the core to a depth of 142 cmbs (Figure 7.1.7). These sediments contain shell hash lenses and evidence of bioturbation. A horizon of stacked shell, including individual pieces measuring 6cm

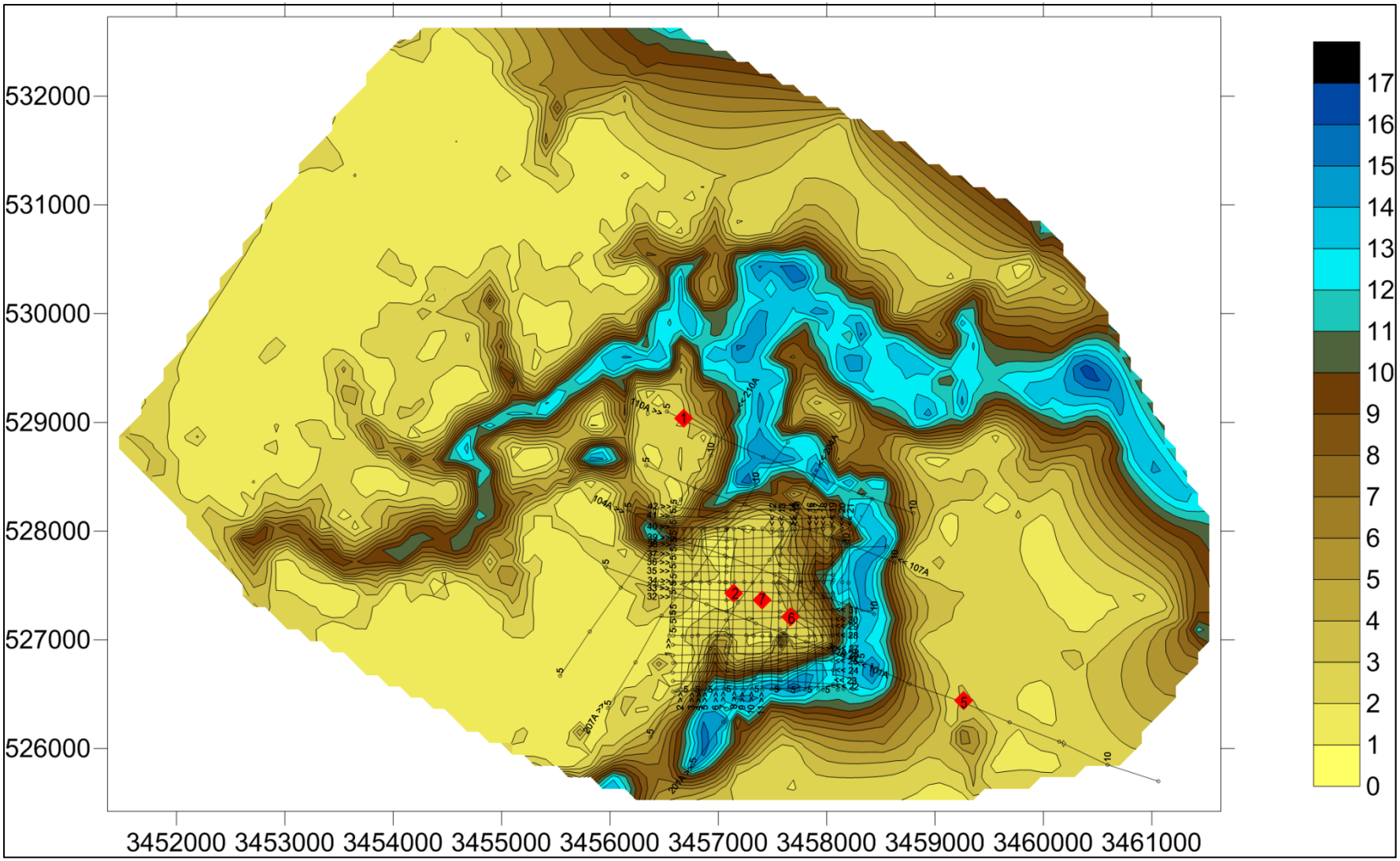

Figure 7.1.1 Core locations are depicted on the interpreted channel system contours as interpreted from the three available data sets (2007, 2008, and 2009). The 2008 survey lines are superimposed over the channel system in black; primary survey lines are spaced 25 m (82 ft) apart. Depths are in meters below the seafloor.

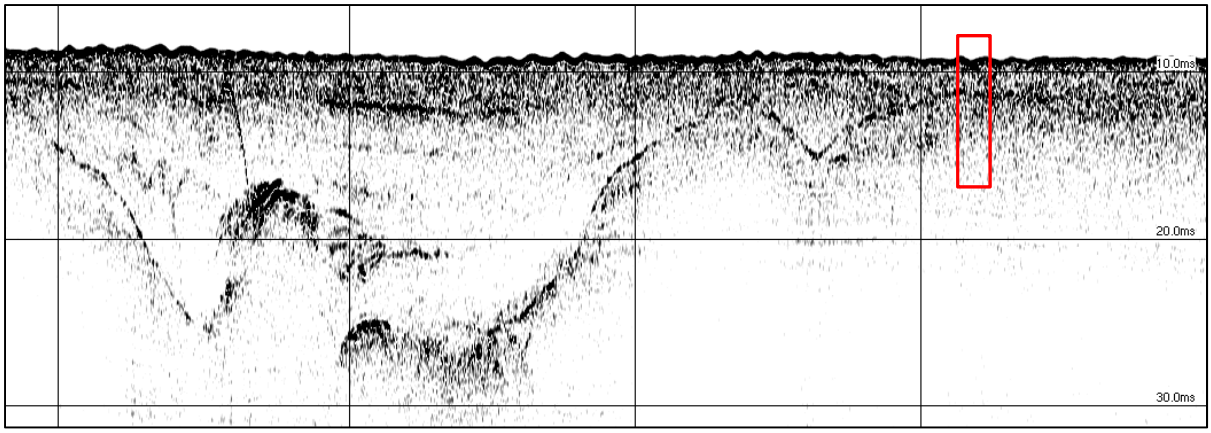

Figure 7.1.2 Annotated subbottom profiler image of core no. 1 location (outlined in red). Vertical scale lines are in 150 m intervals; horizontal scale lines are in 7.5 m intervals.

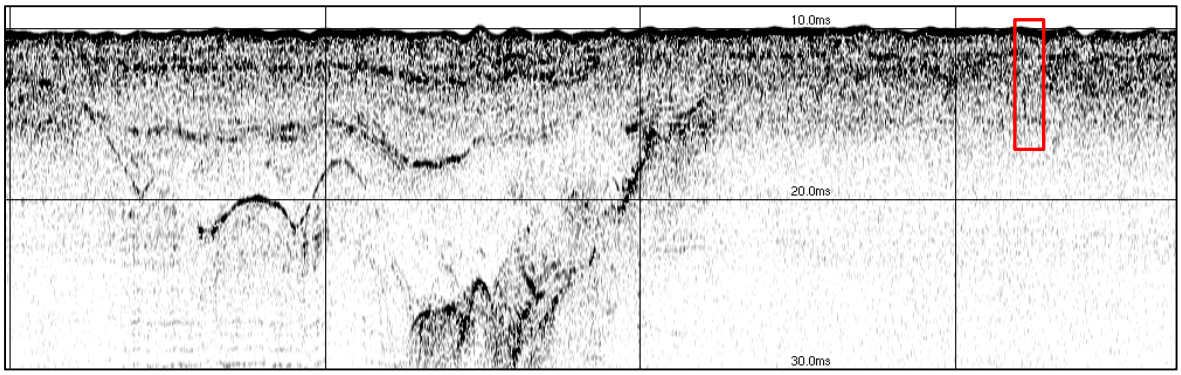

Figure 7.1.3 Annotated subbottom profiler image of survey line 504, with core no. 2 location outlined in red). Vertical scale lines are in 150 m intervals; horizontal scale lines are in 7.5 m intervals.

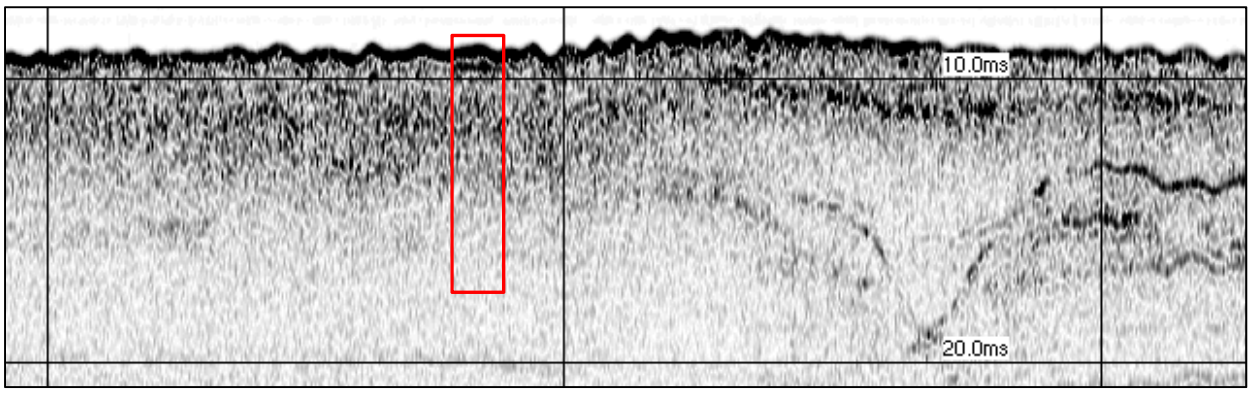

Figure 7.1.4 Annotated subbottom profiler image of survey line 507, showing core no. 5 location outlined in red. Vertical scale lines are in 150 m intervals; horizontal scale lines are in 7.5 m intervals.

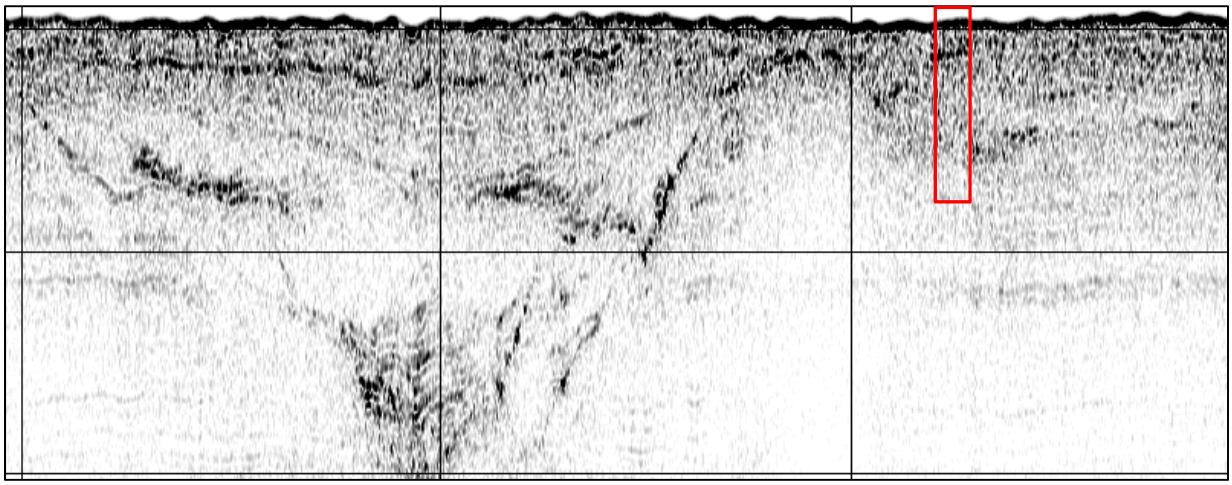

Figure 7.1.5 Annotated subbottom profiler image of survey line 506 showing core no. 6 location outlined in red. Vertical scale lines are in 150 m intervals; horizontal scale lines are in 7.5 m intervals.

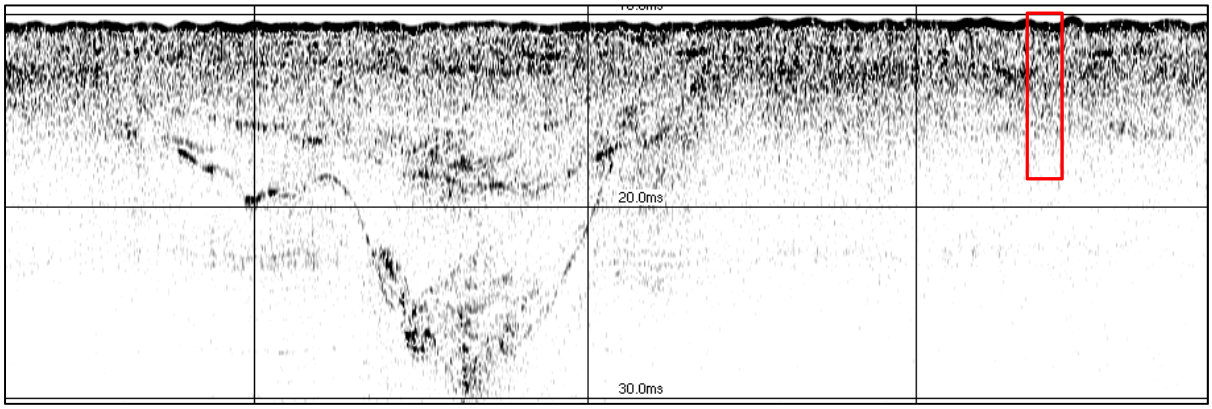

Figure 7.1.6 Annotated subbottom profiler image of survey line 505 showing core no. 7 location outlined in red. Vertical scale lines are in 150 m intervals; horizontal scale lines are in 7.5 m intervals.

x 3cm, immediately underlies the probable Holocene sediments to a depth of 160 cmbs. The remaining sediments within Core no. 2 consist of silty sand interspersed with carbonate nodules and exhibit significant lenses of oxidized sediment.

Core no. 7 represents the feature originally identified from the 2007 survey data. Like Core no. 2 the uppermost sediments consist of probable modern marine and estuarine sediments with occasional disarticulated shell fragments, however this unit does not extend past 93 cmbs (Figure 7.1.8). The remaining sediments within Core no. 7 consist of silty sand exhibiting increased oxidation with depth. Unlike Core no. 2, only a single carbonate nodule was identified, at a depth of 248 cmbs.

Core no. 6 is more similar to Core no. 2 than it is to Core no. 7, despite its closer proximity to Core no. 7. The uppermost sediments of Core no. 6 consist of probable modern marine and estuarine sediments to a maximum depth of 191 cmbs (Figure 7.1.9). This uppermost unit contains discrete lenses of shell hash and disarticulated shell fragments, as well as evidence of bioturbation. An intrusive shell hash lens is present between 90.5 and 108.5 cmbs. Sediments within the remainder of the opened core consist of silty sand interspersed with dark staining, possibly indicative of organic material, and exhibits increasing oxidation with depth.
Core no. 5 consists of approximately 63.5 cm of probable modern marine and estuarine sediment overlying silty sand to a depth of 493 cmbs (Figure 7.1.10). Substantial carbonate nodules are located within the silty sand horizon, beginning at 152 cmbs; evidence of bioturbation is not evident below a depth of 90 cmbs.

Based on the contoured acoustic survey data, core no. 5 is outside of the channelized area and likely represents modern marine sediments over an estuarine transgressive unit that overlies the formerly exposed Pleistocene surface. Cores no. 2, 7, and 6 form a profile across a natural levee feature, which is overlain by modern marine sediment and an estuarine transgressive unit of variable thickness. Acoustic survey contours depict the probable Pleistocene-aged levee at depths ranging from 1 to 2 m BSF, which is reflected by the sediment units from these cores (Figure 7.1.11).

Sedimentary units were initially developed based on qualitative features such as sediment texture and Munsell color; additional attributes such as presence or degree of oxidation and bioturbation were also used to separate cores into discrete sedimentary units. Following core descriptions and

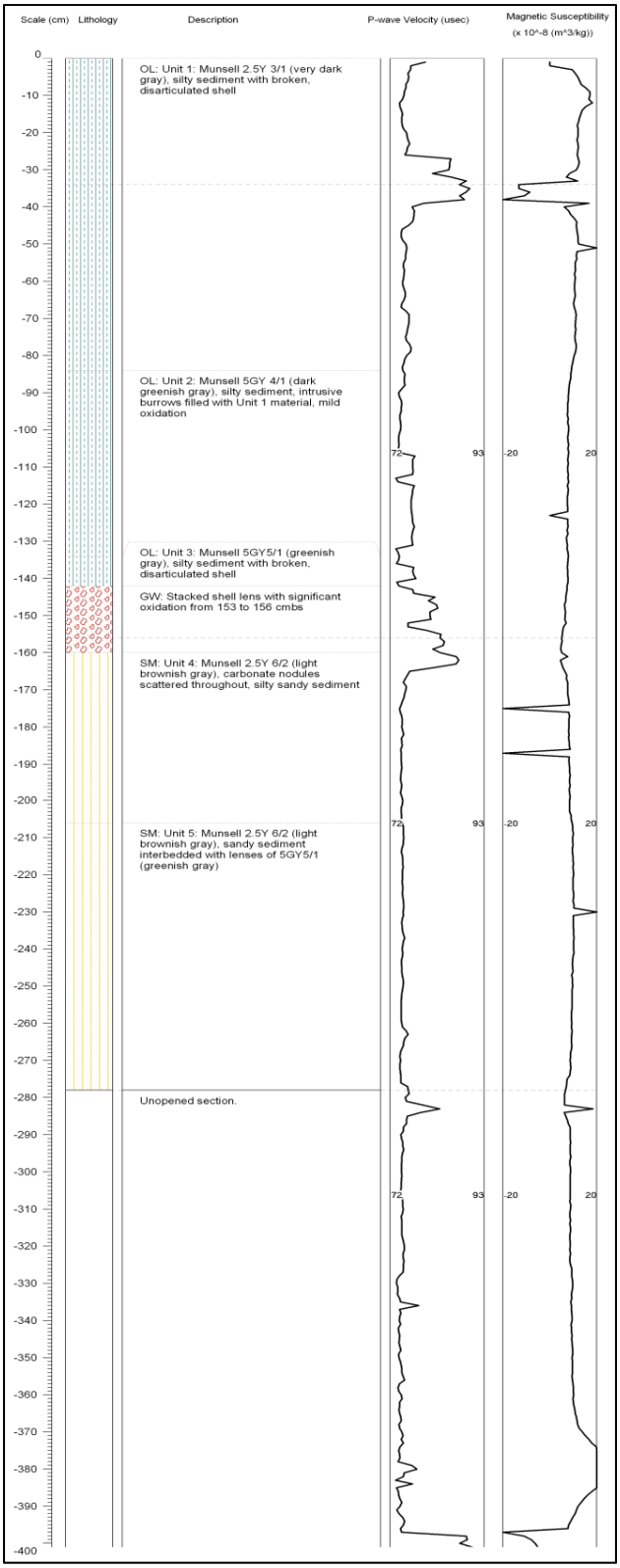

Figure 7.1.7 Core log prepared for No. 2 depicts the sediment units, as well as P-wave measurements (usec) and MS (volume) as measured from the Geotek MSCL (full size core logs are in Appendix B).

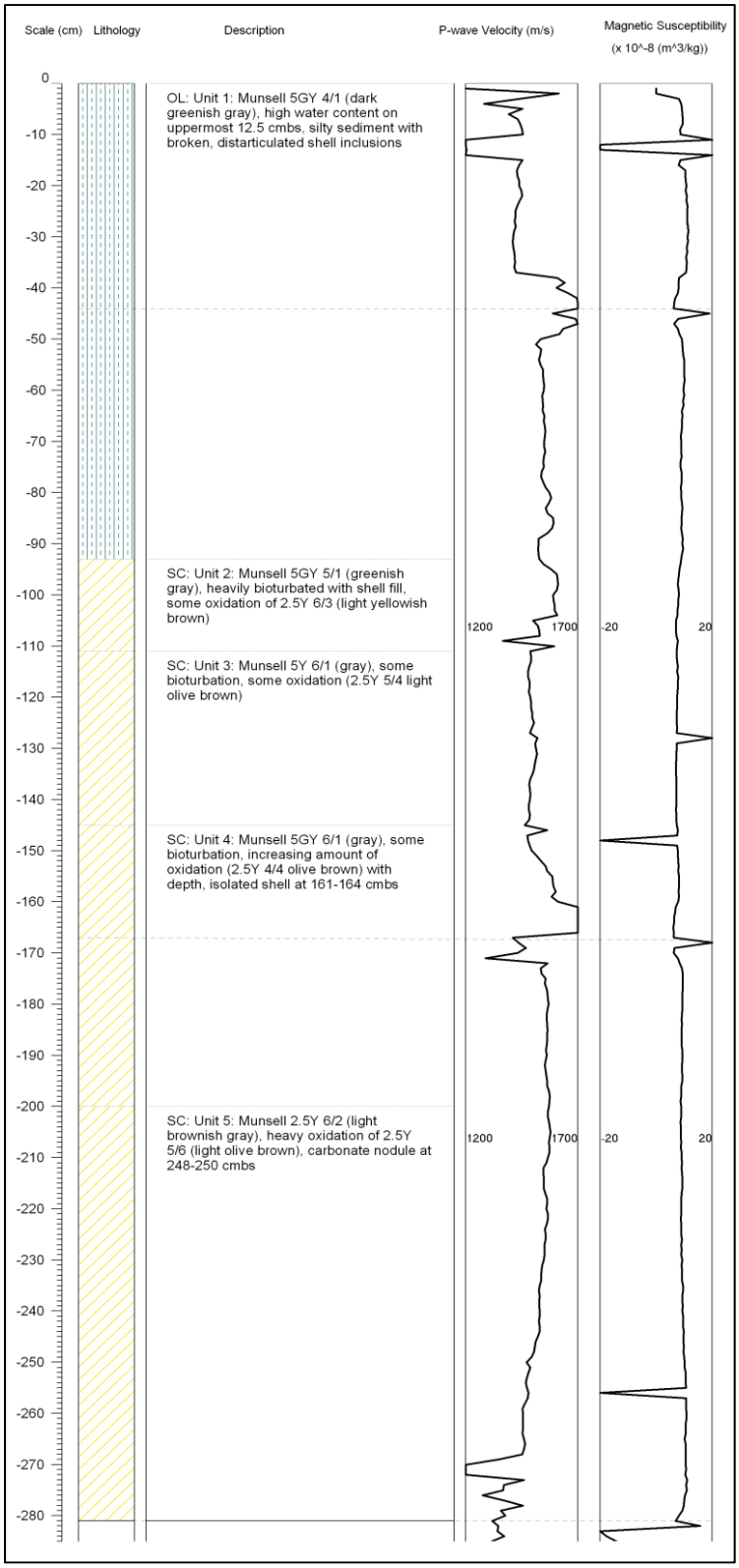

Figure 7.1.8 Core log prepared for No. 7 depicts the sediment units, as well as P-wave measurements (m/s) and MS (volume) as measured from the Geotek MSCL (full size core logs are in Appendix B).

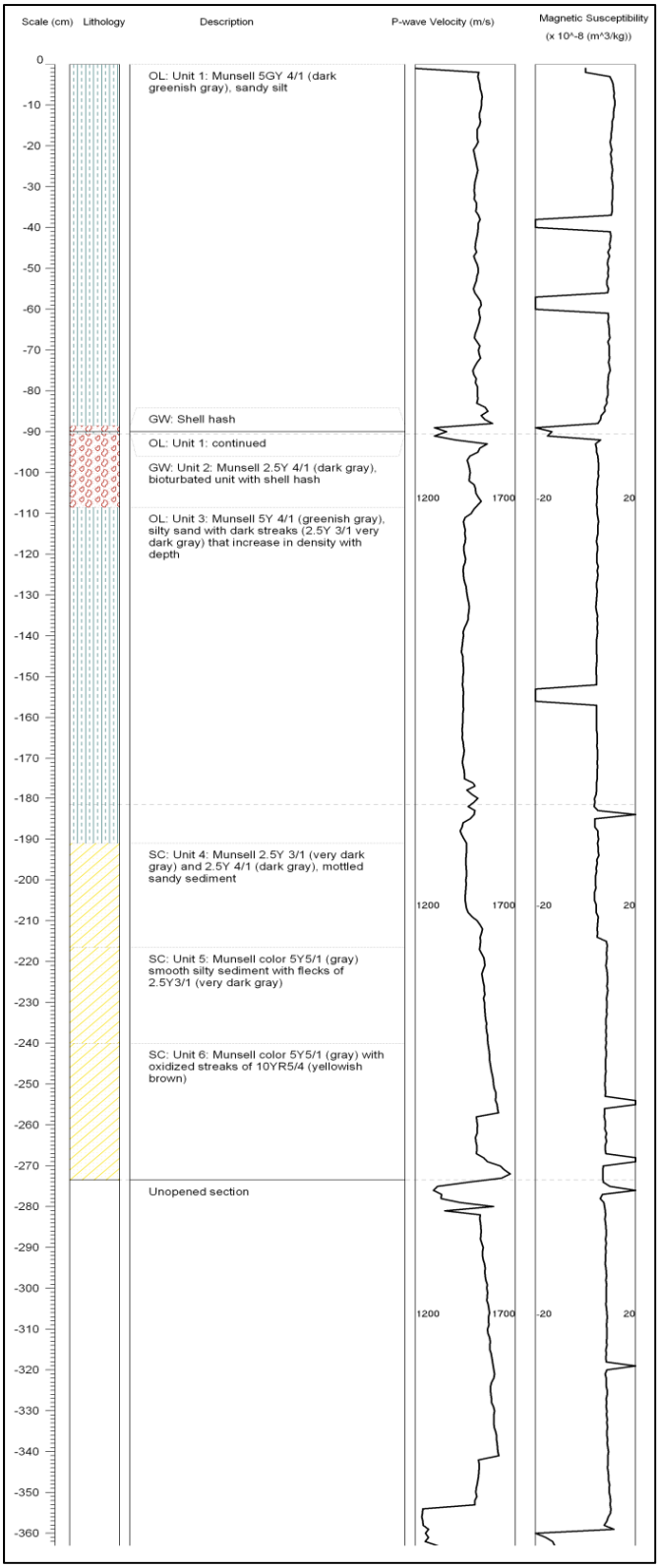

Figure 7.1.9 Core log prepared for No. 6 depicts the sediment units, as well as P-wave measurements (m/s) and MS (volume) as measured from the Geotek MSCL (full size core logs are in Appendix B).

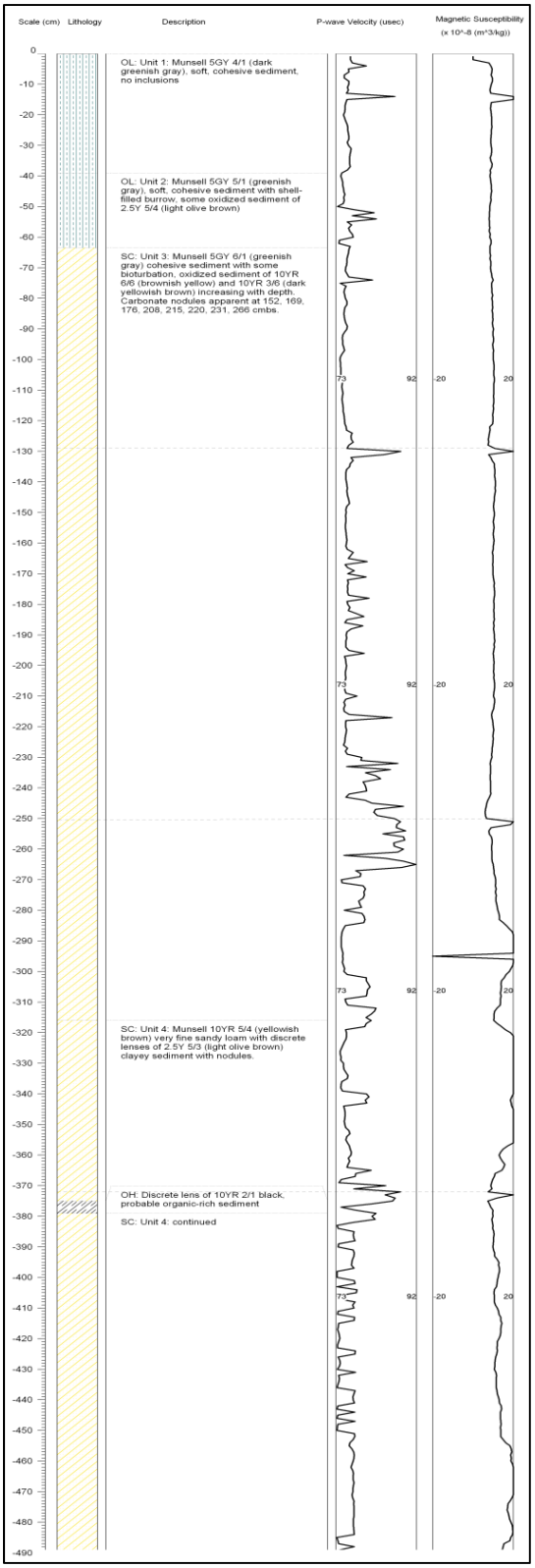

Figure 7.1.10 Core log prepared for No. 5 depicts the sediment units, as well as P-wave measurements (usec) and MS (volume) as measured from the Geotek MSCL (full size core logs are in Appendix B).

initial assessment, physical samples were collected for grain size analysis and mass-specific measurements of magnetic susceptibility.

Physical samples were collected from Core no. 7 for grain size analysis; one sample was collected per unit based on the initial core description. Raw grain size values were plotted as s-curves, then calculated as both median grain size and graphic mean and rounded to the nearest hundredth (Table 7.2; Figure 7.1.12). Due to the similarity of the observed sedimentary units, results from Core no. 7 were assumed to be representative across cores no. 2, 5, and 6.

Table 7.2 Representative Grain Sizes for Core no. 7, HI 178

Sample No.	Sample Depth (cmbs)	Median (Md_{mm})	Graphic Mean Mz (mm)	Wentworth Classification
1	6	0.075	0.088	very fine sand
2	52	0.049	0.063	coarse silt / very fine sand
3	97	0.035	0.069	coarse silt / very fine sand
4	128	0.01	0.043	fine silt / coarse silt
5	172	0.045	0.073	coarse silt / very fine sand
6	240	0.106	0.098	very fine sand

Magnetic susceptibility (MS) was used in this study for multiple reasons: to determine if the observed stratigraphy correlated with discrete depositional events as indicated by the MS values; if plotted MS data would result in the identification of additional units not apparent through qualitative analysis; to detail charcoal horizons or units with significant charcoal; and as a proxy climate indicator. Unlike magnetic susceptibility measurements obtained from the Geotek MSCL, which were obtained as volume-specific values, independent MS measurements were made specific to the individual mass of each sample. Cores no. 2, 7, 6, and 5 were sampled continuously from the top of the core down through the interpreted marine and estuarine sediments, into the Pleistocene surface where observed oxidation suggested subaerial exposure (Figure 7.1.13).

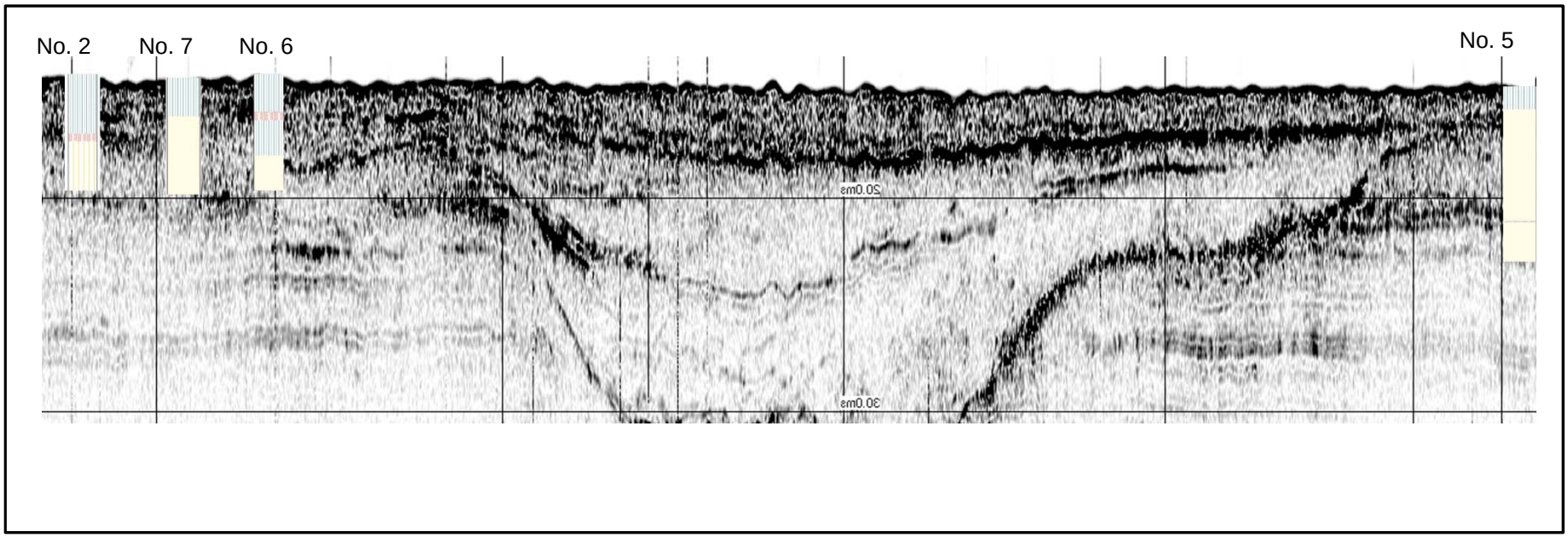

Figure 7.1.11 Core logs superimposed over the acoustic profile depict the sedimentary units and their representative places on the acoustic profile. Core logs and the acoustic profile are shown at the same vertical scale; horizontal scales are not equal.

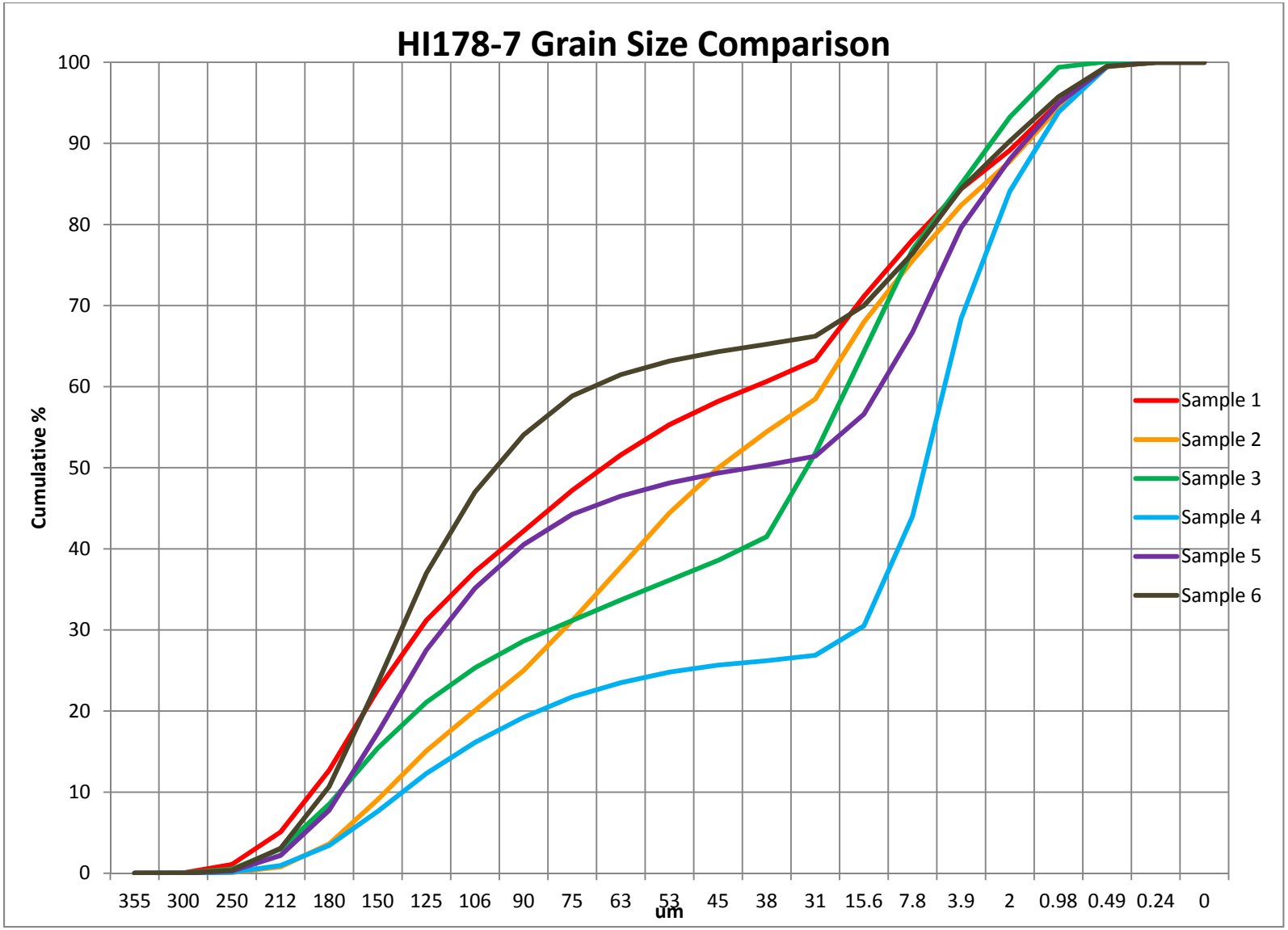

Figure 7.1.12 Comparison of grain size S-curves based on samples from HI 178 core no. 7.

Each of the MS curves prepared from Cores no. 2, 7, 6, and 5 depict a general trend in which the uppermost MS values are relatively high, but exhibit significant variability to a depth of approximately 50 cmbs (Figure 7.1.14). The uppermost sediments likely represent modern marine sediments that have experienced punctuated episodes of scour, mixing, and redeposition that have resulted in a fluctuating but overall increasing MS value. The next sequence of MS values is located between depths of 60 and 100 cmbs and represents a trend of MS values that are slightly lower than the overlying horizon and that exhibit less variability. The base of this sequence is identified by a significant increase from the next underlying MS value sequence, which represent the lowest values recorded in each profile. These values likely represent colder and drier climatic conditions, but without absolute dates it is not possible to determine the exact time period represented by this unit. Core no. 6 was the deepest profile measured for mass MS values and indicates that sediments within the lowest unit of the MS profile represent a time period associated with warmer and or wetter climate conditions. Profiles from cores no. 2, 7, and 5 are truncated at the top of this horizon but suggest that this sequence is found in all cores.

7.1.2 Interpreted Terrace

Core no. 1 was acquired from an interpreted terrace feature located approximately 550 m (1,820 ft) north-northwest of cores no. 2, 6, and 7. This terrace is bounded on the west, north, and east by a channel, with a channel fragment or possible meander loop bounding the southern margin. Core no. 1 was interpreted as having probable Holocene sediment to a depth of approximately 1 m to 1.5 m (3 to 5 ft) BSF, where a horizon of increased reflectivity suggested the depth of the subaerially exposed terrace surface. The sedimentary structure observed in Core no. 1 was much more complex than the sequence observed in cores no. 2, 7, 6, and 5 suggesting a completely different depositional environment.

The uppermost sediments of Core no. 1 consist of approximately 119 cm of soft, cohesive, probable modern marine sediment occurring from the top of the core, with discrete lenses of shell hash (Figure 7.1.15). Unlike any of the other HI 178 cores, the next sedimentary unit observed in Core no. 1 consists of soft, well consolidated sediment interspersed with peat or

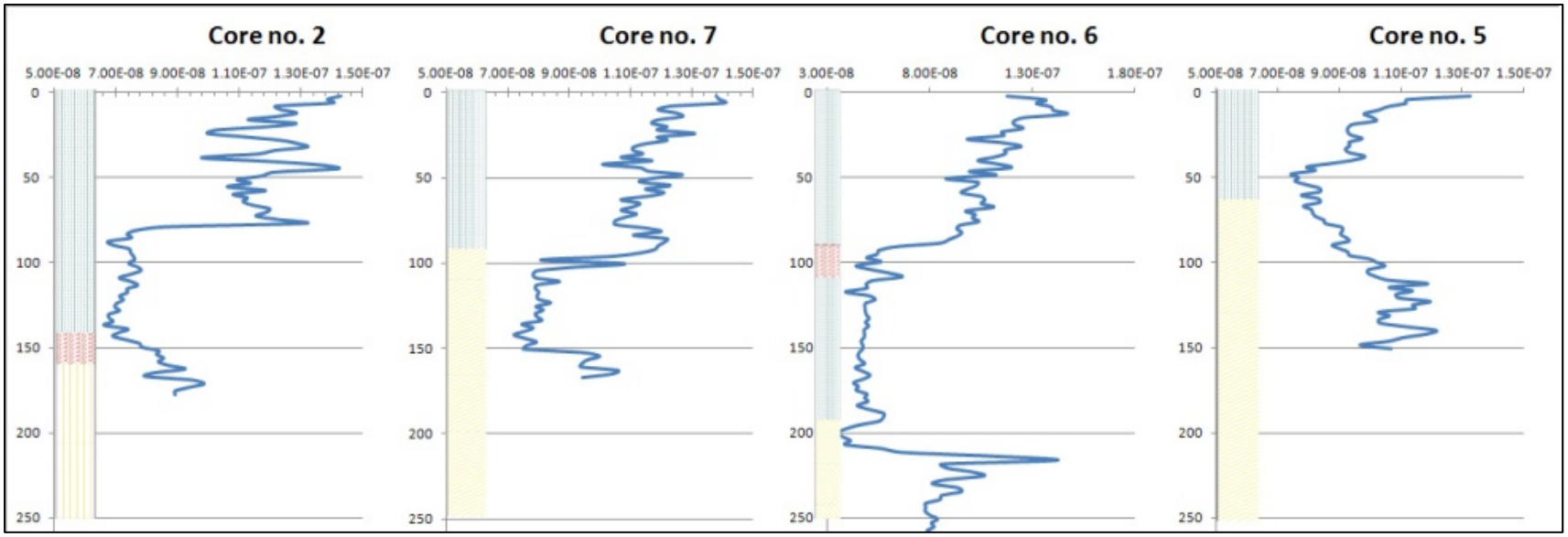

Figure 7.1.13 Diagram depicting MS data obtained from Cores no. 2, 7, 6, and 5 (as collected west-east), and interpreted sedimentary horizons.

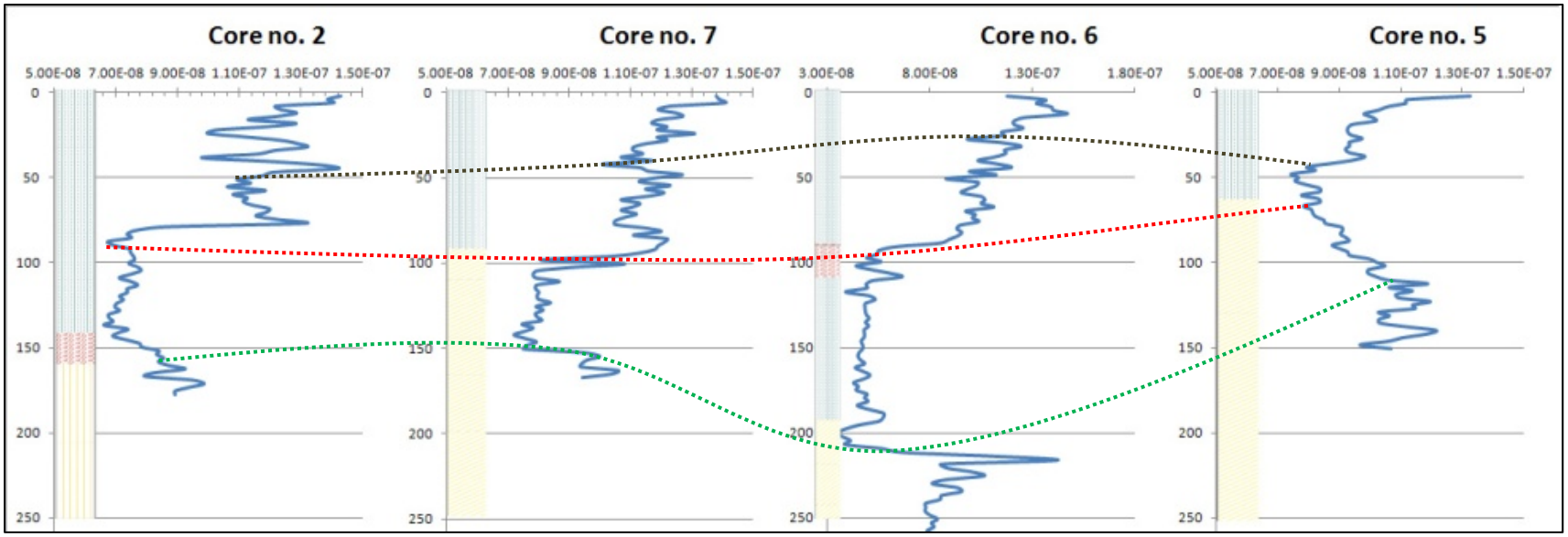

Figure 7.1.14 Annotated diagram depicting MS data obtained from Cores no. 2, 7, 6, and 5 (as collected west-east) depicting the probable ravinement surface indicating the maximum depth of modern marine sediments (as indicated in brown), the lower boundary of the probable estuarine sediment unit deposited during sea-level transgression (as indicated in red), and an anomalously low range of MS values that may indicate a discrete period of lower temperatures following the last glacial maximum (as indicated in green).

other highly organic material and charcoal flecks; a 2 cm thick charcoal lens is contained within this unit starting at a depth of 122 cmbs. This unit continues to a depth of 277 cmbs and contains two other intrusions; a 1 cm thick lens of silty sand located at a depth of 144 cmbs, and a 4 cm thick lens of cohesive sediment lacking any organic material located at a depth of 181.5 cmbs. A unit of silty sandy sediment, similar to those observed in Cores no. 2, 7, 6, and 5 begins at a depth of 277 cmbs and continues to the end of the recovered sediment, exhibiting increased oxidation with depth. The observed sedimentary sequence correlates with the expected stratigraphy from the acoustic profile (Figure 7.1.16).

As with the previous cores, sedimentary units were initially developed based on qualitative features such as sediment texture and Munsell color; additional attributes such as presence or degree of oxidation and bioturbation were also used to separate cores into discrete sedimentary units. Following core descriptions and initial assessment, physical samples were collected for grain size analysis and mass-specific measurements of magnetic susceptibility.

Physical samples were collected from Core no. 1 for grain size analysis; samples were collected at regular 10-cm intervals down the core. Additional samples were acquired between intervals when a distinctly different sediment horizon was encountered that would otherwise remain unsampled. Raw grain size values were plotted as s-curves, then calculated as both median grain size and graphic mean and rounded to the nearest hundredth (Table 7.3; Figure 7.1.17).

Core no. 1 was sampled continuously for magnetic susceptibility from the top of the core down through the interpreted marine and estuarine sediments, into the Pleistocene surface where observed oxidation suggested a former period of subaerial exposure (Figure 7.1.17).

The MS curve prepared from Core no. 1 depicts a general trend in which the uppermost MS values are relatively high, but exhibit significant variability to a depth of approximately 70 cmbs (Figure 7.1.17). It is probable that these uppermost sediments represent modern marine sediments that have experienced punctuated episodes of scour, mixing, and redeposition that have resulted in fluctuating MS values.

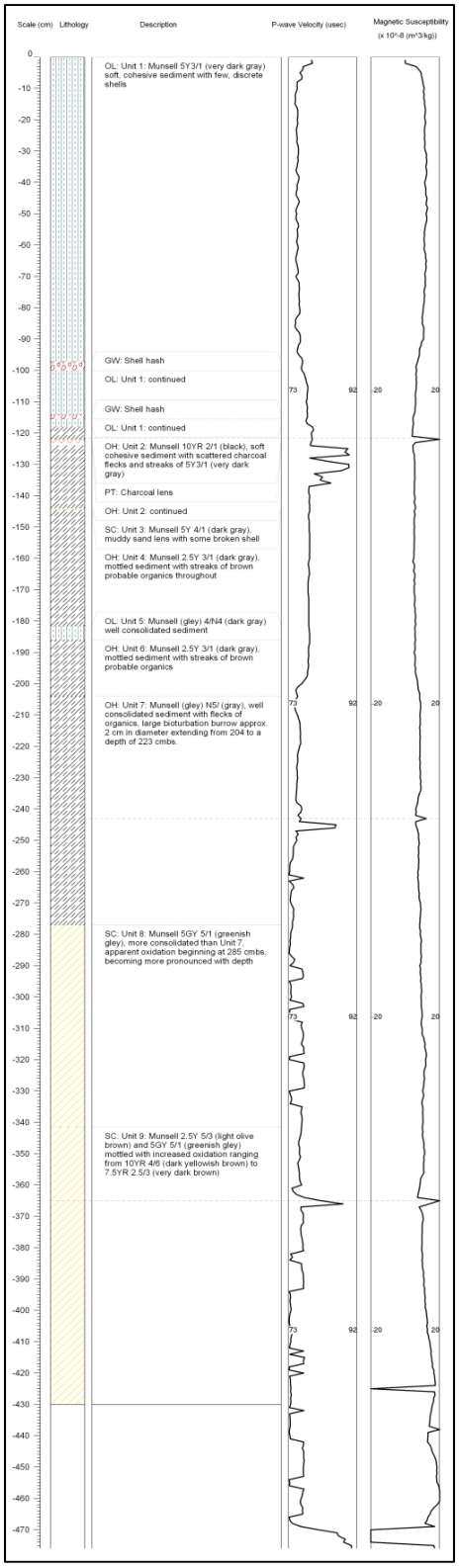

Figure 7.1.15 Core log prepared for No. 1 depicts the sediment units, as well as P-wave measurements (usec) and MS (volume) as measured from the Geotek MSCL (full size core logs are in Appendix B).

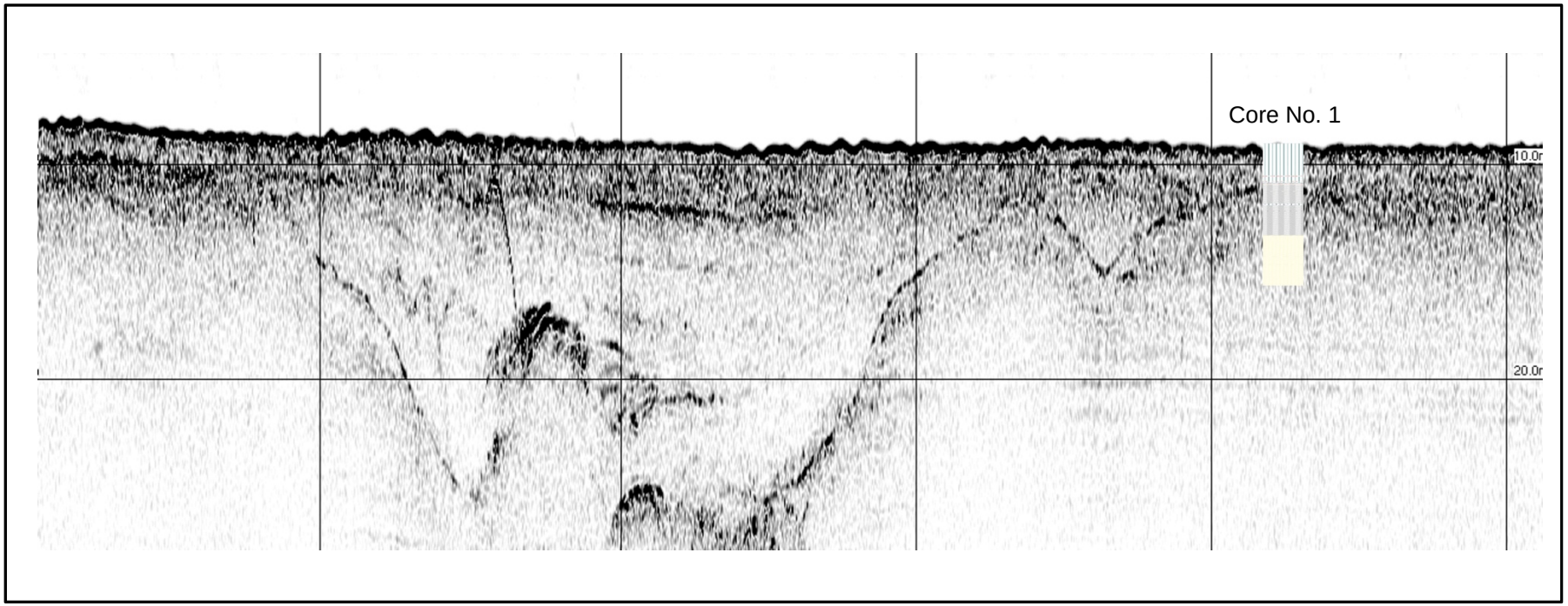

Figure 7.1.16 Core log no. 1 superimposed over the acoustic profile depicts the sedimentary units and their representative places on the acoustic profile. The core log and acoustic profile are shown at the same vertical scale; horizontal scales are not equal.

Table 7.3 Representative Grain Sizes for Core no. 1, HI 178

Sample No.	Sample Depth (cmbs)	Median (Md_{mm})	Graphic Mean Mz (mm)	Wentworth Classification
1	10	0.081	0.088	very fine sand
2	20	0.05	0.071	coarse silt / very fine sand
3	30	0.031	0.041	coarse silt
4	40	0.044	0.048	coarse silt
5	50	0.042	0.047	coarse silt
6	60	0.053	0.064	coarse silt / very fine sand
7	70	0.031	0.045	coarse silt
8	80	0.021	0.045	medium / coarse silt
9	90	0.031	0.055	coarse silt
37	93	0.023	0.050	medium / coarse silt
38	96	0.014	0.034	fine / coarse silt
10	100	0.031	0.053	coarse silt
39	104	0.006	0.013	very fine / fine silt
40	107	0.010	0.029	fine / medium silt
11	110	0.008	0.022	fine / medium silt
41	112	0.006	0.011	very fine / fine silt
12	115	0.003	0.005	clay / very fine silt
42	117	0.003	0.005	clay / very fine silt
43	119	0.007	0.024	very fine / medium silt
13	120	0.003	0.006	clay / very fine silt
14	124	0.003	0.005	clay / very fine silt
44	126	0.003	0.004	clay
45	128	0.003	0.005	clay / very fine silt
46	130	0.004	0.008	clay / very fine silt
47	135	0.003	0.006	clay / very fine silt
15	140	0.002	0.003	clay
16	143	0.004	0.006	clay / very fine silt
17	150	0.004	0.012	clay / fine silt
18	160	0.003	0.004	clay
19	170	0.021	0.060	very fine / medium silt
20	180	0.004	0.007	clay / very fine silt
21	183	0.004	0.006	clay / very fine silt
22	190	0.004	0.006	clay / very fine silt
23	200	0.042	0.055	coarse silt
24	210	0.021	0.033	medium / coarse silt
25	220	0.019	0.027	medium silt
26	230	0.018	0.032	medium / coarse silt

(Table 7.3 continued)

Sample No.	Sample Depth (cmbs)	Median (Md_{mm})	Graphic Mean Mz (mm)	Wentworth Classification
27	240	0.015	0.022	fine / medium silt
28	250	0.013	0.017	fine / medium silt
29	260	0.011	0.015	fine silt
30	270	0.005	0.007	very fine silt
31	280	0.018	0.025	medium silt
32	290	0.009	0.015	fine silt
33	300	0.011	0.014	fine silt
34	310	0.014	0.015	fine silt
35	320	0.013	0.015	fine silt
36	330	0.005	0.007	very fine silt

The sharp decline in MS values exists from 70 to 100 cmbs, at which point MS values remain consistently low to a depth of 190 cmbs; a noticeable spike in MS values is present at 122 cmbs, correlating with the charcoal lens observed in the core. MS values increase significantly from 190 to 210 cmbs, at which point MS values represent a third, distinct sequence of mid-range values with internal variability.

Samples were selected from Core no. 1 for radiocarbon sampling to provide absolute ages for use in correlating the magnetic susceptibility data. Since the charcoal lens represented a unique horizon specific to core no. 1, samples were taken above, below, and within this unit. All samples were submitted to Beta Analytic for testing (Table 7.4; Appendix C). Calibrated ages were calculated, however conventional radiocarbon ages are used in subsequent figures to allow direct comparison against previous sea-level data sets (Figure 7.1.18).

Table 7.4 Radiocarbon Sample Results for Core no. 1, HI 178

Sample	Sample Depth (cmbs)	Conventional Radiocarbon Age (BP)	Calibrated (2 Sigma) Radiocarbon Age (BP)
1	97-100	7,420 +/ 50	7,780 – 7,970
2	114-115.5	7,720 +/- 50	8,070 – 8,310
3	121.5-122	8,530 +/- 60	9,460 – 9,550
4	125	8,630 +/- 40	9,530 – 9,670
5	170.5	8,600 +/- 70	9,480 – 9,700
6	202	8,790 +/- 40	9,670 – 9,920

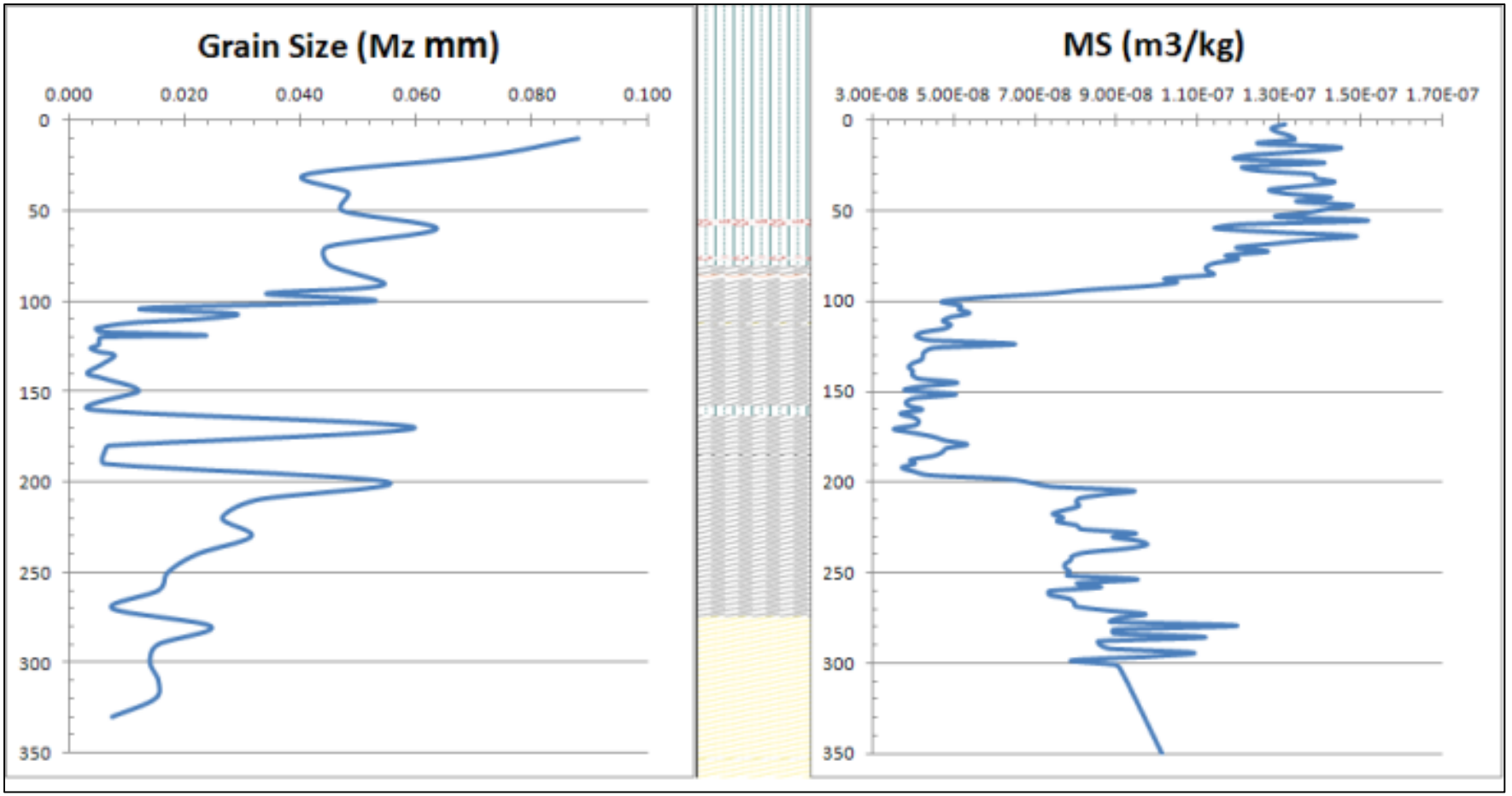

Figure 7.1.17 Diagram depicting grain size (graphic mean) and MS data obtained from Core 1, with sedimentary units provided for correlation.

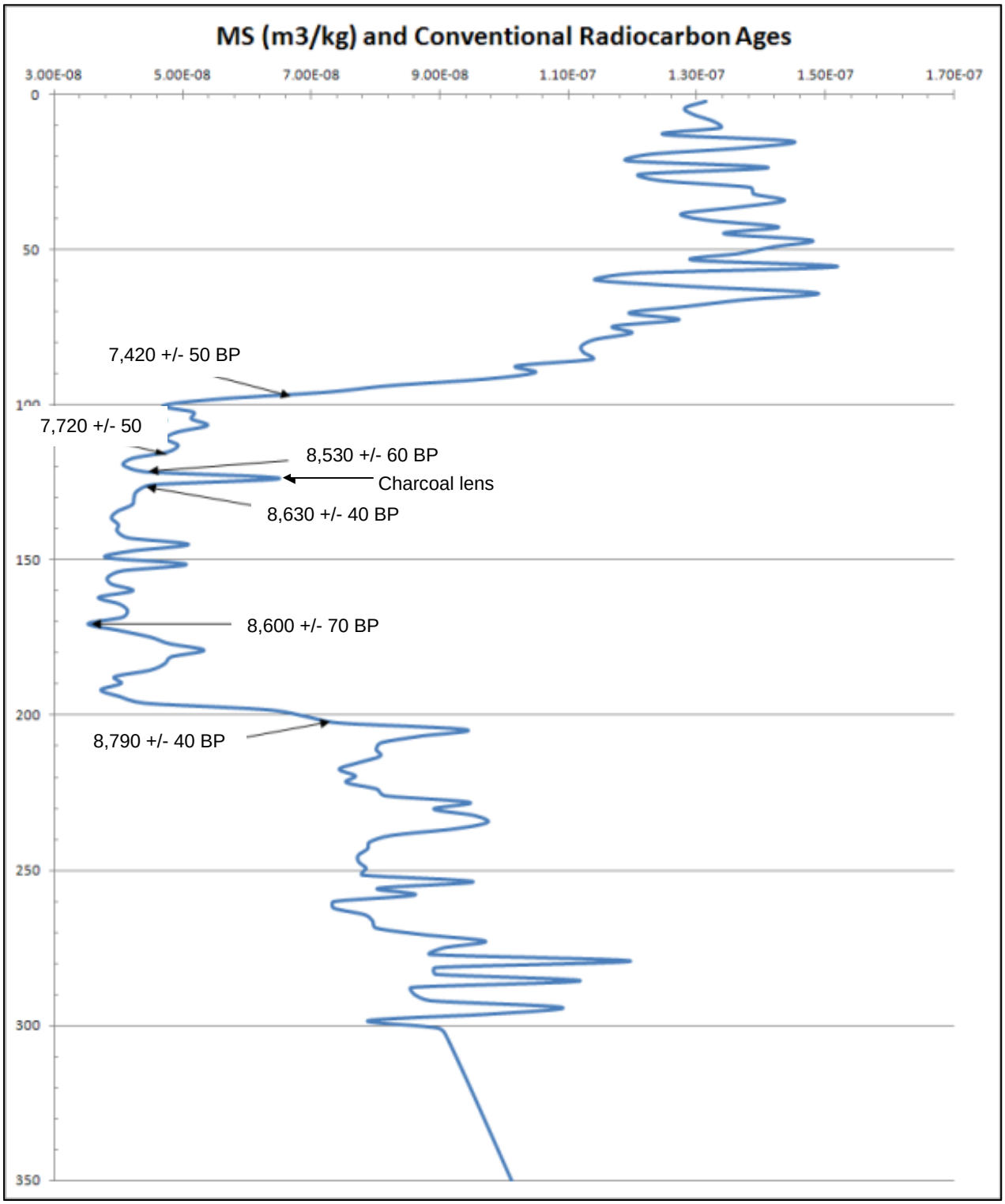

Figure 7.1.18 MS curve from Core no. 1 samples with conventional radiocarbon ages plotted at depth.

7.2 Galveston Area 426

Coring locations were selected from the combined 2007 and 2008 geophysical data (Figures 7.2.1 and 7.2.2). Based on the interpreted subbottom data, cores no. 1 and 2 were placed across the topographic feature as identified from the 2008 data, and represented the westernmost cores. During coring operations, core no. 2 was moved away from core no. 1 to approximate the lateral extent of the shell deposit observed within the sleeve for core no. 1. Cores were not acquired in numerical order and during operations core no. 3, which had been intended to sample a laterally migrating terrace extending north of the topographic feature, was cancelled in the field due to its proximity to the already acquired cores no. 7 and 8. Core no. 4 was positioned over a possible levee to the south of the southernmost channel. Core no. 5 was selected as an offsite control in an area of parallel bedded sediment with no visible channeling, located between the southernmost channel and the outcropping diapir feature. Core no. 6 was positioned over the topographic feature as identified from the 2007 data. Cores no. 7 and 8 were positioned due north of core no. 6 in order to test the interpreted inset terrace extending northward from the topographic feature. Core no. 9 was positioned adjacent to core no. 4 in order to increase the likelihood of coring through the possible levee feature, however this core location was moved in the field. Core no. 9 was relocated in order to acquire additional samples from the same surface location as core no. 1 after densely packed shell was observed in the core sleeves during retrieval. A combination of factors including the impending arrival of Hurricane Dolly and the presence of densely packed shells in the core sleeves for cores no. 1 and 9 resulted in the acquisition of two supplemental cores from Galveston Area 426. Cores no. 10 and 11 were acquired using the same surface location as core no. 1. Although the vessel drifted north during live-boat placement of the coring rig prior to acquisition of core no. 10, the intent was to acquire a large enough sample from the shell feature to determine if it represented a naturally-occurring or anthropogenic deposit. A total of 10 cores were acquired from this study area. Actual locations of all cores are shown in Figure 7.2.2.

All cores from the Galveston 426 area were acquired on June 30 and July 1, 2009. Core recovery ranged from 65% to 101% of the possible 6 meters maximum; sediment recovery within each core ranged from 95% to 101% (Table 7.5).

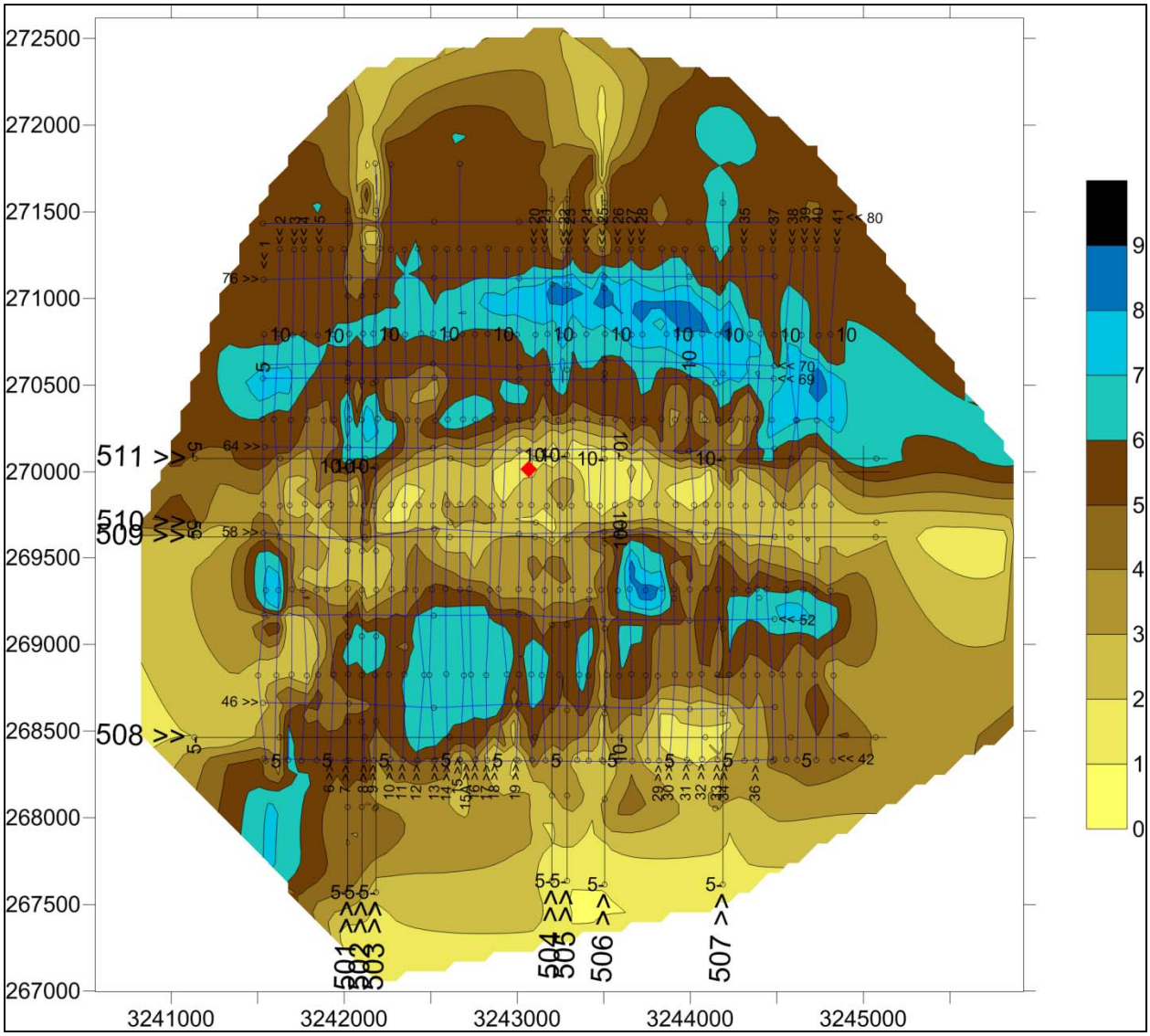

Figure 7.2.1 Contours depict the channel system as interpreted from the combined data sets. The topographic feature is indicated by a red diamond. The survey lines are superimposed over the channel system. Primary survey lines are spaced 25 m (82 ft) apart; 500 series lines were acquired in 2011. Depths are in meters below the seafloor.

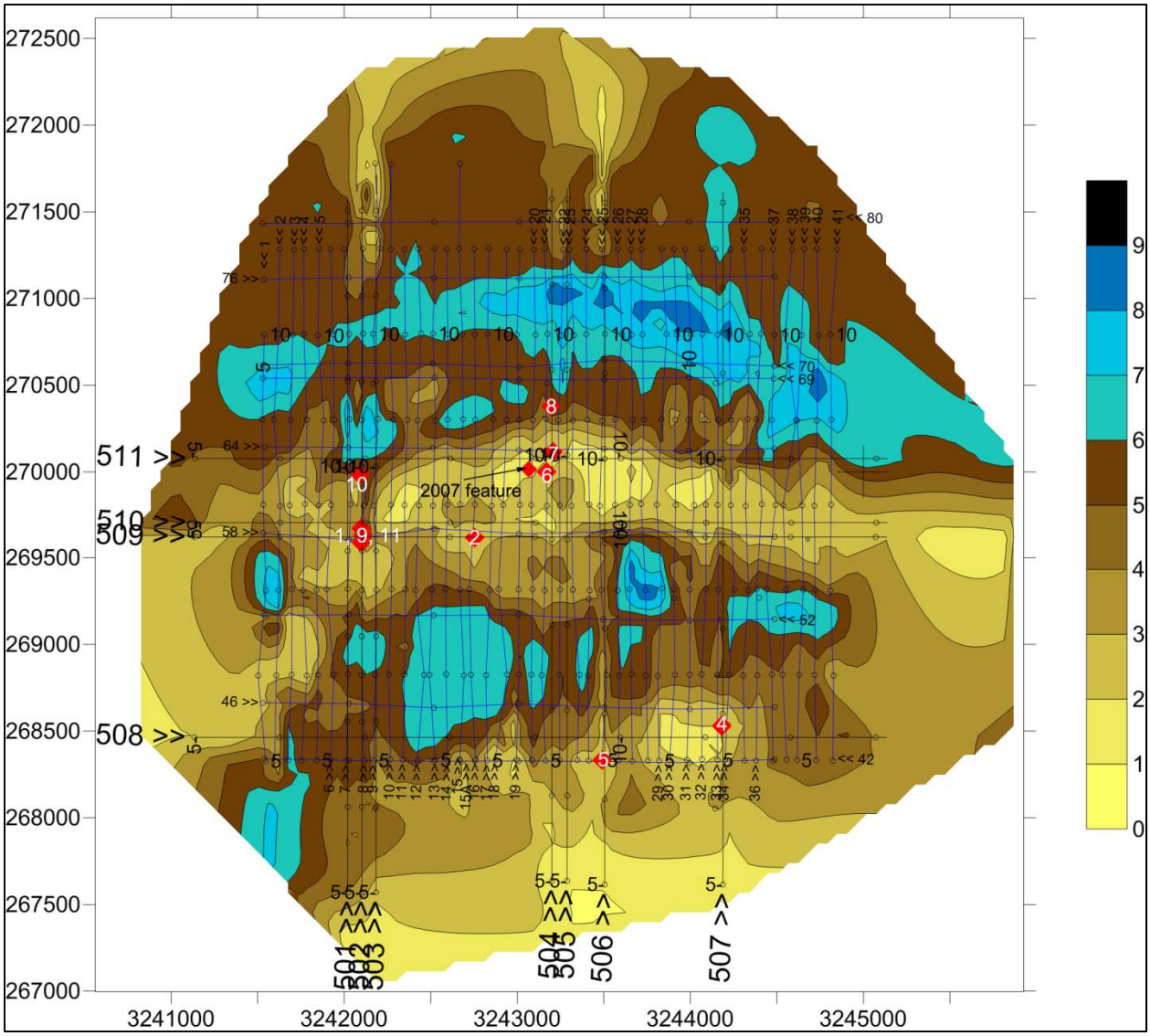

Figure 7.2.2 Core locations are labeled on the channel system contours as interpreted from the combined data sets. The 2008 survey lines are superimposed over the channel system in black. Primary survey lines are spaced 25 m (82 ft) apart; 500 series lines were acquired in 2011. Depths are in meters below the seafloor. Red diamonds indicate core locations.

Table 7.5 Core Penetration and Sediment Recovery, Galveston 426

Core No.	Maximum Core Depth (m)	Maximum Core Depth (%)	Sediment Recovery (m)	Sediment Recovery (%)
1	5.92	98	5.80	98
2	5.42	90	5.45	101
4	6.12	101	6.04	99
5	4.54	75	4.45	98
6	5.99	99	5.89	98
7	4.74	78	4.50	95
8	5.43	90	5.25	97
9	4.48	74	4.29	96
10	5.95	98	5.87	99
11	3.94	65	3.90	99

Once the cores were opened it became apparent that cores no. 1, 2, 9, 10, and 11 reflected similar sedimentary units related to a significant shell deposit (Figure 7.2.3). Cores no. 6, 7, and 8 form a profile across the southern margin of the northernmost channel, including an inset terrace (Figure 7.2.4). Core no. 4 (Figure 7.2.5) represents a possible intact levee, while core no. 5 (Figure 7.2.6) represents parallel to subparallel sediments outside of the channel system. Cores no. 4 and 5 represent isolated samples and are not included in the following discussion.

7.2.1 Interpreted Shell Deposit

Cores 1, 9, and 11 represent a significant shell deposit located between channels on the western boundary of the area surveyed in 2008. Core no. 10 is located 106 m (350 ft) north of the common surface location for Cores no. 1, 9, and 11; core no. 2 is located approximately 197 m (650 ft) east of the common surface location. All five cores were interpreted as having probable Holocene sediment to a depth of approximately 1.5 m (5 ft) BSF, at which point the channel system and associated features appeared to be relatively intact.

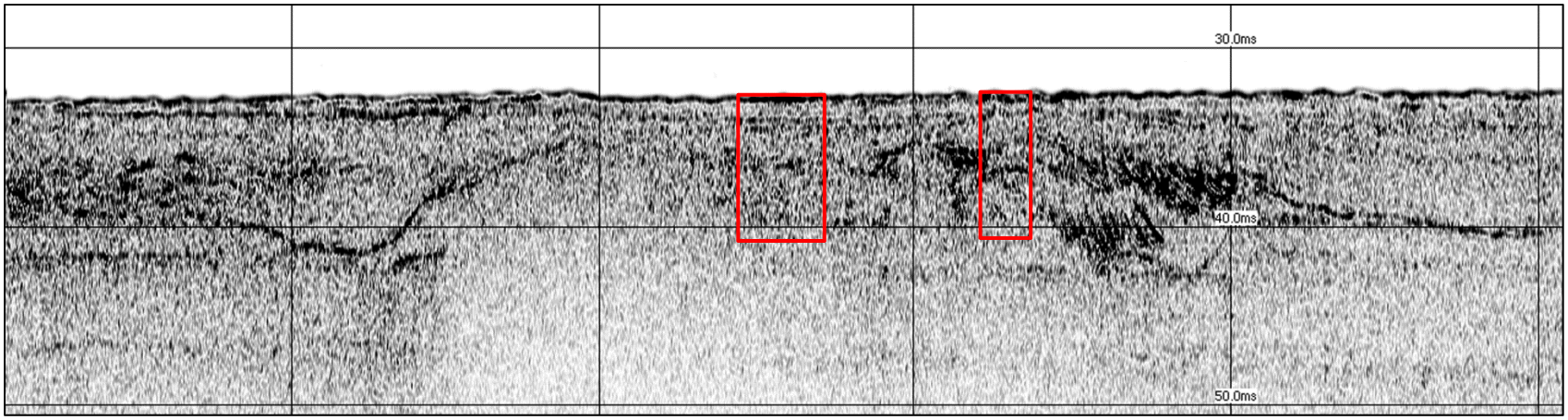

Figure 7.2.3 Annotated subbottom profiler image of survey line 502 showing the common surface location for cores no. 1, 9, and 11 (left) and core no. 10 (right) outlined in red. Vertical scale lines are in 150 m intervals; horizontal scale lines are in 7.5 m intervals; north is at right.

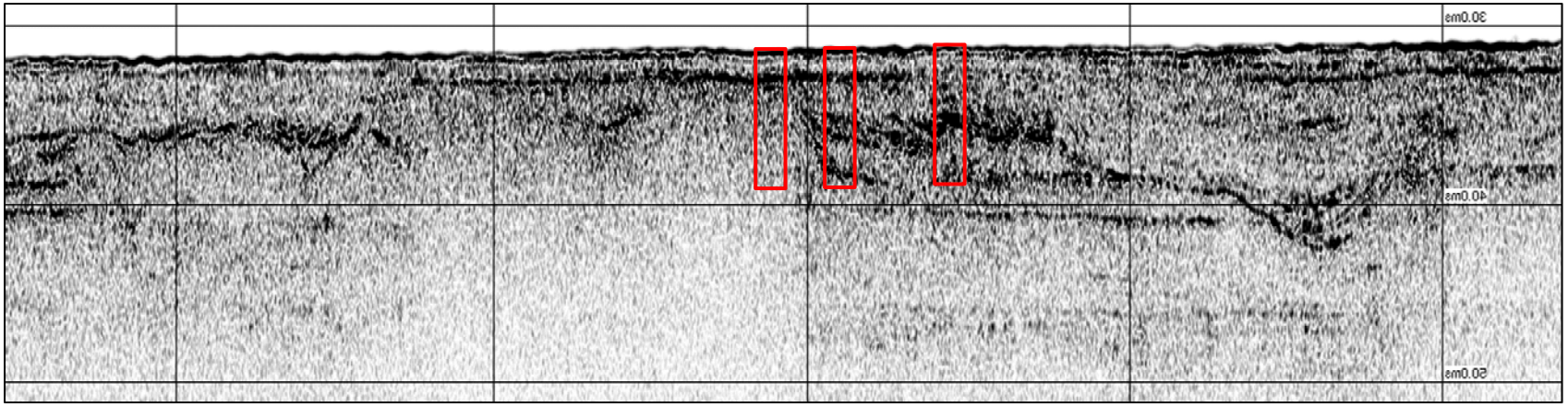

Figure 7.2.4 Annotated subbottom profiler image of survey line 504 showing the common surface location for cores no. 6 (left), 7 (middle), and 8 (right) outlined in red. Vertical scale lines are in 150 m intervals; horizontal scale lines are in 7.5 m intervals; north is at right.

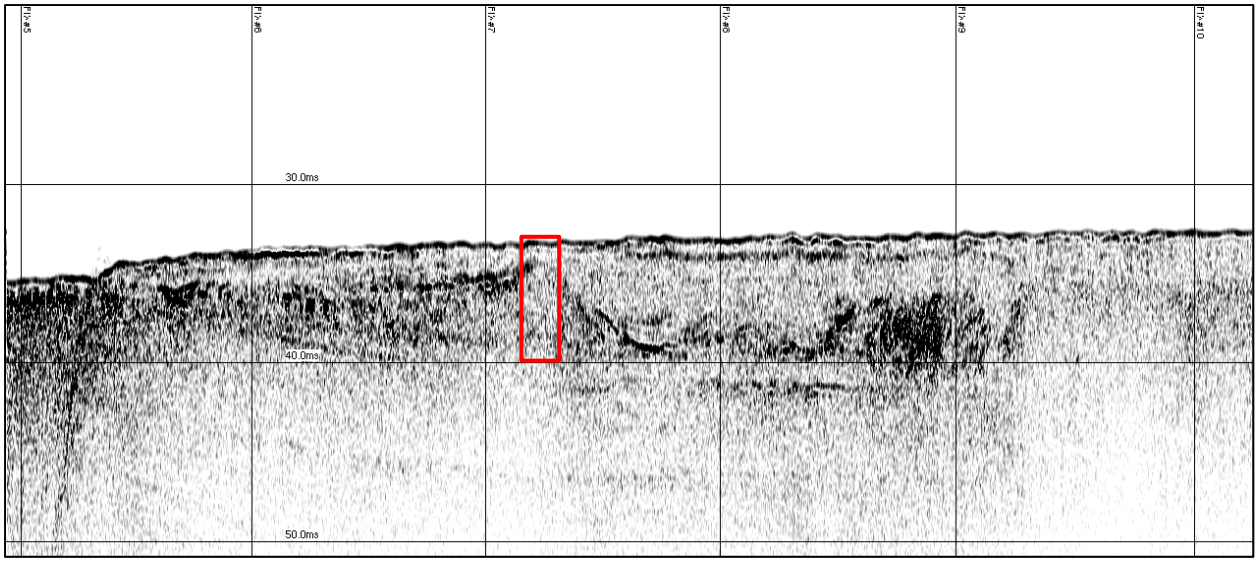

Figure 7.2.5 Annotated subbottom profiler image of survey line 507 showing the location for core no. 4 outlined in red. Vertical scale lines are in 150 m intervals; horizontal scale lines are in 7.5 m intervals; north is at right.

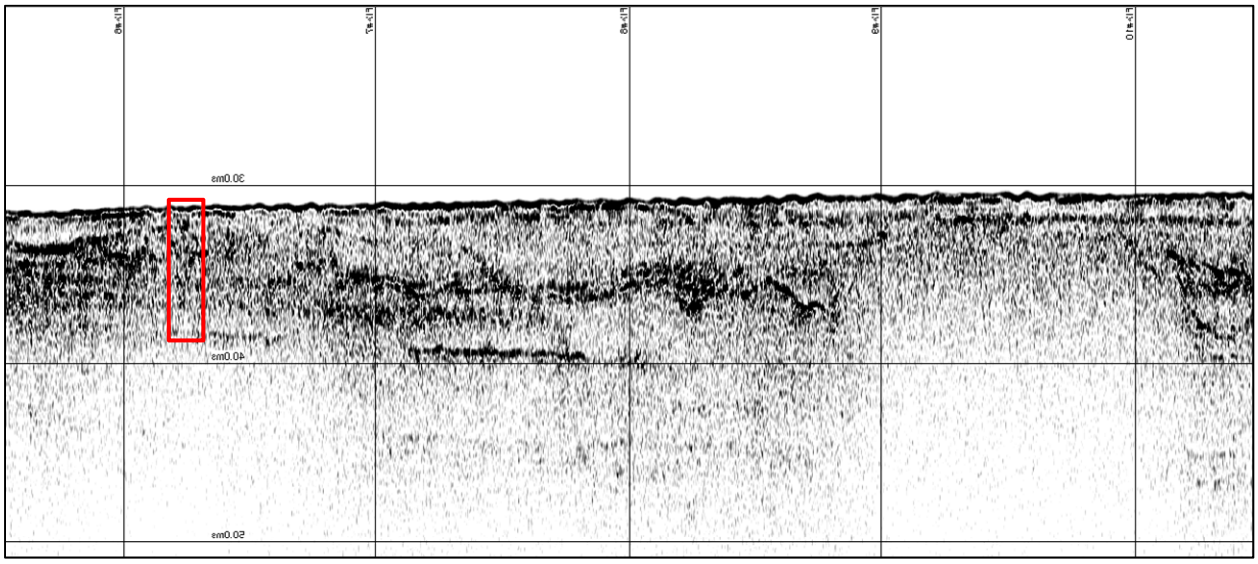

Figure 7.2.6 Annotated subbottom profiler image of survey line 506 showing the location for core no. 5 outlined in red. Vertical scale lines are in 150 m intervals; horizontal scale lines are in 7.5 m intervals; north is at right.

Core no. 1 was the first core acquired through the shell deposit, and once opened was found to contain approximately 85 cm of probable Holocene sediment with discrete shell lenses. This same sedimentary unit was found in cores no. 9, and 11, which were collected from the same

surface location (Figure 7.2.7). The penetrometer, used to monitor core depth and potential refusal, was not functioning properly during acquisition of cores at this location, therefore cores were timed and withdrawn after an estimated duration, resulting in artificially shortened cores 9 and 11. The next sediment unit across all three cores represents possible estuarine sediments with organic material. This unit overlies sediment units that include increasing amounts of coarser grained material with depth that overlie the densely packed shell deposit. The shell deposit continues past the captured ends of cores no. 1 and 11, but does not persist to the end of core no. 9 likely because of stratigraphic mixing caused by the common surface location.

Similar stratigraphic units were identified in cores no. 10 and 2, located due north and due east of cores no. 1, 9, 11, respectively. The uppermost sedimentary unit in core no. 10 is the same as those within cores no. 1, 9, and 11; all four cores are within 106m (350 ft) of one another. Although core no. 2 lacks this same sedimentary unit at the top of the core, the remaining sequence is similar to that of core no. 10 (Figure 7.2.8). Core no. 10 contains approximately 220 cm of densely packed shell, similar to core no. 1, while core no. 2 has a much thinner lens of densely packed shell overlying coarse grained sediment with evidence of oxidation.

Based on the contoured acoustic survey data, all five cores are located along the ridge of a topographic high area between the two observed channels. It is apparent that the shell deposit is concentrated in the area surrounding cores no. 1, 9, 10, and 11, but extends to a lesser extent to the east at least as far as core no. 2. While the shell deposit is a significant feature, variable horizons are evident when the acoustic profiles and sediment units are compared (Figure 7.2.9).

Sedimentary units were initially developed based on qualitative features such as sediment texture and Munsell color; additional attributes such as presence or density of shell and degree of oxidation were also used to separate cores into discrete sedimentary units. Following core descriptions and initial assessment, physical samples were collected for grain size analysis and mass-specific measurements of magnetic susceptibility from representative cores.

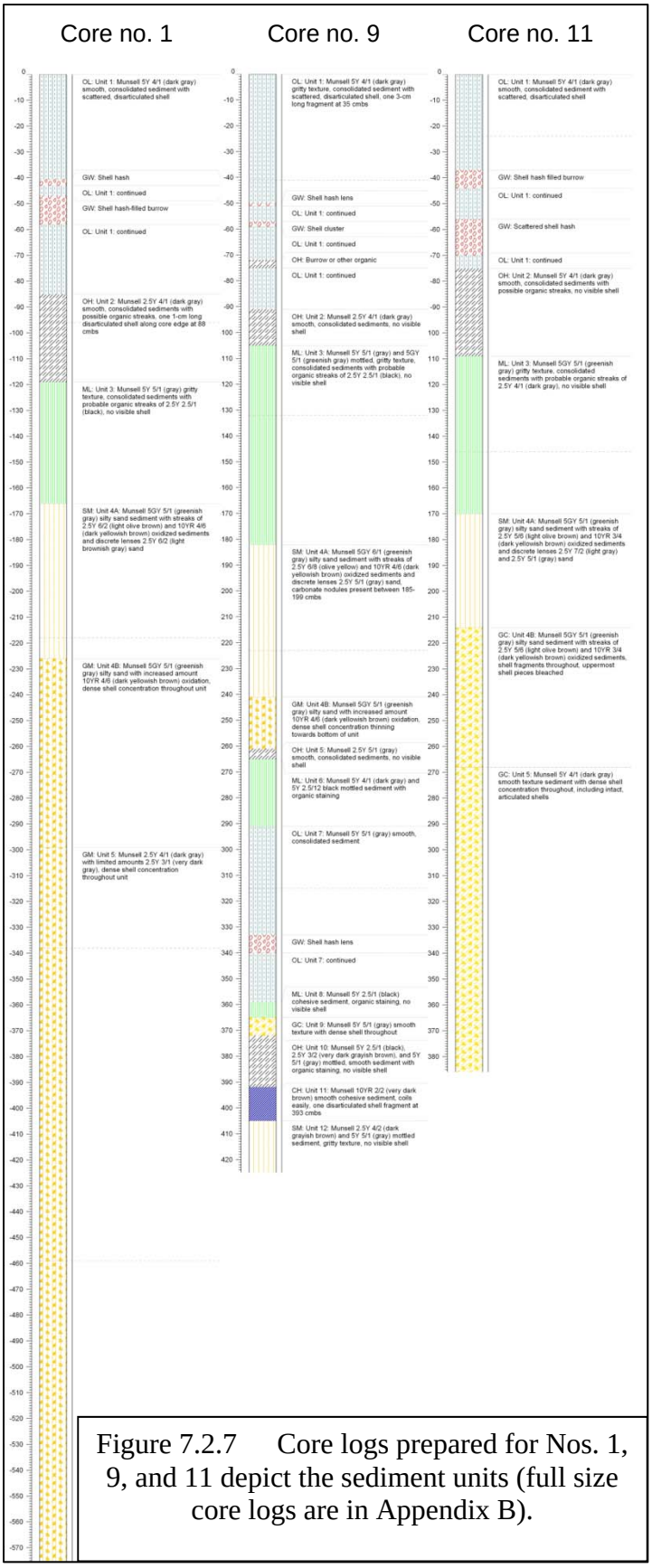

Figure 7.2.7 Core logs prepared for Nos. 1, 9, and 11 depict the sediment units (full size core logs are in Appendix B).

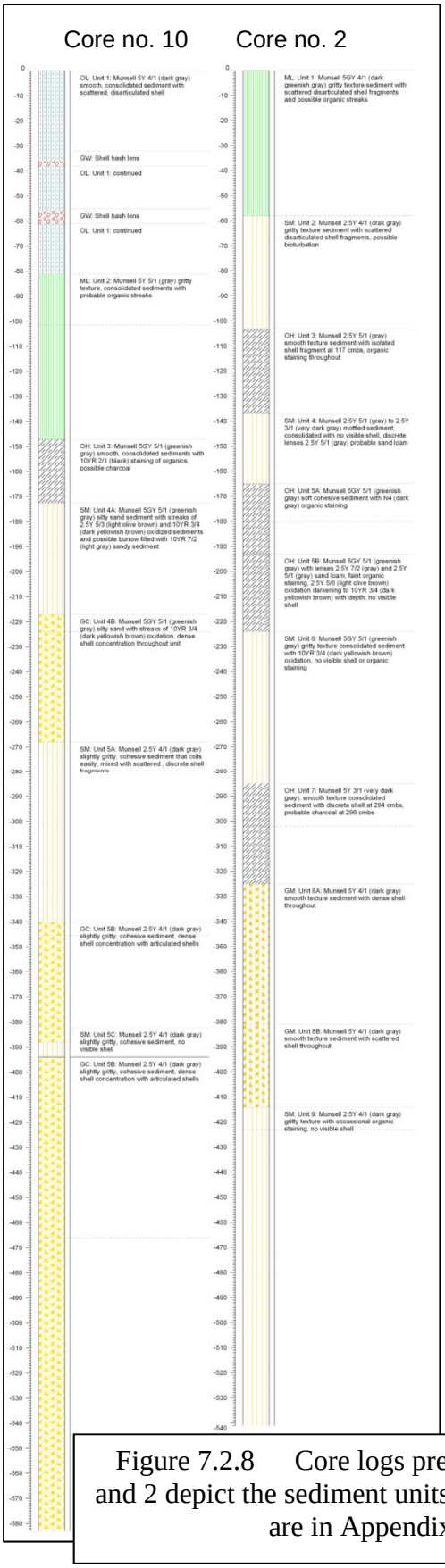

Figure 7.2.8 Core logs prepared for Nos. 10 and 2 depict the sediment units (full size core logs are in Appendix B).

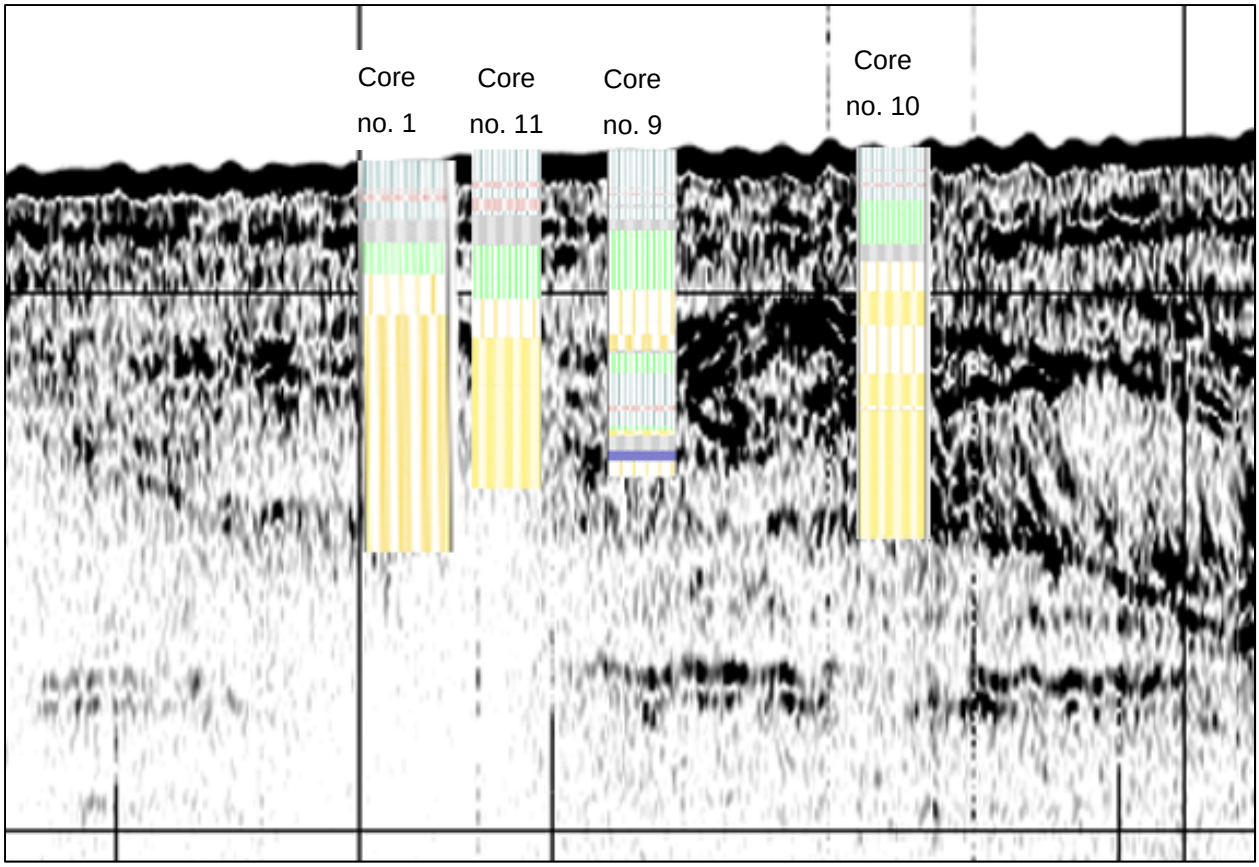

Figure 7.2.9 Core logs superimposed over the acoustic profile depict the sedimentary units and their representative places on the acoustic profile. Core logs and the acoustic profile are shown at the same vertical scale; horizontal scales are not equal. North is at right.

Physical samples were collected from Core no. 10 for grain size analysis; one sample was collected every 10 cm down the core for the first two meters; the remaining samples were collected from the dense shell deposit at arbitrary levels based on the ability to capture enough sediment between shells for processing. Raw grain size values were plotted as s-curves, then calculated as both median grain size and graphic mean and rounded to the nearest hundredth (Table 7.6; Figure 7.2.10). Median grain sizes were generally smaller than the calculated graphic mean size. Sediment classes range from fine sand to very fine silt; no clay was observed within the calculated grain sizes. Due to the similarity of the observed sedimentary units, results from Core no. 10 were assumed to be representative for similar units within cores from this area within GA 426.

Table 7.6 Representative Grain Sizes for Core no. 10, GA 426

Sample No.	Sample Depth (cmbs)	Median (Md_{mm})	Graphic Mean Mz (mm)	Wentworth Classification
1	10	0.082	0.093	very fine sand
2	20	0.031	0.065	coarse silt / very fine sand
3	30	0.036	0.054	coarse silt
4	40	0.038	0.044	coarse silt
5	50	0.034	0.042	coarse silt
6	60	0.028	0.045	medium / coarse silt
7	70	0.045	0.083	coarse silt / very fine sand
8	80	0.098	0.108	very fine sand
9	90	0.017	0.062	medium / coarse silt
10	100	0.005	0.007	very fine silt
11	110	0.007	0.015	very fine / fine silt
12	120	0.058	0.063	coarse silt / very fine sand
13	130	0.087	0.077	very fine sand
14	140	0.070	0.070	very fine sand
15	150	0.066	0.068	very fine sand
16	160	0.053	0.059	coarse silt
17	170	0.022	0.046	medium / coarse silt
18	180	0.084	0.073	very fine sand
19	190	0.078	0.070	very fine sand
20	200	0.069	0.063	very fine sand
21	250	0.090	0.088	very fine sand
22	280	0.071	0.064	very fine sand
23	330	0.102	0.084	very fine sand
24	390	0.010	0.044	fine / coarse silt
25	464	0.012	0.042	fine / coarse silt
26	550	0.102	0.202	very fine / fine sand

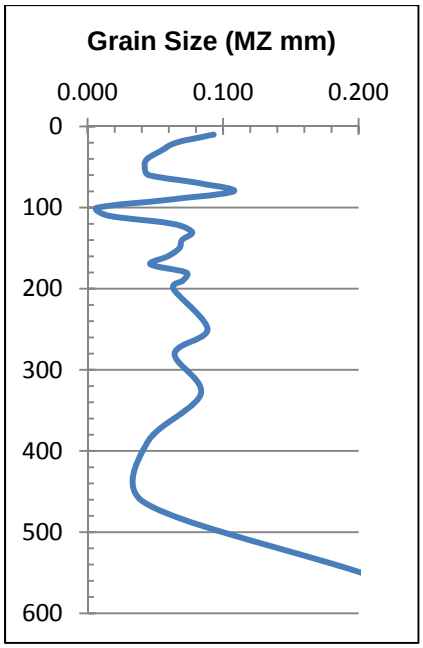

Figure 7.2.10 Graphic mean grain size curve for Core no. 10.

Core no. 10 was sampled continuously for magnetic susceptibility from the top of the core down through the interpreted marine and estuarine sediments and throughout the entire shell deposit. The upper half of Core no. 9 was sampled at arbitrary intervals, based on stratigraphy but reflects a similar pattern of MS values (Figure 7.2.11).

Each of the MS curves prepared from Cores no. 9 and 10 depict a general trend in which the uppermost MS values are relatively higher than values at the bottom of the core, but exhibit a significantly increased unit between depths of 50 and 100 cmbs. Similar peaks within the MS data recorded during core logging indicate that this unit is a real artifact of the sedimentary record and is not a spike within the data.

Samples were selected from Core no. 10 for radiocarbon sampling to provide absolute ages for use in correlating the magnetic susceptibility data. All samples were submitted to Beta Analytic for testing (Table 7.7; Appendix C). Calibrated ages were calculated, however conventional radiocarbon ages are used in text and in subsequent figures to allow direct comparison against previous sea-level data sets.

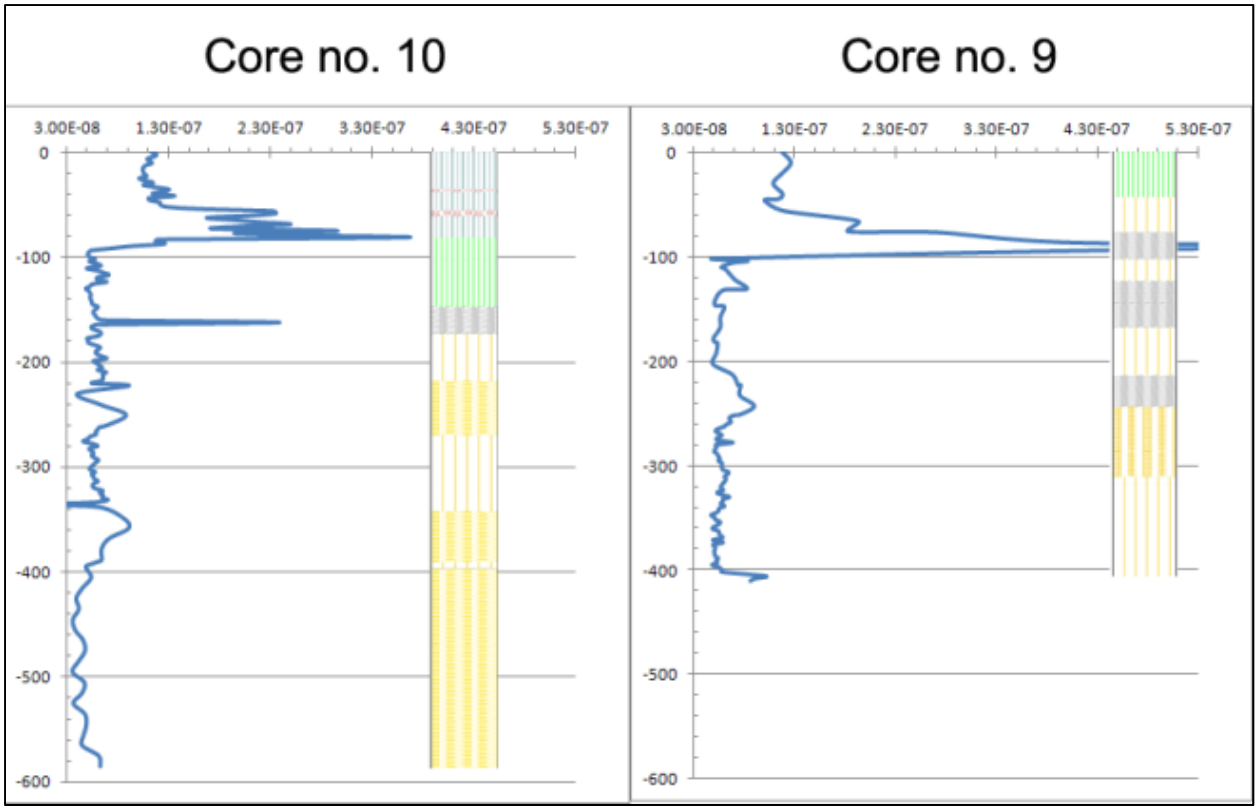

Figure 7.2.11 Diagram depicting MS data obtained from Cores no. 10 and 9 with their interpreted sediment horizons.

Table 7.7 Radiocarbon Sample Results for Core no. 10, GA 426

Sample	Sample Depth (cmbs)	Conventional Radiocarbon Age (BP)	Calibrated (2 Sigma) Radiocarbon Age (BP)
1	39	9,890 +/ 50 BP	10,610 – 11,050
2	85	9,870 +/- 50 BP	10,600 – 11,020
3	105	9,980 +/- 50 BP	11,250 – 11,640
4	106	10,070 +/- 60 BP	11,320 – 11,840
5	149	41,660 +/- 620 BP	Outside of calibration range
6	254	38,880 +/- 900 BP	Outside of calibration range
7	390.5	>43,500	---
8	460.5	>43,500	---

Radiocarbon ages suggest a long history of sediment deposition within this area, spanning over 33,000 years. When correlated with the MS curve for Core no. 10, the radiocarbon ages demonstrate that the sedimentary units have been formed as punctuated events, rather than one continuous event (Figure 7.2.12).

7.2.2 Interpreted Inset Terrace Profile

Cores 6, 7, and 8 represent a profile along an interpreted inset terrace on the southern margin of the northernmost channel surveyed in 2008. The interpreted Holocene sediment depth increases from core no. 6, which represents the highest point along the channel margin, to core no. 8, ranging from approximately 1.5 m (5 ft) to 3 m (10 ft) BSF (Figure 7.2.4) as calculated from the acoustic profiles.

Core no. 6 is located on the upper margin of the channel, and captured the longest sediment profile of the three cores (Figure 7.2.13). With varying intrusions this unit was observed consistently in cores no. 7 and 8 to depths of 130 to 165 cmbs. Cores no. 6 and 7 are most similar in profile, and it is likely that the variable unit thicknesses across the cores is attributed to the slope on which core no. 7 was acquired, grading into the channel system. The second sedimentary unit in these cores features oxidized sediment, suggesting these sediments were exposed as dry land in the recent past. Core no. 8 lacks this same unit, and instead features a thin horizon of consolidated sediment streaked with dark, probable organic material. The third sedimentary unit in all three cores consists of densely packed shell with oxidized sediment. Underlying sediments in Core no. 6 transition from gritty sediment with few scattered shells at the bottom of the shell deposit to sediments streaked with possible organic flecks throughout. Core no. 7 has the same gritty sediment with evidence of oxidation at the bottom of the shell deposit but lacks the organic-streaked sediment unit; this may be because Core no. 7 is the shortest of this series and did not penetrate into this sediment unit. The lowest sedimentary units in Core no. 8 include alternating lenses of sandy and organic streaked sediment, suggesting this area saw repeated episodes of deposition and scour, possibly during terrace formation.

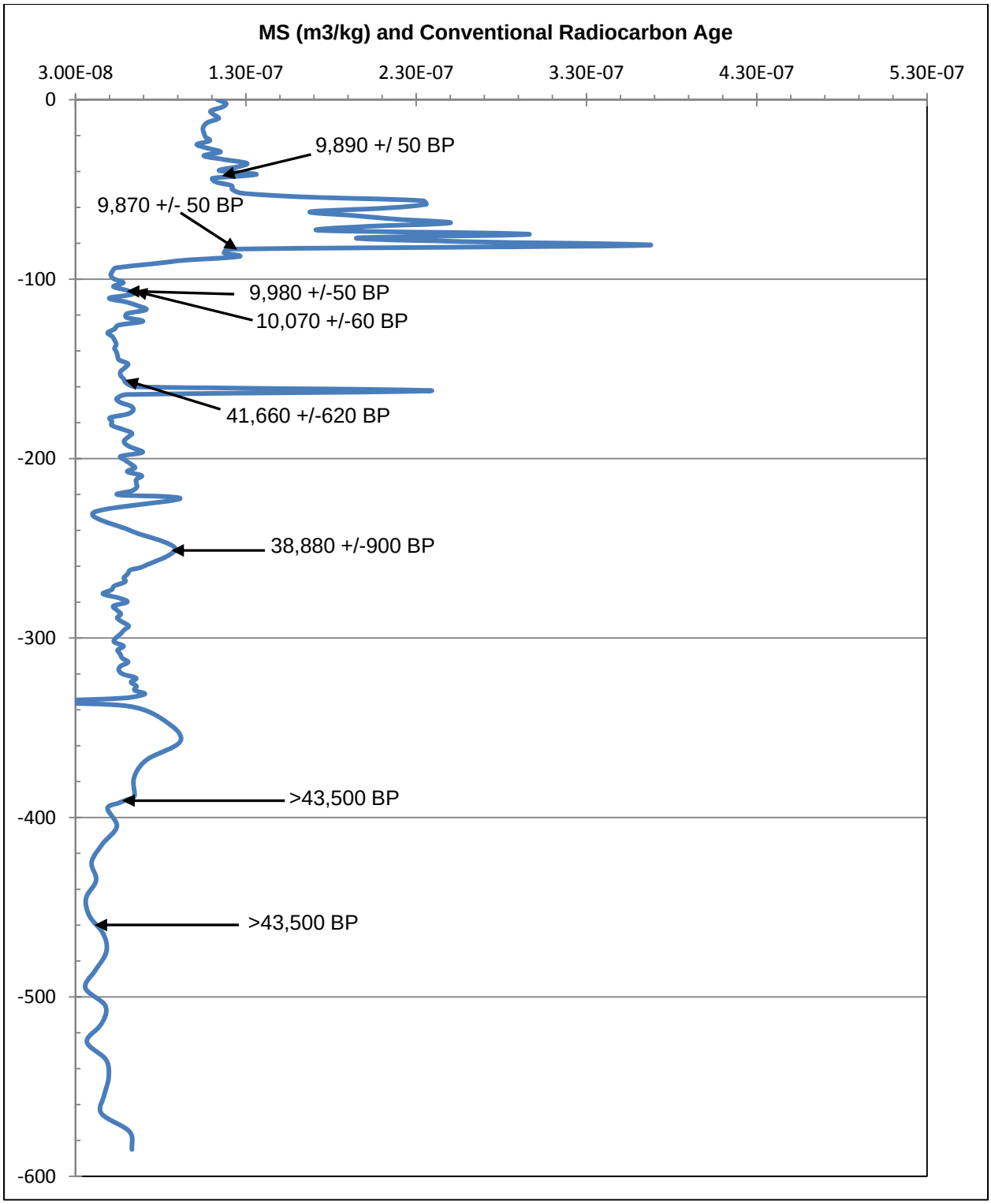

Figure 7.2.12 MS curve from Core no. 10 samples with conventional radiocarbon ages plotted at depth.

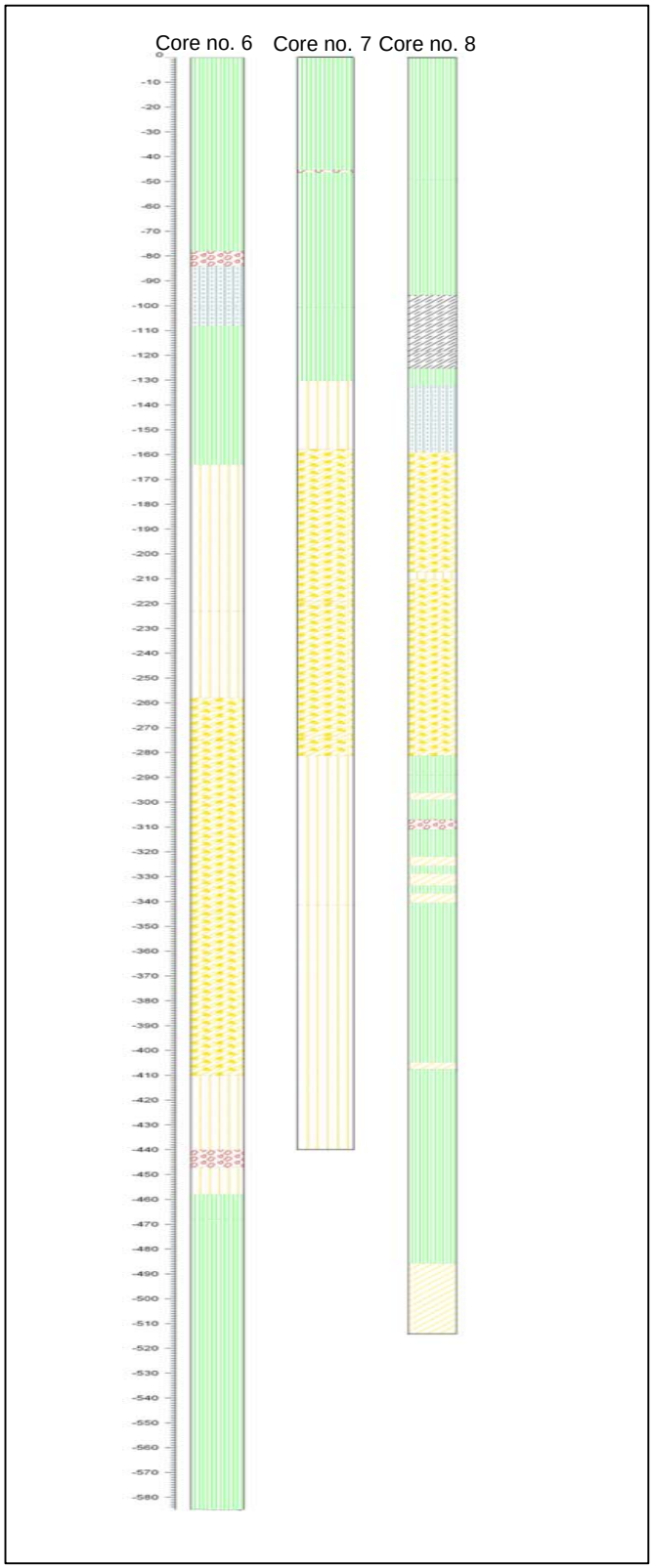

Figure 7.2.13 Core logs prepared for Nos. 6, 7, and 8 depict the sediment units (full size core logs are in Appendix B).

Based on the contoured acoustic survey data, the three cores should not have uniform stratigraphic units as they represent different elevations of the channel's inset terrace and margin (Figure 7.2.14).

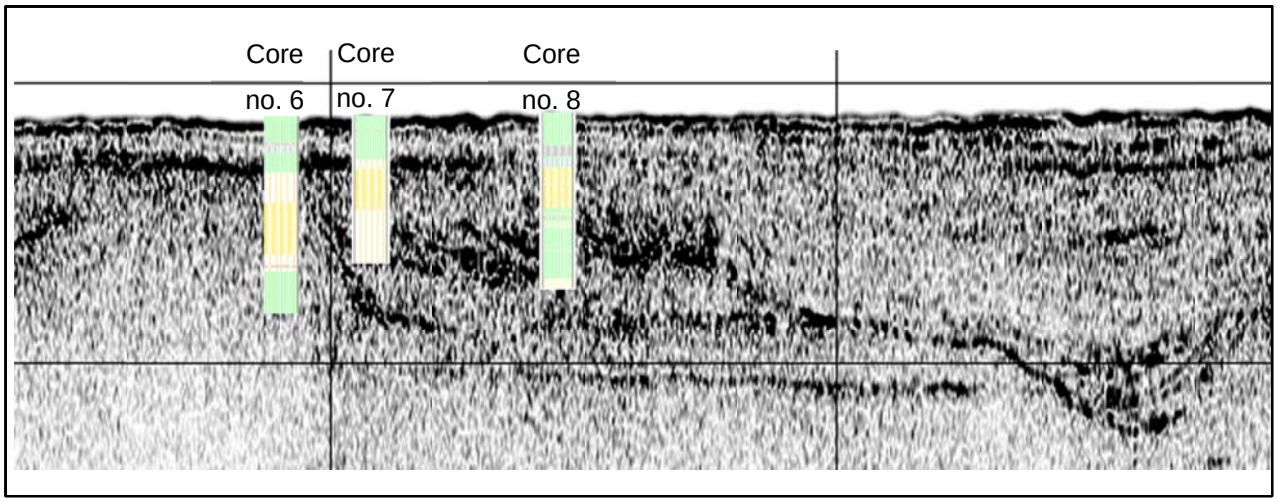

Figure 7.2.14 Core logs superimposed over the acoustic profile depict the sedimentary units and their representative places on the acoustic profile. Core logs and the acoustic profile are shown at the same vertical scale; horizontal scales are not equal. North is at right.

As with the previous cores, qualitative attributes were used to distinguish sedimentary units. Physical samples were collected subsequently from Core no. 6 for grain size analysis; one sample was collected within each qualitative unit, and from intrusive lenses observed within units. Raw grain size values were plotted as s-curves, then calculated as both median grain size and graphic mean and rounded to the nearest hundredth (Table 7.7; Figure 7.2.15). Median grain sizes were generally smaller than the calculated graphic mean size. Sediment classes range from very fine sand to very fine silt; no clay was observed within the calculated grain sizes. Due to the similarity of the observed sedimentary units, results from Core no. 6 were assumed to be representative for similar units along this channel margin.

Table 7.8 Representative Grain Sizes for Core no. 6, GA 426

Sample No.	Sample Depth (cmbs)	Median (Md_{mm})	Graphic Mean Mz (mm)	Wentworth Classification
1	39	0.025	0.038	medium / coarse silt
2	93	0.010	0.023	fine / medium silt
3	112	0.075	0.072	very fine sand
4	140	0.092	0.082	very fine sand
5	181	0.031	0.054	coarse silt
6	216	0.027	0.051	medium / coarse silt
7	246	0.006	0.013	very fine / fine silt
8	267	0.045	0.059	coarse silt
9	309	0.090	0.098	very fine sand
10	383	0.007	0.024	very fine / medium silt
11	434	0.016	0.036	medium / coarse silt
12	523	0.077	0.069	very fine sand

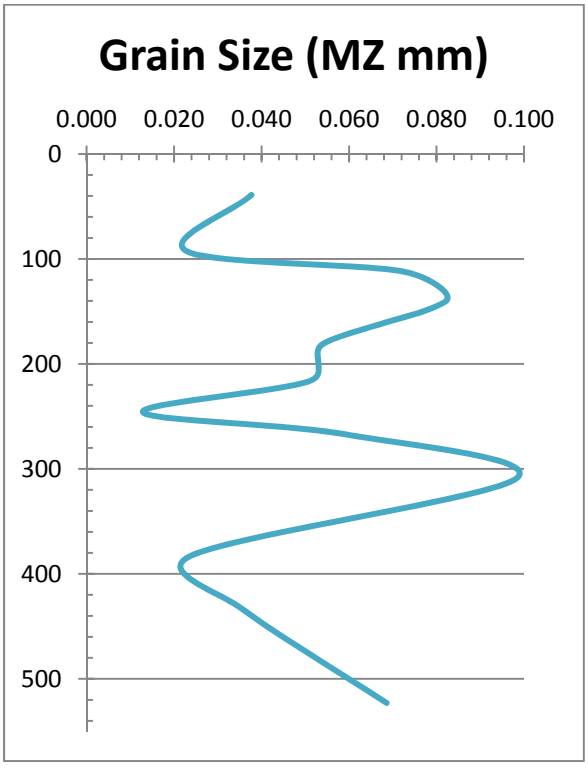

Figure 7.2.15 Graphic mean grain size curve for Core no. 6.

CHAPTER 8. 'REAL' ENVIRONMENTS

It was hypothesized at the beginning of this project that geographical, operational, and modified environments could be identified on the OCS through a spatial application of middle-range theory using indices recorded from geophysical survey and sampling. Site formation process variables were identified as they relate to environmental changes from a subaerial landscape to the modern marine environment on the OCS (Chapter 2). Terrestrial patterns of landscape exploitation demonstrated the types of features most likely to be associated with archaeological sites, providing guidance in the identification of the geographical environment (Chapter 3). Additional indices of anthropogenic activity were culled from previous studies in the GOM region and from other submerged contexts (Chapter 4), and were identified from some of the geophysical data sets (Chapters 6 and 7). Geographical and operational environments were identified in both survey areas, and two possible examples of modified environments were identified from the geophysical and environmental data.

8.1 Geographical Environments

The physical landscape, or geographical environment, available for possible exploitation by human populations was readily identified from the acoustic profile data. At close interval survey line spacing, depths for the interpreted landscape horizons for the two survey areas were contoured. The resulting renderings (provided in Chapter 6) effectively stripped off the overlying sediments, consisting of modern marine and estuarine strata, leaving the paleolandscape visible. In this manner it was possible to identify paleochannels as possible freshwater resources, as well as inset terraces and intact topographic features. Both the inset terraces and topographic features have been previously identified as indices for prehistoric site occurrence and preservation. Based on a qualitative assessment of the acoustic profile data it was possible to identify the geographical environment in each survey area from the corresponding geophysical data. Gross landscape interpretation was based on an assumption that subsurface depths for the interpreted landscape could be calculated using an assumed constant speed of sound.

Acoustic survey profiles were interpreted by using the average speed of sound in saltwater (1,500 m/sec) to calculate depth. Minimum and maximum depths for observed features within each horizon were then plotted against the composite sea-level curve presented in

Chapter 2 to determine if the paleolandscape dated to a time correlating with known occupation of the Gulf coast region. In both survey areas it was assumed that the average speed of sound would be accurate enough to determine depth within the shallow subsurface. Following this method, the geographical environments in HI 178 and GA 426 were dated to approximately 5,000 BP to 10,200 BP, and 7,800 BP to 11,800 BP respectively (as previously presented in Figure 6.3.1). Although these are wide ranges for possible occupation, they correlate with the Paleoindian and Early Archaic cultural-chronological periods in Texas and Louisiana. This was sufficient evidence to continue forward with environmental sampling (coring) in each area.

All of the cores acquired from this study were logged prior to opening using a Geotek multi-sensor core logger, which produced primary wave, or p-wave, velocity profiles for each core section. The p-wave data were initially recorded in μsec (seconds per foot) and processed to calculate downcore acoustic wave penetration in meters per second. Acoustic data profiles are recorded within the subbottom profiler as a function of time, therefore using the average speed of sound in two-way time travel each second of data is equivalent to 750 meters in depth. The acoustic data profiles displayed in this study are presented on a millisecond (ms) scale; horizontal scales are plotted in 10 ms intervals, therefore 10 ms are equal to 7.5 m, or 1 ms is equal to 0.75m.

The actual speed of sound was found to vary considerably within each survey area, and between neighboring cores. This suggests that age estimates based on depths calculated using the average speed of sound may contain errors. In the HI 178 survey area, measured p-wave velocity from cores no. 6 and 7, when plotted against the average speed of sound, demonstrate this variability (Figure 8.1.1).

The measured p-wave velocities within HI 178 ranged from a minimum of 1,100 m/sec to a maximum 1,825 m/sec. When calculated as depth, 1 ms of data is equal to a vertical distance of 0.55 m to 0.913 m. Depths calculated from the acoustic profiles using the average speed of sound are therefore accurate within a margin of 0.36 m. This error does not significantly impact the date ranges for landscape age as determined using constant velocity-derived depths on the composite sea-level curve.

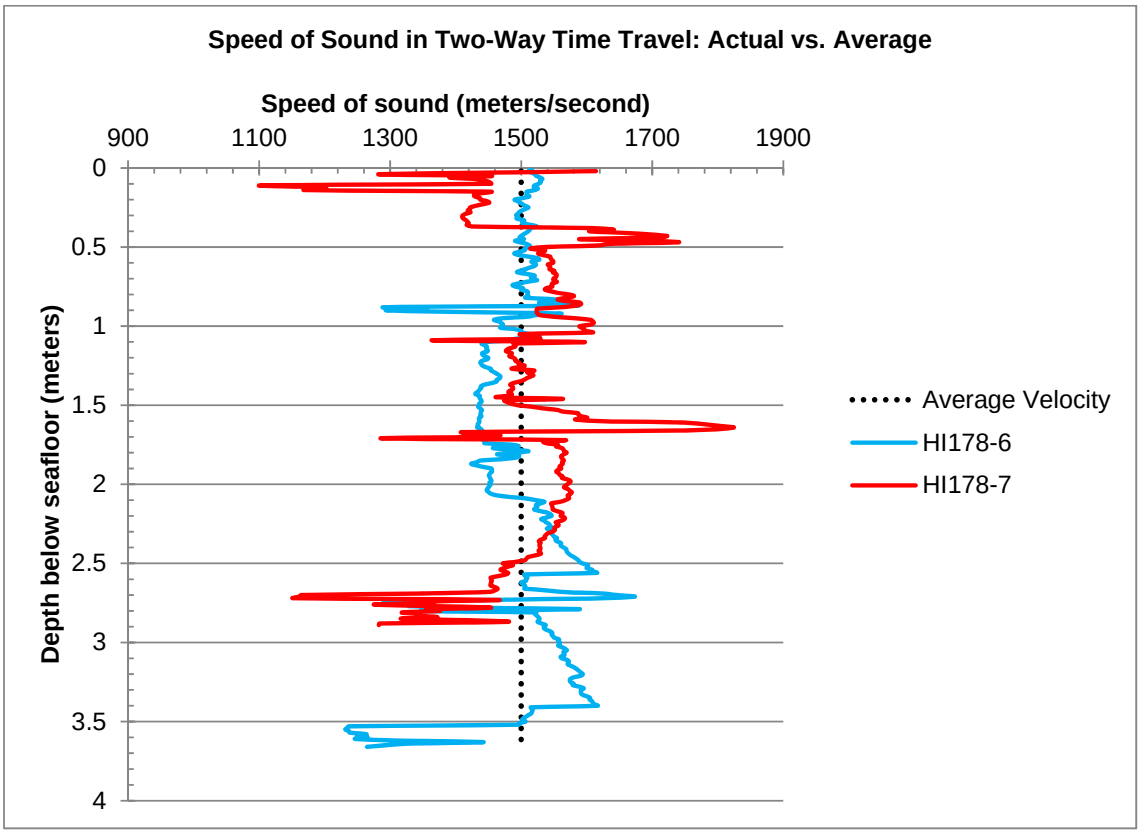

Figure 8.1.1 Measured p-wave velocities for HI 178 Cores no. 6 and 7 compared to the average speed of sound.

Cores from GA 426 show similar variability in the p-wave profiles (Figures 8.1.2 and 8.1.3). The measured p-wave velocities within the interpreted shell deposit in GA 426 range from a minimum of 915 m/sec to a maximum 1,800 m/sec while those along the interpreted channel margin range from 980 m/sec to 1,835 m/sec. Depths calculated within the shell deposit are considered accurate within a margin of 0.44 m, while depths along the channel margin profile are accurate within a margin of 0.43 m.

In addition to their utility in calculating accurate depths below the seafloor, seismic wave velocities have been used to characterize marine sediments in geology for over 40 years (Ayres and Theilen 1999:431). In engineering applications, abrupt changes in p-wave velocity are used to identify stratigraphic features, such as the presence of the groundwater tables, within 1 m depth accuracy (Bellana 2009:14). Normal marine sediments exhibit increased shear strength at the seafloor due to compression caused by the weight of the overlying water column (Ayres and Theilen 1999:433), but the p-wave profile under the

water/sediment interface may be used to categorize lithologic facies (Hamilton and Bachman 1982). Of specific application to the cores from HI 178 and GA 426, mean grain size and percent clay fraction directly impact velocity (Hamilton and Bachman 1982:1899).

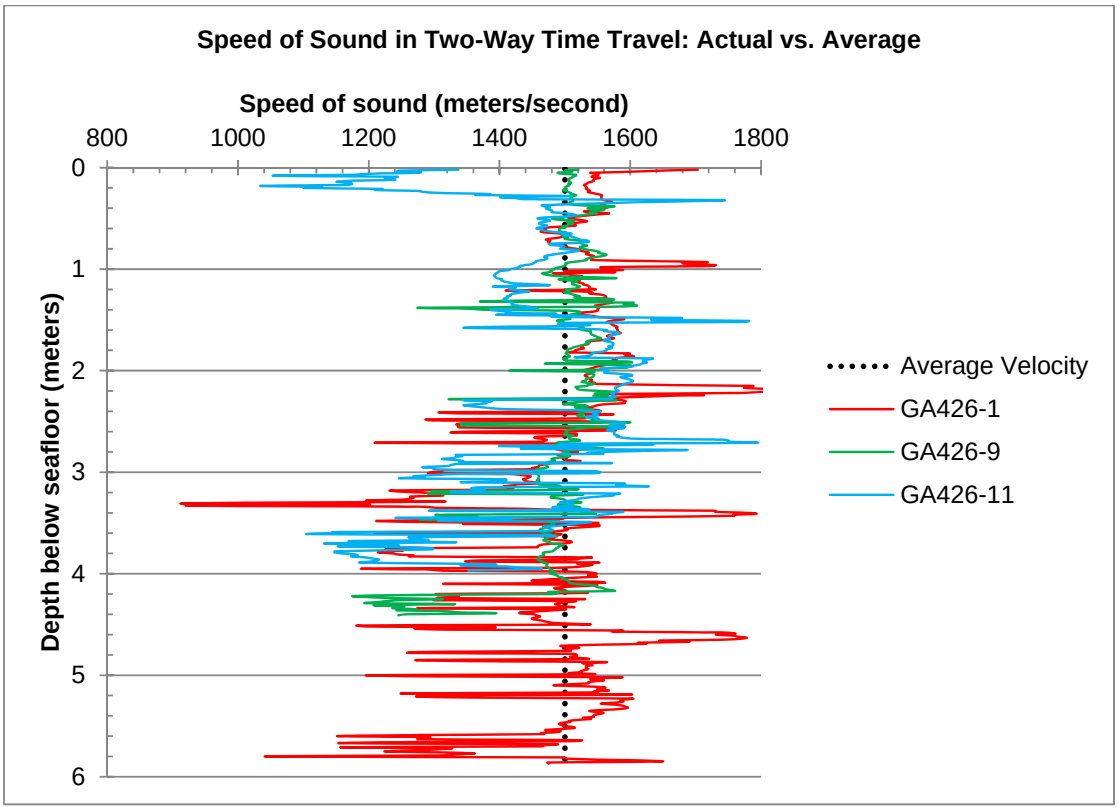

Figure 8.1.2 Measured p-wave velocities for GA 426 Cores no. 1, 9, and 11 compared to the average speed of sound.

P-wave velocities (V_p) for sediments within the study area ranged from 915 m/sec to 1,835 m/sec. Mid-range values within this data set correlate with measured p-wave velocities of marine sediments, which can be between 1,400 and 1,700 m/sec (Ayres and Theilen 1999:434). Previous studies have correlated marine sediments and V_p, producing expected values for material type and sediment classes (Table 8.1).

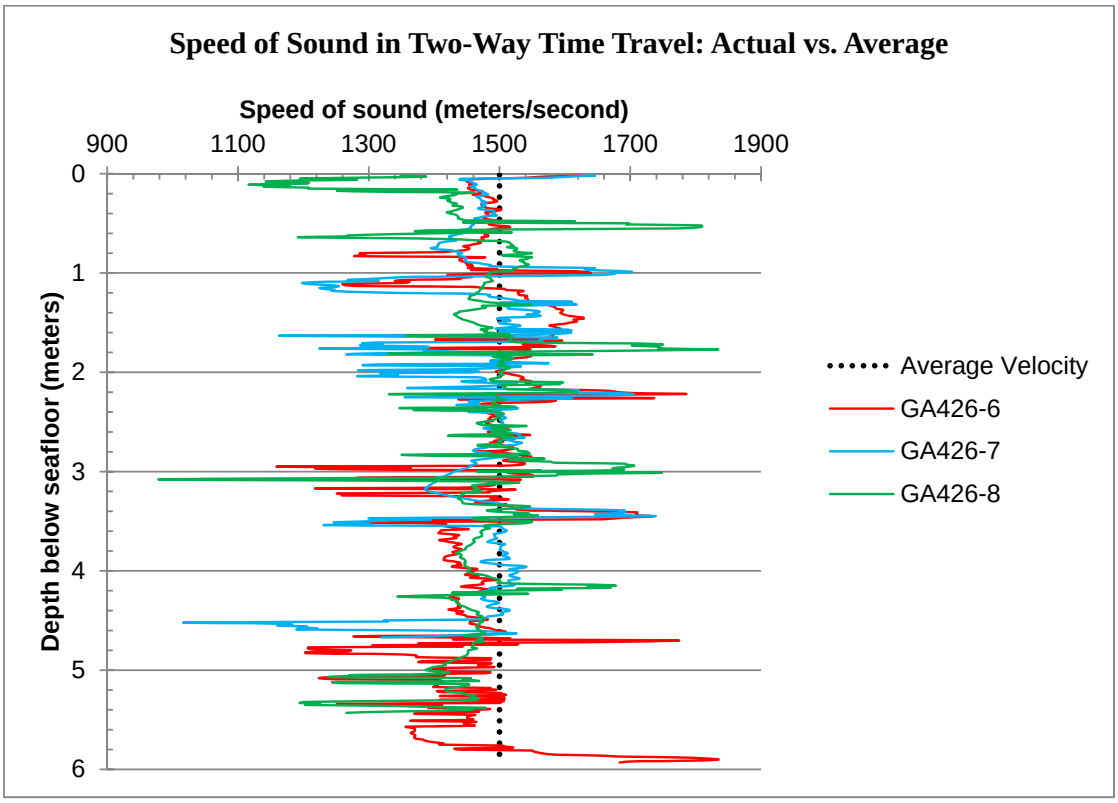

Figure 8.1.3 Measured p-wave velocities for GA 426 Cores no. 6, 7, and 8 compared to the average speed of sound.

Table 8.1 P-wave velocities of Specific Materials

Material type	Sediment classification	V_p (m/sec)
Air [b]		320
Water [b]		1,500
Ice [b]		3,200
Clastic sediment [b]		1,400 – 5,300
	Very fine sand [a]	1,709
	Silty sand [a]	1,658
	Sandy silt [a]	1,644
	Silt [a]	1,615
	Sand-silt-clay [a]	1,582
	Clayey silt [a]	1,546
	Silty clay [a]	1,517
Sandstone [b]		4,300
Salt [b]		3,800 – 5,200
Source: (a) Hamilton and Bachman 1982; (b) Bormann et al. 2012		

Velocity is impacted by many factors, for example decreasing in direct relation to decreasing sediment porosity and water content, therefore similar sediment types may react differently under various conditions (Ayres and Theilen 1999:434). P-wave velocity in clay particles varies from approximately 200 to 1,400 m/sec when dry but increases to between 1,200 to 2,200 m/sec when wet, suggesting that it may be possible to correlate grain size and p-wave velocity with prolonged subaerial exposure. In the case of the shell deposit identified in GA 426, core depths correlating with the densest areas of shell show V_p that is consistently lower than the average (1,500 m/sec). No corresponding p-wave velocities could be found for shell mounds or middens, therefore it is assumed that the p-wave values recorded in the core logs is based on the sediment within these dense shell horizons.

Acoustic profiling has been consistently referred to as the first step in searching for submerged prehistoric environments, but typically relies on data acquired using an assumed, or average, velocity of sound. The measured p-wave profiles from cores acquired in this study demonstrate that horizon depths calculated from the acoustic survey data were accurate within approximately half a meter. This is an important finding given that much of the survey work done to identify potential prehistoric geographical environments in the GOM consists entirely of acoustic profiling, without the benefit of supplemental physical samples, however there is not a direct correlation between geographical environment depth and time range of subaerial exposure.

Depths calculated from p-wave velocities or even assumed speeds of sound were plotted on sea-level curves in order to determine the potential dates of exposure and final inundation, but do not always accurately indicate the horizon's age. Radiocarbon testing was conducted on sediment and shell samples obtained from cores in both HI 178 and GA 426. The geographical landscape in HI 178 was dated to approximately 5,000 BP to 10,200 BP using the composite sea-level. Radiocarbon dates from samples between 16.4 m and 17.4 m BSL yielded absolute dates of 7,420 +/- 50 BP [7,780 – 7,970 cal BP] from this area. The absolute dates for this geographical environment correlated with the expected dates of landscape exposure as indicated from the acoustic profile depths (Figure 8.1.4). Radiocarbon dates from GA 426 proved problematic. The geographical environment was dated between 7,800 BP and 11,800 BP using the composite sea-level curve, however dates from samples taken at depths between 31.3 m and 35.9 m BSL yielded absolute dates ranging from 9,890 +/ 50 BP [10,610 – 11,050 cal BP] to greater than 43,000 BP. These dates suggest either a long period

of exposure with little to no sediment accretion followed by a punctuated period of deposition, or a significant unconformity possibly caused by scour or sediment removal. No other radiocarbon dates were run from this area, therefore it is not possible to state with certainty if samples from similar total depths BSL on other geographical features, such as the inset terrace indicated by Core no. 8, are any younger or if the shell deposit represents an anomaly in the radiocarbon profile of this geographical landscape. What is clear from the GA 426 radiocarbon dates is that the uppermost sections of the shell deposit were exposed, or in the shallow subsurface, and possibly available for exploitation as part of the operational environment during periods correlating with known human occupation of the Gulf coast.

8.2 Operational Environments

Four distinct features were identified within the overall geographical environments in HI 178 and GA 426, including two inset terraces (HI 178 and GA 426), an intact topographic feature (HI 178), and a shell deposit (GA 426). By themselves, these features do not confirm or refute the possible presence of humans on the OCS, but they do form a landscape available for exploitation. It is necessary then to identify any resources available for subsistence, which would create an operational environment within the geographical landscape.

The cultural chronological periods that coincide with subaerial exposure of the geographical environments in HI 178 and GA 426 include both the Paleoindian and Early Archaic. Both of these periods include populations of hunter gatherers who left scant evidence of their presence in terms of material culture. In a review of prehistoric sites between Sabine Lake and Corpus Christi, Texas, Aten (1971:1-2) found that the most common type of archaeological site was the shell midden, which ranged in extent from refuse deposits created during temporary occupation to periodic occupation over hundreds of years. Relative to operational environments, these shell middens typically consisted of clam, oysters, faunal materials, and in later prehistoric periods pottery and projectile points (Aten 1971:1-2).

Given the paucity of artifacts associated with Paleoindian and Early Archaic period sites, and the relatively small core diameter used for physical sampling, it is not surprising that no artifacts were identified in any of the cores recovered in the study areas. It is still possible, however, to identify elements within the landscape that could have supported anthropogenic subsistence systems. Proxy data indicated by the magnetic susceptibility profiles provide

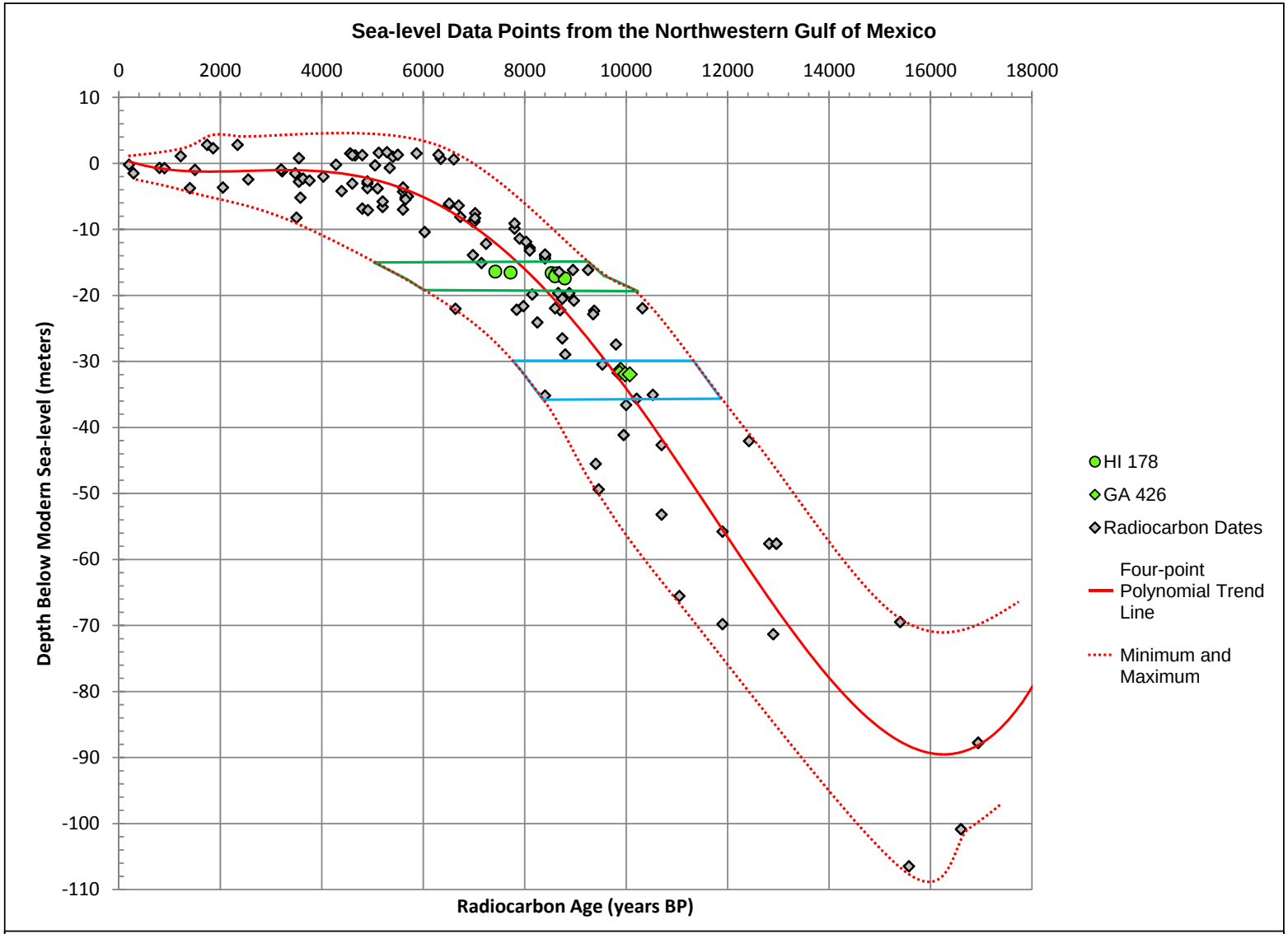

Figure 8.1.4 Composite sea-level curve with radiocarbon dates and estimated ages (based on acoustic profiles) shown.

evidence of possible climate conditions, while shell samples and pollen analysis provide evidence of available fauna and flora capable of supporting subsistence.

8.2.1 Magnetic Susceptibility

As discussed in Chapter 5, magnetic susceptibility has been used to identify anthropogenic activities and evidence of prehistoric activity (Evans and O'Connor 1999). As used in this study, measurements of magnetic susceptibility are used to develop a proxy record of climate conditions within each core sediment profile, since increases in temperature and moisture typically result in higher MS values. By itself, the MS profile is merely a relative profile devoid of absolute dates. As previously stated in Chapter 5, MS data have inherent limitations; in and of itself the data will only result in a relative curve of conditions and change. MS data from the study areas cores have been tied into the stratigraphic record using the absolute radiocarbon dates obtained during lab analyses.

An archaeological application of MS data serving as a climate proxy was conducted in inland Texas, and demonstrates its utility within the Gulf coast region. In fact, sediment data from Hall's Cave, Texas demonstrated that MS data were a more accurate indicator of the end of full glacial climate conditions than sediment lithology (Ellwood and Gose 2006).

Data compiled by Ellwood and Gose (2006) correlated local climate variations and MS data from Hall's Cave, Texas, with global events to create a timeline of climate change. Full glacial conditions existed between approximately 14 and 19 kya BP, a trend supported by lower relative MS values. An anomalously high range of MS values recorded at Hall's Cave at approximately 17 – 17.5 kya BP correlates with the global date of 16,800 +/- 255 for the Heinrich H1 event, which resulted in milder conditions along the western Atlantic and Gulf coast region (Ellwood and Gose 2006). A steady increase in MS values, which was consistent with changes noted in the faunal assemblage, suggested that the end of full glacial conditions occurred at the site by 14,200 yr BP (Ellwood and Gose 2006). An overall warming trend from 2 – 14 kya BP was interrupted by a temporally restricted decrease in MS values between 11 – 14 kya BP. This decrease approximately correlated with the Younger Dryas climate event, which has been dated to 11.5 – 12.5 kya BP (Ellwood and Gose 2006).

From 8,250 BP to 8,050 BP, MS values at the Hall's Cave site increased, a pattern which was correlated with the 8,200 yr BP event, hypothesized as the final pulse of glacial melt

freshwater into the Gulf of Mexico (Ellwood and Gose 2006). Data from the Greenland Ice Sheet Project (GISP) 2 have identified this meltwater pulse as occurring between 8,250 and 8,180 yr BP, although this event could not be identified in all of the GISP cores (Ellwood and Gose 2006). At approximately 4,300 yr BP an anomalous increase in MS values at the Hall's Cave site was correlated to a 4,400 yr BP event in British Columbia, and interpreted as an increase in rainfall that subsequently increased volume to the marine system (Ellwood and Gose 2006).

Magnetic susceptibility was measured in two ways for this study; as mass-specific and volume-specific values. Volume MS profiles were recorded continuously down each core section during core logging. Individual cores were sampled either continuously or at intervals as mass-specific values during lab sampling and analyses. Mass-specific MS measurements are preferred over volume-specific MS due to the potential for introduced error related to potential sediment compaction within samples (Thacker and Ellwood 2007. Mass-specific measurements were not always conducted as continuous samples however, and the use of arbitrary levels resulted in overly simplified curves. In future studies it is suggested that continuous sampling be conducted to allow for direct comparison with p-wave, grain size, and radiocarbon results. To allow for continuous curves, volume-based measurements are presented in the following graphics.

Magnetic susceptibility curves for HI 178 and GA 426 indicate relatively similar values for measured MS between 7,000 and 10,000 yrs BP (Figures 8.2.1, 8.2.2, 8.2.3, and 8.2.4). The dominant MS values within this period measured approximately 6.0E-8 to 8.0E-8 m^3/kg. Spikes and oscillations observed within the data are most likely attributed to shells or sediment unconformities caused by erosion, but may also represent artifacts of the core logging process. Core sections were logged unopened, in the core sleeve liners, complete with the caps at each end of the individual core sections. The plastic caps and air pockets at the end of some cores may have resulted in erroneous spikes at the top and/or bottom of core sections. Not all core sections had observed data errors. Therefore, the following graphs include all data points, and the locations of core section caps are annotated on the complete core logs (Appendix B).

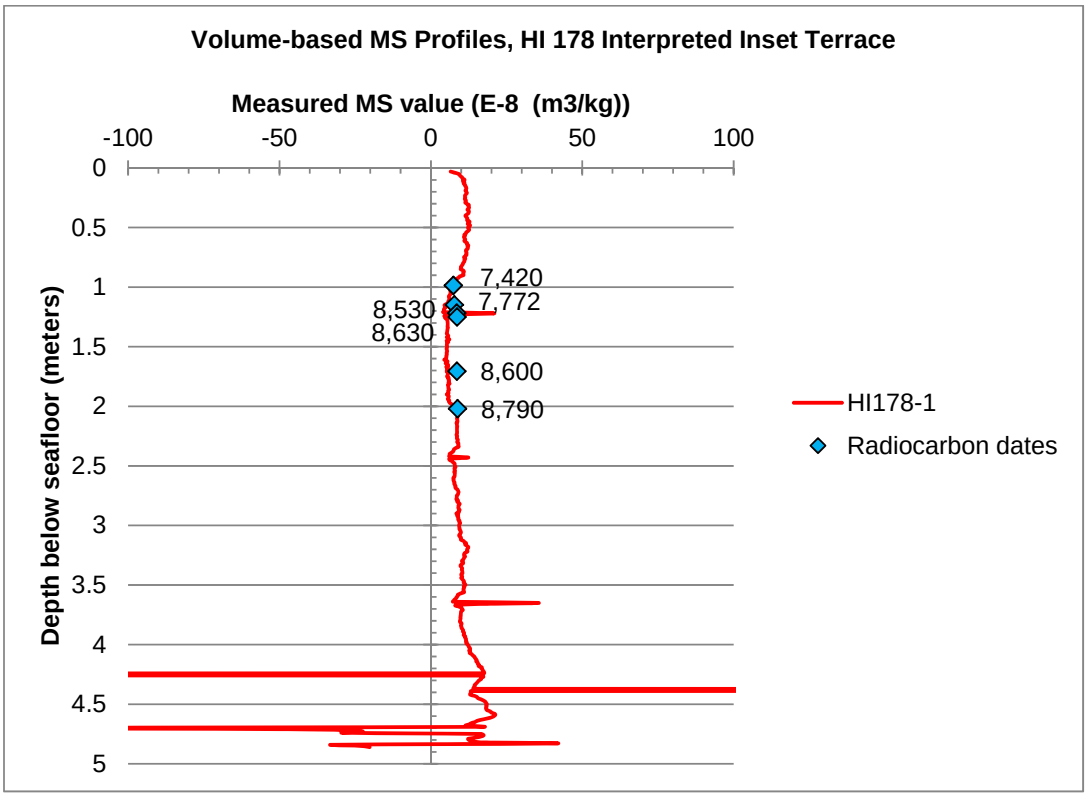

Figure 8.2.1 MS curve from HI 178 Core no. 1 with radiocarbon dates annotated at depth; charcoal horizon is at 1.21 m below seafloor.

Of particular interest on the MS curves is that the inset terrace features from both HI 178 and GA 426 appear to have fewer data oscillations than geographical features with high elevation, suggesting fewer stratigraphic interruptions. Core no. 1, HI 178 in particular has very few oscillations within the MS curve, and the one spike that does appear at a depth of 1.20 m is attributed to the charcoal layer observed in the sediment lithology. The interpreted topographic feature from HI 178, cores no. 2, 6, and 7 shows significant spikes in the uppermost 60 cm of data, with the most variability observed on Core no. 6, which was also the highest point on the topographic feature. It is very likely that scour related to sea-level transgression and subsequent storms has impacted the uppermost stratigraphy, a hypothesis supported by the presence of discrete shell and or sand lenses within the uppermost sedimentary units (Appendix B). Climate as indicated by the MS curves from HI 178 appears to have remained relatively consistent during the period of subaerial exposure and possible occupation.

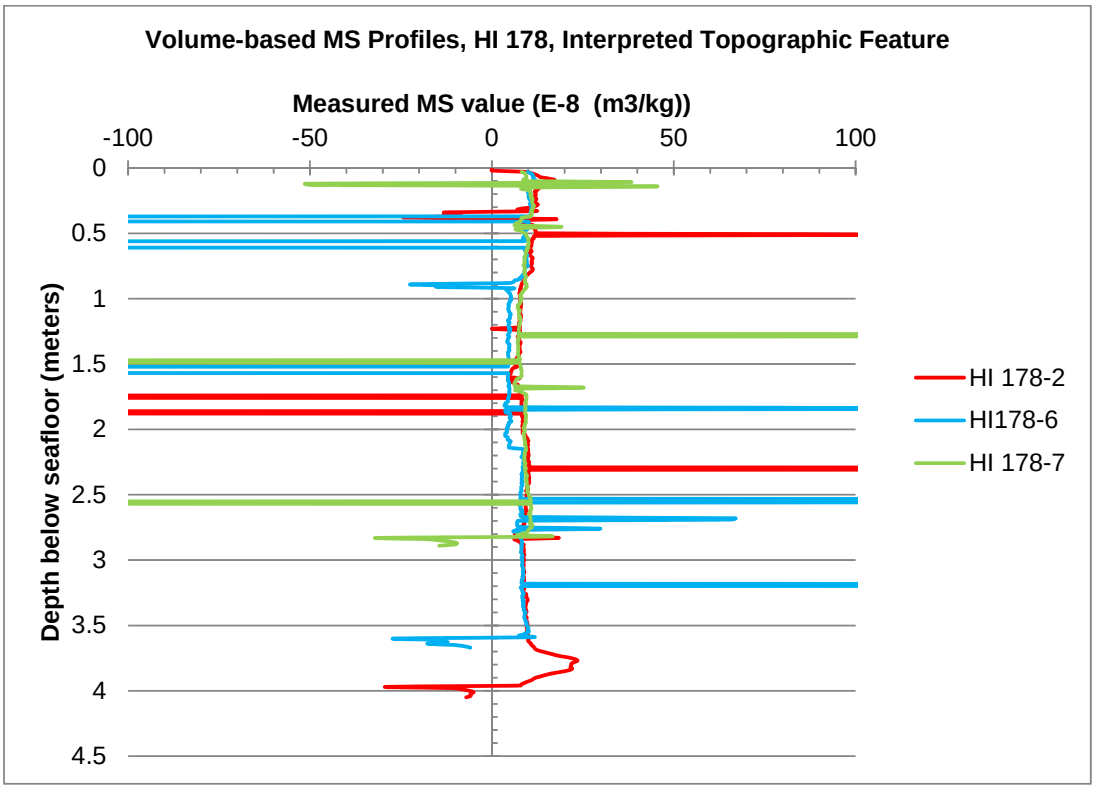

Figure 8.2.2 MS curves from HI 178 Core nos. 2, 6, and 7.

MS curves for the shell deposit noted in GA 426 demonstrate a possible warming period within the overall MS profile, occurring between 10,070 [11,320 – 11,840 cal BP] and 9,890 BP [10,610 – 11,050 cal BP]. This same interpreted warming trend is apparent in the terrace profile of Cores no. 6, 7, and 8, but to a lesser degree. This potential warming trend does not correlate with any previously known climate trends identified from terrestrial settings in the Gulf coast region, such as Milliken et al.'s (2008) Holocene-era flooding events, or the 8,200 year BP event which was associated with an increased meltwater pulse. Cores no. 6 and 8 do provide some indication of a possible locally-specific cooling event, such as the Younger Dryas (approximately 12,000 yrs BP). Each MS profile depicts higher than modern MS values at depth, overlain by a sequence of lower than modern MS values. The depths of these lower and higher MS values are not consistent across the cores, but this is likely due to the fact that the geographical surface of Core no. 6 was at a higher elevation than the interpreted contemporary terrace surface at Core no. 8.

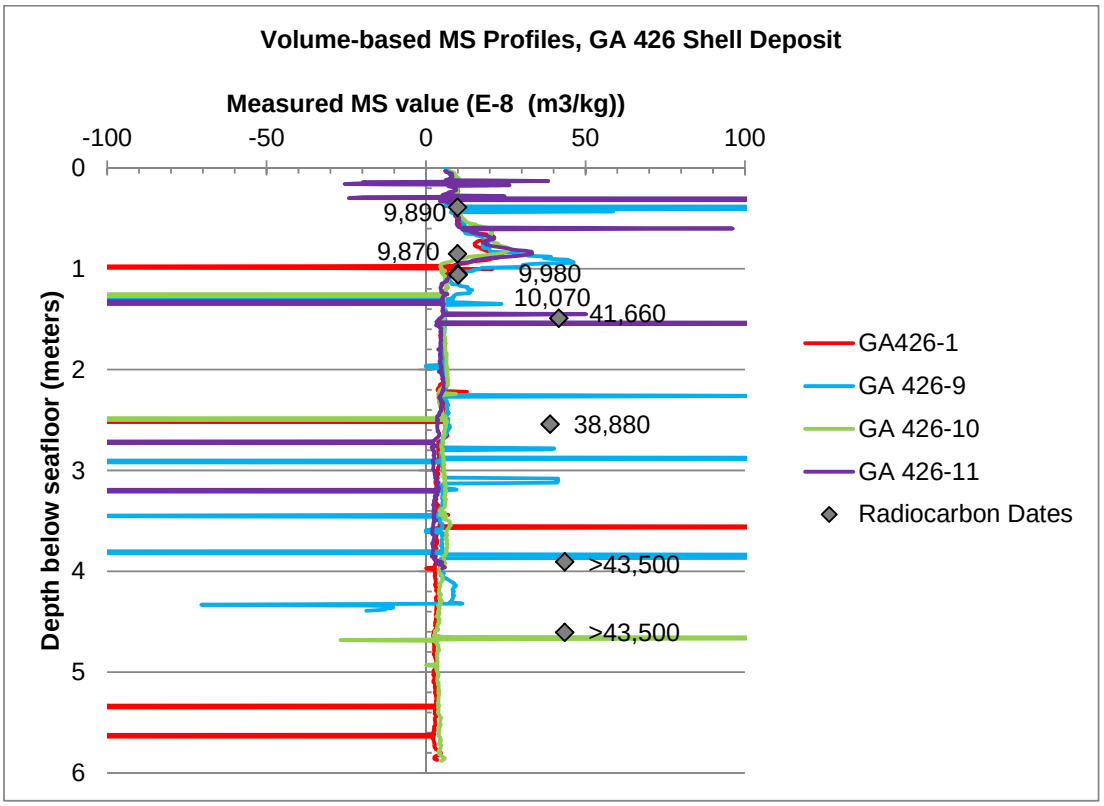

Figure 8.2.3 MS curves from GA 426 Cores no. 1, 9, 10, and 11 with radiocarbon dates annotated at depth.

Complications arise when attempting to compare MS profiles across cores in both survey areas. With the exception of Cores no. 1, 9, and 11 in GA 426, the cores represent discrete surface locations where the observed geographical landscape is at a different depth below the seafloor than in the adjacent cores. Oceanographic modeling of storm related scour indicates that the seafloor in HI 178 and GA 426 is likely to experience episodes of scour, followed by redeposition of sediments, resulting in mixed and possibly scrambled near-surface stratigraphy at least once every 18 months (Curray 1960; Rego et al. 2011). Based on the core logs and the observed sediment lithology, it is expected that modern marine and possible estuarine sediments represent the uppermost sections of each MS profile, and it is therefore expected that these areas will exhibit MS data interruptions due to scour.

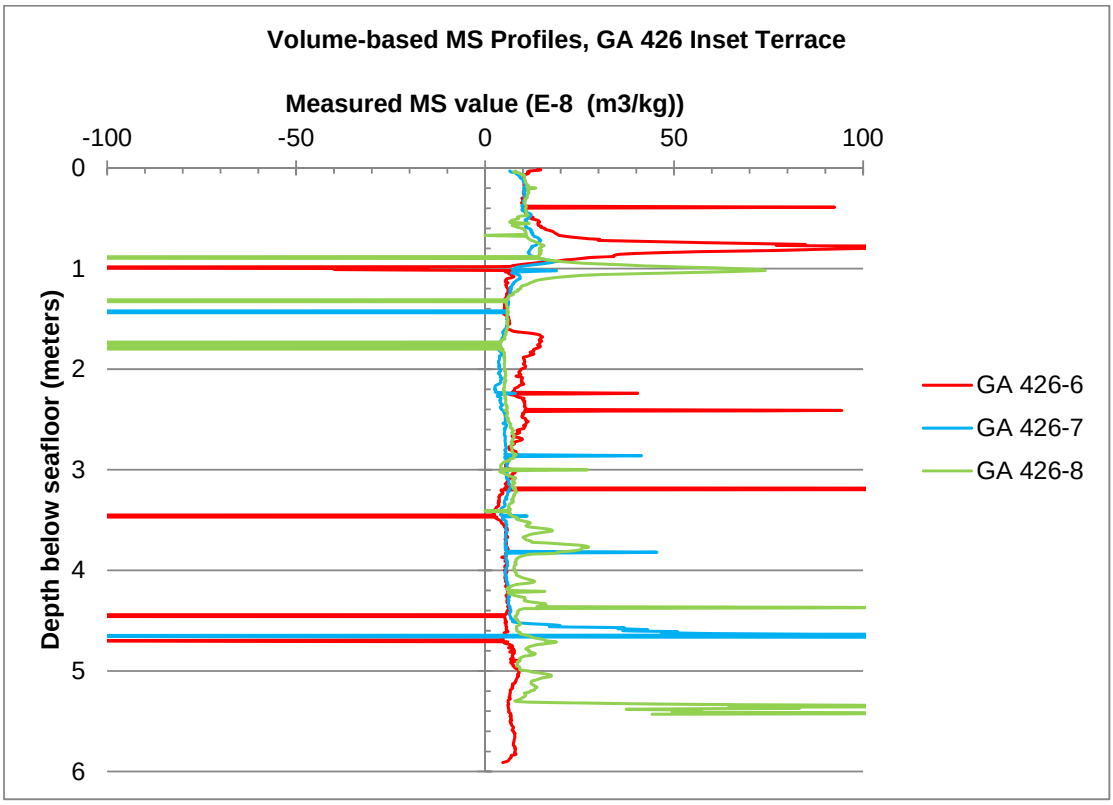

Figure 8.2.4 MS curves from GA 426 Core nos. 6, 7, and 8.

8.2.2 Shell Resources

Prehistoric shellfish and marine exploitation is not uncommon, especially in areas where terrestrial resources are lacking (Erlandson et al. 2008, 2011). Areas in California's Channel Islands provide evidence of marine exploitation dating to approximately 10,000 yrs BP (Erlandson et al. 2008). However, most Paleoindian and Early Archaic sites in the northwestern GOM are associated with projectile points and faunal remains from land mammals (as discussed in Chapter 3). This fact is not to suggest that marine exploitation did not occur in the GOM during the Paleoindian and Early Archaic periods. Instead, evidence to that effect is not likely to have been preserved at what would have been inland sites far removed from the contemporary coastline. Estuarine exploitation is more typical of GOM sites, and *Rangia cuneata* shells were a focus of the previous investigation of offshore landscapes (Pearson et al. 1986). Shells collected within the cores from HI 178 and GA 426 have been used to assist in identifying stratigraphic sections, and also serve as climate indicators.

Donax shells were identified in almost all of the cores, as intrusive lenses in the uppermost sediments. The two dominant *Donax* species, *texasianus* and *variabilis* are typically found in the surfzone, or intermediate shallow surf zone (Tunnell et al. 2010:373). Living *Donax* occur at depths of up to 11 m (36ft); their presence within the uppermost core sediments suggests mixing of modern marine sediments and discrete storm deposit layers (Tunnell et al. 2010:373).

Representative shells and shell fragments collected from HI 178 Core no. 2 at depths of 81 and 93 cmbs include the species *Anadara transversa* and *Mulinia lateralis* (dwarf surf clam). Both are bivalves that are abundant in bays (Hicks 2010:39). Dwarf surf clams are not tolerant of high-energy environments and are typically found in calm water mid-bay environments where salinity ranges from 15 to 35 ppt (Hicks 2010:39). Their presence on the topographic high feature along a channel margin may be explained as preferential deposition following flooding events, or possible deposition on the channel margins following exploitation by another organism. The shells identified in Core no. 2 were likely the result of either intensive or extensive human exploitation, due to the relatively small numbers recovered, but this does not preclude their exploitation by other species.

Shells within the deposit identified across GA 426, especially cores no. 1, 2, 9, 10, and 11 are composed almost exclusively of *Crassostrea virginica*, or eastern oyster. This species is known to occur in areas with moderate salinity (12 to 25 ppt) and are found in naturally accumulating reefs (Hicks 2010:41). Oyster reefs are formed over successive generations as new organisms attach to and live on the shell substrate of their predecessors (Hicks 2010:41). Naturally occurring reefs of *Crassostrea virginica* have been identified off the Texas coast measuring 6 – 8 km (3.5 – 5 mi) in length (Hicks 2010:41). The uppermost portions of some large reefs are exposed to air at low tides, which may explain oxidation observed in the sediment profiles along the upper boundaries of shell deposits within the cores from GA 426. Tidally-exposed portions of oyster reefs are located in the intertidal zone, referred to as "hogbacks", may consist entirely of dead oyster shells (Hicks 2010:41). Living portions of oyster reefs are typically subtidal (Hicks 2010:41). It is possible that the oyster reef identified in GA 426 extends below the maximum core depths; documented oyster reefs in San Antonio Bay extend to depths of 24 m (80 ft) below the seafloor, and date to over 8,500 yrs BP (Hicks 2010:41).

The dates obtained from *Crassostrea virginica* shells within the deposit in Core no. 10 are too old to coincide with known human occupations in the region. There is additional evidence to suggest that this is a naturally occurring deposit. In many cases, articulated shells were discovered, and no evidence of worked shell was observed on any of the recovered samples. One sample in particular, recovered from Core no. 10 at a depth of 235cmbs, consisted of an intact, articulated *Crassostrea virginica*, whose largest valve contained sediment infilling with barnacle plates and fragments, and whose inner surface contained encrusted bryozoans (*Laurie Anderson, personal communication*). This pattern is consistent with an oyster shell *in situ* within a reef environment.

Shells recovered from the uppermost portions of the shell deposits indicate a transition to a bay-like environment, and possible sea-level transgression. Cores no. 6 and 7 contained *Anomalcordia auberiana,* and *Terebra protexta* among the uppermost *Crassostrea virginica* deposits. *Terebra protexta* are found just offshore at depths less than 1 m BSL to depths of over 100 m BSL (Tunnell et al. 2010:240), while *Anomalcordia auberiana* are located in hypesaline bays (Tunnell et al. 2010:357).

A single *Geukensia demissa* specimen was identified from the lower boundary of estuarine sediment in Core no. 8, GA 426, immediately overlying the *Crassostrea virginica* deposit, at approximately 160 cmbs. *Geukensia demissa,* or ribbed mussels, are filter-feeders commonly found attached to the stalks of Spartina (Moris 1973:17) and indicate a low energy, sediment rich environment.

8.2.3 Pollen and FTIR Analysis

Pollen samples were acquired from the inset terrace indicated by Core no. 1, HI 178 and the shell deposit in GA 426 (cores no. 2, 9 and 10). Pollen samples from HI 178 core no. 1 were analyzed by two independent labs; Dr. Sophie Warny at Louisiana State University examined one set of pollen samples, and a second set was analyzed by PaleoResearch Institute (Appendix C). All samples from GA 426 were analyzed by researchers at PaleoResearch Institute.

Pollen samples were acquired from Core no. 1, HI 178 and analyzed closest to the charcoal horizon, from depths of 116, 124, and 135 cmbs. Analysis by Warny et al. (2012) indicated preserved examples of Hornworts (*Anthocerotophyta*) within the samples acquired above and

below the charcoal horizon (located at 121.5 cmbs). Hornworts are one of three phyla of bryophyte (non-vascular land plants), along with liverworts and mosses (Warny et al. 2012:7). In terms of environmental reconstruction, and specifically identification of the operational environment, the presence of hornworts provides a significant amount of information. Hornworts require a damp environment and are often found on streams, river banks, and wet floodplains; they are associated with shady, moist areas that correlate with warm and relatively wet conditions conducive to swamp development but are not salt-tolerant, suggesting a freshwater environment (Warny et al. 2012:14). Hornworts have a very fine tolerance for moisture; they cannot survive desiccation, nor can they be permanently submerged (Warny et al. 2012:14), suggesting a relatively stable water level. The core's location on an inset terrace correlates with the environmental requirements for successful hornwort colonization, and provides additional details about this potential freshwater resource. Also noted in the pollen profile for the sediment samples from HI 178 were abundant *Helianthoid* (including members of the sunflower family) and *Chenopodiaceae* (including species of the goosefoot family). *Chenopodiaceae* are related to *Amaranthaceae* and commonly referred to as "cheno-ams" (McConnell 1998:179). *Chenopodiaceae* are a common pollen species associated with prehistoric sites and have been found in diverse environments ranging from Australia (McConnell 1998) to submerged contexts off the coast of Israel (Galili and Weinstein-Evron 1985) to the eastern (McLauchlan 2003) and southwestern US (Hill 1966). They are commonly associated with pioneering species in areas that have been cleared or denuded (Coile and Artaud 1997). In addition to their nutritional use, Chenopodium have been used variously as a vermifuge and insecticide, and for medicinal purposes in a variety of cultures (Core 1967:206; Coile and Artaud 1997:4).

Two samples surrounding the charcoal lens in Core no. 1, at depths of 121 and 123 cmbs, were examined by Paleoresearch Institute for pollen analysis and FTIR (Fourier Transform Infrared Spectroscopy), which was used to identify organic residue. Probable *Thalictrum* pollen dominated the samples, followed by *Poaceae* pollen indicative of large grass populations (Cummings and Logan 2011:12). Additional species identified through pollen analysis included: *Quercus* (oak) and Cheno-am pollen (goosefoot and saltbush); and *Juglans, Pinus, and Alnus,* pollen (walnut, pines, and wetland-adjacent alder). Some examples of diploxylon *Pinus* (red pine) pollen were observed. According to Cummings and Logan (2011:12), smaller quantities of *Artemisia*, Low- and High-spine *Asteraceae*, *Boraginaceae*, *Cyperaceae*, *Fabaceae*, *Plantago*, and *Rosaceae* were also identified, and

represent “sagebrush or wormwood, marshelder or similar plants, other members of the sunflower family, wild onion or a similar plant, members of the borage, sedge, and legume families, plantain, and a member of the rose family”. The pollen identified from the sediments surrounding the charcoal horizon supports the dominant pollen interpretation that the surrounding environment was a meadow with adjacent freshwater remaining at relatively stable levels.

FTIR analysis of the sediments from the same horizons as the pollen resulted in the identification of the following: *Achillea* (yarrow) stems, *Cicuta* (hemlock) stems, *Poaceae* (grass family) stems and joints, *Helianthus* (*sunflower*) seed shells, and *Prunus* (choke cherry) and *Ribes* (currant) fruit. These plant species are consistent with the interpretation of a meadow environment, with some species also found in drainages (Cummings and Logan 2011:12-13). FTIR analysis identified polysaccharide galactoglucomannan, indicative of woody and fibrous tissues from coniferous plants (Gymnosperms) (Cummings and Logan 2011:13). FTIR peaks correlating with the amino acid glutamate indicate the presence of fish within the sample, however this is expected for sediment recovered from below the seafloor in a modern marine environment (Cummings and Logan 2011:13).

At the time the sediments immediately above and below the charcoal horizon were deposited, the inset terrace surrounding core no. 1 was subaerially exposed. Plant species identified include sunflowers, goosefoot, chokecherry, and currants, all of which would have provided ample subsistence to foragers, including most commonly black bears, raccoons, chipmunks, deer mice, and birds (USDA NRCS 2004). While there is no direct evidence of exploitation by human populations at this location, historic Native American populations are known to have exploited chokecherry, goosefoot, and sunflower seeds (Hill 1966; Core 1967; McLauchlan 2003; USDA NRCS 2004). Cultivation of several of these species is known, but from later periods in prehistory (McLauchlan 2003). Indirectly, animals known to consume these species can also be interpreted as part of the operational environment, since this location would have been an ideal place for Paleoindian and Early Archaic hunters to target game animals.

Pollen and FTIR analysis was initially conducted on a sample from the dense shell concentration within core no. 9, GA 426, at a depth of 399 cmbs; this sample was submitted before the radiocarbon dating results determined the antiquity of the reef structure. The

pollen record for this sample had high amounts of *Quercus*, indicating the presence of oak trees (Cummings and Logan 2011:10). Additional species identified include: *Betula*, *Carya*, *Pinus*, and *Ulmus* (hickory, pine, and elm trees); diploxylon *Pinus* pollen (red pine); and a large quantity of *Poaceae* pollen (grasses) (Cummings and Logan 2011:10). Cheno-am pollen frequency suggested the presence of saltbush, goosefoot, or a similar plant. Additional species identified included: Low- and High-spine *Asteraceae*, *Cyperaceae*, *Eriogonum*, *Phlox*, and *Rosaceae* (marshelder and rabbitbrush/sunflower, sedges, wild buckwheat, phlox); and possibly *Prunus* (chokecherry) (Cummings and Logan 2011:10). The presence of the Low-spine *Asteraceae* and *Cyperaceae* suggests that the area was part of a wetland. This is consistent with conditions necessary for oyster reef development.

FTIR analysis of this same sample provided additional species identification, all of which was consistent with the interpretation of a wetland environment with adjacent areas capable of supporting terrestrial plant species. It is probable that these plants would have grown in areas adjacent to estuarine zones and river channels. According to Cummings and Logan (2011:11) some of these additional species are similar to those surrounding HI 178, and include: *Achillea* (yarrow) stems; *Schoenoplectus* (bulrush) stems; *Cicuta* (hemlock) stems; *Helianthus* (sunflower) seed shells; ground Cheno-am seeds; dried, ground *Thalia dealbata* (alligator flag) seeds; dried *Cylindropuntia* (cholla cactus) buds; and wet *Sambucus* (elderberry). Of note among the FTIR results is the identification of matches consistent with cricket proteins and reptilian, probably turtle, blood (Cummings and Logan 2011:11).

Following the return of radiocarbon dates for the shell deposit in GA 426, additional samples were submitted for pollen analysis, targeting the top of the shell deposit, and the interpreted estuarine sediments that date more closely to periods of possible human occupation. These samples were prepared from core no. 2 at depths of 104, 131, and 136 cmbs, and from core no. 10 at depths of 86, and 105 cmbs.

Identified pollen species observed from core no. 2, at a depth of 136, was similar in pollen profile to the previously examined sample from Core no. 10, at a depth of 399 cmbs (Cummings and Varney 2011). The dominant species, which included pine, hickory, oak, elm, sunflower, sagebrush, and marshelder suggest proximity to a wetland with an adjacent open area and elevated ground (Cummings and Varney 2011:2). Of particular interest in this

sample was a moderate amount of charcoal, visible in the sedimentary unit as "organic staining throughout" (Appendix B).

The overlying sample from 131 cmbs was collected from the same lithologic unit but represented a changing environment. Microscopic charcoal was identified throughout this sample, as in the previous sample. An increased amount of oak pollen was identified, as well as evidence of alder, juniper, and fir (Cummings and Varney 2011:2). Decreases in the amount of High-spine *Asteraceae* suggest fewer sunflower-type plants, which were replaced by increases in marshelder plants (Cummings and Varney 2011:2). Of particular note is the presence of *Apiaceae,* or umbel, which are characteristic of plants including carrot, parsley, dill, fennel, and onion (Cummings and Varney 2011:2). An overall increase in preserved pollen from <10,000 pollen per cc of sediment to >47,000 pollen per cc of sediment indicates that this sedimentary unit was part of a stable surface (Cummings and Varney 2011:2). Based on the rapid change in radiocarbon age noted in Core no. 10, it is very likely that this environment remained relatively unchanged for a significant period of time.

The uppermost sample from Core no. 2 was collected from a depth of 104 cmbs, and indicated an increase in pine from the previously discussed samples. Cummings and Varney (2011:3) attributed this to either a decrease in other vegetation resulting in overrepresentation in the sample, or a simple increase in the amount of pine within the immediate area. Larger pieces of charcoal were identified in this sample, however pollen amounts in the sample are not low-enough to suggest complete landscape clearing through fire (Cummings and Varney 2011:3). Instead, it is more probable that this sample represents an environment with an increased number of pine trees. Generally, the pollen record for Core no. 2 suggests a relatively stable environment over time, with an increase in sediment dryness, which is supported by observed oxidation within the sediment profile.

Two samples were analyzed from Core no. 10, from depths of 85 and 106 cmbs; these samples correspond to samples dated for radiocarbon age. The sample from 106 cmbs dates to 9,890 BP [10,610 – 11,050 cal BP], and is similar in pollen profile to Core no. 2, at 136 cmbs (discussed above). This pollen profile identified similar species, suggesting an environment dominated by grasses, with some pine and oak stands, as well as *Apiaceae*, *Artemisia*, Low-spine *Asteraceae*, *Caryophyllaceae*, *Cyperaceae*, *Plantago*, *Rosaceae*, *Salix*, and *Typha*; these species indicate a member of the umbel family, sagebrush, members of the

sunflower family, a member of the pink family, sedges, plantain, a member of the rose family, willow, and cattails (Cummings and Varney 2011:4).

A total pollen concentration of 18,000 pollen per cc of sediment suggests a relatively stable surface, and a moderately large quantity of microscopic charcoal from this sample provide evidence of a potential surface that was exposed and available for exploitation (Cummings and Varney 2011:4).

The overlying sediment sample from 86 cmbs correlates with a radiocarbon age of 9,870 +/- 50 BP [10,600 – 11,020 cal BP]. The pollen profile suggests a stable, forested landscape interspersed with grassy meadows, with high amounts of hickory, juniper, pine, and oak and smaller quantities of alder and hemlock (Cummings and Varney 2011:4). Local vegetation in this sample was similar to Core no. 2 and included evidence of umbel, sagebrush, sunflower, wild buckwheat, legumes, as well as microscope charcoal (Cummings and Varney 2011:4).

As with HI 178, the pollen and FTIR results indicate that the operational landscape of GA 426 would have supported numerous species of flora available for both hunter gatherer populations and game animals, including species known to have been important to prehistoric cultures in other parts of the United States (Hill 1966; McLauchlan 2003). Pollen species identified in both study areas include *Chenopodiaceae*, identified by Warny, and Cheno-ams identified by Paleoresearch. During the Middle Archaic (Louisiana) / coastal Archaic (Texas) period, approximately 3,950-3,450 BP, *Chenopodium* and *Helianthus* were domesticated by prehistoric populations in the eastern United States where they were grown on disturbed landscapes, and associated with land clearance (McLauchlan 2003:557). The dates for the pollen samples in this study are very early compared with known dates for cultivation, and there is no other direct evidence to suggest that these plants were being modified, however there are known linkages between these species and land clearance. Evidence of microscopic charcoal was noted in the GA 426 samples, but was not evident in the core lithology as a discrete lens, as was the case in HI 178. Both examples of charcoal, however, may provide evidence of a modified environment.

8.3 Modified Environments

People require an operational landscape that will support their subsistence needs. Given enough time, people will modify their environment through frequent or effective activity (Butzer 1982:253). In the case of HI 178 and GA 426, discrete evidence of charcoal within the sediment profiles suggests fire, but in neither case is there concrete evidence that the fire is intentional, or anthropogenic.

As identified by Warny et al. (2012:16), charcoal was identified in the same samples as the hornwort and cheno-am pollen. It was suggested that the charcoal itself may explain the abundance of hornwort species in the pollen profile. Bryophytes, including hornworts, and cheno-ams are among the early pioneering species during secondary succession, or recolonization of a landscape following a burning event (Coile and Artaud 1997; Warny et al. 2012:16). No other evidence of charcoal was identified from any of the other cores at HI 178, however core no. 1 was an isolated sample. Core no. 1 was acquired from an inset terrace over 550 m north-northwest of the other cores in this area. Although there is evidence that prehistoric populations manipulated the landscape through use of fire (e.g., Fowler and Konopik 2007), it is not possible based on a single core to determine if the charcoal in Core no.1 represents a locally-discrete burn feature such as a midden or intentional land clearance. It is just as likely, based on the evidence presented here, that the charcoal is related to a naturally occurring fire or lightning strike.

Charcoal was identified from GA 426 in multiple cores, spanning a horizontal distance of approximately 106 m. Unlike HI 178, the charcoal identified at this location was observed as microscopic fragments throughout a sedimentary unit, and was not located within one discrete unit. While it is possible that this charcoal represents a geographical landscape-wide burn event there is insufficient evidence to suggest that the fire(s) was anthropogenic in nature, and may just as easily be explained as a wildfire, or lightening-induced burning event.

Evidence from HI 178 and GA 426 indicate that it is possible to use geophysical evidence and environmental data to identify geographical and operational environments, however there was no irrefutable evidence of an anthropogenically-modified environment. It is possible that subsequent testing could indicate anthropogenic alterations to the operational landscape.

8.4 Summary

The geophysical and environmental data were used to successfully identify both geographical and operational environments in both of the study areas. The acoustic survey data alone were used to construct contour maps of the interpreted geographical environment. When viewed as part of the total data set, the acoustic survey data comprise the single most important data set that form the building block on which all subsequent testing was based.

The use of p-wave data, which have not been extensively cited in published studies of submerged landscapes, were effective in correlating the calculated depths of features from the acoustic data with the actual depths of features in the observed sediment stratigraphy. Inferences concerning sediment type and environmental conditions were based on p-wave data. Specifically, slower velocities were correlated with oxidized sediment to suggest subaerial exposure of hogback portions of the GA 426 oyster reef.

Volume-based measurements of magnetic susceptibility were used to generalize climate conditions at each study area. Inferences were made about sediment scour and disturbance based on oscillations within the MS curves, since sediment discontinuities are known to cause anomalous spikes.

Shell species were identified and used to identify the environmental conditions present at that depth. The oysters and dwarf clams represent potential food resources for human populations, but there was no evidence of worked shell or selective disposal of shell species/size/seasonality. The shells represent species within a healthy ecosystem, though, and contribute information concerning the operational environment.

The pollen and FTIR data provided information on the types of species, allowing inferences to be made about the operational environment within each study area at different points in time. The HI 178 pollen data suggested a wetland environment with adjacent terrestrial plants, indicative of a stable waterline and relatively stable conditions. Species known to have been utilized by prehistoric populations were identified in association with the charcoal horizon, and suggest that this area would have provided significant resources to any populations in the area. The pollen from GA 426 indicated a long period of exposure and a relatively stable environment, with many of the same species as HI 178. The GA 426 environment was identified as a meadow-type ecosystem with adjacent freshwater. Again,

this type of environment would have provided a reliable source of diverse resources for a population present in the area.

The modified environment was the most difficult to identify. At present, there is no conclusive evidence of human modification at either HI 178 or GA 426, although both areas warrant further investigation.

CHAPTER 9. SUMMARY AND FUTURE RESEARCH DIRECTIONS

The investigation of submerged prehistoric sites in the northwestern Gulf of Mexico region is an archaeological task firmly rooted in physical geography. The modified and operational aspects of the geographical environment form the basis for the real environment, which can be empirically tested using methods of sediment sampling, acoustic surveying, and environmental analysis. Without the physical aspects of the environment, it is not possible to begin to make inferences as to the perceived environment, which is at the heart of human behavior and archaeology's ultimate goals.

The methods used in this study was based on the concept of middle-range theory but was applied in a spatial rather than temporal manner. Known indices of archaeological sites dating to the Paleoindian and Early Archaic periods from terrestrial contexts in Louisiana and Texas were applied to geographical environments identified on the outer continental shelf dating to similar points in time. A combination of acoustic surveying and physical sampling provided all of the data used in this study.

A review of existing sea-level curves was conducted, and a new composite curve created specifically for use in this study. The composite sea-level curve was deemed necessary to account for local variations in sea-level rise attributed to uplift or subsidence, and provide the maximum possible date range for potential subaerial exposure and corresponding prehistoric occupation. The composite sea-level curve accounted for all of the dates corresponding with the operational environment identified in HI 178, but did not account for anomalously old dates within the shell deposit identified in GA 426. These dates are beyond the range for material reliably dated by ^{14}C dating and therefore would not be expected to fall within the known sea-level curve for the late Pleistocene. Additional dates, such as OSL dates from non-shell features in GA 426 may provide a better record of the age-depth relationships. If possible, dates at regular intervals should be acquired for the sediment profile above and through the shell feature in GA 426 Core no. 2, to correlate with the pollen data. Additional dates could also be obtained from samples across the channel profile in HI 178, in cores 2, 6, 7, and 5.

Acoustic survey data were used to delineate large-scale geographical environments within both study areas. Evidence of the operational environments in both HI 178 and GA 426 demonstrate that each area could have supported subsistence systems essential for human occupation. Independent data sets correlated to provide a more detailed reconstruction of the operational environments, but were not without problems. Mass-specific magnetic susceptibility was not measured continuously down each core, resulting in MS profiles with significant gaps between data points that did not allow for direct comparison with other data sets. Although volume-based MS measurements may contain erroneous or misleading readings due to differential compaction, these measurements were found to be better suited for comparison across data sets in this study. If future testing includes mass-specific MS measurements, the samples must be collected continuously down the core.

Although not all elements were found in the current study, future research should continue to search for elements of the real environment in buried and submerged contexts through a spatial application of middle-range theory using geophysical data. Evidence of fire was identified from Paleoindian-age operational environments in both HI 178 and GA 426. Charcoal was only identified in one core from HI 178, indicating the fire was spatially restricted to the terrace feature sampled by Core no. 1. No evidence of fire was indicated by the remaining cores. However, the firemay refer to a discrete localized burn, such as a hearth, or a terrace-wide burning event. Additional coring, conducted systematically across this terrace feature could help to resolve this question. Charcoal identified across several cores in GA 426 suggests a wider burn area, but again it is unclear if this is due to a natural fire, or was intentionally set by humans to modify the landscape.

Pollen species identified in the cores from both HI 178 and GA 426 represent food sources exploited by prehistoric populations, and even species developed as cultigens in later contexts (Hill 1966; Core 1967; McLauchlan 2003). In North America, chenopods especially became an important staple crop of prehistoric populations, but at later points in time than the area in HI 178 (McConnell 1998:181). Without additional cores from the terrace feature sampled via Core no. 1, HI 178 it is not possible at this time to determine if the pollen shows any evidence of cultivation, seasonal selection, manipulation, or is naturally occurring. Similarly, pollen data

from GA 426 indicated Cheno-ams associated with charcoal. This finding alone does not indicate human landscape modification. Future coring or sediment sampling strategies should be designed to allow for pollen analysis relative to seasonality or other indicators that would allow for distinction between likely periods for wildfire so as to identify modification of the operational environment.

Further acoustic surveying at either of the locations tested in this study is unlikely to result in significantly new data. The macro-scale environment clearly contains operational features that correlate with prehistoric populations. The challenge now is to recover sufficient data from the subsurface environment to identify anthropogenic environmental modification. This step can only be done through physical sampling of the horizons associated with potential human occupation.

LITERATURE CITED

Adelsberger, Katherine A. and Tristam R. Kidder
2007 Climate Change, Landscape Evolution and Human Settlement in the Lower Mississippi Valley, 5,500 – 2,400 Cal BP. In, Reconstructing Human-Landscape Interactions, L. Wilson, P. Dickinson, and J. Jeandron (eds.), pp. 84-108. Cambridge Scholars Publishing, Newcastle, UK.

Adovasio, J.M. and D.R. Pedler
2005 A Long View of Deep Time at Meadowcroft Rockshelter. In Paleoamerican Origins: Beyond Clovis, edited by R. Bonnichsen, B.T. Lepper, D. Stanford, and M.R. Waters, pp. 23-28. Center for the Study of the First Americans, Texas A&M University, College Station.

Adovasio, J.M. and C. Andy Hemmings
2011 Geoarchaeological Explorations on the Inner-Continental Shelf of the Florida Gulf of Mexico. BOEM Information Transfer Meeting, March 23, 2011, New Orleans, LA.

Allison, M.A., G.C. Kineke, E.S. Gordon, and M.A. Goñi
2000 Development and Reworking of an Annual Flood Deposit on the Inner Continental Shelf off the Atchafalaya River. Continental Shelf Research 20:2267-2294.

Anderson, John B.
2007 The Formation and Future of the Upper Texas Coast. Texas A&M University Press, College Station.

Anderson, David G.
1996 Models of Paleoindian and Early Archaic Settlement. In, The Paleoindian and Early Archaic Southeast, David G. Anderson and Kenneth E. Sassaman, eds., pp. 29-57, University of Alabama Press, Tuscaloosa, AL.

Anuskiewicz, Richard J.
1992 Using Remote Sensing as a Tool for Middle-Range Theory Building in Maritime and Nautical Archaeology. In Underwater Archaeology Proceedings from the Conference on Underwater and Historical Archaeology, D.H. Keith and T.L. Carrell (eds.), pp. 92-99. Society for Historical Archaeology, Tucson, AZ.

Aten, Lawrence E.
1971. A study of the effects of petroleum exploration and production activities on archaeological and historical resources along the Texas coast prepared for the Galveston District, US Army Corps of Engineers. Research Report No. 3. Texas Archaeological Salvage Project. University of Texas at Austin.

———. 1983 Indians of the Upper Texas Coast. Academic Press, New York.

Ayres, Arthur and Friedrich Theilen
1999 Relationship Between P- and S-Wave Velocities and Geological Properties of Near Surface Sediments of the Continental Slope of the Barents Sea. Geophysical Prospecting 47(4):431–441.

Balsam, W.L. and J.P. Beeson
2003 Sea-Floor Sediment Distribution in the Gulf of Mexico. Deep-Sea Research I 50:1421–1444.

Bailey, Geoff and J. Parkington (eds.)
1988 The Archaeology of Prehistoric Coastlines. Cambridge University Press, Cambridge.

Bailey, Geoff and Nic C. Flemming
2008 Archaeology of the Continental Shelf: Marine Resources, Submerged Landscapes, and Underwater Archaeology. Quaternary Science Reviews, 27, 2153-2165.

Balsillie, J. H. and J.F. Donoghue
2004 High resolution Sea-Level History for the Gulf of Mexico Since the Last Glacial Maximum. Florida Geological Survey, Report of Investigations No. 103, Tallahassee, FL.

Bellana, Naresh
2009 Shear Wave Velocity as Function of SPT Penetration Resistance and Vertical Effective Stress at California Bridge Sites. Masters thesis, Department of Civil and Environmental Engineering, University of California, Los Angeles.

Benjamin, Jonathan
2010 Submerged Prehistoric Landscapes and Underwater Site Discovery: Reevaluating the 'Danish Model' for International Practice. Journal of Island and Coastal Archaeology 5(2):253-270.

Benjamin, Jonathan, Clive Bonsall, Catriona Pickard, and Anders Fischer
2011 Submerged Prehistory. Oxbow Books, London, UK.

Bentley, S.J., T.R. Keen, C.A. Blain, and W.C. Vaughan
2002 The Origin and Preservation of a Major Hurricane Bed in the Northern Gulf of Mexico: Hurricane Camille, 1969. Marine Geology 186:423– 446.

Bernard, H.A.
1970 Preliminary Report of Geology, Soil Character and Soil Stability in the Louisiana Offshore West of the Mississippi Delta. Shell Development Company, Houston, TX.

Bernard, Hugh A. and Rufus J. LeBlanc.
1965 Resume of the Quaternary Geology of the Northwestern Gulf of Mexico Province. In, H.E. Wright Jr. and D.G. Frey (eds.) The Quaternary United States, pp. 137-185. Princeton University Press, Princeton, NJ.

Berryhill, Jr., H.L.
1984. Distribution and Thickness of Holocene Sediments. Shallow Geology of the Continental Shelf and Upper Continental Slope, Port Arthur, Texas. OCS Map Series MMS 84-003. New Orleans, LA.

Binford, Lewis R.
1978 Nunamiut Ethnoarchaeology. Academic Press Inc., New York, NY.

———. 1981 Bones: Ancient Men and Modern Myths. Academic Press Inc., New York, NY.

Bird, Eric C.
1993 Submerging Coasts: The Effects of a Rising Sea-Level on Coastal Environments. John Wiley and Sons, Chichester, UK.

Bird, Dale E., Kevin Burke, Stuart A. Hall, and John F. Casey.
2011 Tectonic Evolution of the Gulf of Mexico Basin. In, N.A. Buster and C.W. Holmes (eds.) Gulf of Mexico Origins, Waters, and Biota, Volume 3, Geology, pp. 3-16. Texas A&M University Press, College Station.

Blondel, Philipe
2009 The Handbook of Side Scan Sonar. Praxis. Chichester, UK.

Blum, Michael D., T.J. Misner, E.S. Collins, D.B. Scott, R.A. Morton, and A. Aslan
2001 Middle Holocene Sea-level Rise and Highstand at +2m, Center Texas Coast. Journal of Sedimentary Research 71(4):581-588

Blum, Michael D. J.H. Tomkin, A. Purcell, and R.R. Lancaster
2008 Ups and Downs of the Mississippi Delta. Geology 36, 675-678.

BOEM (see U.S. Department of the Interior)

Bousman, C. Britt, Barry W. Baker, and Anne C. Kerr.
2004 Paleoindian Archeology in Texas. In, The Prehistory of Texas, Timothy K. Perttula (ed.), pp. 15-97, Texas A&M University Press, College Station.

Bonnichsen, R.
2005 An Introduction to Paleoamerican Origins. In Paleoamerican Origins: Beyond Clovis, edited by R. Bonnichsen, B.T. Lepper, D. Stanford, and M.R. Waters, pp. 1-8. Center for the Study of the First Americans, Texas A&M University, College Station.

Bonnichsen, R. and B.T. Lepper.
2005 Changing Perceptions of Paleoamerican Prehistory. In Paleoamerican Origins: Beyond Clovis, edited by R. Bonnichsen, B.T. Lepper, D. Stanford, and M.R. Waters, pp. 9-19. Center for the Study of the First Americans, Texas A&M University, College Station.

Bormann, Peter, Bob Engdahl, and Rainer Kind
2012 Seismic Wave Propagation and Earth Models. In, New Manual of Seismological Observatory Practice, P. Bormann (ed.), pp. 1-70. IASPEI, GFZ German Research Centre for Geosciences, Potsdam.

Breitzke, Monika
2000 Acoustic and Elastic Characterization of Marine Sediments by Analysis, Modelling, and Inversion of Ultrasonic P Wave Transmission Seismograms. Journal of Geophysical Research 105(B9):21,411–21,430.

Browne, I.
1994 Seismic Stratigraphy and Relict Coastal Deposits off the East Coast of Australia. Marine Geology 121:81-107.

Burroughs, William J.
2005 Climate Change in Prehistory: The End of the Reign of Chaos. Cambridge University Press, Cambridge, UK.

Butzer, Karl W.
1982 Archaeology as Human Ecology: Method and Theory for a Contextual Approach. Cambridge University Press, Cambridge, UK.

Camidge, K., P. Holt, C. Johns, L. Randall, and A. Schmidt
2010 Developing Magnetometer Techniques to Identify Submerged Archaeological Sites: Theoretical Study Report. HE Report No. 2010R012. Cornwall Council, Historic Environment, Environment, Planning, and Economy, Cornwall, UK.

Catt, J.A.
1986 Soils and Quaternary Geology: A Handbook for Field Scientists. Clarendon Press, Oxford, UK.

Chappell, J., A. Omura, T. Esat, M. McCulloch, J. Pandolfi, Y. Ota, and B. Pillans
1996 Reconciliation of Late Quaternary Sea Levels Derived from Coral Terraces at Huon Peninsula with Deep Sea Oxygen Isotope Records. Earth and Planetary Science Letters 141:227-236.

Coastal Environments, Inc. (CEI)
1977 Cultural Resources Evaluation of the Northern Gulf of Mexico Continental Shelf. Prepared for Interagency Archaeological Services Office of Archaeology and Historical Preservation, National Park Service, U. S. Department of the Interior, Baton Rouge, LA.

Coile, Nancy C. and Carlos R. Artaud
1997 Chenopodium ambrosiodes L., (Chenopodiaceae): Mexican-tea, Wanted Weed? Botany Circular No. 33, Florida Department of Agriculture and Consumer Services, Division of Plant Industry.

Coleman, James M. and Harry H. Roberts
1988 Late Quaternary Depositional Framework of the Louisiana Continental Shelf and Upper Continental Slope. Transactions – Gulf Coast Association of Geological Societies, Volume 38, 1988.

Coleman, James H., Harry H. Roberts, and William R. Bryant.
1991 Late Quaternary Sedimentation. In, The Geology of North America, Vol. J., The Gulf of Mexico Basin, Amos Salvador (ed.), pp. 325-352. Geological Society of America, Boulder, CO.

Core, Earl L.
1967 Ethnobotany of the Southern Appalachain Aborigines. Economic Botany 21(3):199-214.

Cummings, Linda Scott and Melissa Logan
2011 Pollen and Organic Residue (FTIR) Analysis of Samples from Sites GA426 And HI178, Texas Gulf Coast. PaleoResearch Institute Technical Report 10-119 Prepared for Dr. P. Hesp, Louisiana State University, Baton Rouge.

Cummings, Linda Scott and R.A. Varney
2011 Pollen Analysis of Cores from Site GA426,Offshore Near Galveston, Texas. PaleoResearch Institute Technical Report 11-079 Prepared for Dr. P. Hesp, Louisiana State University, Baton Rouge.

Curray, J.
1960 Sediments and History of Holocene Transgression, Continental Shelf, Northwest Gulf of Mexico. In Recent Sediments Northwest Gulf of Mexico, edited by F. Shepard and T.J. Van Andel. American Association of Petroleum Geologists Symposium, 221–266.

Dearing, J.
1994 Environmental Magnetic Susceptibility : Using the Bartington MS2 System. Bartington Instruments Limited, Oxford.

Dix, Justin, Rory Quinn, and Kieran Westley
2004 A Reassessment of the Archaeological Potential of Continental Shelves. Final Report Submitted to English Heritage as part of the Aggregates Levy Sustainability Fund. University of Southampton.

Dixon, E. James.
1999 Bones, Boats, and Bison: Archaeology and the First Colonization of Western North America. University of New Mexico Press, Albuquerque.

Dott, Robert H., Jr.
1992 An Introduction to the Ups and Downs of Eustasy. In, Dott, R.H., Jr., ed., Eustasy: The Historical Ups and Downs of a Major Geographical Concept. Boulder, CO. Geological Society of America Memoir, 180.

Dunbar, James S.
1983 A Model for the Predictability of Clovis/Suwannee Paleo-Indian Site Clusters in Florida – A Revival of W.T. Neill's Oasis Hypothesis. Paper presented at the 35th Annual Meeting of the Florida Anthropological Society, Tallahassee.

———. 1991 Resource Orientation of Clovis and Suwannee Age Paleoindian Sites in Florida. In, Clovis: Origins and Adaptations, R. Bonnichsen and K. Turnmier, eds., pp. 185 – 213, Center for the First Americans, University of Oregon, Corvallis, OR.

Dunbar, James S. and B.I. Waller.
1983 A Distribution Analysis of the Clovis/Suwannee Paleo-Indian Sites of Florida. Florida Anthropologist 36:18-30.

EdgeTech
2003 Discover Sub-Bottom Profiler Processor Software Technical and User's Manual Revision 2.1. West Wareham, MA.

Ellwood, Brooks B. and B. Burkart
1996 Test of Hydrocarbon-Induced Magnetic Patterns in Soils: the Sanitary Landfill as Laboratory. In Hydrocarbon Migration and Its Near-Surface Expression, D. Schumacher and M.A. Abrams, eds., AAPG Memoir 66, 91 – 98.

Ellwood, Brooks B., F.B. Harrold, S.L. Benoist, P. Thacker, M. Otte, D. Bonjean, G.L. Long, A.M. Shahin, R.P. Hermann, and F. Grandjean
2004 Magnetic Susceptibility Applied as an Age-Depth-Climate Relative Dating Technique Using Sediments from Scladina Cave, a Late Pleistocene Cave Site in Belgium. Journal of Archaeological Science 31, 283-293.

Ellwood, Brooks B., W. L. Balsam and Harry H. Roberts
2006 Gulf of Mexico Sediment Sources and Sediment Transport Trends from Magnetic Susceptibility Measurements of Surface Samples. Marine Geology 230: 237–248.

Ellwood, Brooks B. and W.L. Gose
2006 Heinrich H1 and 8,200 Year B.P. Climate Events Recorded in Hall's Cave, Texas. Geology 34, 753-756.

Enright, J.M., R. Gearhart II, D. Jones, and J. Enright
2006 Study to Conduct National Register of Historic Places Evaluations of Submerged Sites on the Gulf of Mexico Outer Continental Shelf. U.S. Department of the Interior, Minerals Management Service, Gulf of Mexico OCS Region, New Orleans, L.A. OCS Study MMS 2006-036.

Erlandson, Jon M., Madonna L. Moss, and Matthew Des Lauriers
2008 Life on the Edge: Early Maritime Cultures of the Pacific Coast of North America. Quaternary Science Reviews 27:2232-2245

Erlandson, Jon M., Torben C. Rick, Todd J. Braje, Molly Casperson, Brendan Culleton, Brian Fulfrost, Tracy Garcia, Daniel A. Guthrie, Nicholas Jew, Douglas J. Kennett, Madonna L. Moss, Leslie Reeder, Craig Skinner, Jack Watts, and Lauren Willis
2011 Paleoindian Seafaring, Maritime Technologies, and Coastal Foraging on California's Channel Islands. Science 331(6021):1181-1185

Evans, Amanda M.
[n.d.] No Visibility, No Artifacts, No Problem?: Challenges Associated with Presenting Buried Sites and Inaccessible Shipwrecks to the Public. In, Solving Problems in the Public Interpretation of Maritime Cultural Heritage, D. Scott-Ireton (ed.). Springer, New York, NY. In press.

Evans, Amanda M., Antony Firth, and Mark Staniforth
2009 Old and New Threats to Submerged Cultural Landscapes: Fishing, Farming and Energy Development. Conservation and Management of Archaeological Sites, Special Issue: Conserving Marine Cultural Heritage, 11(1):43-53.

Evans, Amanda M. and Matthew E. Keith
2011a Benefit Analysis of a Maritime Cultural Landscape Approach to Submerged Prehistoric Resources, Northwestern Gulf of Mexico. In: Contributions to the Archaeology of Maritime Landscapes, B. Ford (ed.), pp. 169-178, Springer Publishing, New York, NY.

———. 2011b The Consideration of Archaeological Sites in Oil and Gas Drilling. UNESCO

Evans, Amanda M. and Erin E. Voisin
2011 Geophysics, Industry, and Shipwrecks on the Gulf of Mexico OCS. In, Proceedings of the Offshore Technology Conference, Houston, Texas, USA, May 2-5, 2011. Paper 21697.

Evans, Amanda M., Matthew E. Keith, Erin E. Voisin, Patrick Hesp, Greg Cook, Mead Allison, Graziela da Silva, and Eric Swanson.
2012 Archaeological Analysis of Submerged Sites on the Gulf of Mexico Outer Continental Shelf. U.S. Department of the Interior, Bureau of Ocean Energy Management, Gulf of Mexico OCS Region, New Orleans, LA. OCS Study BOEM 2012-0xx. 395p.

Evans, Amanda M., Joe Flatman, and Nic Flemming (eds.)
[n.d.] Submerged Prehistoric Archaeology: How Climate Change and Technology are Rewriting History. Springer, New York, NY. In press.

Evans, J. and T. O'Connor
1999 Environmental Archaeology: Principles and Methods. Sutton Publishing, Gloucestershire.

Fairbanks, R.G.
1989 A 17,000-year Glacio-eustatic Sea Level Record: Influence of Glacial Melting Rates on the Younger Dryas Event and Deep Ocean Circulation. Nature 342:637-642.

———. 1990 The Age and Origin of the "Younger Dryas Climate Event" in Greenland Ice Cores. Paleooceanography 5(6):937-948.

Faught, Michael K.
2008 Archaeological Roots of Human Diversity in the New World: A Compilation of Accurate and Precise Radiocarbon Ages from Earliest Sites. American Antiquity 73(4):670-698.

Faught, Michael K. and J.F. Donoghue
1997 Marine Inundated Archaeological Sites and Paleofluvial Systems: Examples from a Karst-Controlled Continental Shelf Setting in Apalachee Bay, Northeastern Gulf of Mexico. Geoarchaeology 12, 417-458.

Fladmark, Kent
1979 Routes: Alternate Migration Corridors for Early Man in North America. American Antiquity 44:55-69

Fleischer, P., T.H. Orsi, M.D. Richardson, and A.L. Anderson
2001 Distribution of Free Gas in Marine Sediments: A Global Overview. Geo-Marine Letters 21:103-122.

Flemming, Nic C.
1983 Survival of Submerged Lithic and Bronze Age Artefact Sites: a Review of Case Histories. In Quaternary Coastlines and Maritime Archaeology, edited by P.M. Masters and N.C. Flemming, pp.135-173. Academic Press, London.

Foecke, T., L. Ma, M.A. Russell, D.L. Conlin, and L.E. Murphy
2010 Investigation Archaeological Site Formation Processes on the Battleship USS Arizona Using Finite Element Analysis. Journal of Archaeological Science 37:1090-1101.

Folk, R.L.
1980 Petrology of Sedimentary Rocks. Hemphill Publishing Company; Austin, TX.

Food and Agricultural Organization of the United Nations (FAO)
2005 Impacts of Trawling and Scallop Dredging on Benthic Habitats and Communities. Rome, Italy.

Fowler, Cynthia and Evelyn Konopik
2007 The History of Fire in the Southern United States. Human Ecology Review 14(2):165-176.

Frazier, David E.
1974 Depositional Episodes: Their Relationship to the Quaternary Stratigraphic Framework in the Northwestern Portion of the Gulf Basin. Geologic Circular 74-1, Bureau of Economic Geology, University of Texas at Austin.

Gaffney, Vince and Kenneth Thomson
2007 Mapping Doggerland. In, Mapping Doggerland: The Mesolithic Landscapes of the Southern North Sea, V. Gaffney, K. Thomson, and S. Fitch (eds.), pp. Archaeopress, Oxford, UK.

Gagliano, Sherwood M.
1964 An Archaeological Survey of Avery Island. Coastal Studies Institute, Baton Rouge.

———. 1967 Occupation Sequence at Avery Island. Unpublished Ph.D. dissertation, Department of Geography and Anthropology Louisiana State University, Baton Rouge.

———. 1984. Geoarchaeology of the Northern Gulf Shore. In Perspectives on Gulf Coast Prehistory, Dave D. Davis (ed.), pp. 1-40. University Presses of Florida, Gainesville.

Gagliano, Sherwood M., Charles E. Pearson, Richard A. Weinstein, D.E. Wiseman, and C.M. McClendon
1982 Sedimentary Studies of Prehistoric Archaeological Sites: Criteria for the Identification of Submerged Archaeological Sites of the Northern Gulf of Mexico Continental Shelf. National Park Service, Division of State Plans and Grants.

Galili, Ehud and Mina Weinstein-Evron
1985 Prehistory and Paleoenvironments of Submerged Sites Along the Carmel Coast of Israel. Paléorient 11(1):37-52.

Galinat, Walton C.
1985 Domestication and Diffusion of Maize. In, Prehistoric Food Production in North America, R. Ford (ed.), pp. 245-278. University of Michigan Press, Ann Arbor.

Garrison, E. G.,C.F. Giammona, F.J. Kelly, A.R. Tripp, and G.A. Wolff
1989 Historic Shipwrecks and Magnetic Anomalies of the Northern Gulf of Mexico: Reevaluation of Archaeological Resource Management Zone 7- Volume I executive summary. OCS Study MMS 89-0023. US DOI, MMS, Gulf of Mexico OCS Region, New Orleans.

Gilbert, M. Thomas P., Dennis L. Jenkins, Anders Götherstrom, Nuria Naveran, Juan J. Sanchez, Michael Hofreiter, Philip Francis Thomsen, Jonas Binladen, Thomas F. G. Higham, Robert M. Yohe II, Robert Parr, Linda Scott Cummings, and Eske Willerslev
2008 DNA from Pre-Clovis Human Coprolites in Oregon, North America. Science 320(5877):786-789

Goebel, Ted, Michael R. Waters, D.H. O'Rourke
2008 The Late Pleistocene Dispersal of Modern Humans in the Americas. Science 319:1497-1502.

Goldberg, P. and R.I. Macphail
2006 Practical and Theoretical Geoarchaeology. Blackwell Publishing, Malden, MA.

Goodyear, Albert C.
2005 Evidence for Pre-Clovis Sites in the Eastern United States. In Paleoamerican Origins: Beyond Clovis, edited by R. Bonnichsen, B.T. Lepper, D. Stanford, and M.R. Waters, pp. 103-112. Center for the Study of the First Americans, Texas A&M University, College Station.

Gordon, E.S., M.A. Goñi, Q.N. Roberts, G.C. Kineke, and M.A. Allison
2001 Organic Matter Distribution and Accumulation on the Inner Louisiana Shelf. Continental Shelf Research 21:1691-1721.

Hamilton, Edwin L. and Richard T. Bachman
1982 Sound velocity and related properties of marine sediments. Journal of the Acoustical Society of America 72(6):1891-1904.

Harrold, F., Brooks B. Ellwood, P. Thacker, S. Benoist
2004 Magnetic susceptibility analysis of sediments at the Middle-Upper Paleolithic transition for two cave sites in northern Spain. ZILHÃO, J.; D'ERRICO, F. (eds.) The Chronology of the Aurignacian and of the Transitional Technocomplexes. Dating, Stratigraphies, Cultural Implications, Trabalhos de Arqueologia 33. Lisboa, Instituto Português de Arqueologia, 301-310.

Herbert, D. G. Maschner
1996 Middle Range Theory. In The Oxford Companion to Archaeology, Brian M. Fagan (ed.). Oxford Reference Online, Boise State University. <http://www.oxfordreference.com/views/ENTRY.html?subview=Main&entry=t136.e0289> Accessed 20 March 2009

Herz, N. and E.G. Garrison
1998 Geological Methods for Archaeology. Oxford University Press, Oxford, U.K.

Hicks, David W.
2010 Molluscan Ecology and Habitats. In, Tunnell, John W. Jr., Jean Andrews, Noe C. Barrera, and Fabio Moretzsohn (eds.) Encyclopedia of Texas Seashells: Identification, Ecology, Distribution, and History, pps. 28 – 75. Texas A&M University Press, College Station.

Hill, Christopher
2007 Surficial Processes and Pleistocene Archaeology: Context, Landscape Evolution, and Climate Change. In, Reconstructing Human-Landscape Interactions, L. Wilson, P. Dickinson, and J. Jeandron (eds.), pp. 6-36. Cambridge Scholars Publishing, Newcastle, UK.

Hill, James N.
1966 A Prehistoric Community in Eastern Arizona. Southwestern Journal of Anthropology 22(1):9-30.

Holliday, Vance T.
2004 Soils and Archaeological Research. Oxford University Press, Oxford, UK.

Holmes, Charles W.
2011 Development of the Northwestern Gulf of Mexico Continental Shelf and Coastal Zone as a Result of the Late-Pleistocene-Holocene Sea-Level Rise. In, N.A. Buster and C.W. Holmes (eds.) Gulf of Mexico Origins, Waters, and Biota, Volume 3, Geology, pp. 195-208. Texas A&M University Press, College Station.

Johnson, L. L., and M. Stright (eds.)
1992 Paleoshorelines and Prehistory: An Investigation of Method. CRC Press; Baton Raton.

Keith, Matthew and Amanda M. Evans
2009 Proposed Pipeline Route Survey #09-470-13. Report to Minerals Management Service, U. S. Department of the Interior, for Hilcorp Energy GOM, LLC prepared by Tesla Offshore, LLC.

Keith, Matthew and Erika Geresi
2008 Geophysical Lease Survey #07-362-11. Report to Minerals Management Service, U. S. Department of the Interior, for Hydro Gulf of Mexico, LLC prepared by Tesla Offshore, LLC.

Keith, Matthew and Wynn Pryor
2007 Geophysical Lease Survey #07-363-11. Report to Minerals Management Service, U. S. Department of the Interior, for Hydro Gulf of Mexico, LLC prepared by Tesla Offshore, LLC.

Kelly, Robert L. and Lawrence C. Todd.
1988 Coming into the Country: Early Paleoindian Hunting and Mobility. American Antiquity 53(2):231-244.

Lee, Houma J.
1985 State of the Art: Laboratory Determinations of the Strength of Marine Soils. In, Strength Testing of Marine Sediments and In-Situ Measurements, ASTM STP 883, R.C. Chaney and K.R. Demars, eds., American Society for Testing and Materials, Philadelphia, pp. 181-250.

Lewis, R.Barry
2000 Sea-Level Rise and Subsidence Effects on Gulf Coast Archaeological Site Distributions. American Antiquity 65, 525-541.

Lowery, Darrin L., Michael A. O'Neal, John S. Wah, Daniel P. Wagner, and Dennis J. Stanford
2010 Late Pleistocene Upland Stratigraphy of the Western Delmarva Peninsula, USA. Quaternary Science Reviews 29(2010):1472-1480

McClelland Engineers
1979 Strength Characteristics of Near Seafloor Continental Shelf Deposits of North Central Gulf of Mexico. Report Number 0178-043. McClelland Engineers, Houston, TX.

McConnell, Kathleen
1998 The Prehistoric Use of Chenopodiaceae in Australia: Evidence from Carpenter's Gap Shelter 1 in the Kimberley, Australia. Vegetation History and Archaeobotany 7(3):179-188.

McLauchlan, Kendra
2003 Plant Cultivation and Forest Clearance by Prehistoric North Americans: Pollen Evidence from Fort Ancient, Ohio, USA. The Holocene 13(4):557-566.

McNinch, J.E., J.T. Wells, and A.C. Trembanis
2006 Predicting the Fate of Artefacts in Energetic, Shallow Marine Environments: an Approach to Site Management. The International Journal of Nautical Archaeology 35(2):290-309.

Masselink, G. and M.G. Hughes
2003 Introduction to Coastal Processes and Geomorphology. Oxford University Press, New York.

Masters, P. M. and N.C. Flemming (eds.)
1983 Quaternary Coastlines and Marine Archaeology: Towards the Prehistory of Land Bridges and Continental Shelves. Academic Press, New York.

Meltzer, David J.
2009 First Peoples in a New World: Colonizing Ice Age America. University of California Press, Berkeley.

Milanich, Jerald T.
1994 Archaeology of Precolumbian Florida. University Press of Florida, Gainesville, FL.

Milliken, K.T., J.B. Anderson, and A.B. Rodriguez
2008 A New Composite Holocene Sea-Level Curve for the Northern Gulf of Mexico, in Anderson, J.B., and Rodriguez, A.B., eds., Response of Upper Gulf Coast Estuaries to Holocene Climate Change and Sea-Level Rise: Geological Society of America Special Paper 443, pp. 1 – 11.

MMS (see US Department of the Interior)

Momber, Garry
2000 Drowned and Deserted: a Submerged Prehistoric Landscape in the Solent. International Journal of Nautical Archaeology 29:86-99.

Morris, Percy A.
1973 A Field Guide to Shells of the Atlantic and Gulf Coasts and the West Indies. Houghton, Mifflin Company, Boston, MA.

Morton, R.A., J.G. Paine, and Michael D. Blum
2000 Responses of Stable Bay-Margin and Barrier-Island Systems to Holocene Sea-level Highstands, Western Gulf of Mexico. Journal of Sedimentary Research 70:478-490

Muckelroy, Keith
1978 Maritime Archaeology. New Studies in Archaeology. Cambridge University Press, Cambridge, UK.

Mudroch, A. and J.M. Azcue
1995 Manual of Aquatic Sediment Sampling. Lew Publishers, Boca Raton, FL.

Mussett, A.E. and M.A. Khan
2000 Looking into the Earth: An Introduction to Geological Geophysics. Cambridge University Press, Cambridge.

National Commission on the BP Deepwater Horizon Oil Spill and Offshore Drilling
2011 The History of Offshore Oil and Gas in the United States (Long Version). Staff Working Paper No. 22. <http://www.oilspillcommission.gov/resources#staff-working-papers> Accessed 14 June 2011.

NOAA CSC (see U.S. Department of Commerce)

NPS (see U.S. Department of the Interior)

Nelson, Henry F. and Ellis E. Bray
1970 Stratigraphy and History of Holocene Sediments in the Sabine-High Island Area, Gulf of Mexico. In, Deltaic Sedimentation, Modern and Ancient, J.P. Morgan (ed.), pp. 48-77. Society of Economic Paleontologists and Mineralogists Special Publication No. 15, Tulsa, OK.

Neuman, Robert W.
1984 An Introduction to Louisiana Archaeology. Louisiana State University Press, Baton Rouge.

Newcomb, W. W., Jr.
1961 The Indians of Texas from Prehistoric to Modern Times. University of Texas Press, Austin, TX.

Pearson, Charles E., Doug B. Kelley, Richard A. Weinstein, and Sherwood M. Gagliano
1986 Archaeological Investigations on the Outer Continental Shelf: A Study Within the Sabine River Valley, Offshore Louisiana and Texas. Minerals Management Service OCS Study MMS 86-0119. Reston, VA.

Pirazolli, Paolo A.
1991 World Atlas of Holocene Sea-Level Changes. Elsevier Oceanography Series No. 58. Elsevier, Amsterdam.

Plets, Ruth, Justin K. Dix, Alex Bastos, and Angus L. Best
2007 Characterization of Buried Inundated Peat on Seismic (Chirp) Data, Inferred from Core Information. Archaeological Prospection 14(4)1-12.

Pohl, Mary D., Dolores R. Piperno, Kevin O. Pope, and John G. Jones
2007 Microfossil evidence for pre-Columbian Maize Dispersals in the Neotropics from San Andrés, Tabasco, Mexico. Proceedings of the National Academies of Science 104(16):6870-6875

Price, T. Douglas and Gary M. Feinman
2008 Images of the Past, 5th edition. McGraw-Hill, New York, NY.

Quinn, Rory
2006 The Role of Scour in Shipwreck Site Formation Processes and the Preservation of Wreck-Associated Scour Signatures in the Sedimentary Record – Evidence from Seabed and Sub-surface Data. Journal of Archaeological Science 33:1419-1432.

Raab, L. Mark and Albert C. Goodyear
1984 Middle-Range Theory in Archaeology: A Critical Review of Origins and Applications. American Antiquity 49(2):255-268

Rees, Mark A.
2010 Paleoindian and Early Archaic. In Archaeology of Louisiana, Mark A. Rees (ed.), pp . 34-62, Louisiana State University Press, Baton Rouge.

Rego, J., K. Cronin, and D. Vatvani.
2011 Hurricane Bottom Stirring in the Gulf of Mexico. Deltares Report 1204025-000.

Rick, Torben C., Jon M. Erlandson, and René L. Vellanoweth.
2001 Paleocoastal Marine Fishing on the Pacific Coast of the Americas: Perspectives from Daisy Cave, California. American Antiquity 66(4):595-613

Ricklis, Robert A.
2004 The Archeology of the Native American Occupation of Southeast Texas. In, The Prehistory of Texas, Timothy K. Perttula (ed.), pp. 181-202, Texas A&M University Press, College Station.

Ricklis, Robert A. and Michael D. Blum
1997 The Geoarchaeological Record of Holocene Sea Level Change and Human Occupation of the Texas Gulf Coast, Geoarchaeology 12, 287-314.

Schiffer, Michael B.
1987 Formation Processes of the Archaeological Record. University of Utah Press, Salt Lake City, UT.

Shackley, Mary L.
1975 Archaeological Sediments: A Survey of Analytical Methods. Halsted Press, New York, New York.

Shepard, F.P.
1960 Rise of Sea-Level Along Northwestern Gulf of Mexico. In, Recent Sediments, Northwestern Gulf of Mexico, F.P. Shepard (ed.), pp. 338-344. American Association of Petroleum Geologists, Boulder, CO.

Simms, A.R., J.B. Anderson, K.T. Milliken, Z.P. Taha, and J.S. Wellner
2008 Geomorphology and Age of the Oxygen Isotope Stage 2 (Last Lowstand) Sequence Boundary on the Northwestern Gulf of Mexico Continental Shelf, in Davies, R.J., Posamentier, H.W., Wood, L.J., and Cartwright, J.A., eds., Seismic Geomorphology: Applications to Hydrocarbon Exploration and Production. Geological Society, London, Special Publications, 277:29-46.

Stanbury, Myra (ed.)
2003 The Barque Eglinton, Wrecked Western Australia 1852: The history of its loss, archaeological excavation, artefact catalogue and interpretation. Australian National Centre of Excellence for Maritime Archaeology, Special Publication No. 6, AIMA Special Publication No. 13.

Stanford, Dennis and B. Bradley
2012 Across Atlantic Ice: The Origin of America's Clovis Culture. Berkeley: University of California Press, Berkeley.

Stanford, Dennis, R. Bonnichsen, B. Meggers, and D.G. Steele
2005 Paleoamerican Origins: Models, Evidence, and Future Directions. In Paleoamerican Origins: Beyond Clovis, edited by R. Bonnichsen, B.T. Lepper, D. Stanford, and M.R. Waters, pp. 313-353. Center for the Study of the First Americans, Texas A&M University, College Station.

Stewart, D.J.
1999 Formation Processes Affecting Submerged Archaeological Sites: An Overview. Geoarchaeology: An International Journal 14(6):565-587.

Story, Dee Ann
1985 Adaptive Strategies of Archaic Cultures of the West Gulf Coastal Plain. In, Prehistoric Food Production in North America, R. Ford (ed.), pp. 19-56. University of Michigan Press, Ann Arbor.

Stright, Melanie J.
1986 Human Occupation of the Continental Shelf During the Late Pleistocene/Early Holocene: Methods for Site Location. Geoarchaeology 1:347-364.

———. 1999. Spatial Data Analysis of Artifacts Redeposited by Coastal Erosion: a Case Study of McFaddin Beach, Texas. OCS Study MMS 99-0068. US Department of the Interior, Minerals Management Service, Herndon, VA. Siddall et al. 2003

Texas Historical Commission (THC).
1988 State of Texas Archaeological Site Data Form, 41GV101. Recorded by Jeffrey A. Huebner. Document on file Texas Historical Commission, Austin, TX.

Thacker, P.T. and Brooks B. Ellwood
2007 Late Pleistocene paleoclimate and sediment magnetic susceptibility at Lapa dos Coelhos, Portugal. From the Mediterranean basin to the Portuguese Atlantic shore: Papers in Honor of Anthony Marks, Actas do IV Congresso de Arqueologia Peninsular, Ed. Nuno Ferreira Bicho, p.163-171.

Thomas, David Hurst
1989 Archaeology, Second Edition. Holt, Rinehart, and Winston, Inc., Fort Worth, TX.

Tornqvist, Torbjörn E., Santina R. Wortman, Zenon R.P. Mateo, Glenn A. Milne, and John B. Swenson
2006 Did the Last Sea-level Lowstand Always Lead to Cross-Shelf Valley Formation and Source to Sink Sediment Flux? Journal of Geophysical Research 111:FO4002

Toscano, M.A. and I.G. MacIntyre
2003 Corrected Western Atlantic Sea-level Curve for the Last 11,000 years Based on Calibrated ^{14}C Dates from Acropora Palmata Framework and Intertidal Mangrove Peat. Coral Reefs 22:257-270

Tunnell, John W. Jr., Jean Andrews, Noe C. Barrera, and Fabio Moretzsohn.
2010 Encyclopedia of Texas Seashells: Identification, Ecology, Distribution, and History. Texas A&M University Press, College Station.

United Nations Educational Scientific and Cultural Organization (UNESCO)
1958 Convention on the Continental Shelf. Geneva, Switzerland.

United State Department of Agriculture, Natural Resources Conservation Service (USDA NRCS)
2004 Plant Guide: Chokecherry Prunus virginiana L.
<http://plants.usda.gov/plantguide/pdf/cs_prvi.pdf> Accessed January 15, 2011.

United States Congress (97th)
1983 Federal Oil and Gas Royalty Management Act of 1982.
<www.onrr.gov/laws_r_d/PubLaws/PDFDocs/97-451.pdf> Accessed May 1, 2008.

U.S. Department of Commerce, National Oceanic and Atmospheric Administration, Office of Coastal Charts
2006 Mississippi River to Galveston. Chart 11340 1116A. Washington, DC.

U.S. Department of Commerce, National Oceanic and Atmospheric Administration, Coastal Services Center (NOAA CSC)
2009 Maritime Zones and Boundaries, including limits of territorial sea, continguous zone, EEZ and continental shelf.. < http://www.gc.noaa.gov/gcil_maritime.html>. Accessed 16 Nov. 2009.

U.S. Department of the Interior, Bureau of Ocean Energy Management (BOEM)
2005 Notice to Lessees and Operators of Federal Oil, Gas, and Sulphur Leases and Pipeline Right-Of-Way Holders in the Outer Continental Shelf, Gulf of Mexico OCS Region, Archaeological Resource Surveys and Reports, NTL 2005-G07, Gulf of Mexico, OCS Regional Office, Metairie, LA.

U.S. Department of the Interior, National Park Service (NPS)
2006 National Historic Preservation Act. In Federal Historic Preservation Laws: The Official Compilation of US Cultural Heritage Statutes, Part 2. U.S. Department of the Interior, Washington, DC.

Warny, Sophie, David M. Jarzen, Amanda Evans, Patrick Hesp, and Philip Bart
2012 Environmental Significance of Abundant and Diverse Hornwort Spores in a Potential Paleoindian Site in the Gulf of Mexico. Palynology 2012:1-20

Waters, Michael R.
1992 Principles of Geoarchaeology: A North American Perspective. University of Arizona Press, Tucson.

Waters, Michael R., Steve L. Forman, Thomas A. Jennings, Lee C. Nordt, Steven G. Driese, Joshua M. Feinberg, Joshua L. Keene, Jessi Halligan, Anna Lindquist, James Pierson, Charles T. Hallmark, Michael B. Collins, and James E. Wiederdhold.
2011 The Buttermilk Creek Complex and the Origins of Clovis at the Debra L. Friedkin Site, Texas. Science 331:1599-1603.

Weinstein, Richard A., Douglas C. Wells, Thurston H.G. Hahn III, Anne Marie M. Blank, Sherwood M. Gagliano, Amanda Evans, Julia Battle, and Sally A. Morehead
2012 Archaeological Assessment of Sites 16SB64 and 16SB153, St. Bernard Parish, Louisiana. Final Report submitted to Louisiana Governor's Office, Office of Coastal Protection and Restoration, DOA Report No. 22-3893.

Wells, Lisa E.
2001 Archaeological Sediments in Coastal Environments. In Sediments in Archaeological Context, J.K. Stein and W.R. Farrand, eds., pp. 149-182, University of Utah Press.

Wendorf, Fred.
1966 Early Man in the New World: Problems of Migration. American Naturalist 100(912):253-270

Westley, Kieran and Justin Dix
2006 Coastal environments and their role in prehistoric migrations. Journal of Maritime Archaeology 1, 9-28.

Whelan III, Thomas, James M. Coleman, J. N. Suhayda, and Harry H. Roberts
1977 Acoustical penetration and shear strength in gas-charged sediment. Marine Georesources and Geotechnology 2(1-4):147-159.

Wille, P.C.
2005 Sound Images of the Ocean in Research and Monitoring. Springer Verlag, Berlin.

Young, David E., Robson Bonnichsen, Diane Douglas, Jill McMahon, and Lise Swartz.
1994 Low-Range Theory and Lithic Technology: Exploring the Cognitive Approach. In, Method and Theory for Investigating the Peopling of the Americas, R. Bonnichsen and D.G. Steele, eds., pp. 209 – 237. Center for the Study of the First Americans; Corvallis, OR.

APPENDIX A. SEA-LEVEL CURVES

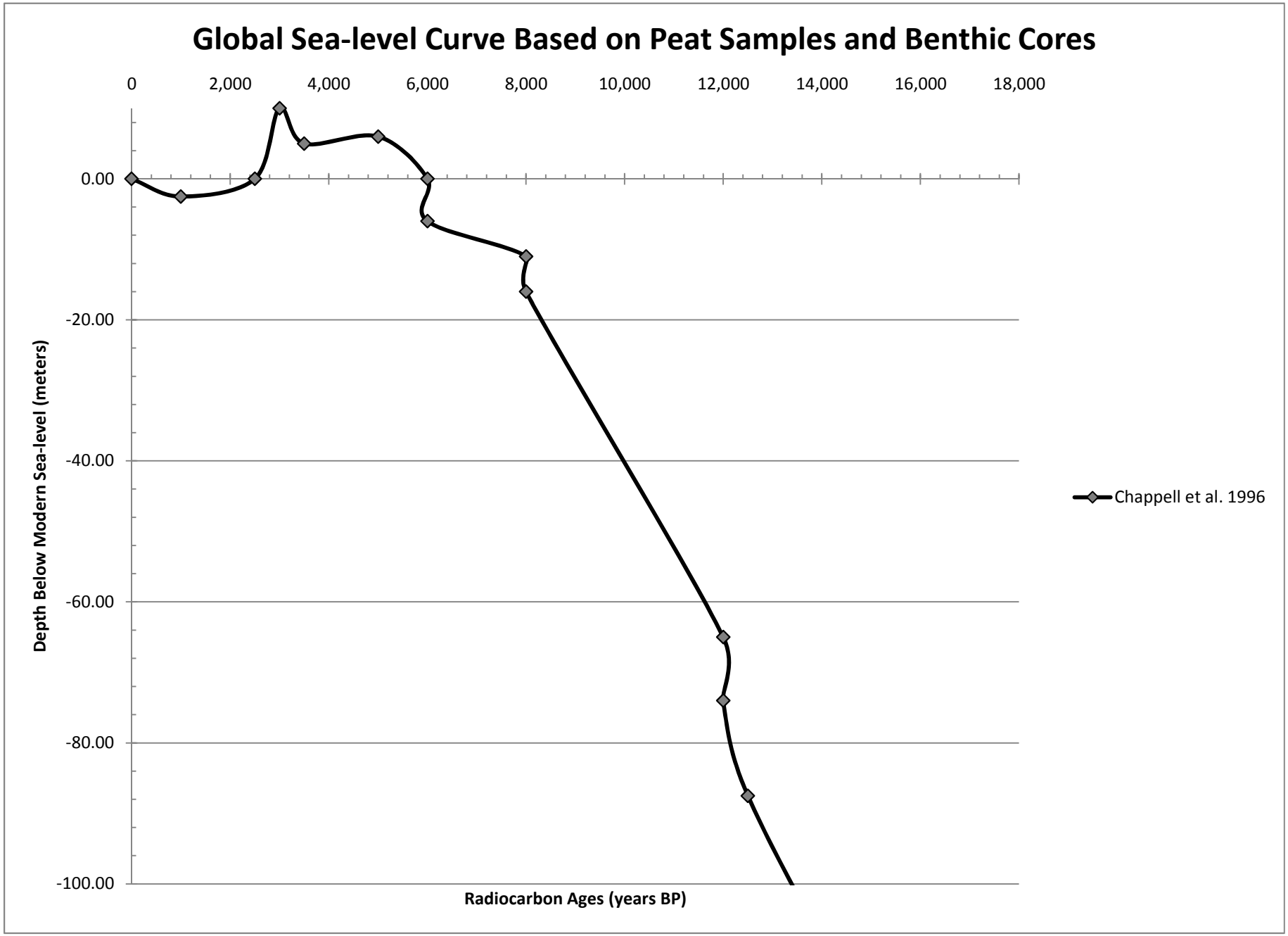
Global Sea-level Curve Based on Peat Samples and Benthic Cores
0
2,000
4,000
6,000
8,000
10,000
12,000
14,000
16,000
18,000
0.00
-20.00
-40.00
-60.00
-80.00
-100.00
Depth Below Modern Sea-level (meters)
Radiocarbon Ages (years BP)
Chappell et al. 1996

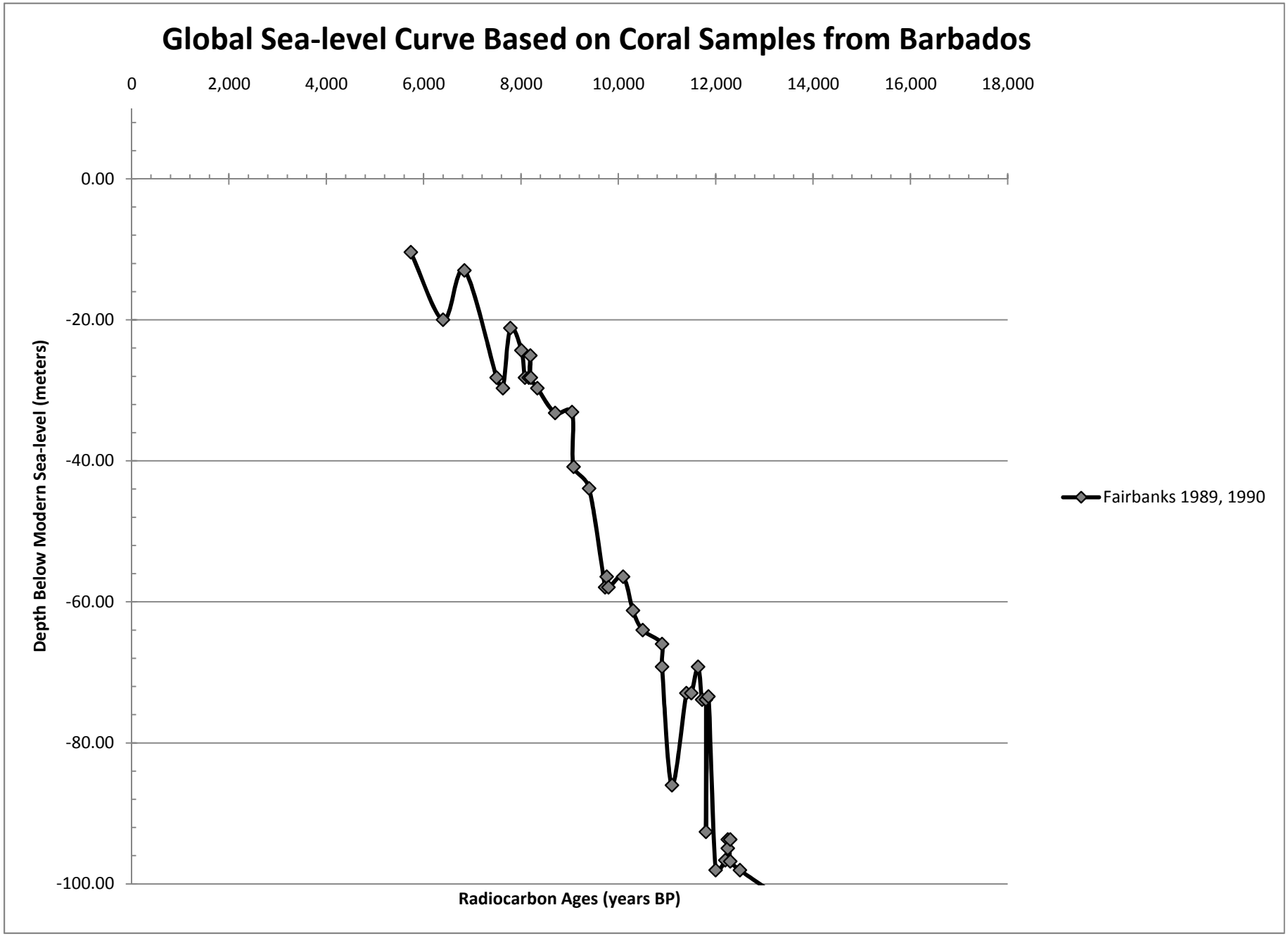
Global Sea-level Curve Based on Coral Samples from Barbados
0
2,000
4,000
6,000
8,000
10,000
12,000
14,000
16,000
18,000
0.00
-20.00
-40.00
-60.00
-80.00
-100.00
Depth Below Modern Sea-level (meters)
Radiocarbon Ages (years BP)
Fairbanks 1989, 1990

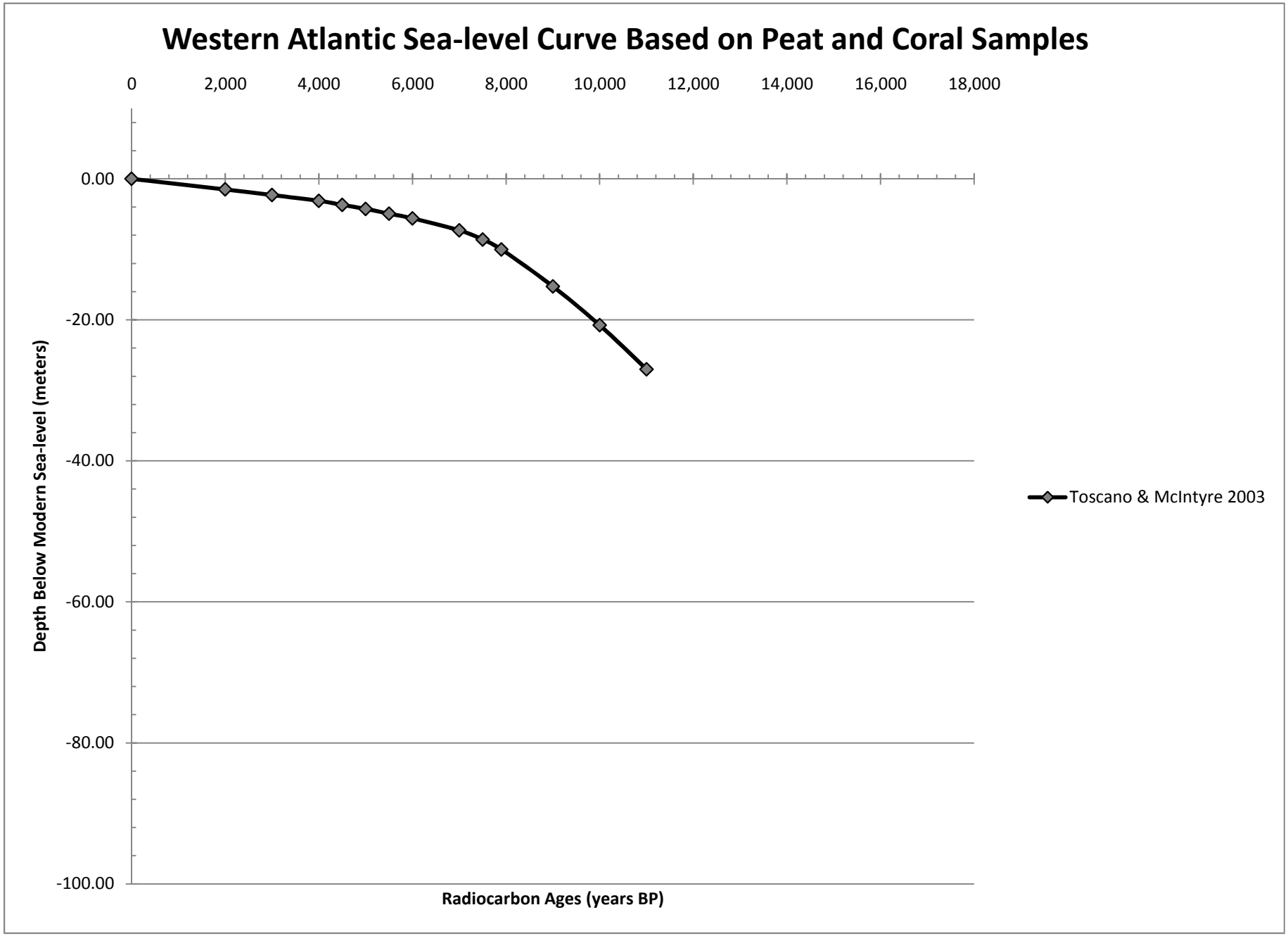
Western Atlantic Sea-level Curve Based on Peat and Coral Samples
0
2,000
4,000
6,000
8,000
10,000
12,000
14,000
16,000
18,000
0.00
-20.00
-40.00
-60.00
-80.00
-100.00
Depth Below Modern Sea-level (meters)
Radiocarbon Ages (years BP)
Toscano & McIntyre 2003

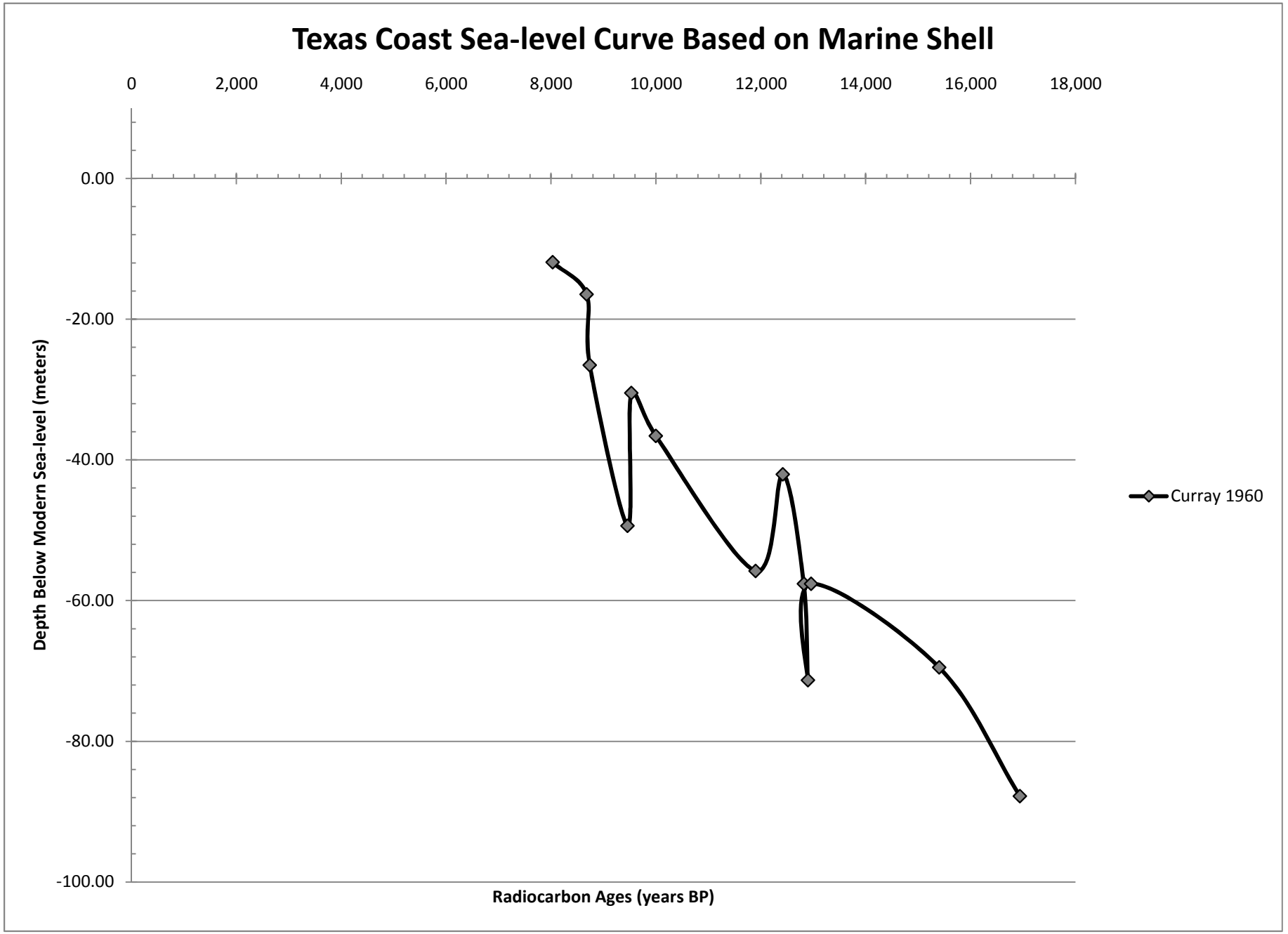
Texas Coast Sea-level Curve Based on Marine Shell
0
2,000
4,000
6,000
8,000
10,000
12,000
14,000
16,000
18,000
0.00
-20.00
-40.00
-60.00
-80.00
-100.00
Depth Below Modern Sea-level (meters)
Radiocarbon Ages (years BP)
Curray 1960

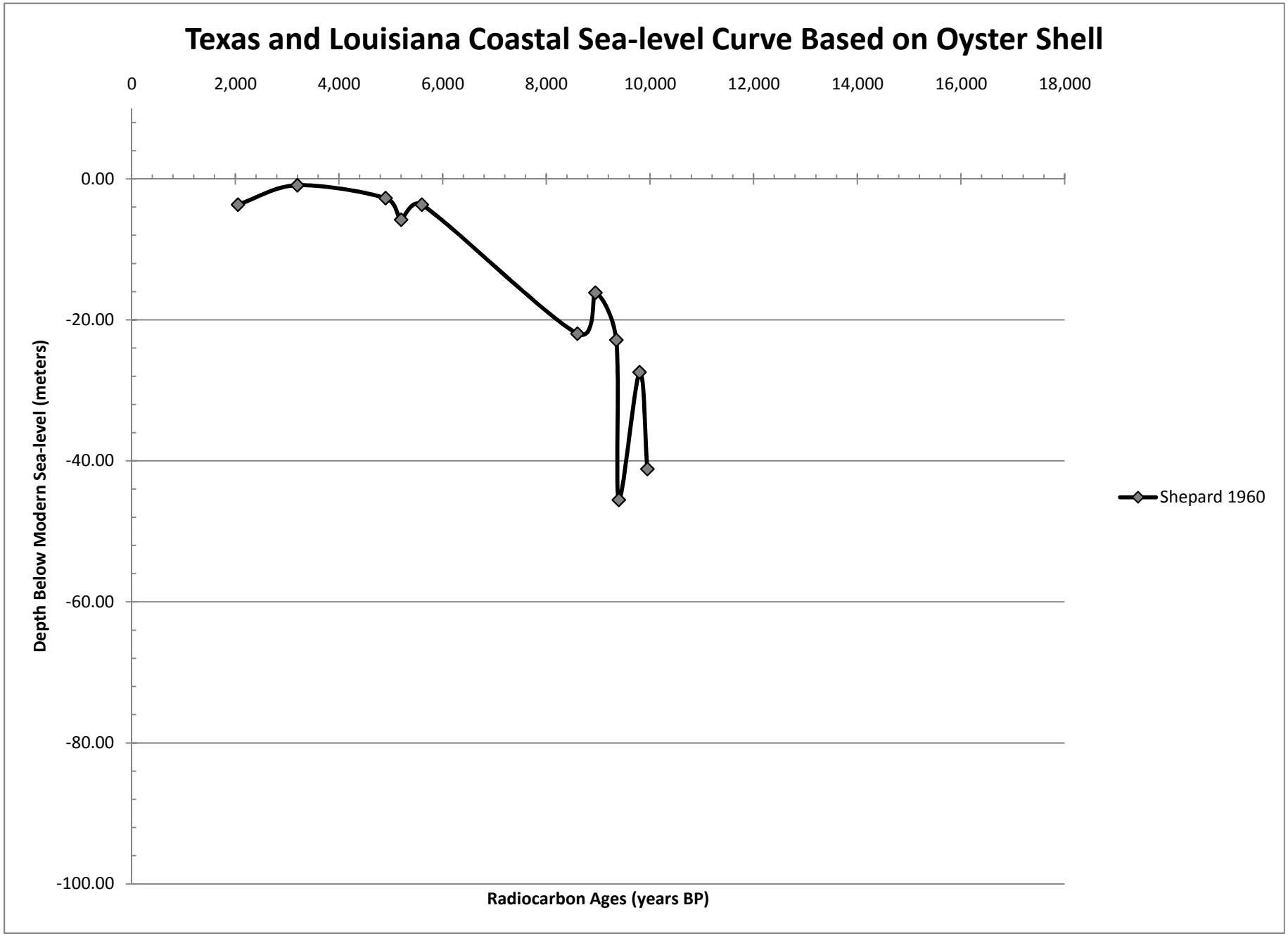
Texas and Louisiana Coastal Sea-level Curve Based on Oyster Shell
0
2,000
4,000
6,000
8,000
10,000
12,000
14,000
16,000
18,000
0.00
-20.00
-40.00
-60.00
-80.00
-100.00
Depth Below Modern Sea-level (meters)
Radiocarbon Ages (years BP)
Shepard 1960

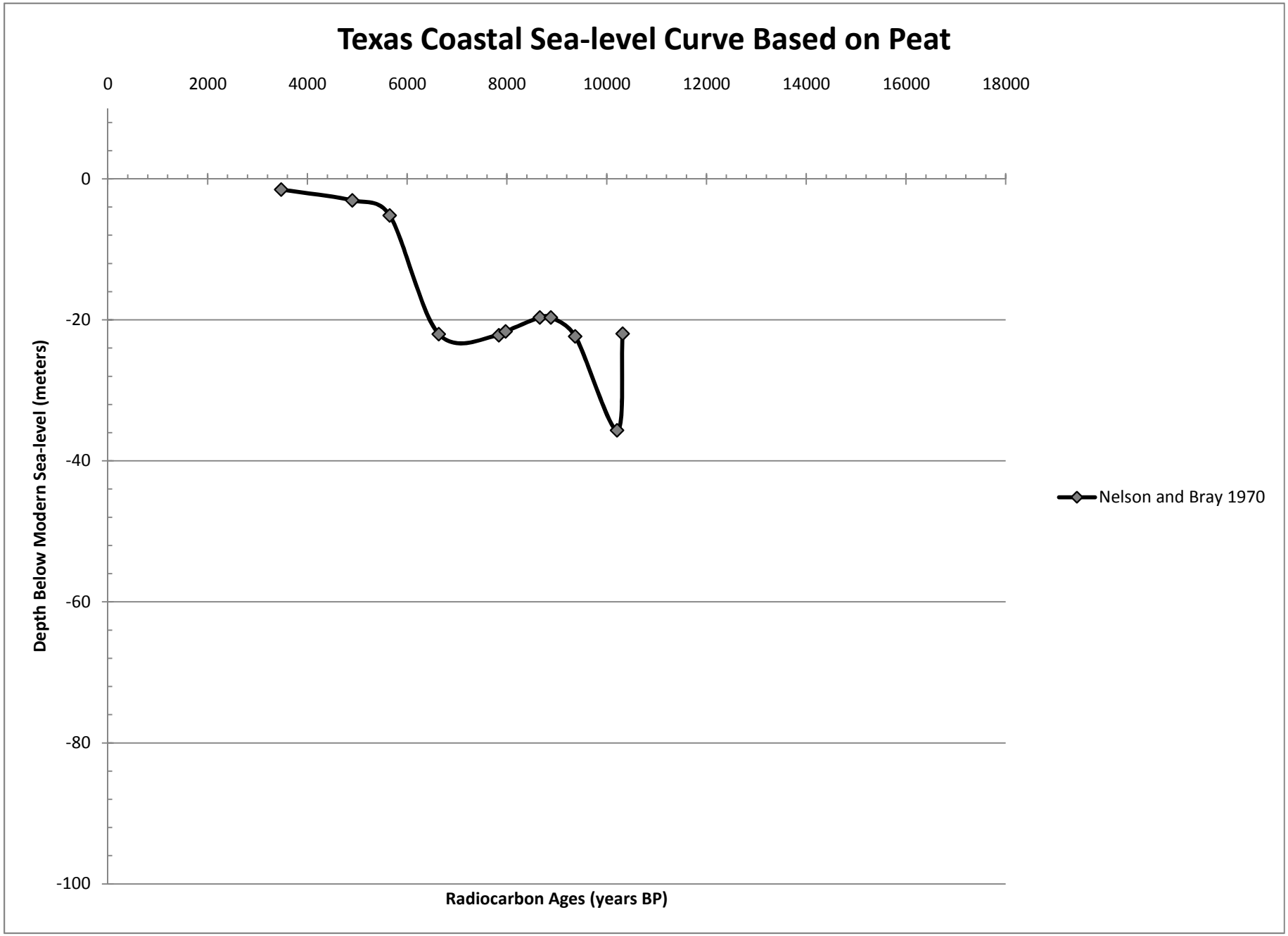
Texas Coastal Sea-level Curve Based on Peat
0
2000
4000
6000
8000
10000
12000
14000
16000
18000
0
-20
-40
-60
-80
-100
Depth Below Modern Sea-level (meters)
Radiocarbon Ages (years BP)
Nelson and Bray 1970

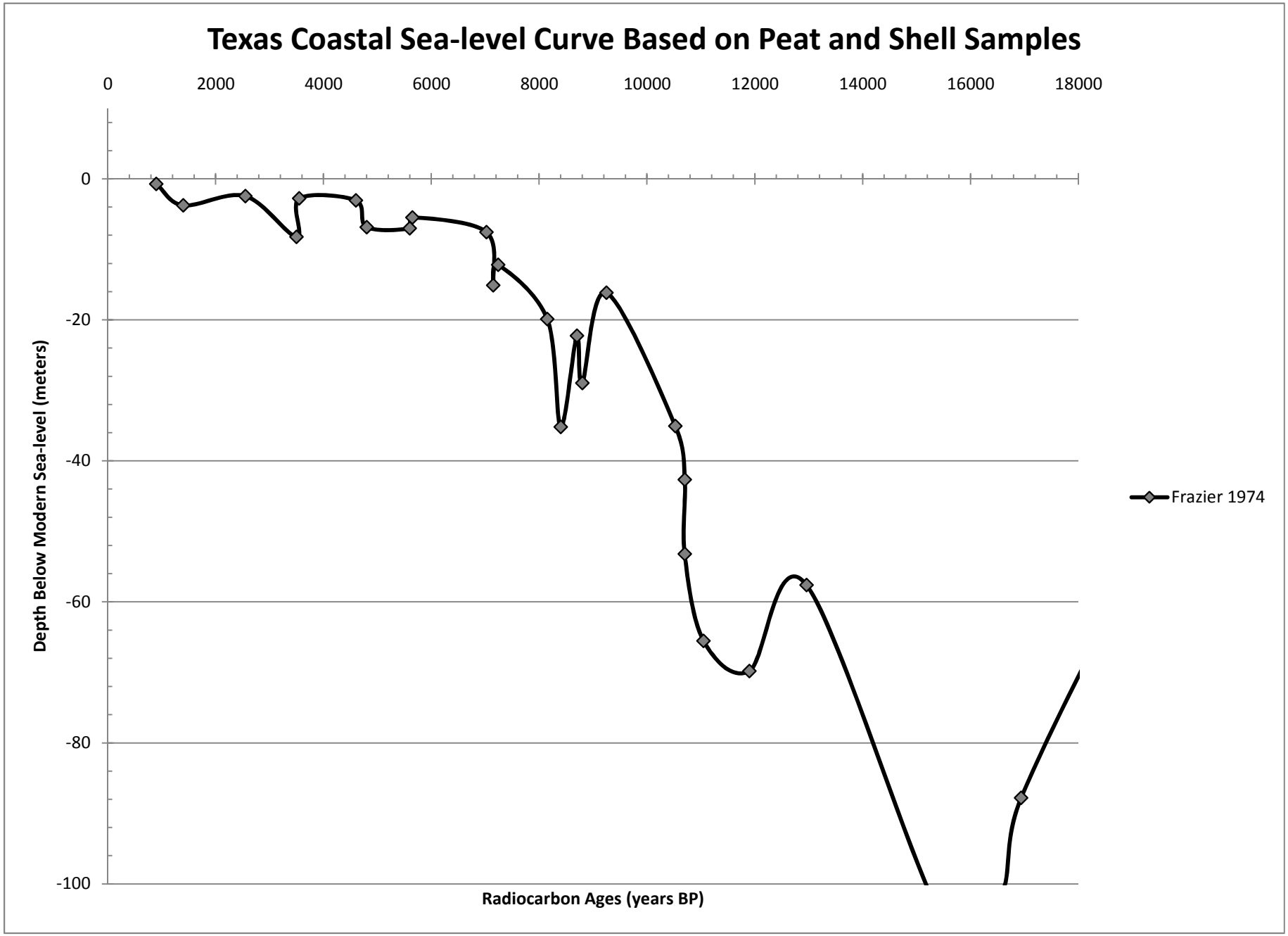
Texas Coastal Sea-level Curve Based on Peat and Shell Samples
0
2000
4000
6000
8000
10000
12000
14000
16000
18000
0
-20
-40
-60
-80
-100
Depth Below Modern Sea-level (meters)
Radiocarbon Ages (years BP)
Frazier 1974

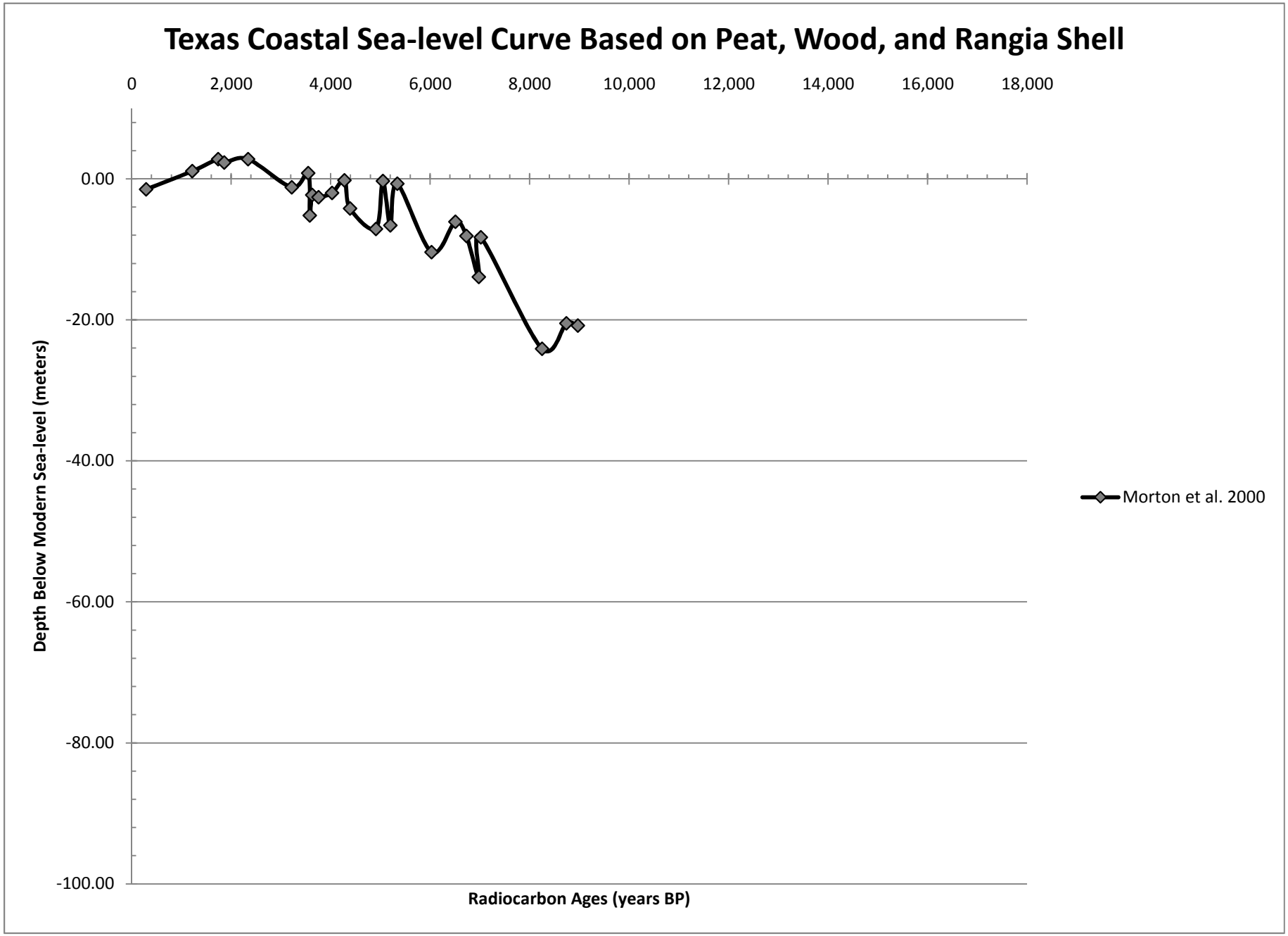
Texas Coastal Sea-level Curve Based on Peat, Wood, and Rangia Shell
0
2,000
4,000
6,000
8,000
10,000
12,000
14,000
16,000
18,000
0.00
-20.00
-40.00
-60.00
-80.00
-100.00
Depth Below Modern Sea-level (meters)
Radiocarbon Ages (years BP)
Morton et al. 2000

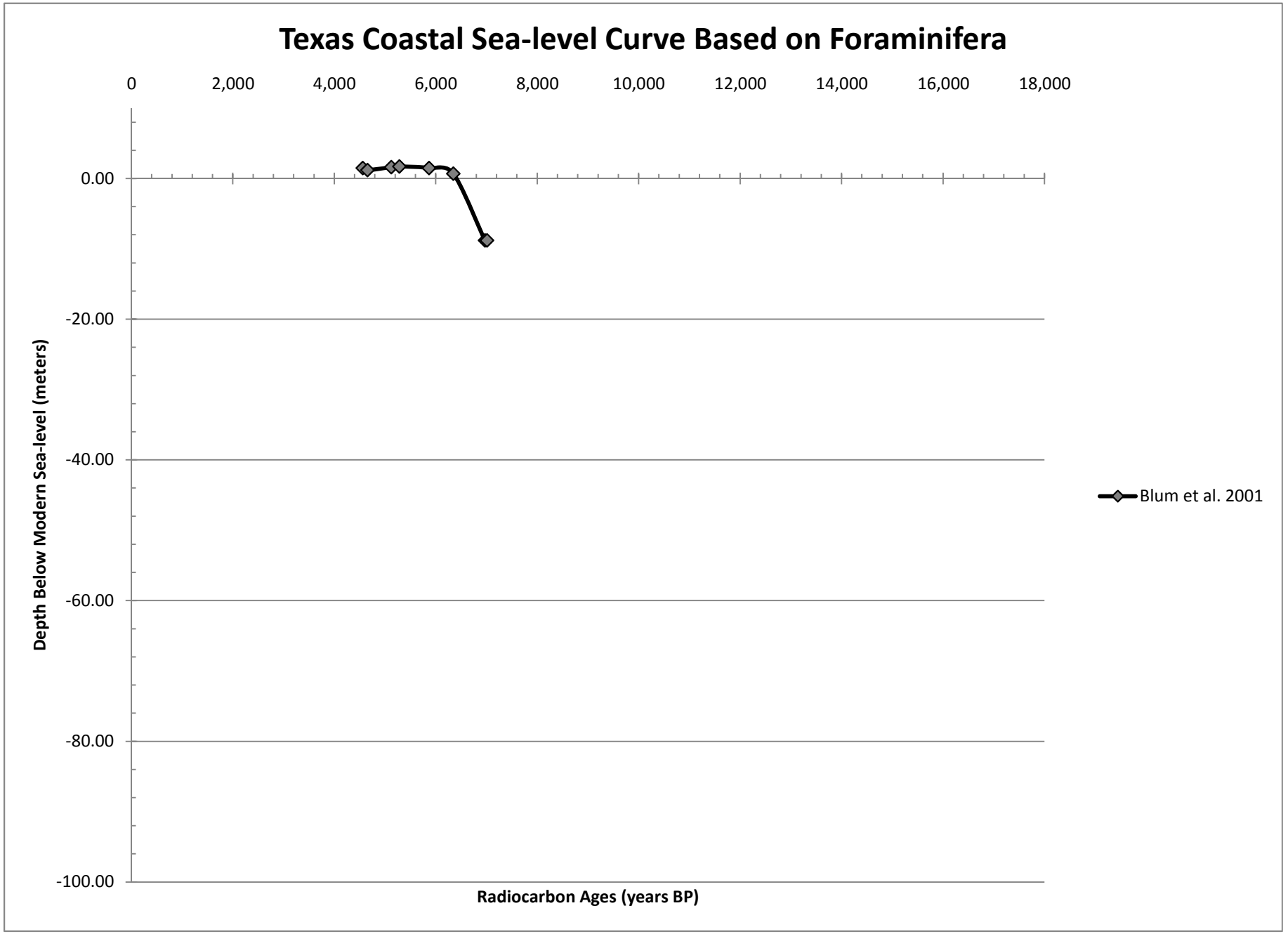
Texas Coastal Sea-level Curve Based on Foraminifera
0
2,000
4,000
6,000
8,000
10,000
12,000
14,000
16,000
18,000
0.00
-20.00
-40.00
-60.00
-80.00
-100.00
Depth Below Modern Sea-level (meters)
Radiocarbon Ages (years BP)
Blum et al. 2001

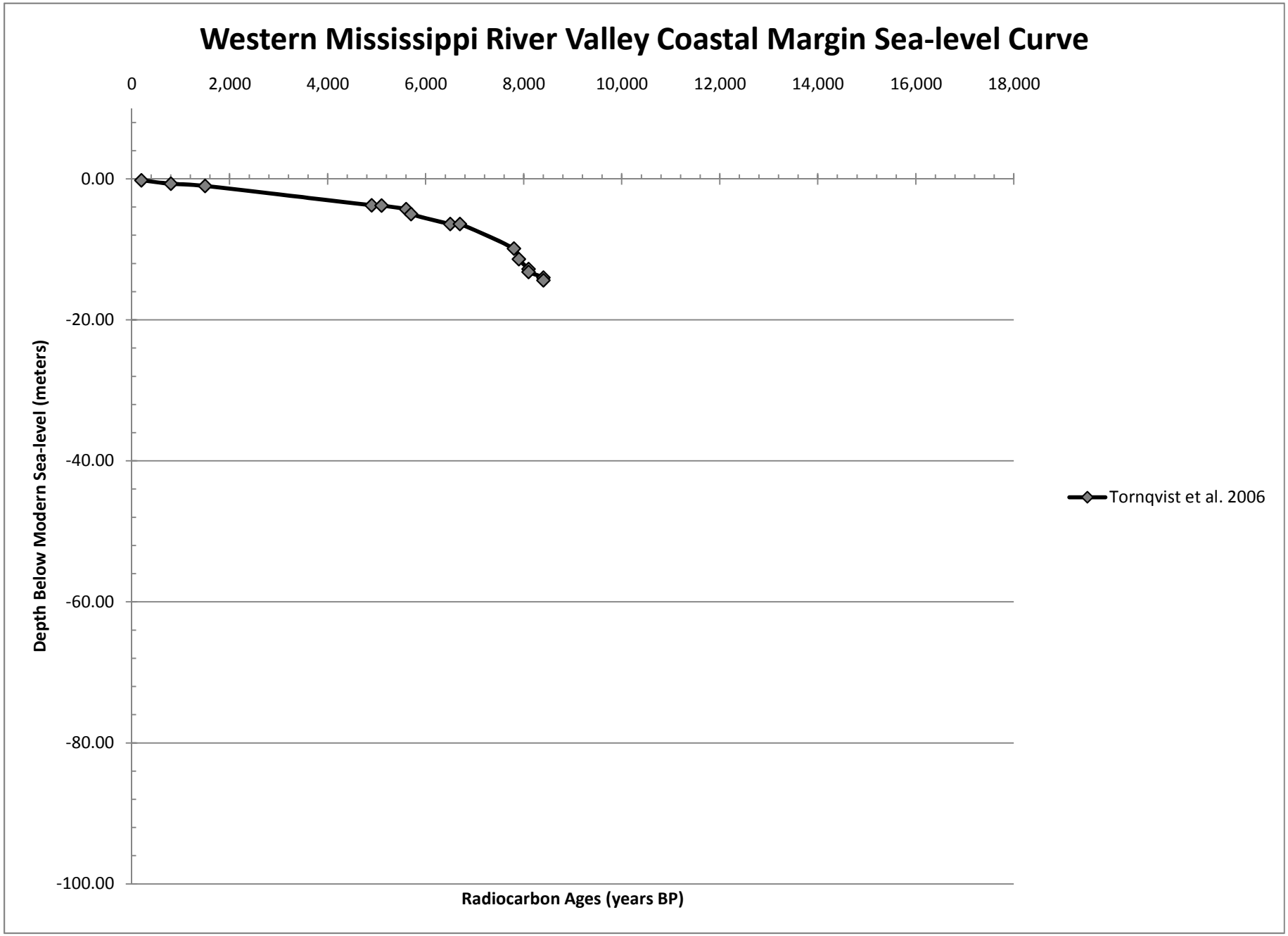
Western Mississippi River Valley Coastal Margin Sea-level Curve
0
2,000
4,000
6,000
8,000
10,000
12,000
14,000
16,000
18,000
0.00
-20.00
-40.00
-60.00
-80.00
-100.00
Depth Below Modern Sea-level (meters)
Radiocarbon Ages (years BP)
Tornqvist et al. 2006

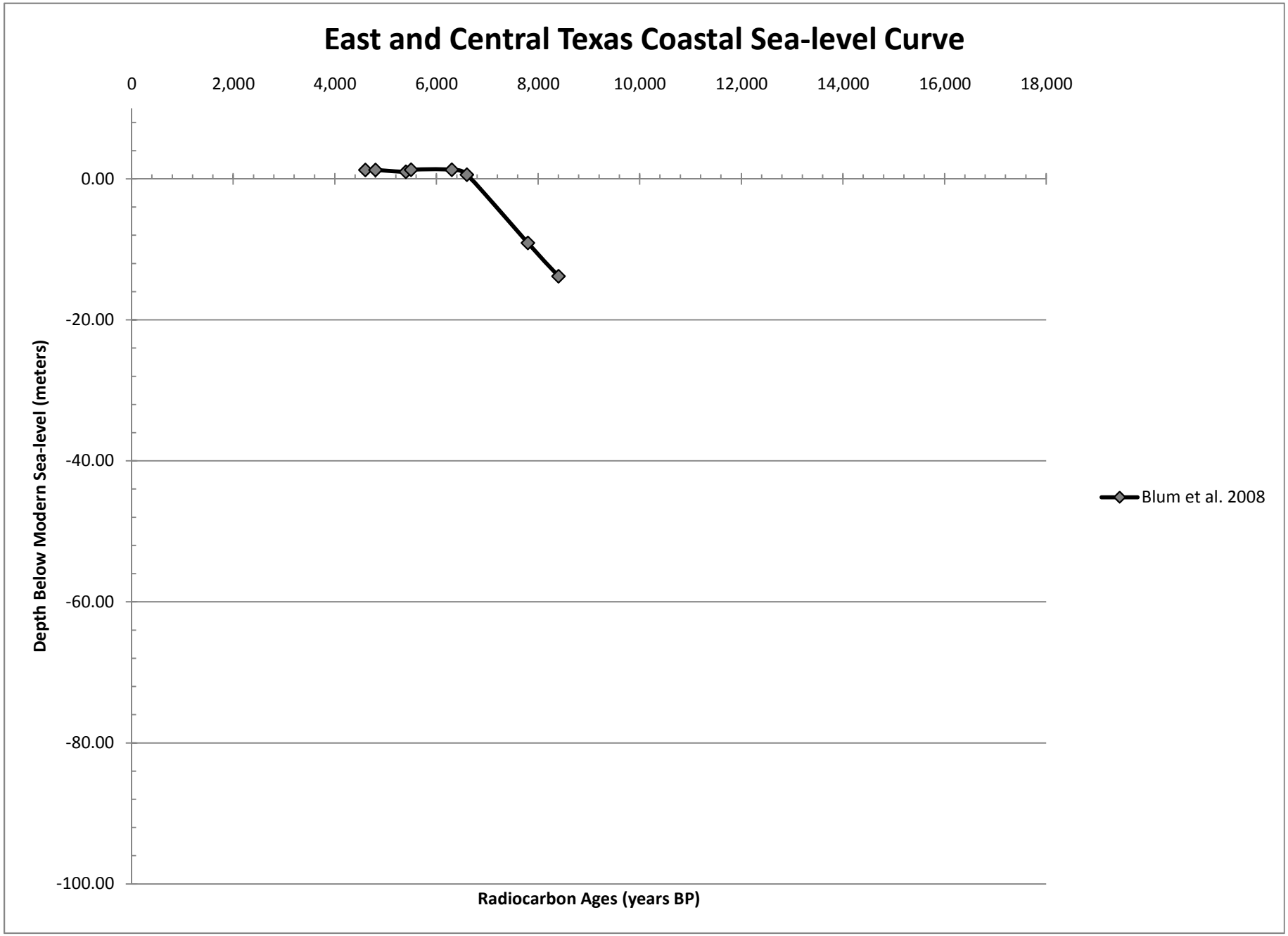
East and Central Texas Coastal Sea-level Curve
0
2,000
4,000
6,000
8,000
10,000
12,000
14,000
16,000
18,000
0.00
-20.00
-40.00
-60.00
-80.00
-100.00
Depth Below Modern Sea-level (meters)
Radiocarbon Ages (years BP)
Blum et al. 2008

APPENDIX B. CORE LOGS

Site No. HI 178 **Collection Date** 28 June 2009

Core No. 1

Water Depth 15.4 m BSL

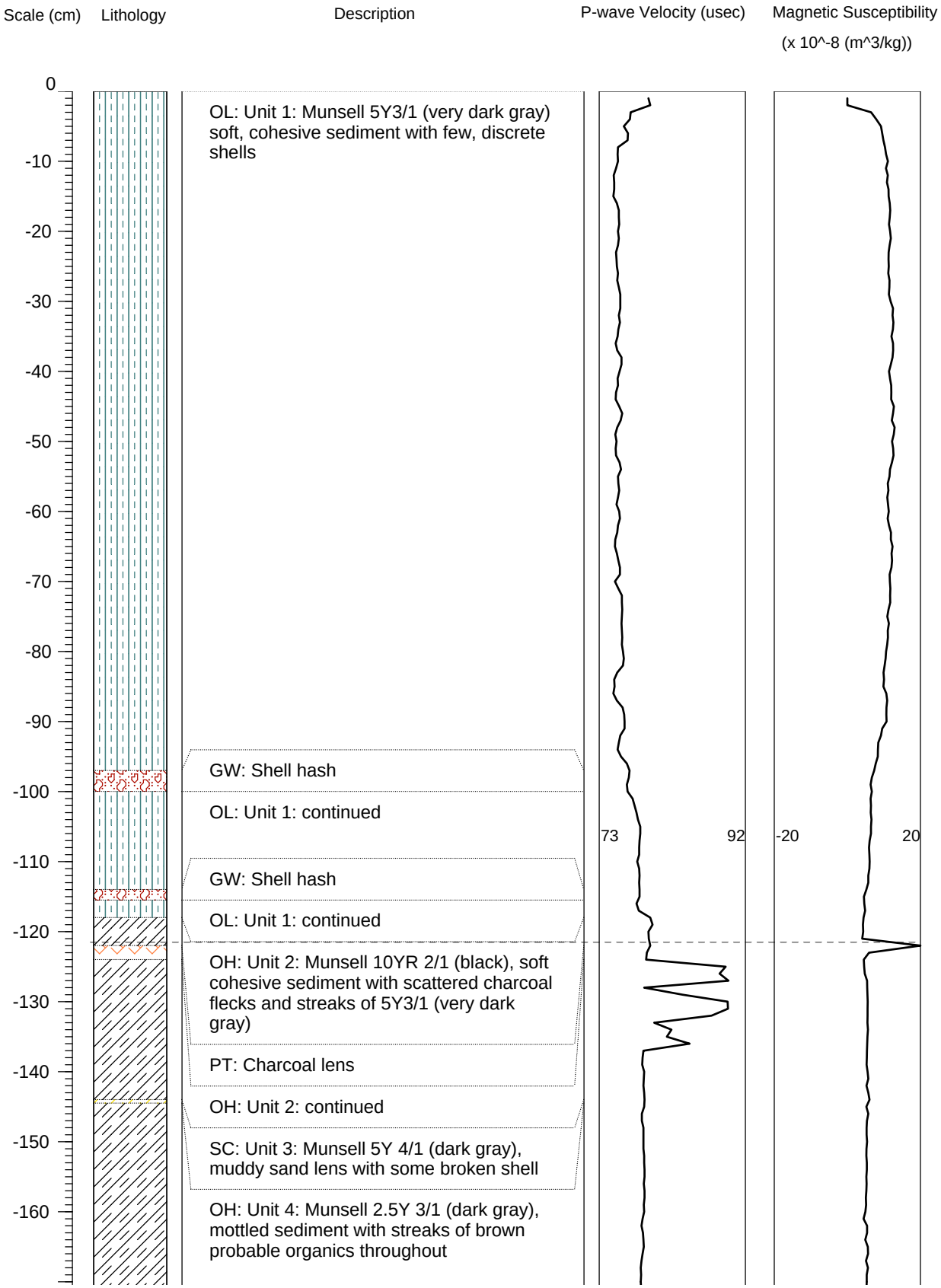

Site No. HI 178 **Collection Date** 28 June 2009

Core No. 1

Water Depth 15.4 m BSL

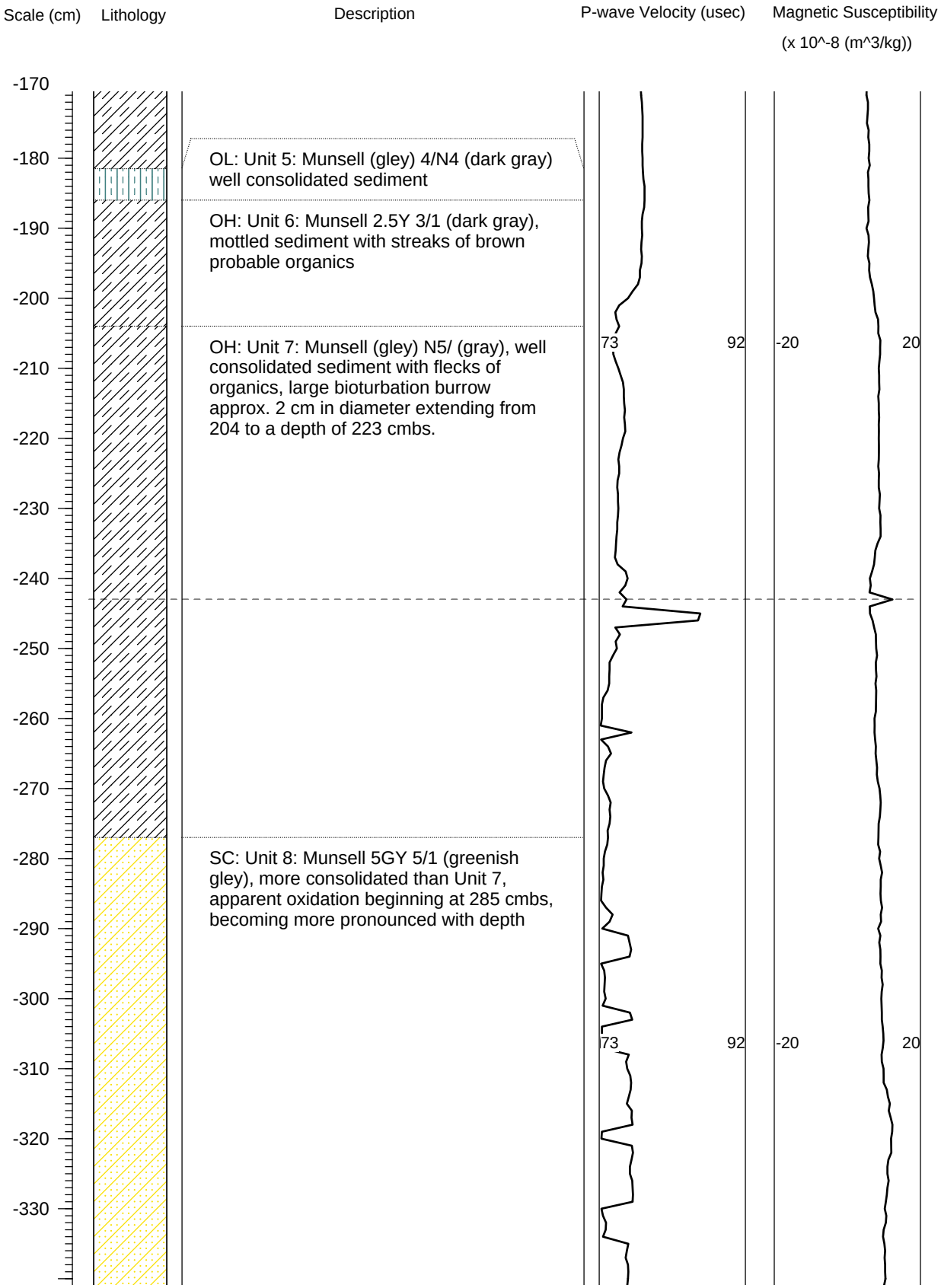

Site No. HI 178 **Collection Date** 28 June 2009

Core No. 1

Water Depth 15.4 m BSL

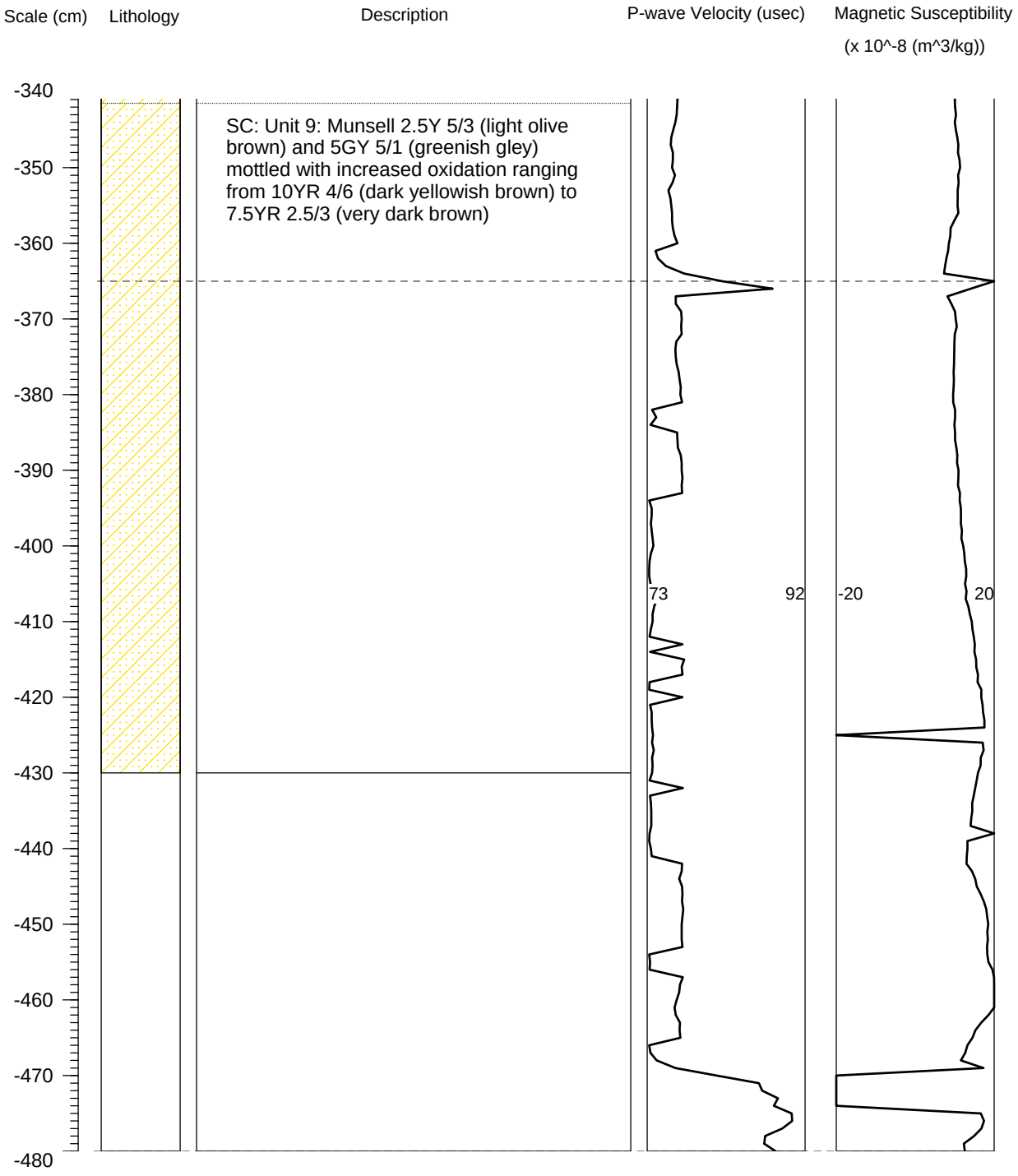

Site No. HI 178 **Collection Date** 28 June 2009

Core No. 2

Water Depth 15.4 m BSL

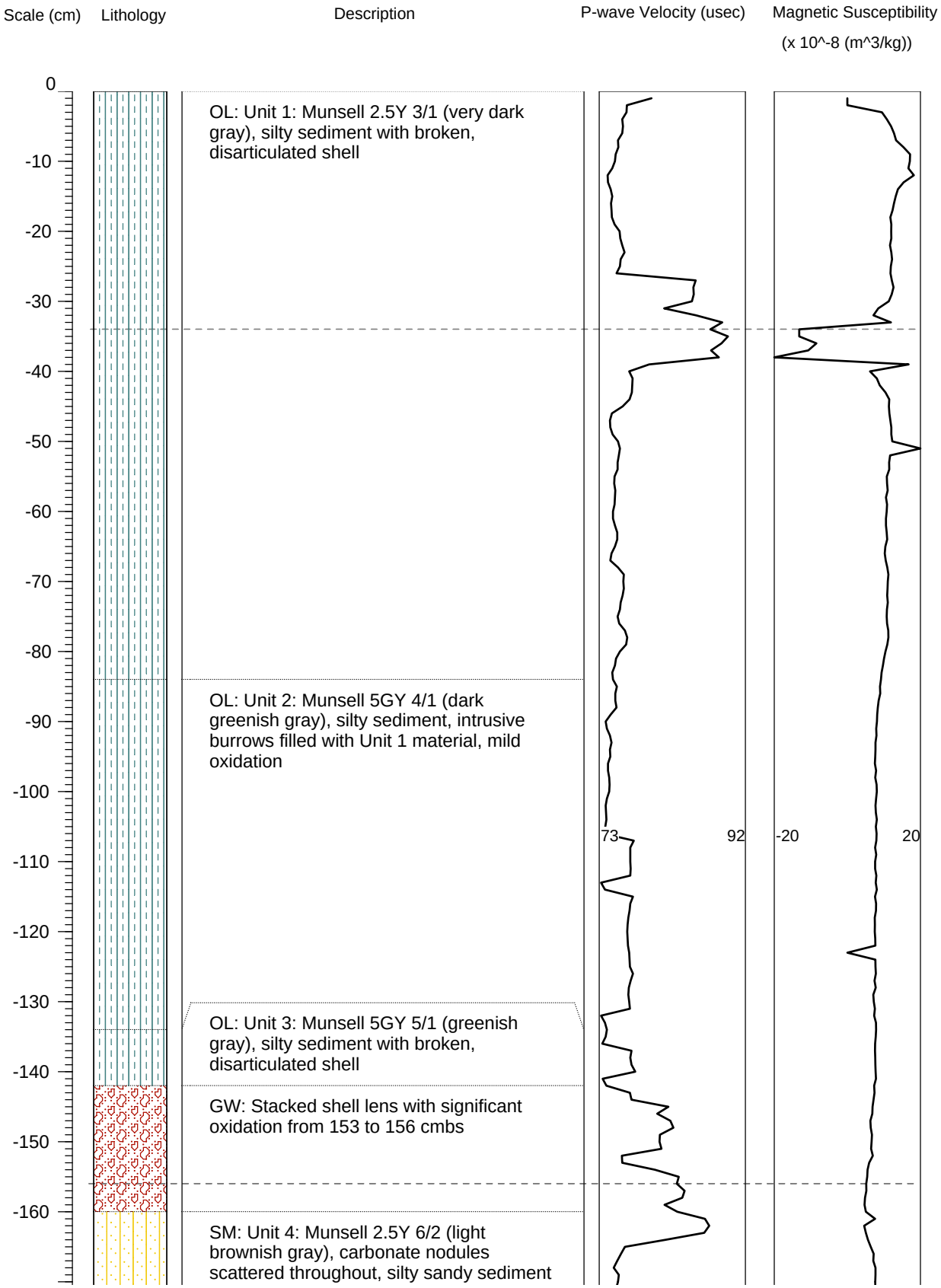

Site No. HI 178 **Collection Date** 28 June 2009

Core No. 2

Water Depth 15.4 m BSL

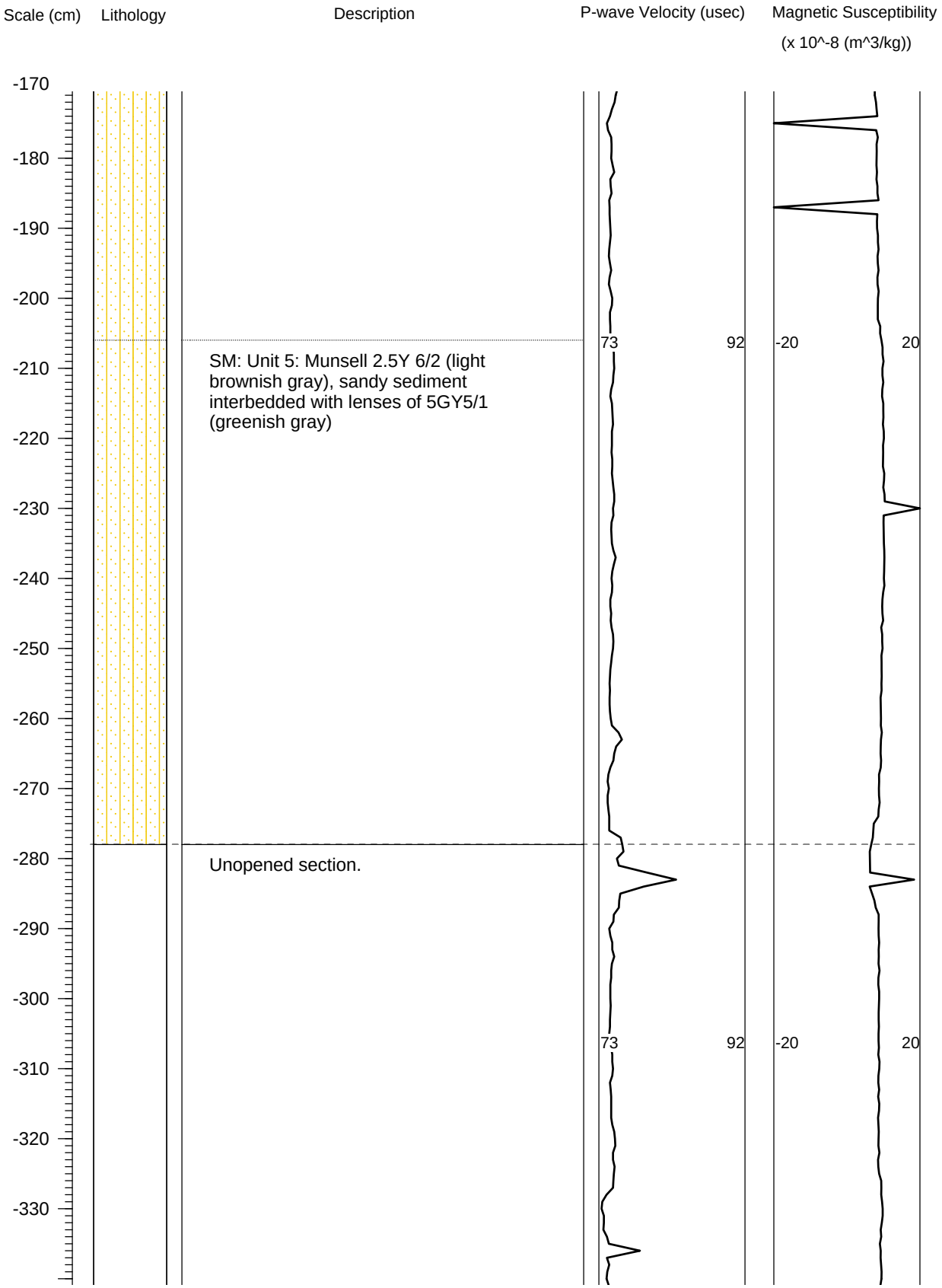

Site No. HI 178 **Collection Date** 28 June 2009

Core No. 2

Water Depth 15.4 m BSL

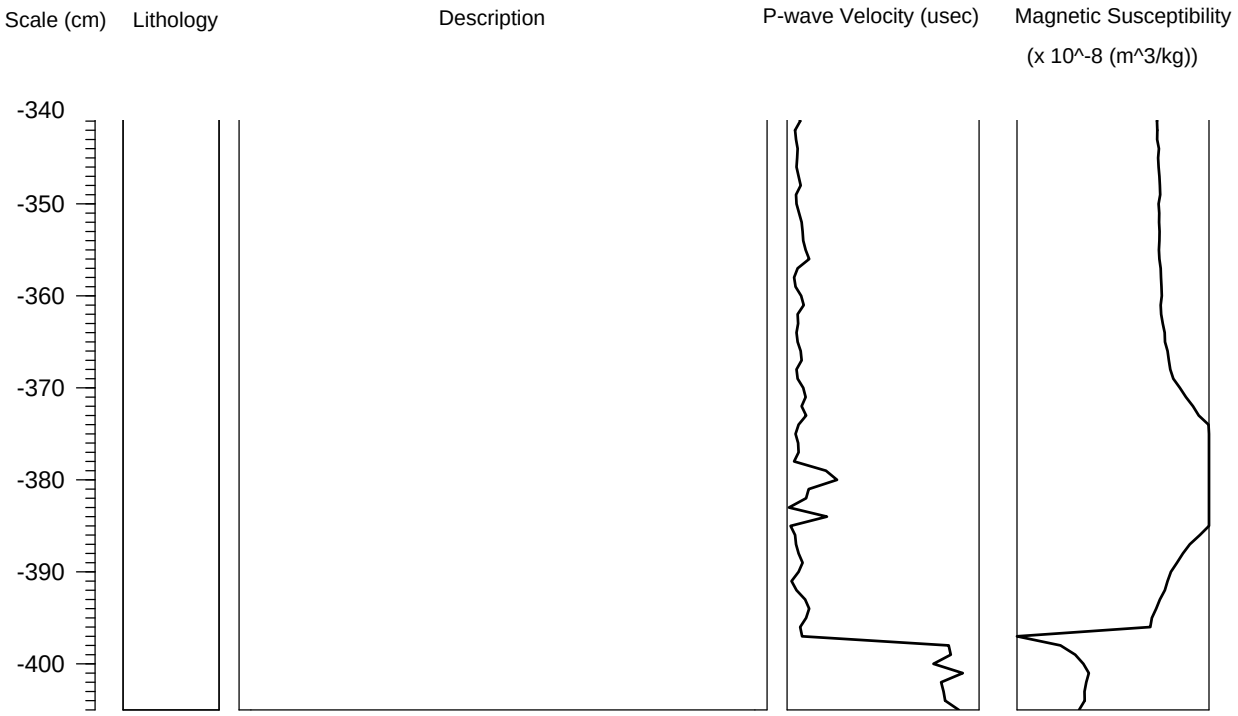

Site No. HI 178 **Collection Date** 28 June 2009

Core No. 5

Water Depth 15.4 m BSL

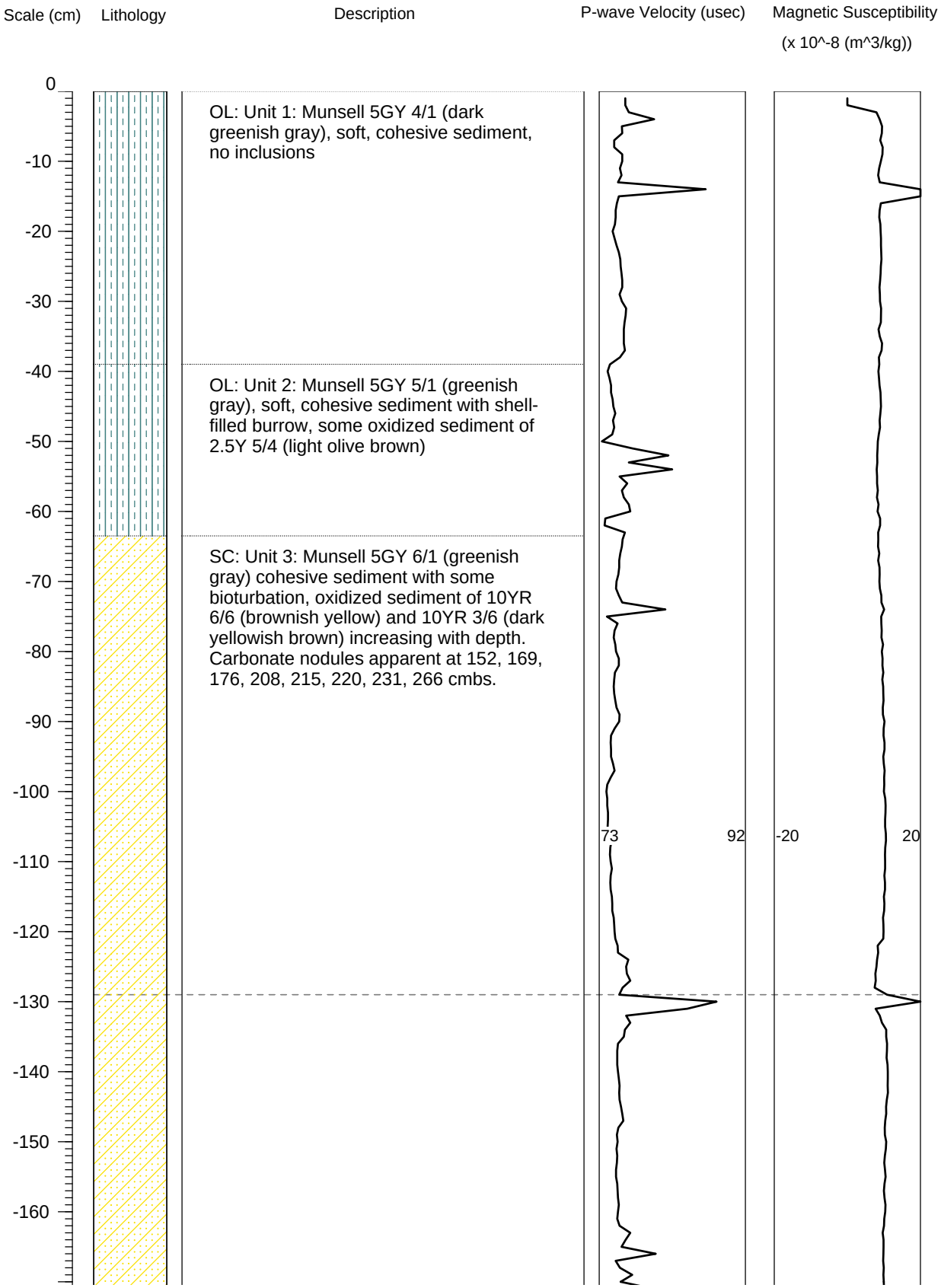

Site No. HI 178 **Collection Date** 28 June 2009

Core No. 5

Water Depth 15.4 m BSL

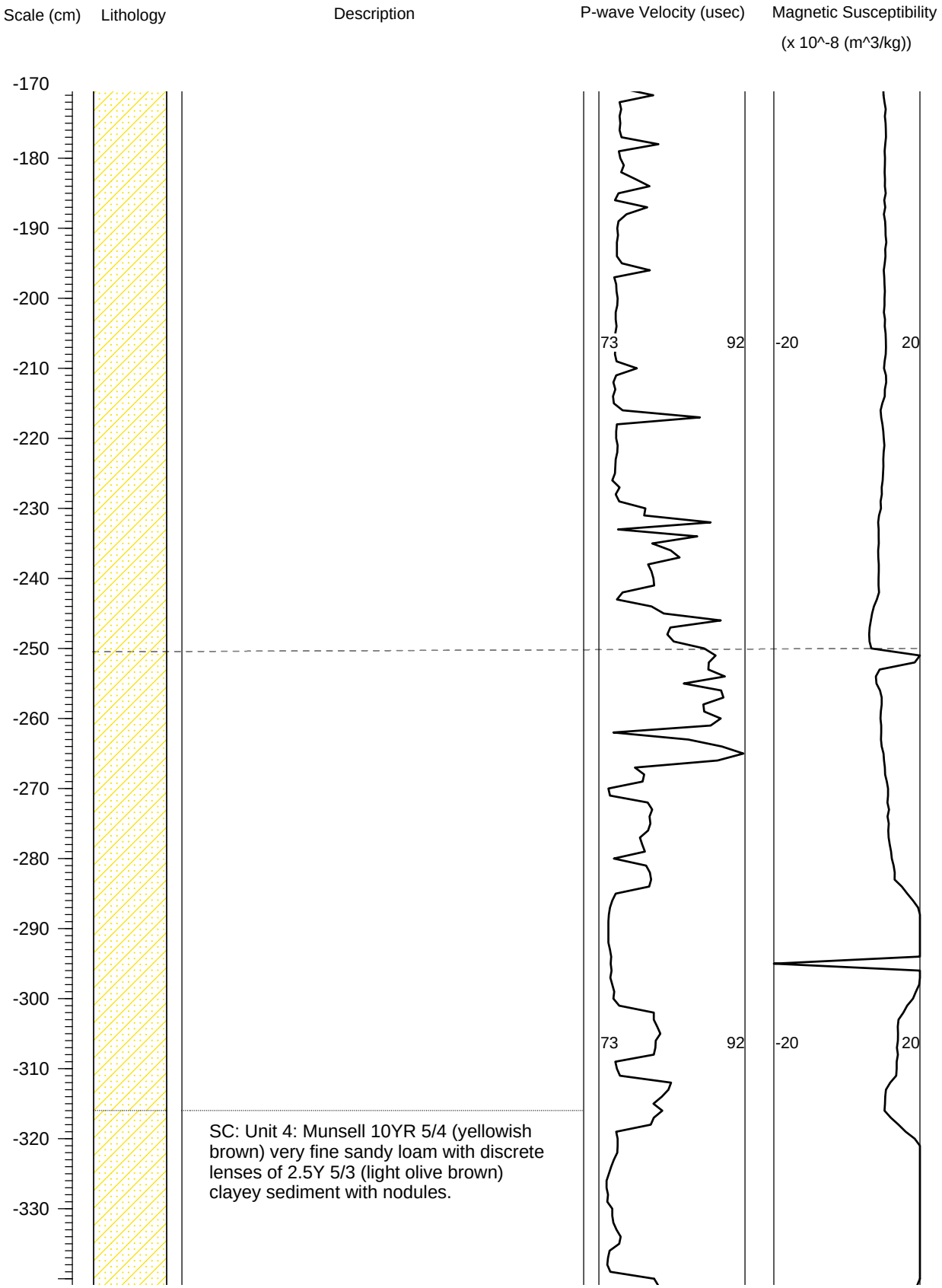

Site No. HI 178 **Collection Date** 28 June 2009

Core No. 5

Water Depth 15.4 m BSL

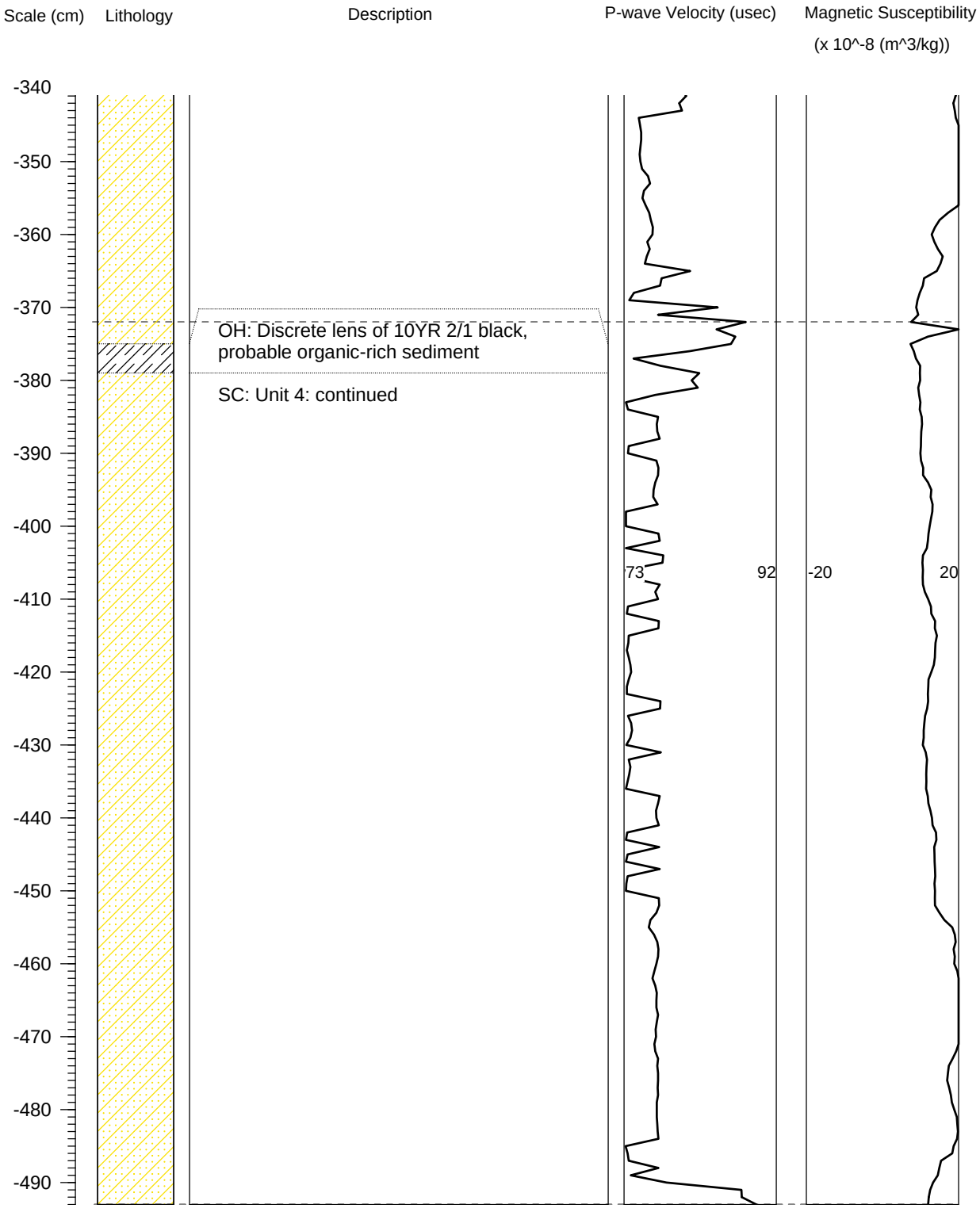

Site No. HI 178 **Collection Date** 28 June 2009

Core No. 6

Water Depth 15.4 m BSL

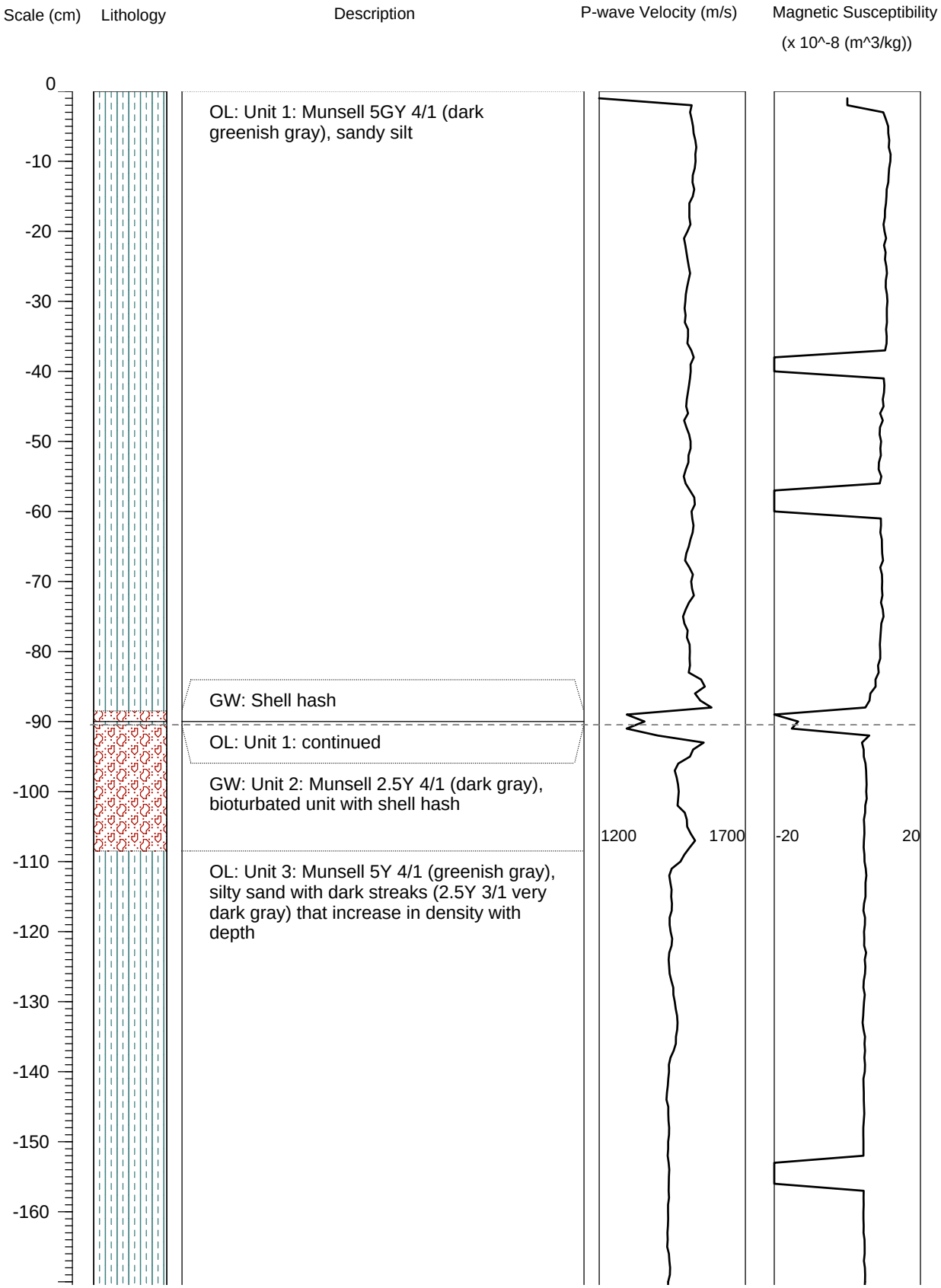

Site No. HI 178 **Collection Date** 28 June 2009

Core No. 6

Water Depth 15.4 m BSL

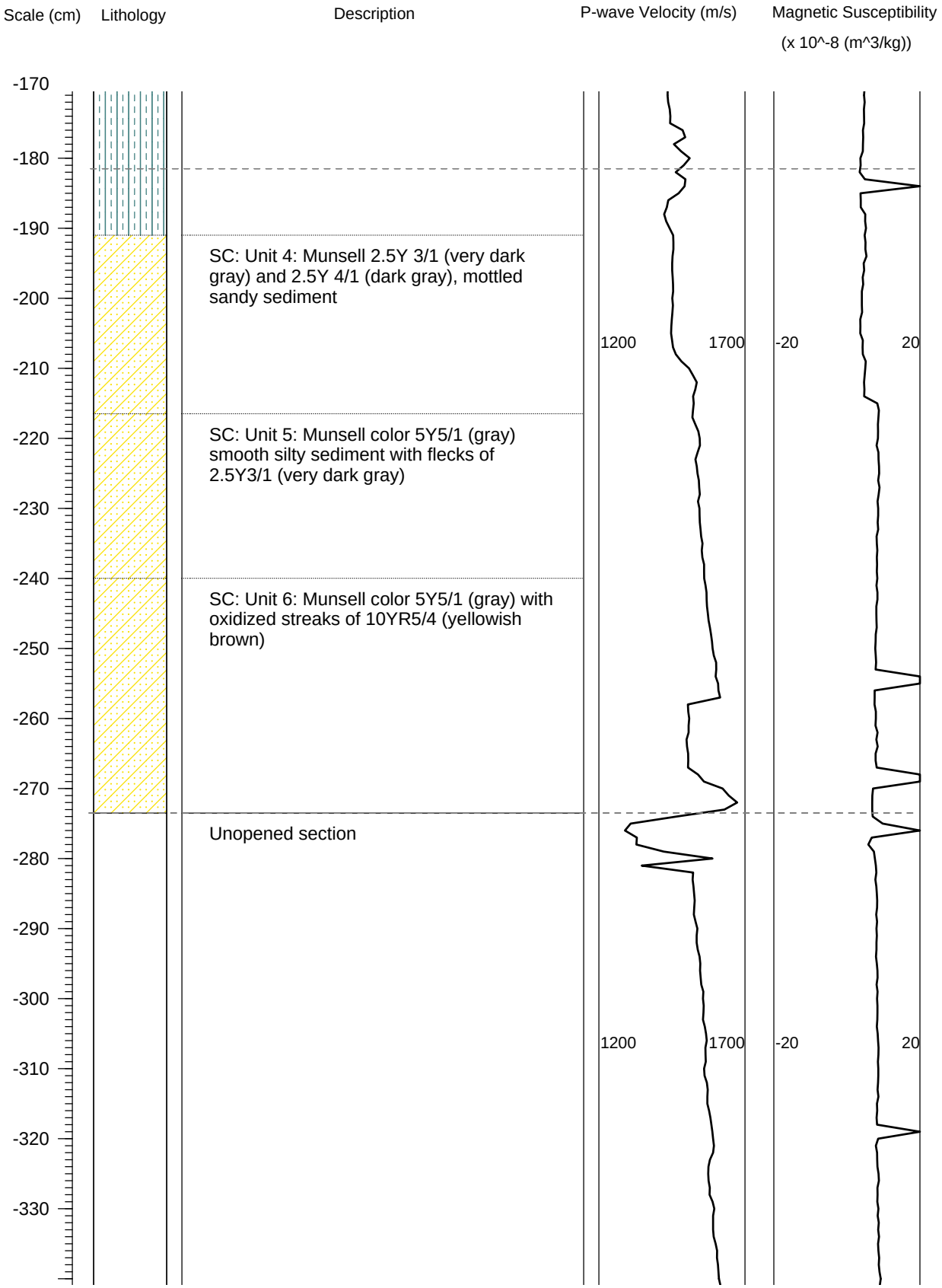

Site No. HI 178 **Collection Date** 28 June 2009

Core No. 6

Water Depth 15.4 m BSL

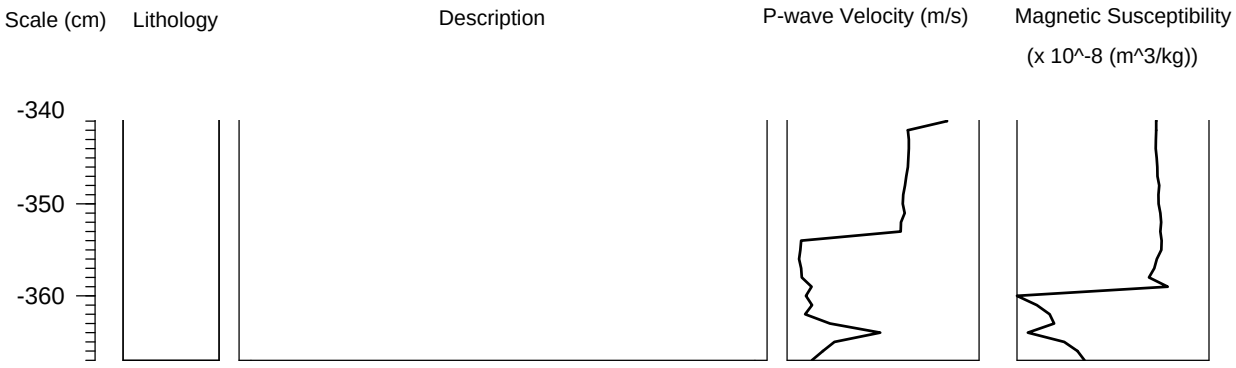

Site No. HI 178 **Collection Date** 28 June 2009

Core No. 7

Water Depth 15.4 m BSL

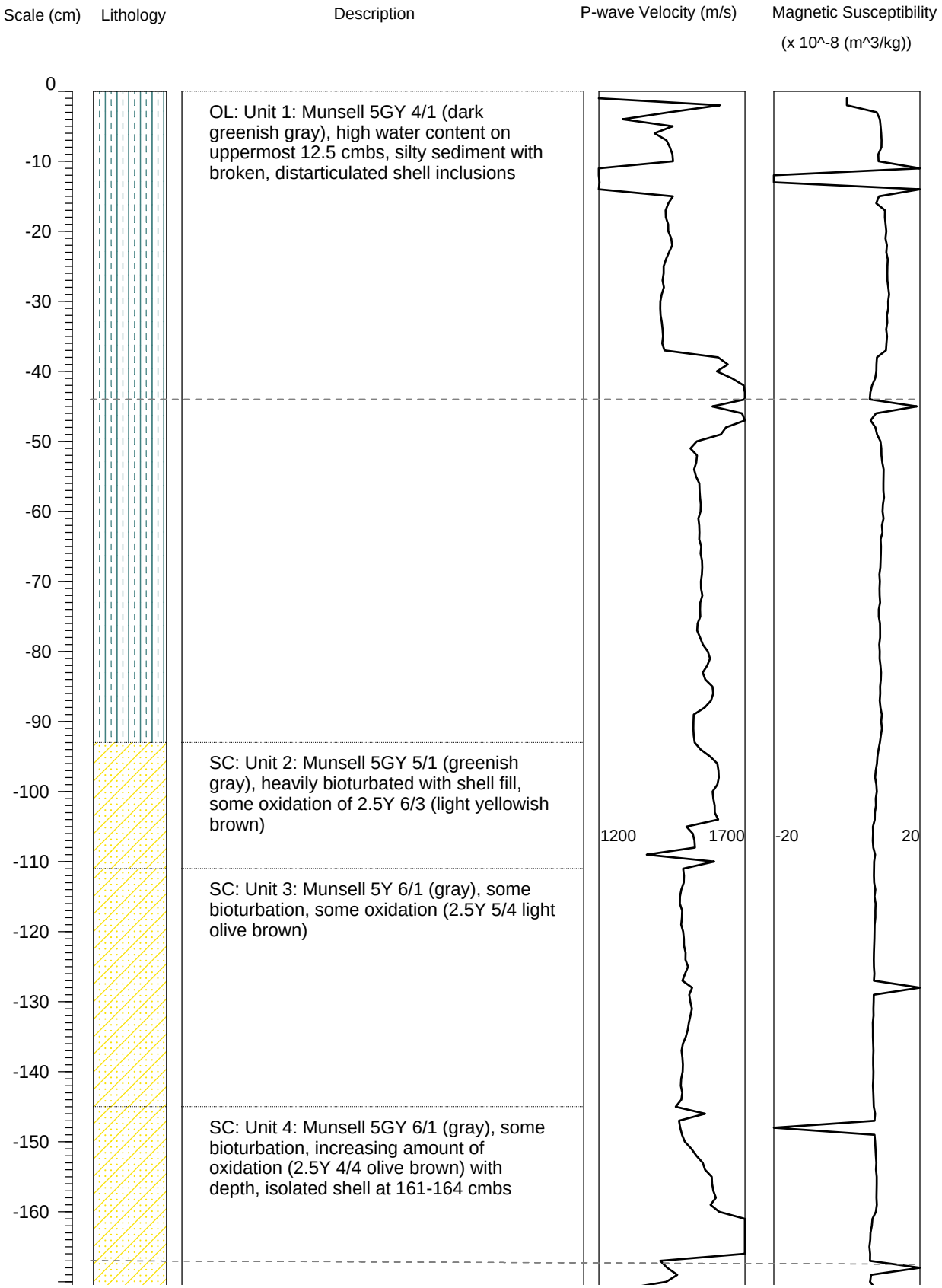

Site No. HI 178 **Collection Date** 28 June 2009

Core No. 7

Water Depth 15.4 m BSL

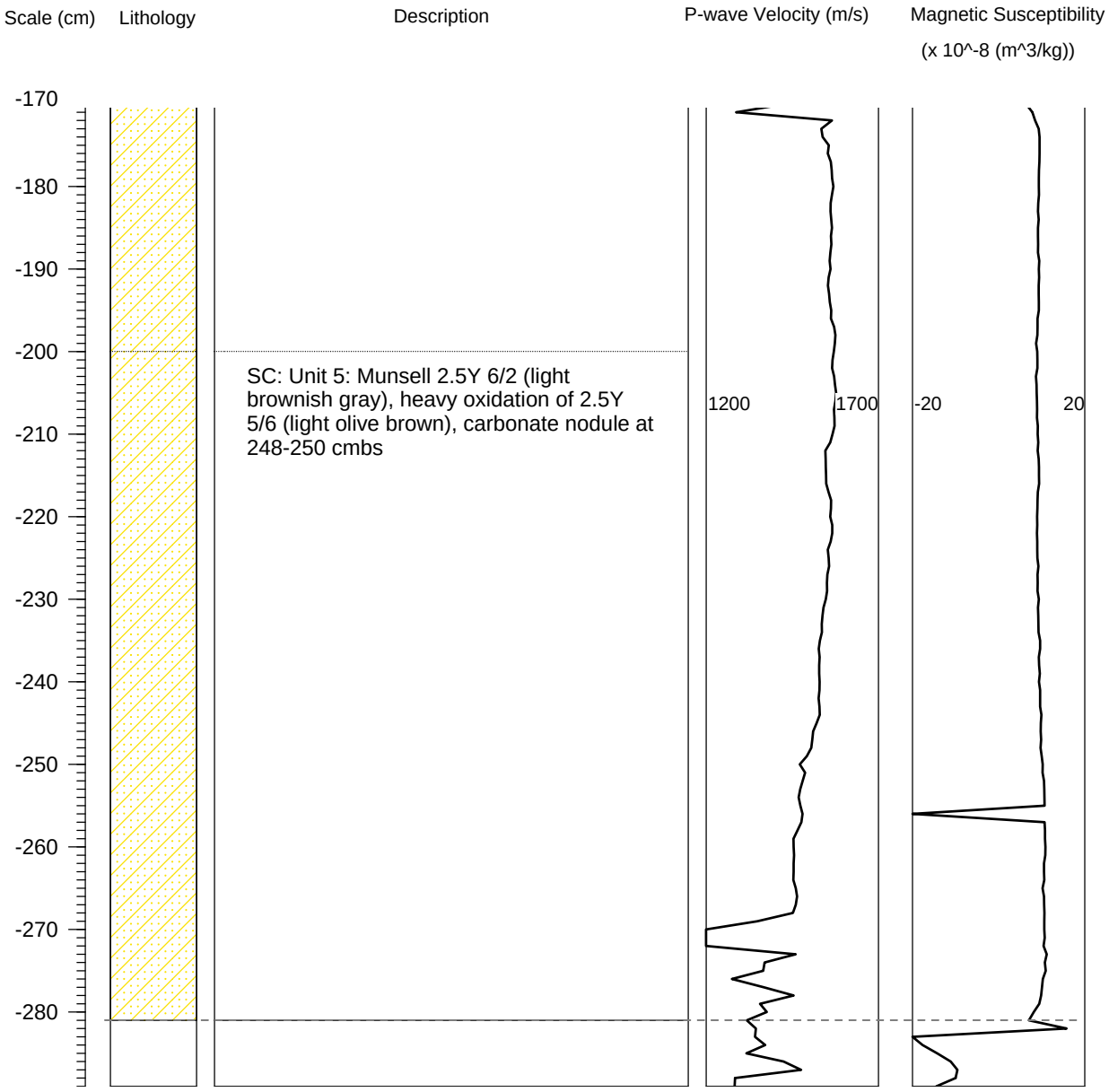

Site No. GA 426 **Collection Date** 30 June 2009

Core No. 1

Water Depth 30.9 m BSL

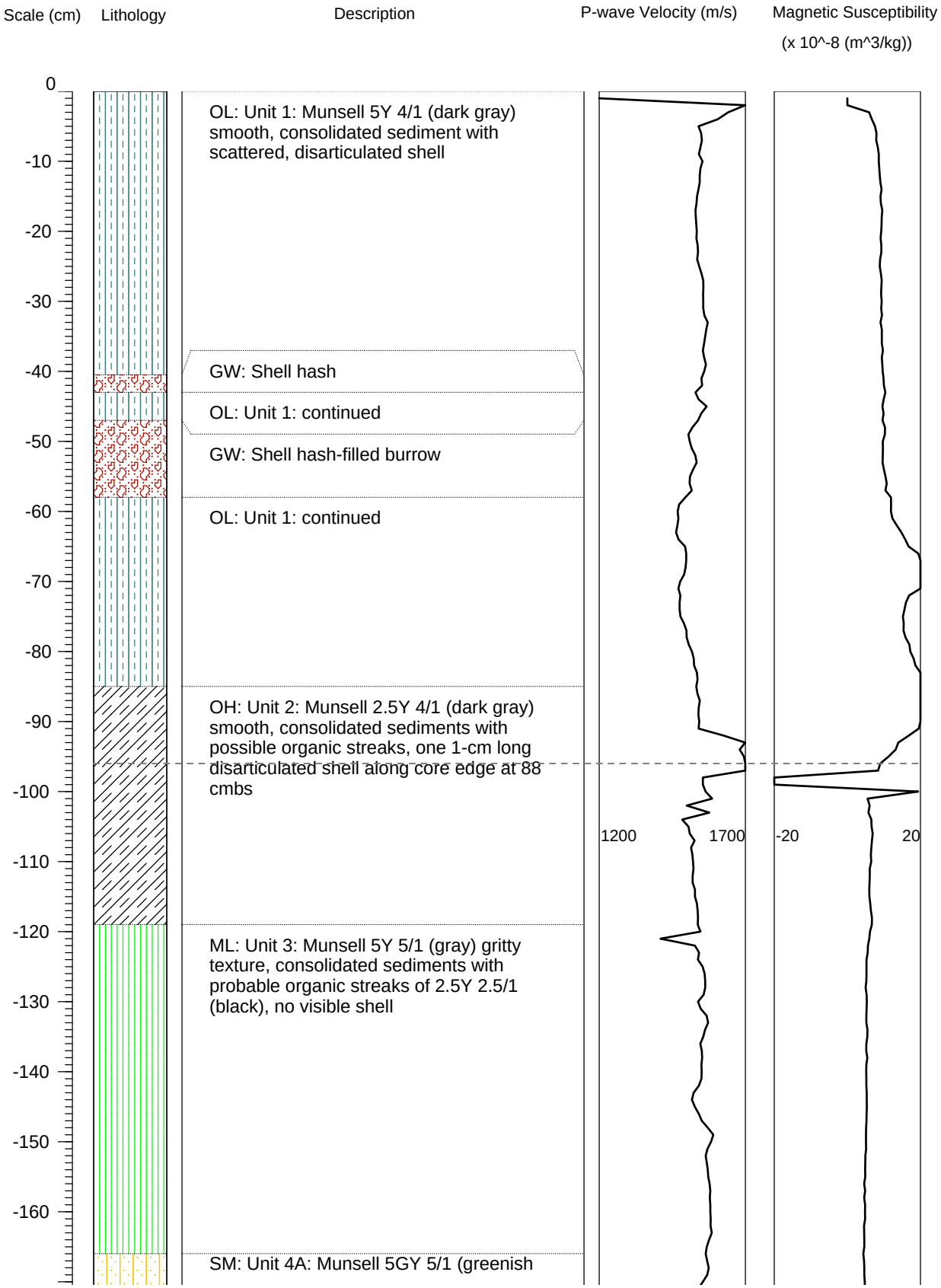

Site No. GA 426 **Collection Date** 30 June 2009

Core No. 1

Water Depth 30.9 m BSL

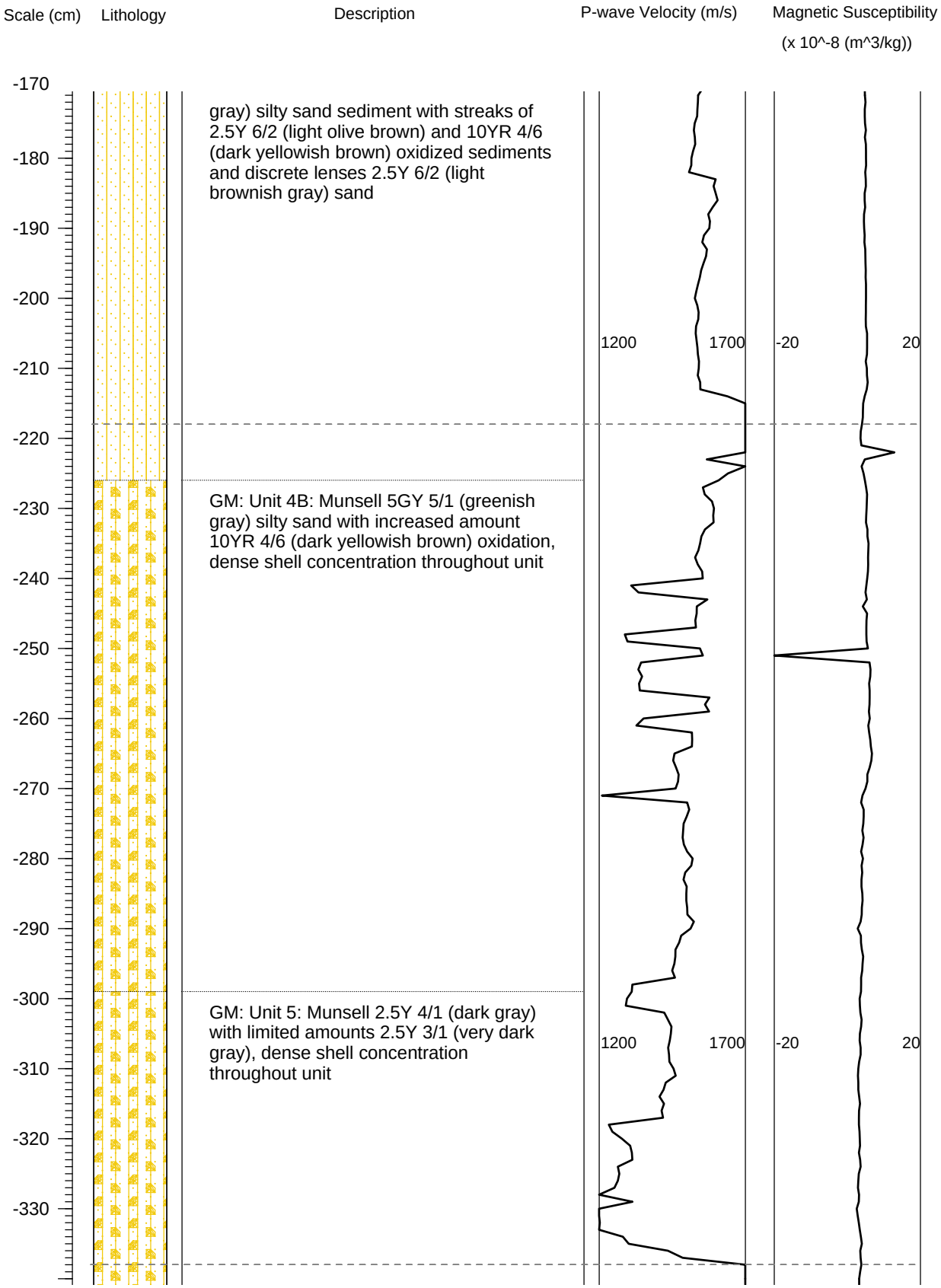

Site No. GA 426 **Collection Date** 30 June 2009

Core No. 1

Water Depth 30.9 m BSL

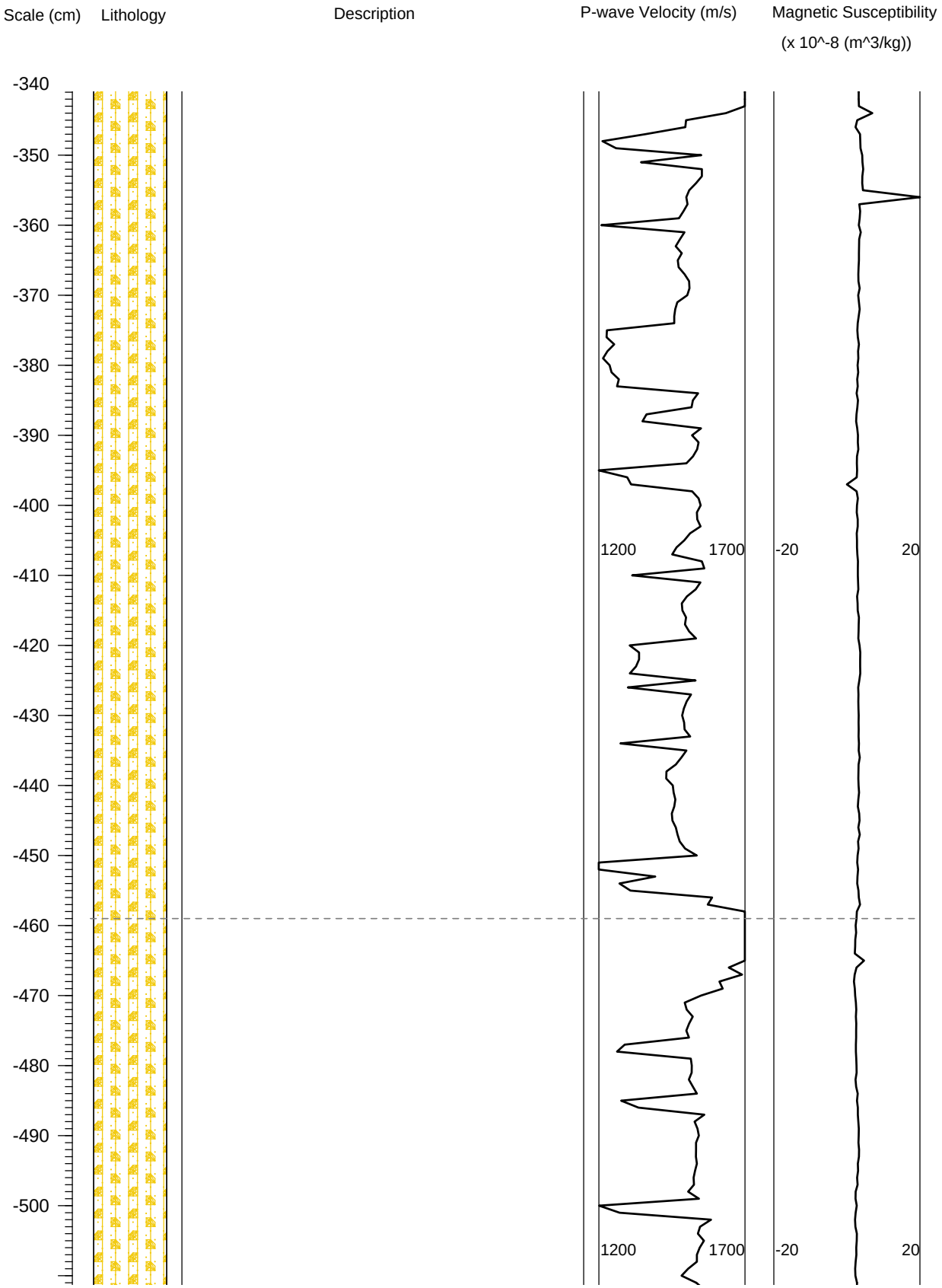

Site No. GA 426 **Collection Date** 30 June 2009

Core No. 1

Water Depth 30.9 m BSL

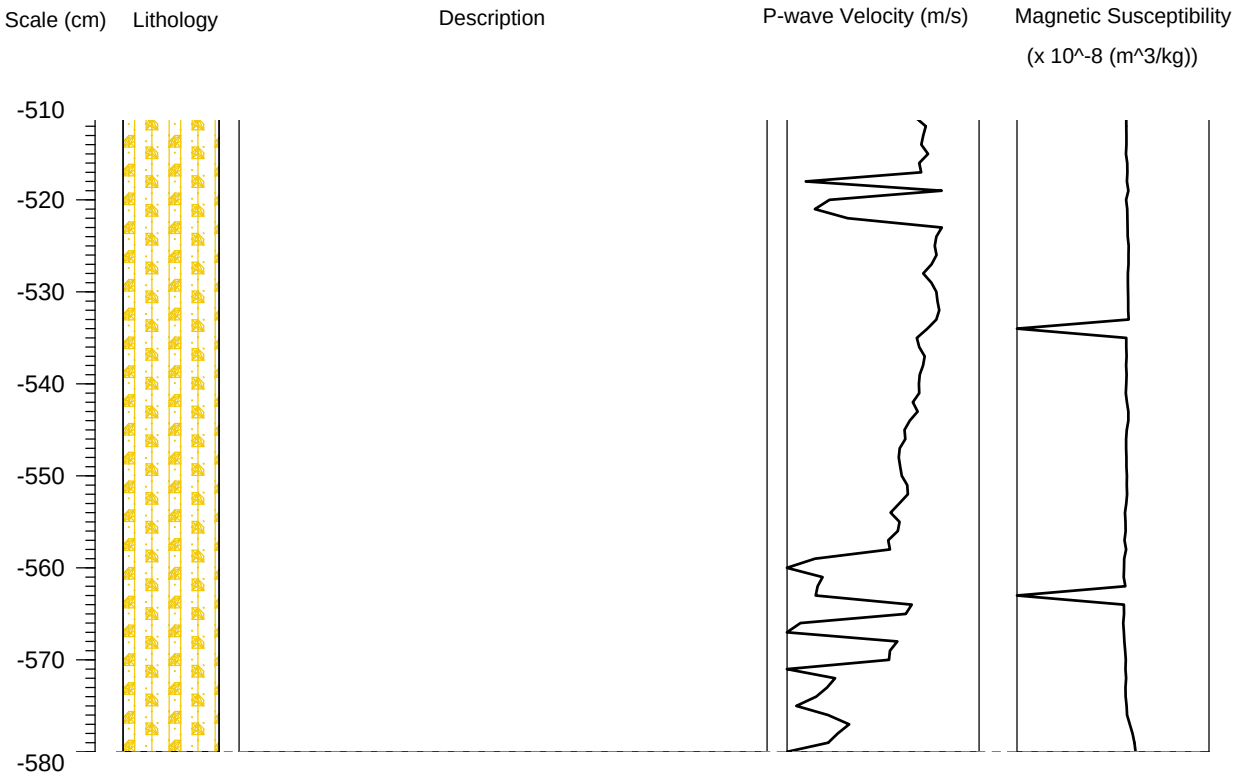

Site No. GA 426 **Collection Date** 1 July 2009

Core No. 2

Water Depth 30.7 m BSL

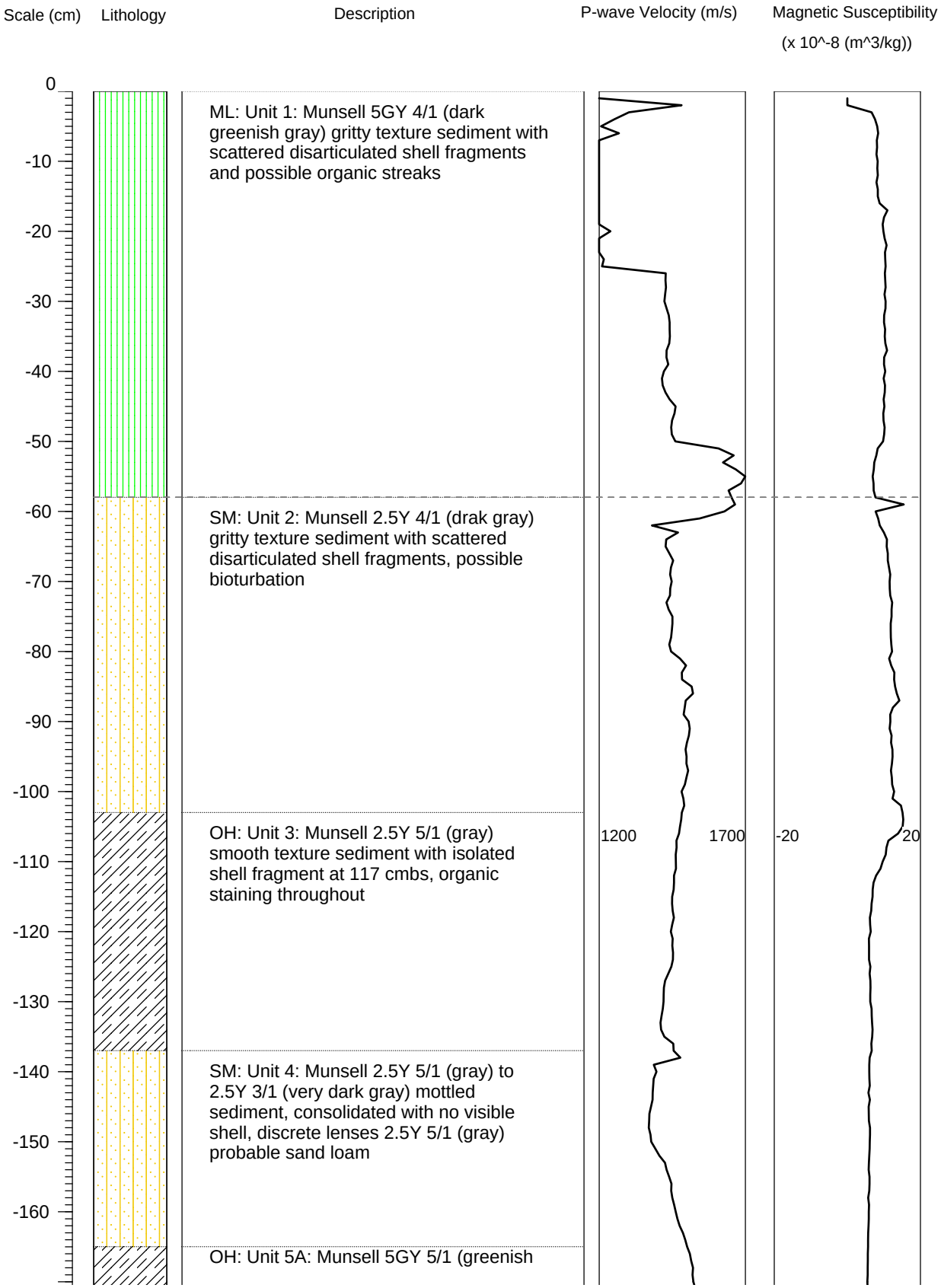

Site No. GA 426 **Collection Date** 1 July 2009

Core No. 2

Water Depth 30.7 m BSL

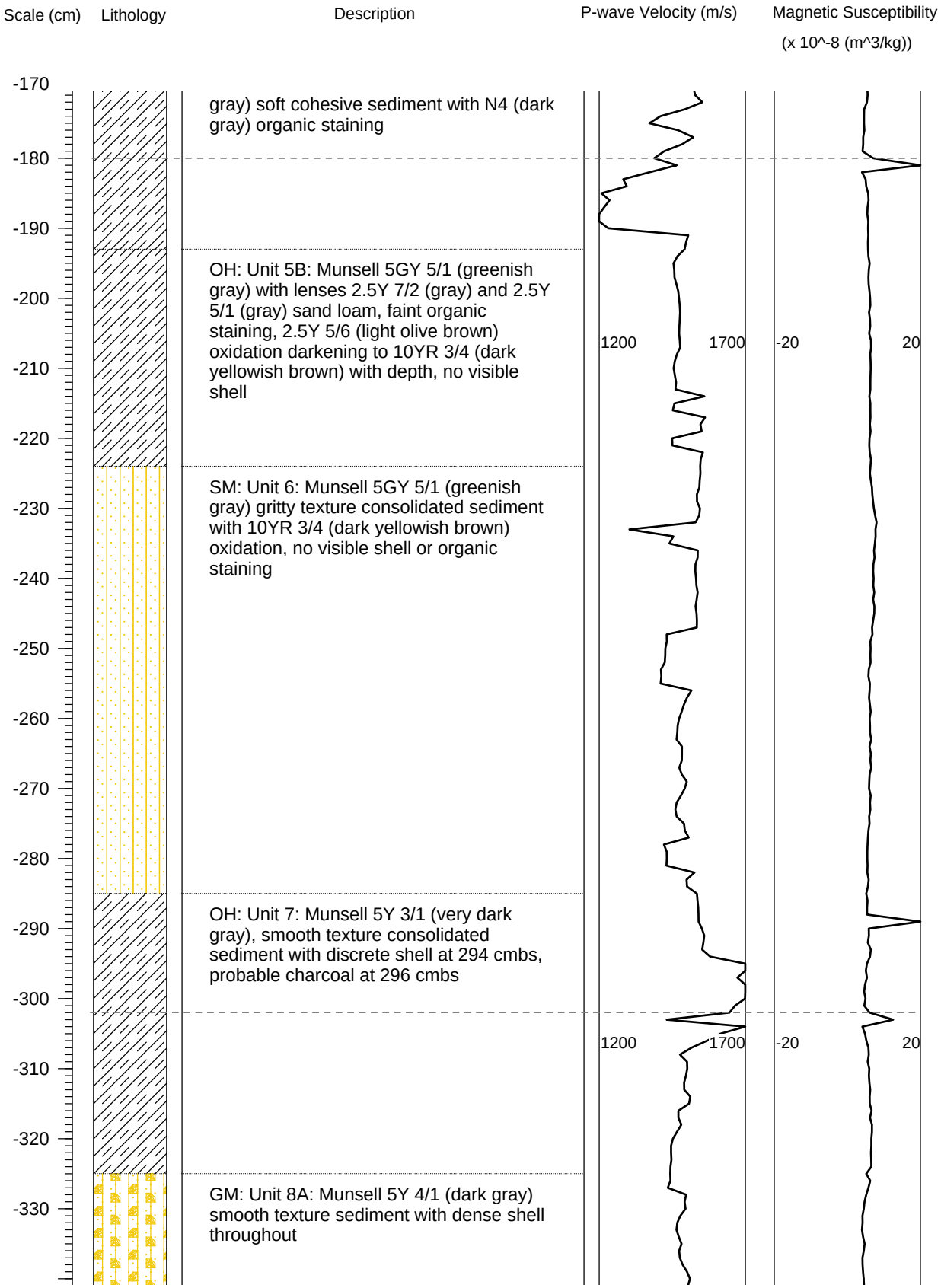

Site No. GA 426 **Collection Date** 1 July 2009

Core No. 2

Water Depth 30.7 m BSL

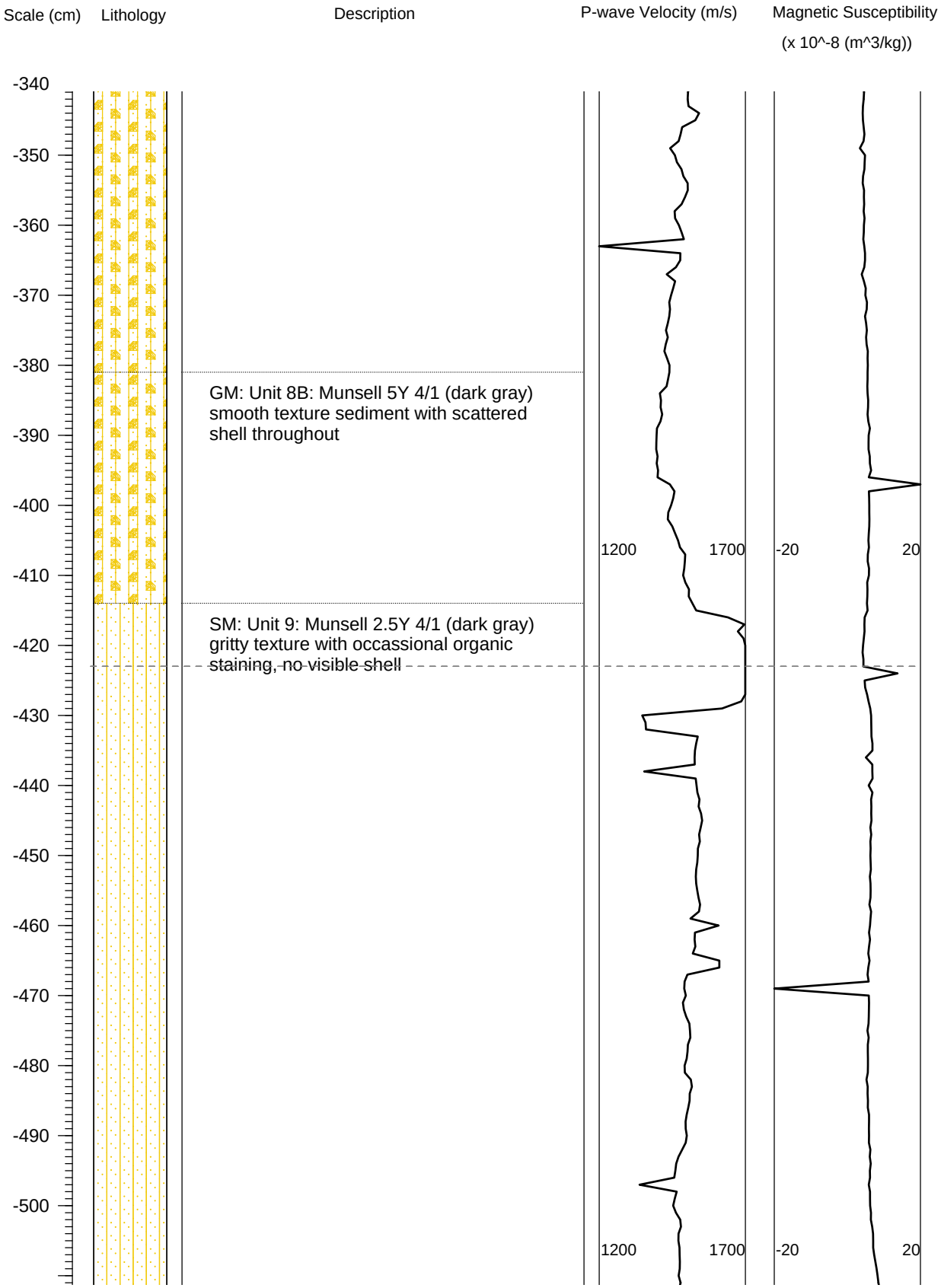

Site No. GA 426 **Collection Date** 1 July 2009

Core No. 2

Water Depth 30.7 m BSL

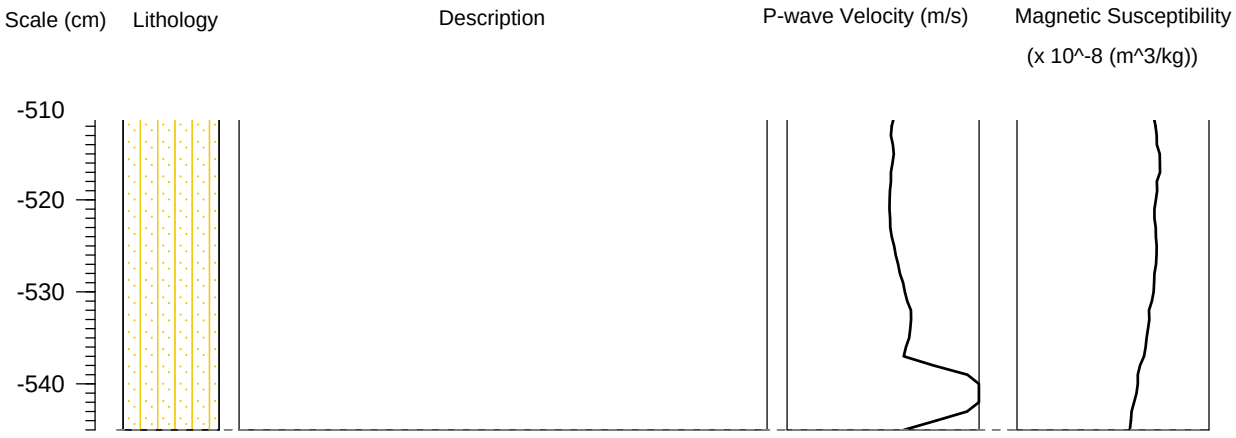

Site No. GA426 **Collection Date** 30 June 2009

Core No. 4

Water Depth 31.09 m BSL

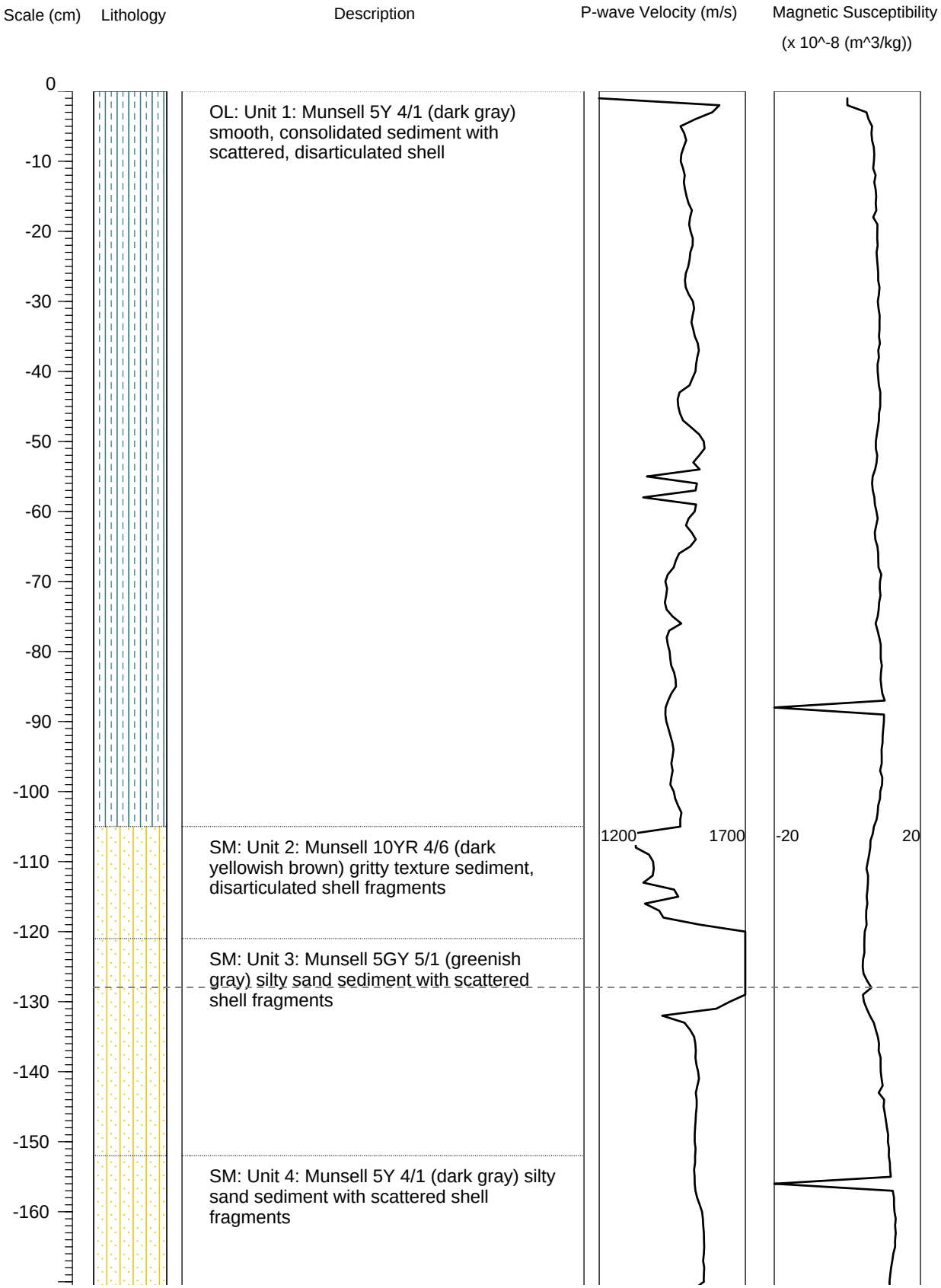

Site No. GA426 **Collection Date** 30 June 2009

Core No. 4

Water Depth 31.09 m BSL

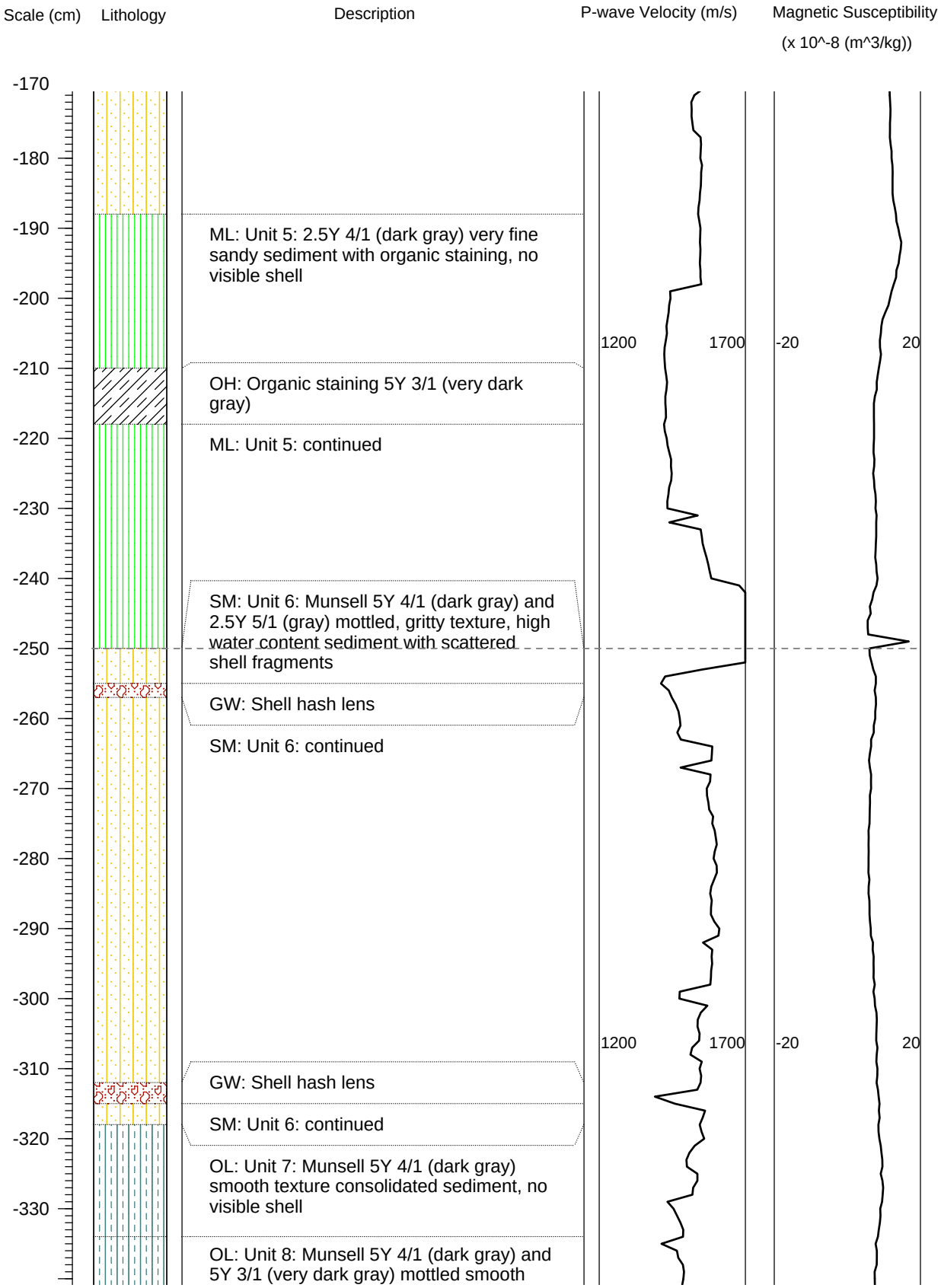

Site No. GA426 **Collection Date** 30 June 2009

Core No. 4

Water Depth 31.09 m BSL

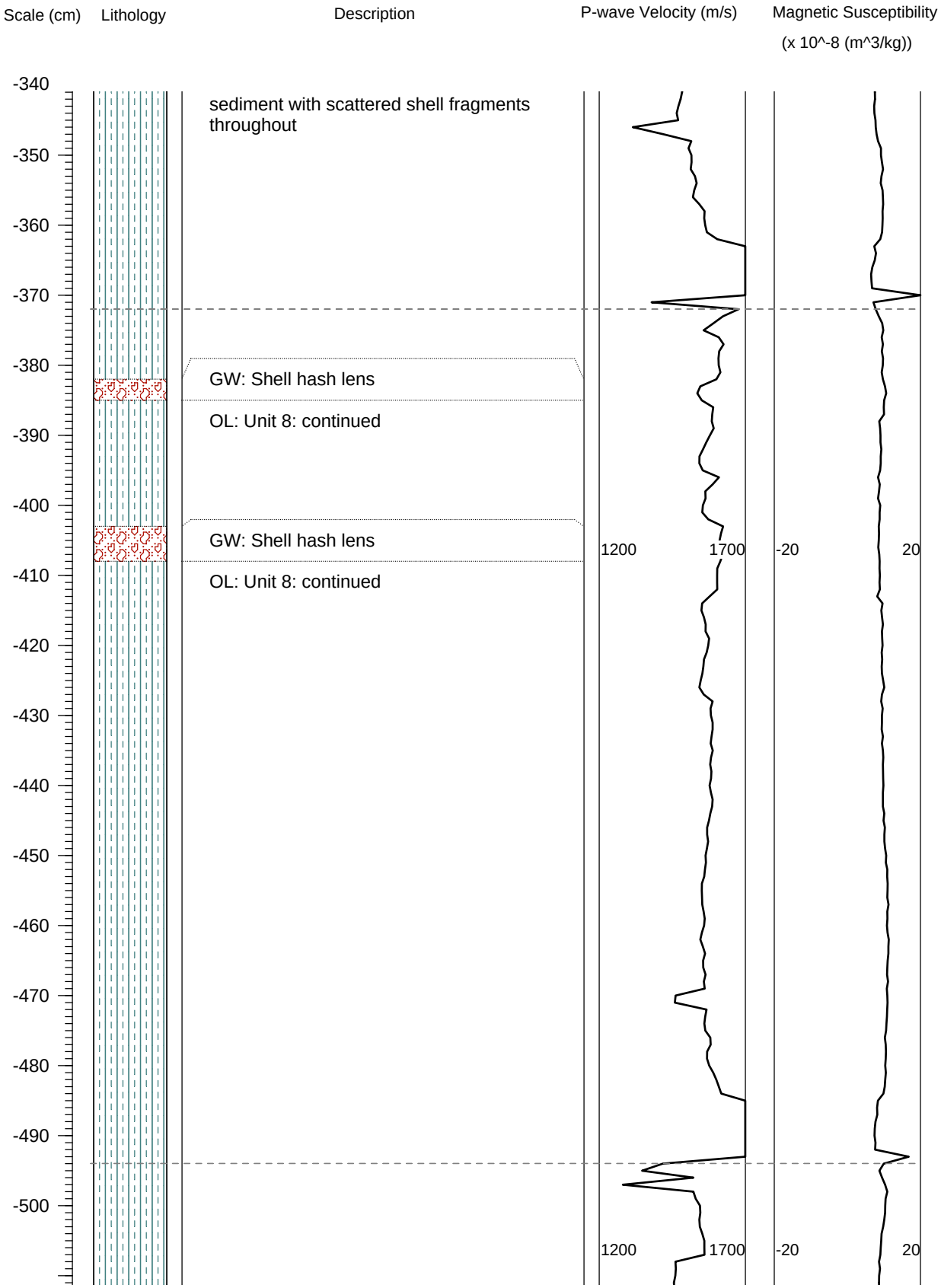

Site No. GA426 **Collection Date** 30 June 2009

Core No. 4

Water Depth 31.09 m BSL

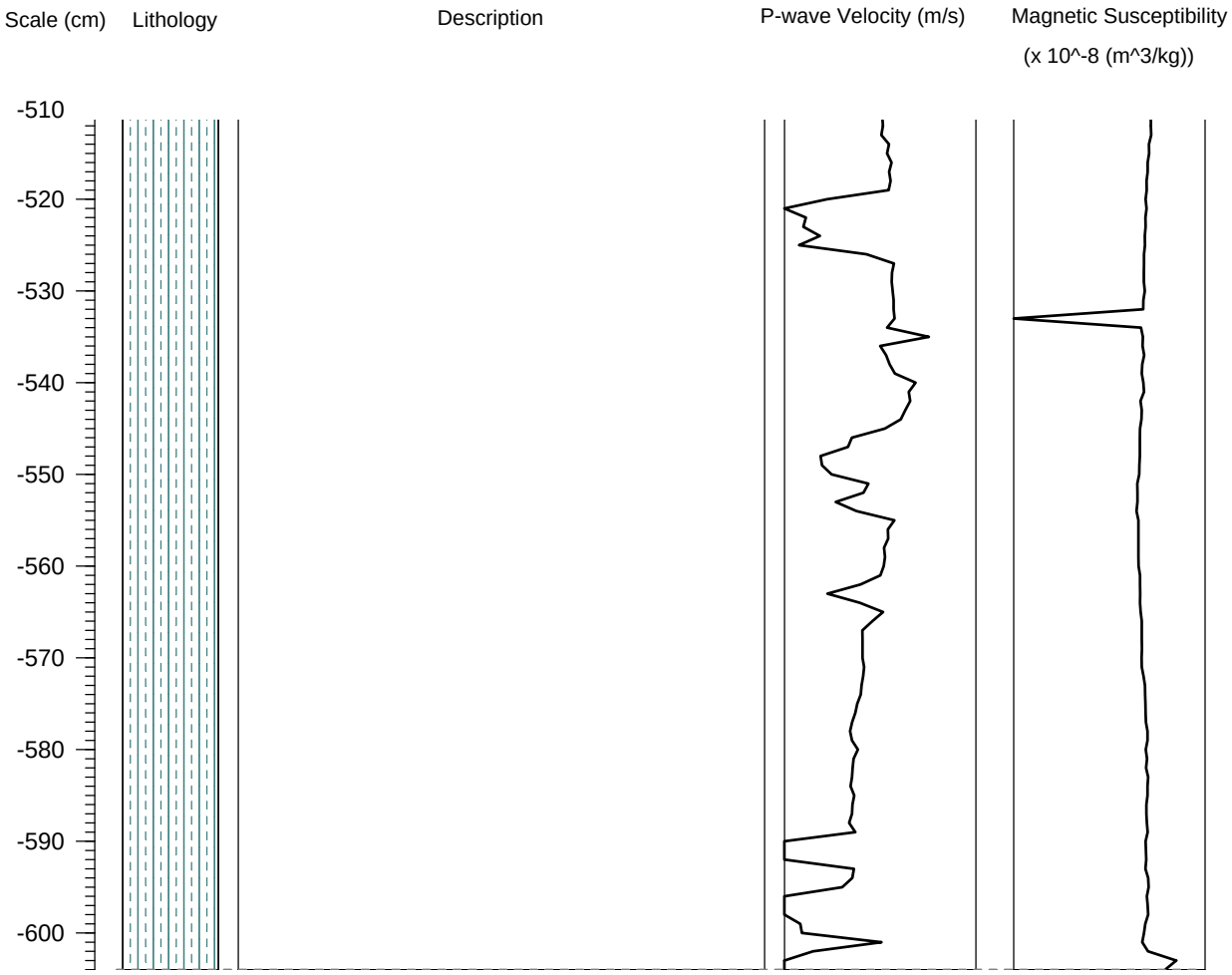

Site No. GA426 **Collection Date** 30 June 2009

Core No. 5

Water Depth 31.3 m BSL

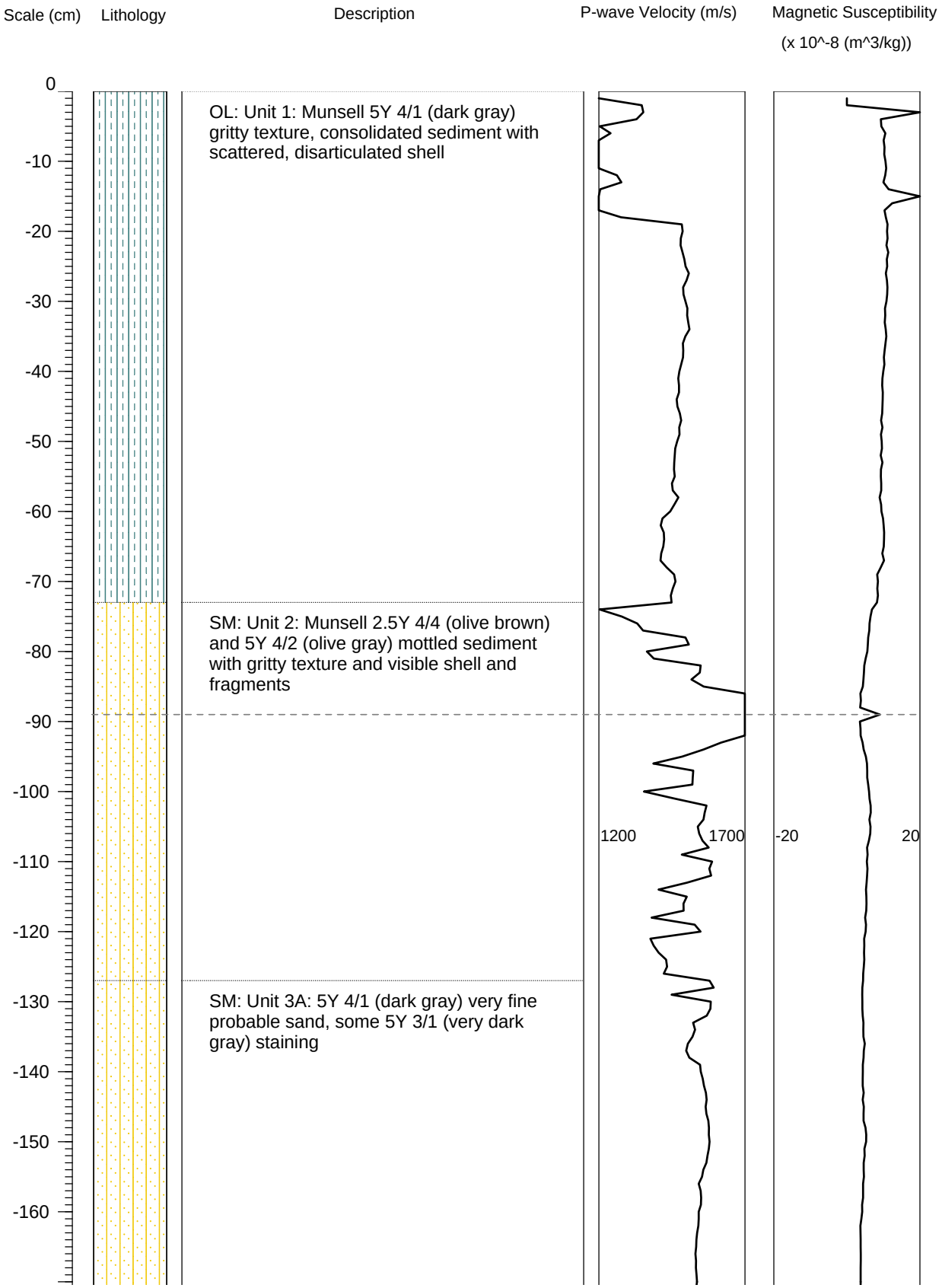

Site No. GA426 **Collection Date** 30 June 2009

Core No. 5

Water Depth 31.3 m BSL

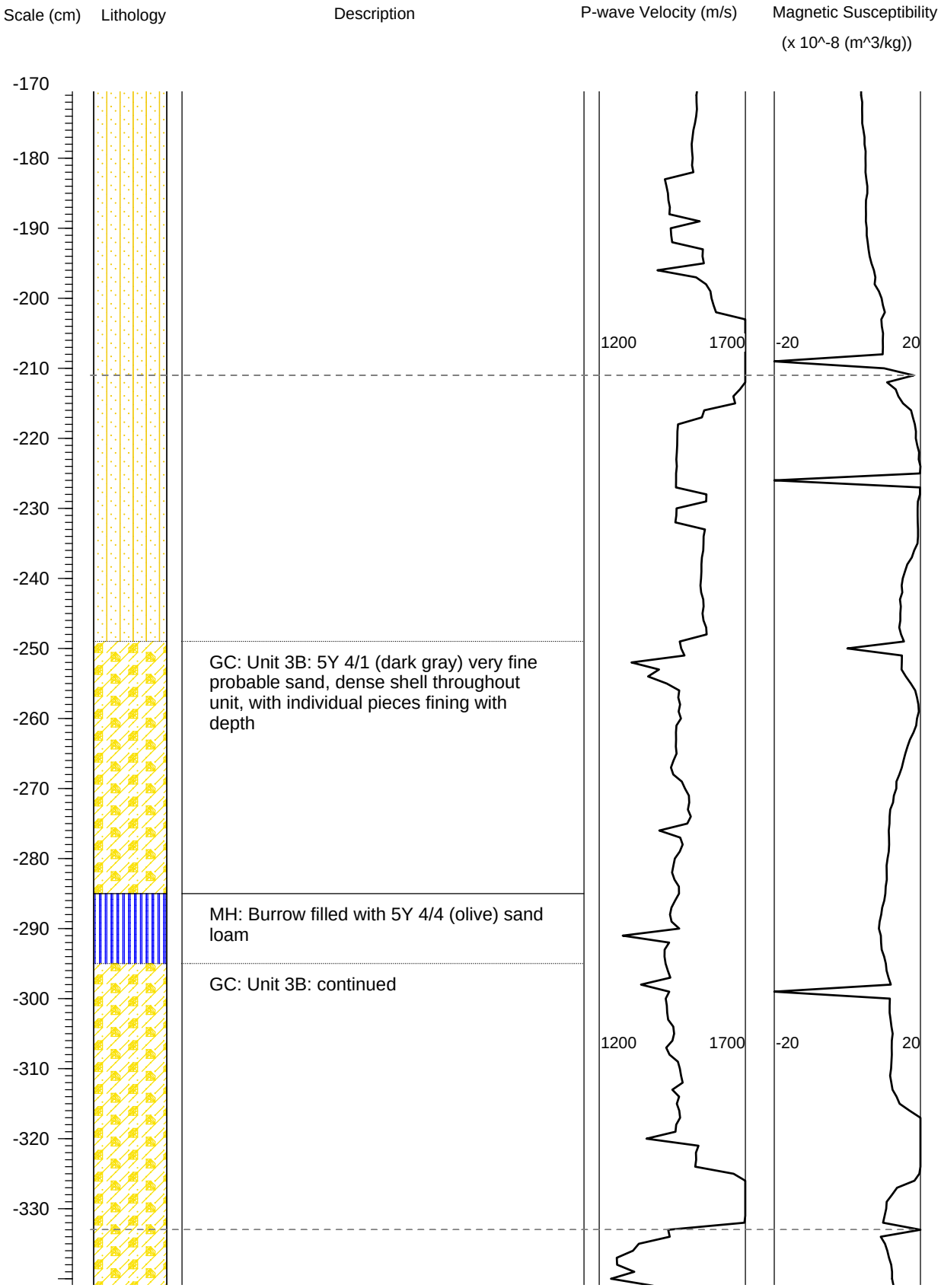

Site No. GA426 **Collection Date** 30 June 2009

Core No. 5

Water Depth 31.3 m BSL

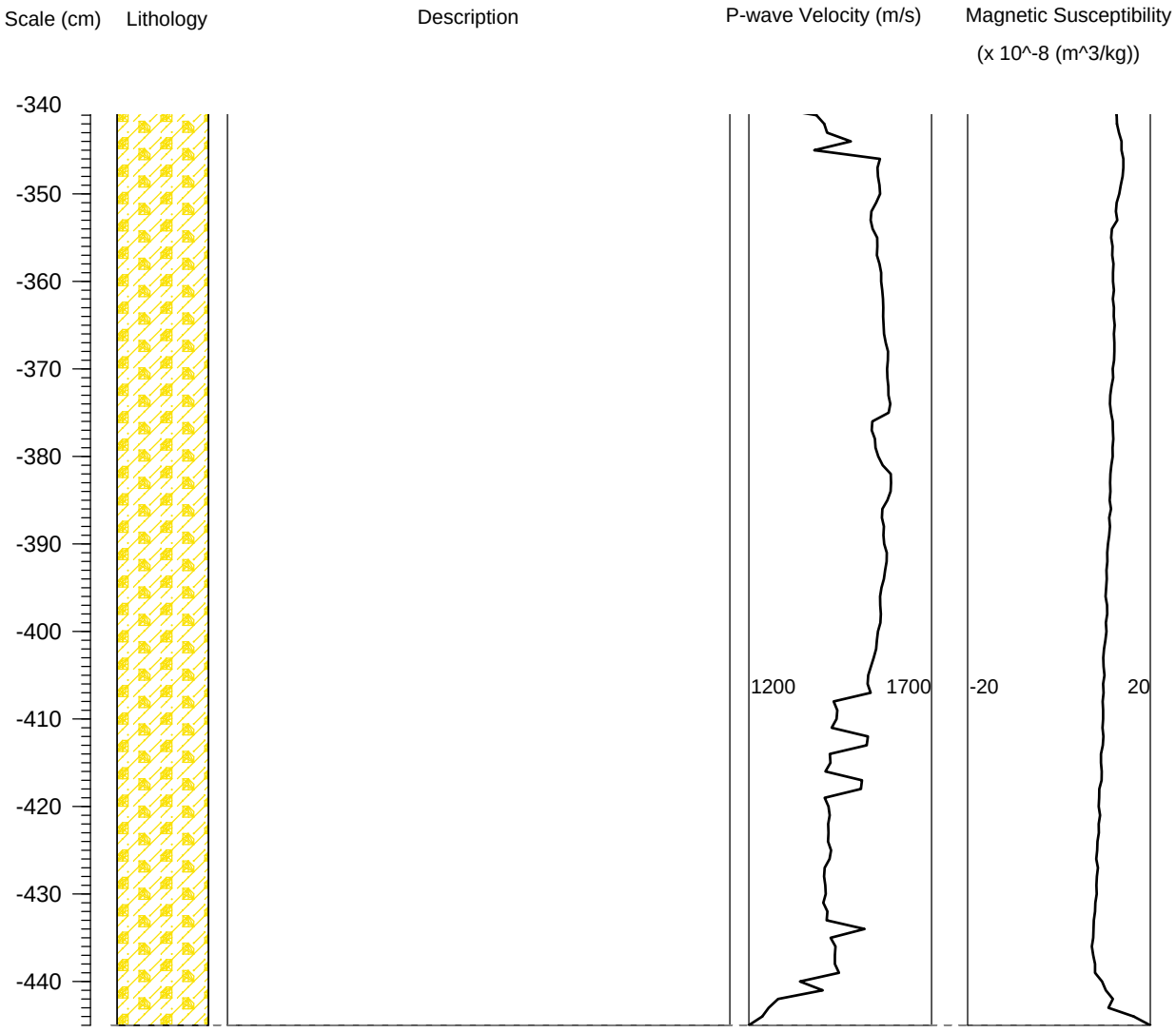

Site No. GA426 **Collection Date** 30 June 2009

Core No. 6

Water Depth 30.9 m BSL

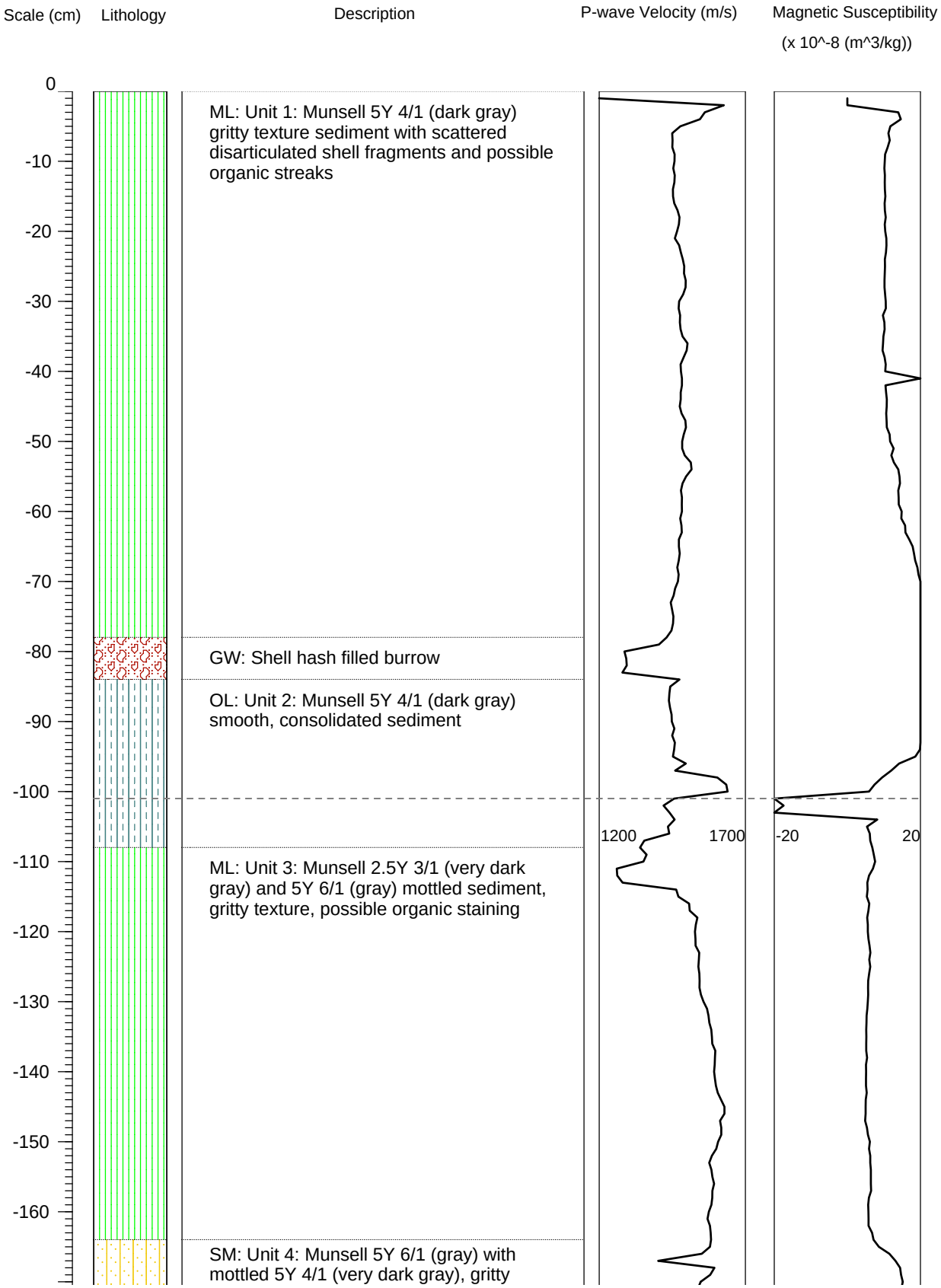

Site No. GA426 **Collection Date** 30 June 2009

Core No. 6

Water Depth 30.9 m BSL

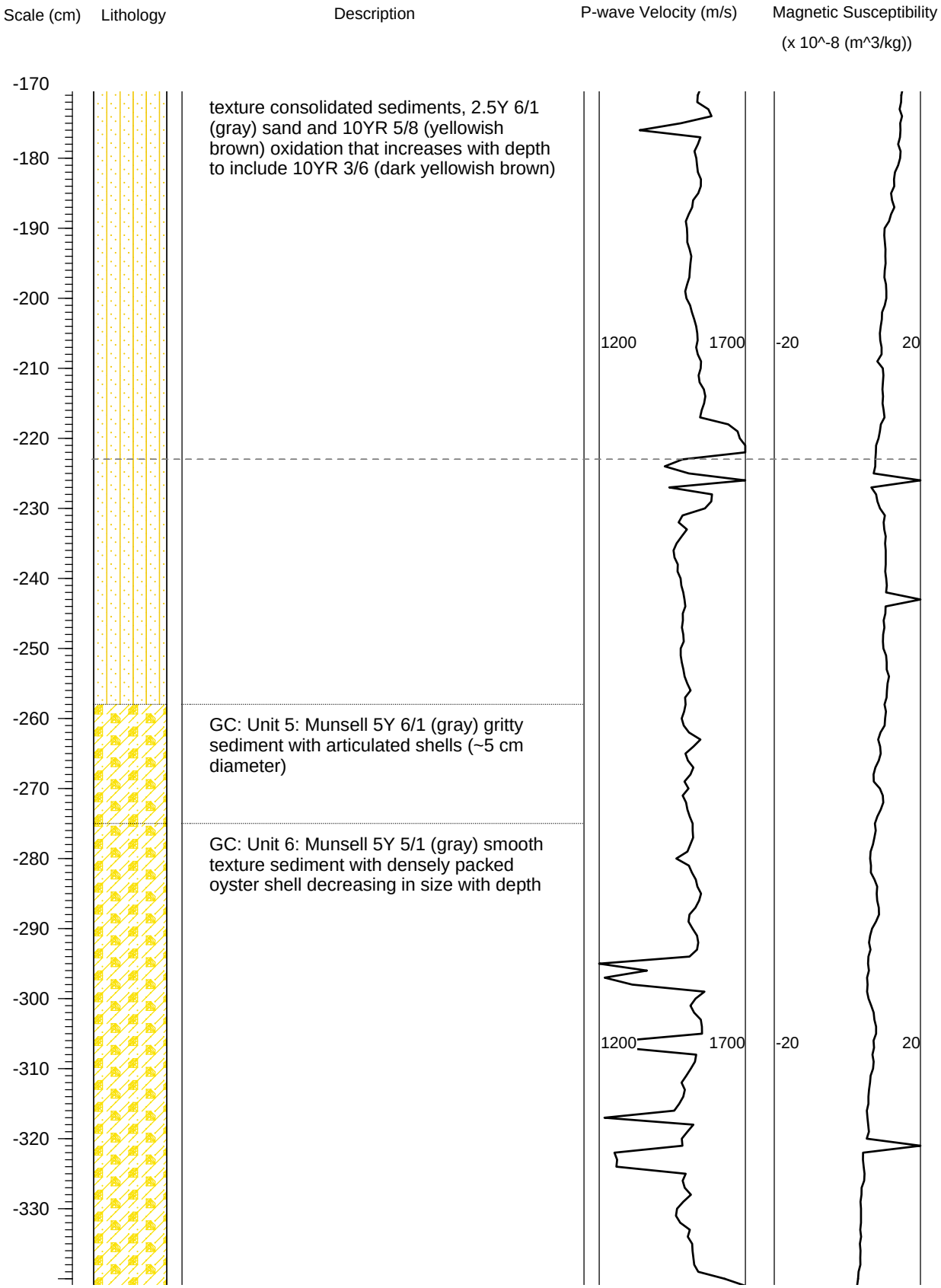

Site No. GA426 **Collection Date** 30 June 2009

Core No. 6

Water Depth 30.9 m BSL

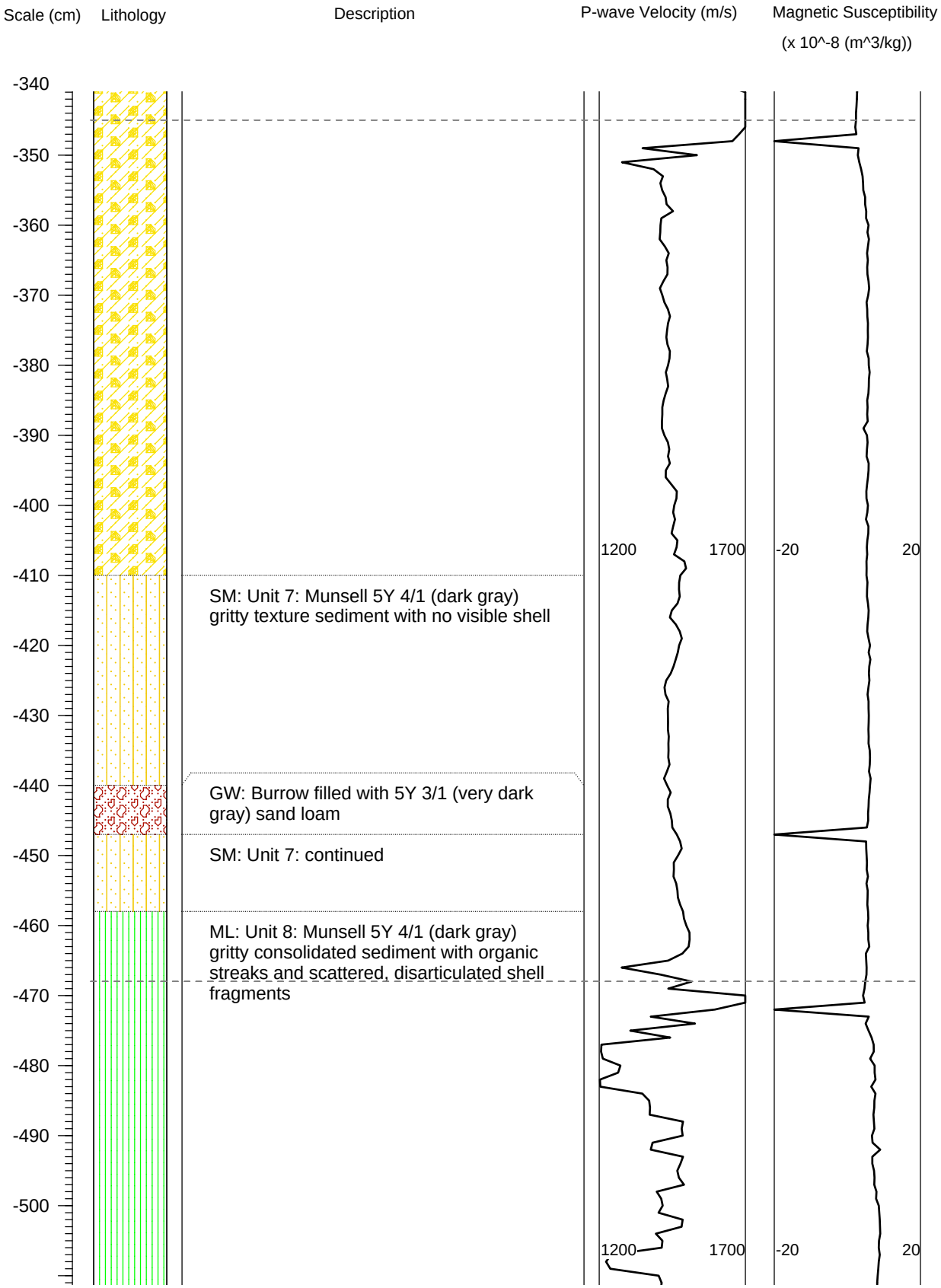

Site No. GA426 **Collection Date** 30 June 2009

Core No. 6

Water Depth 30.9 m BSL

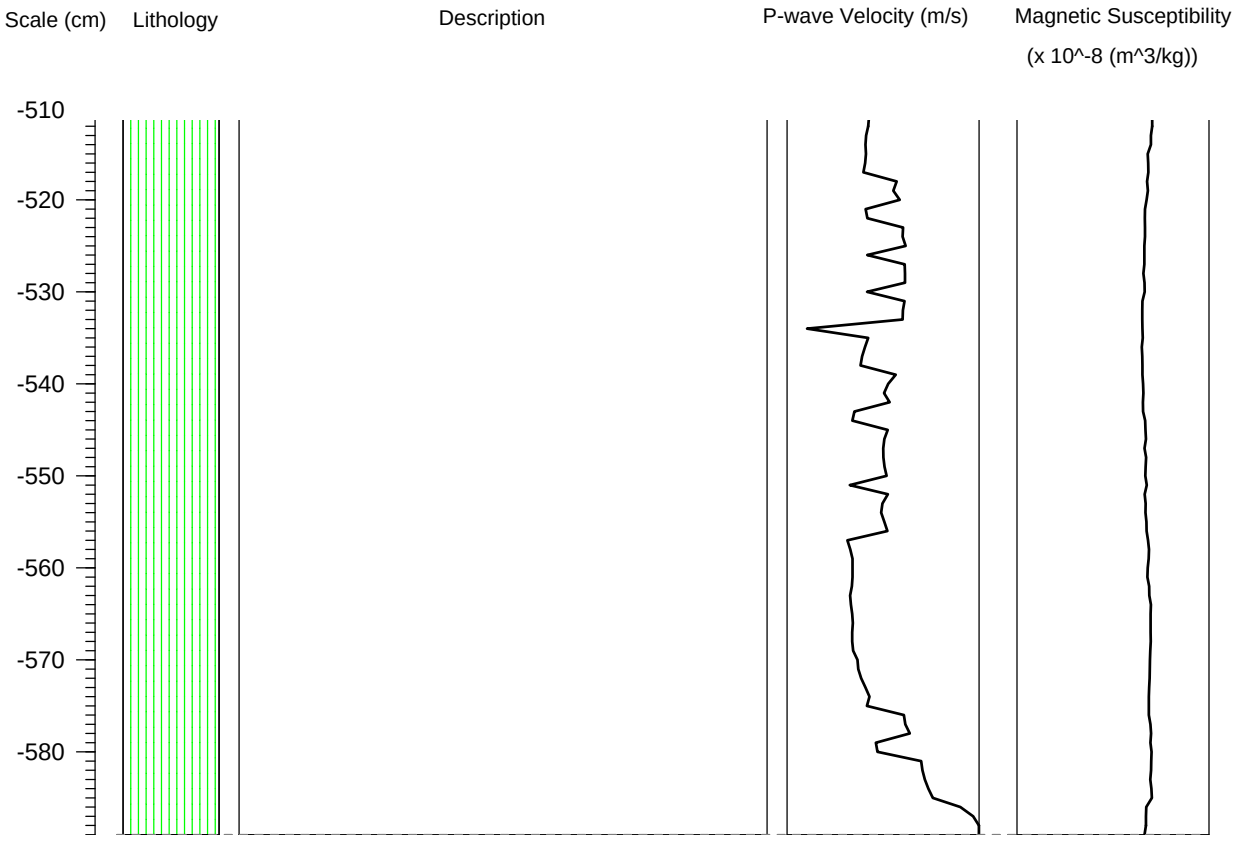

Site No. GA426 **Collection Date** 1 July 2009

Core No. 7

Water Depth 30.8 m BSL

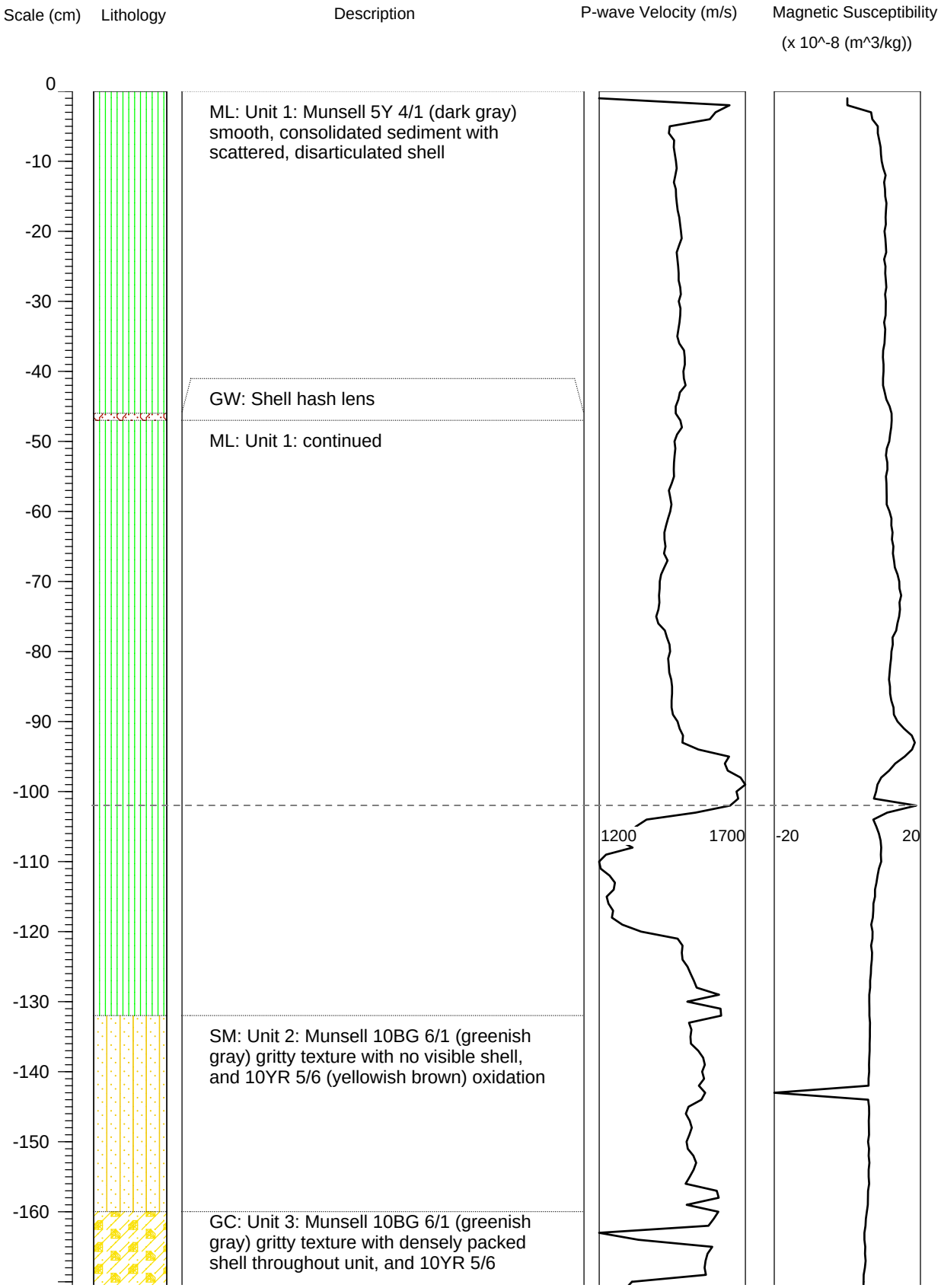

Site No. GA426 **Collection Date** 1 July 2009

Core No. 7

Water Depth 30.8 m BSL

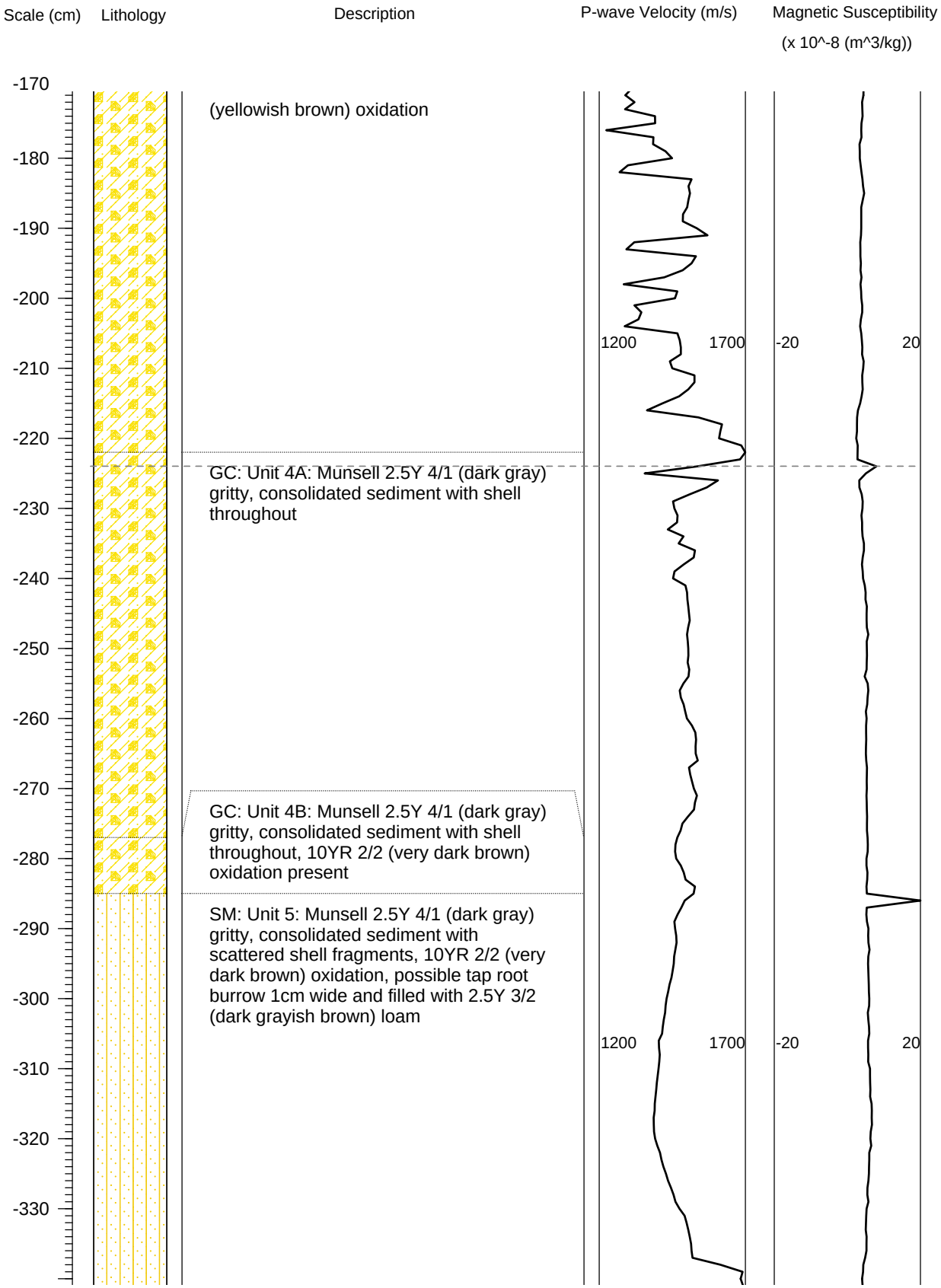

Site No. GA426 **Collection Date** 1 July 2009

Core No. 7

Water Depth 30.8 m BSL

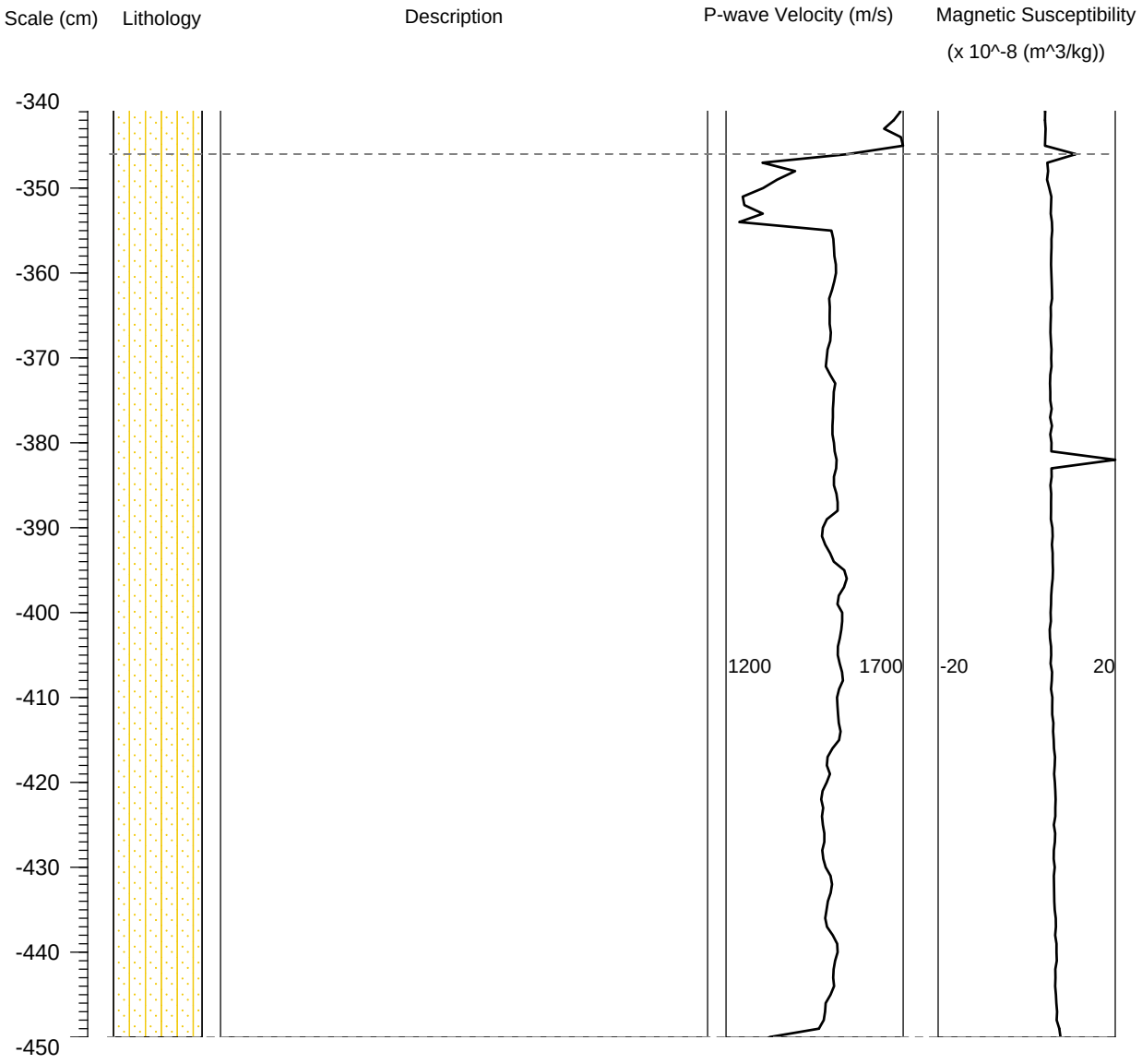

Site No. GA426 **Collection Date** 1 July 2009

Core No. 8

Water Depth 30.7 m BSL

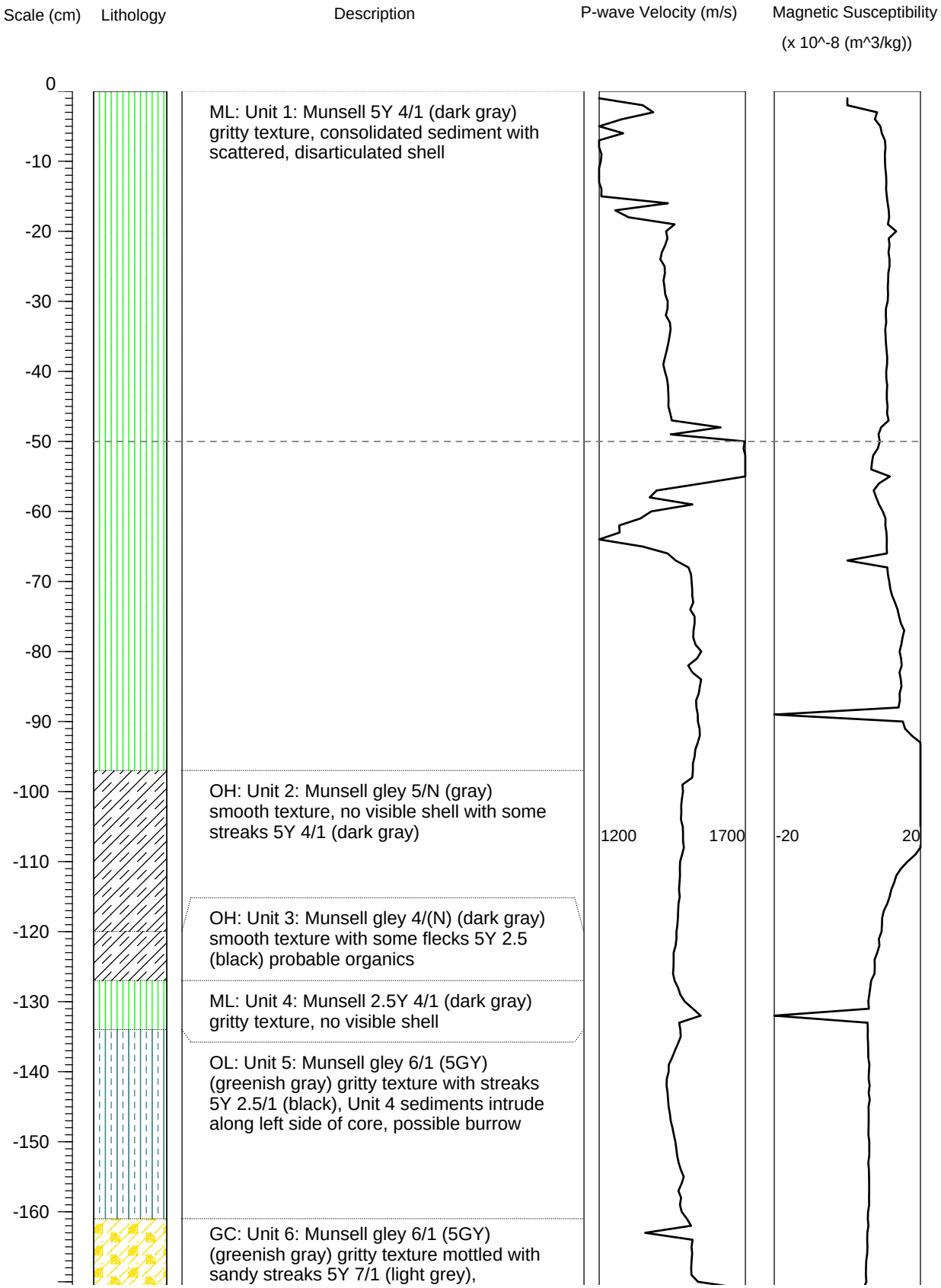

Site No. GA426 **Collection Date** 1 July 2009

Core No. 8

Water Depth 30.7 m BSL

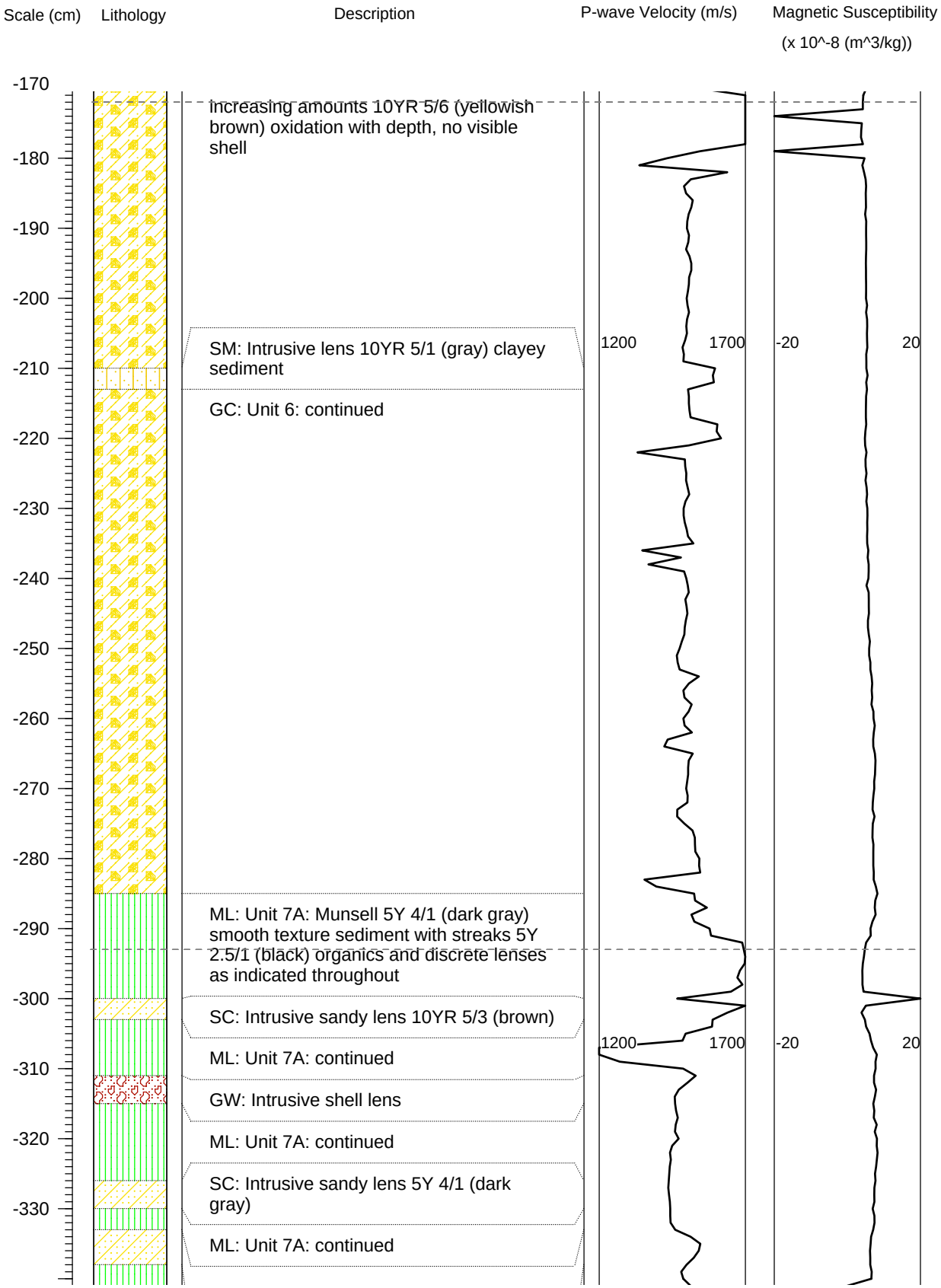

Site No. GA426 **Collection Date** 1 July 2009

Core No. 8

Water Depth 30.7 m BSL

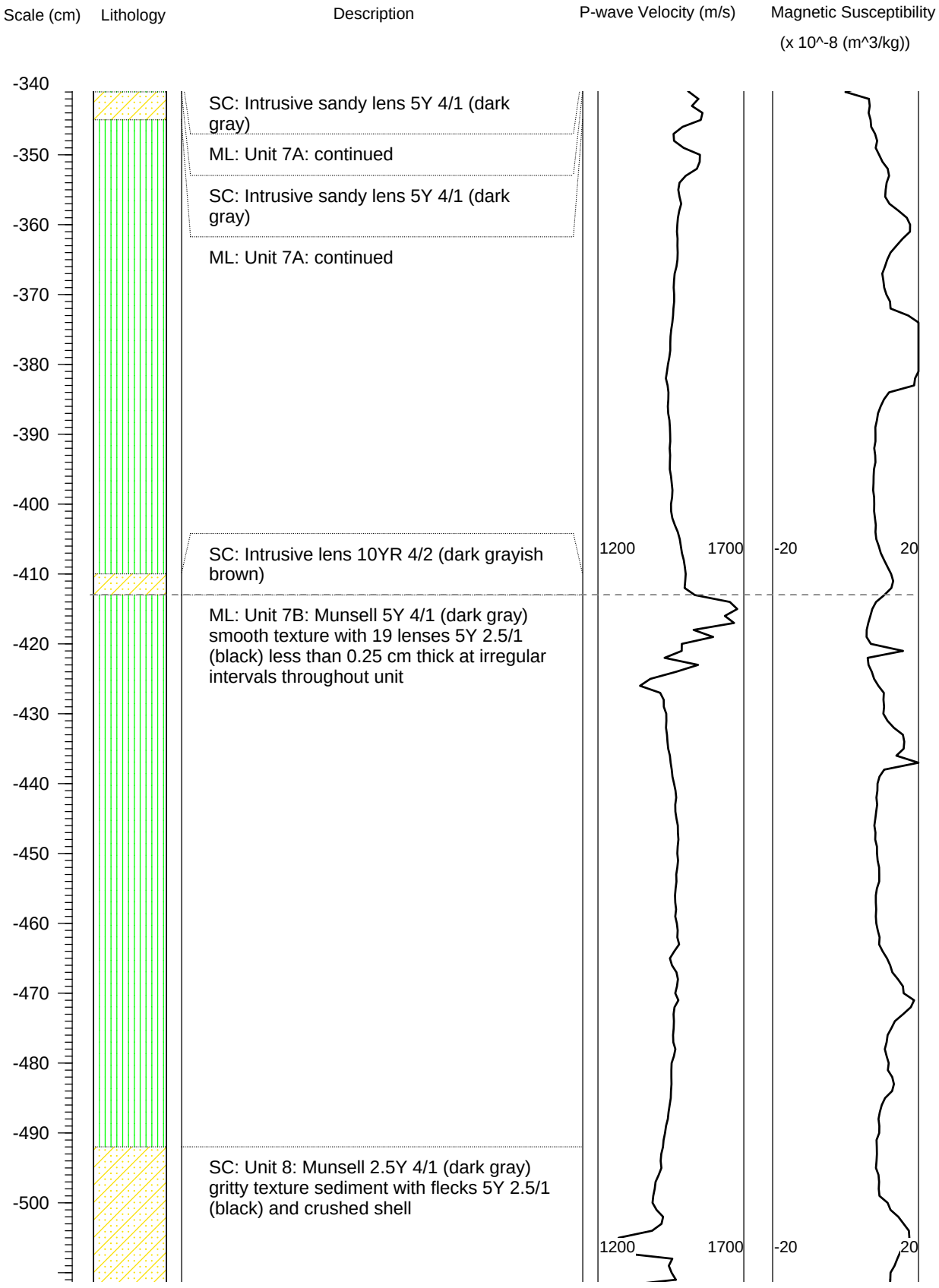

Site No. GA426 **Collection Date** 1 July 2009

Core No. 8

Water Depth 30.7 m BSL

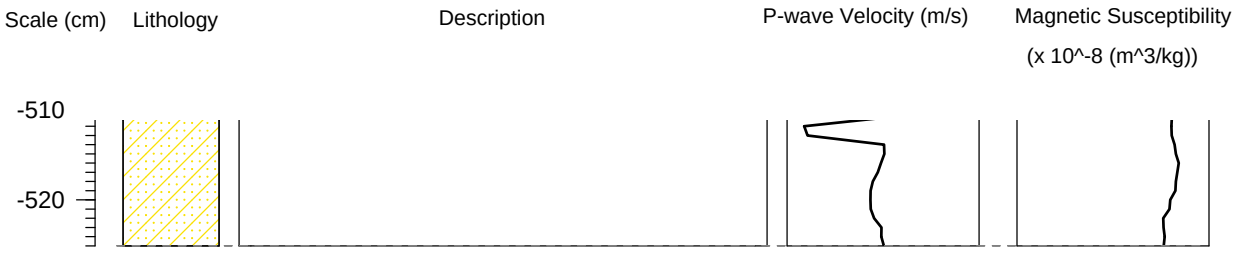

Site No. GA426 **Collection Date** 1 July 2009

Core No. 9

Water Depth 30.9 m BSL

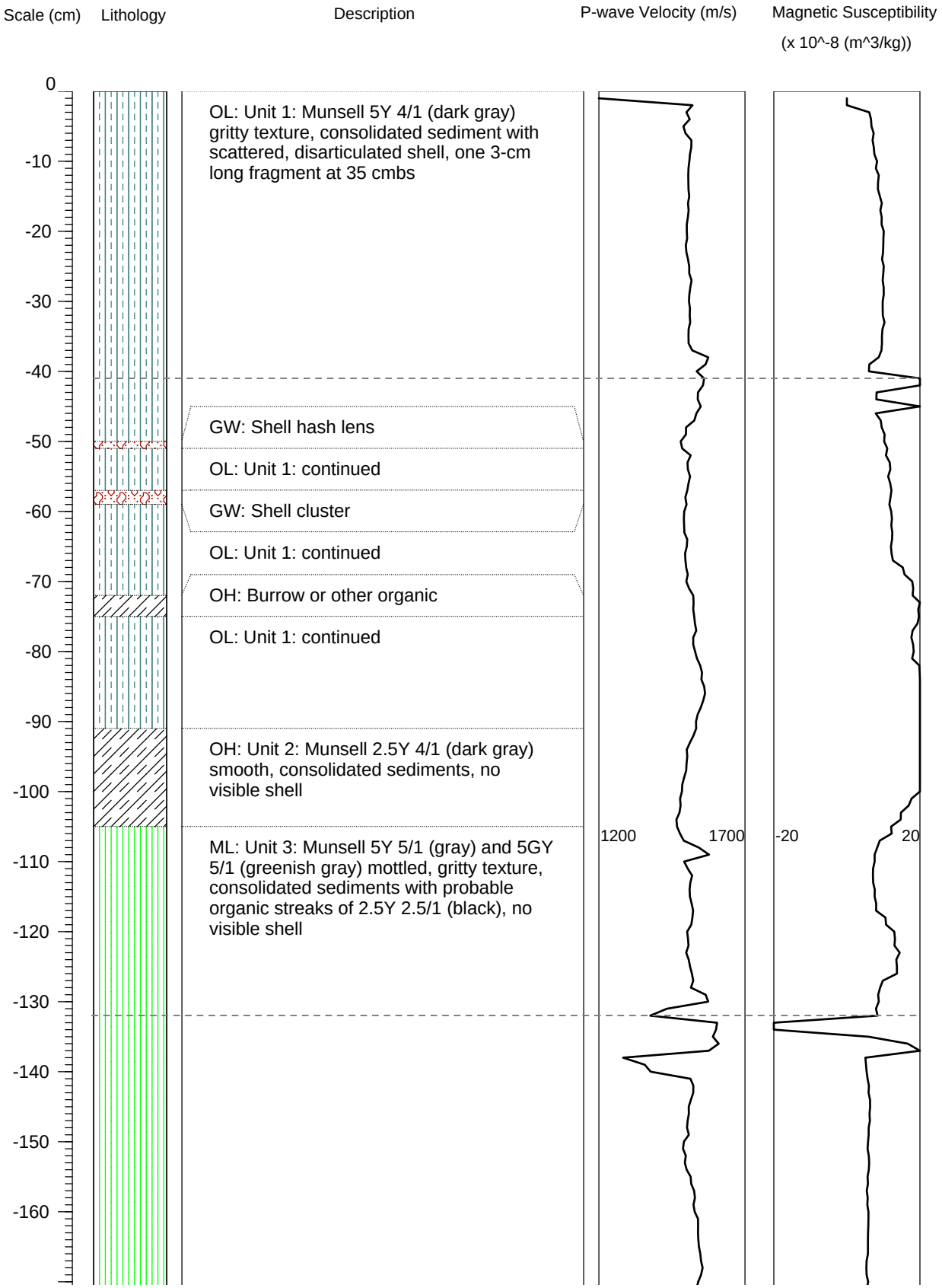

Site No. GA426 **Collection Date** 1 July 2009

Core No. 9

Water Depth 30.9 m BSL

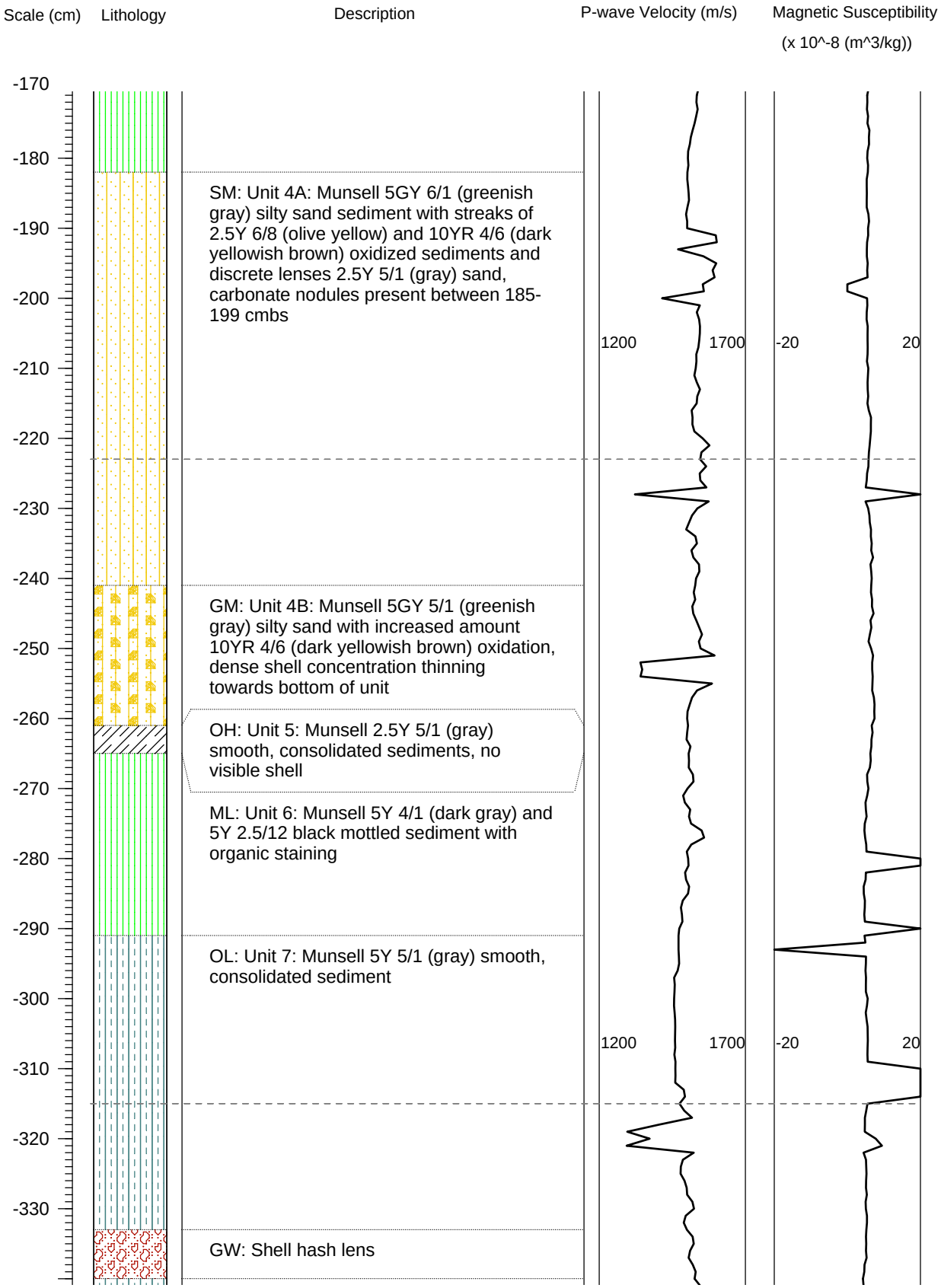

Site No. GA426 **Collection Date** 1 July 2009

Core No. 9

Water Depth 30.9 m BSL

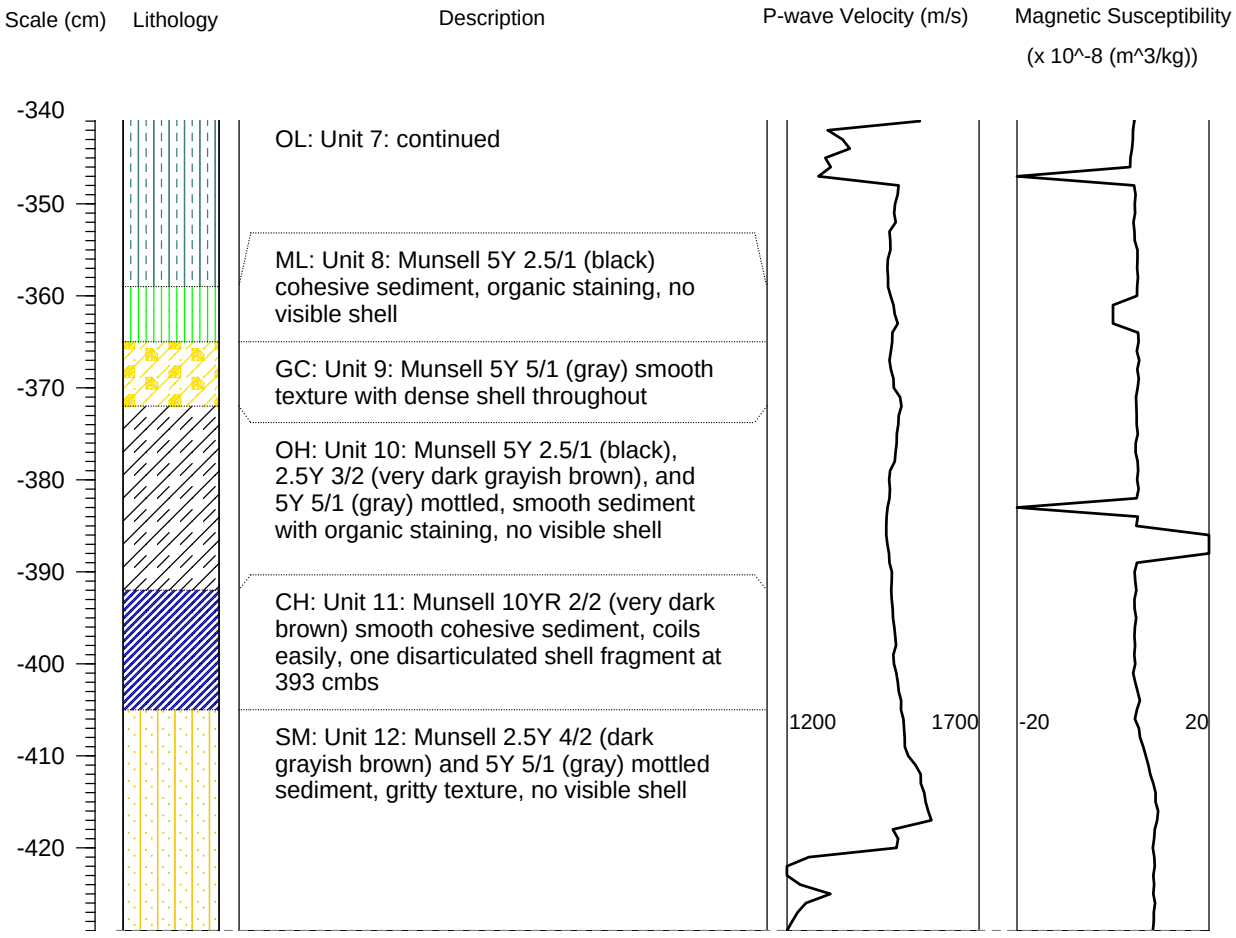

Site No. GA426 **Collection Date** 1 July 2009

Core No. 10

Water Depth 30.9 m BSL

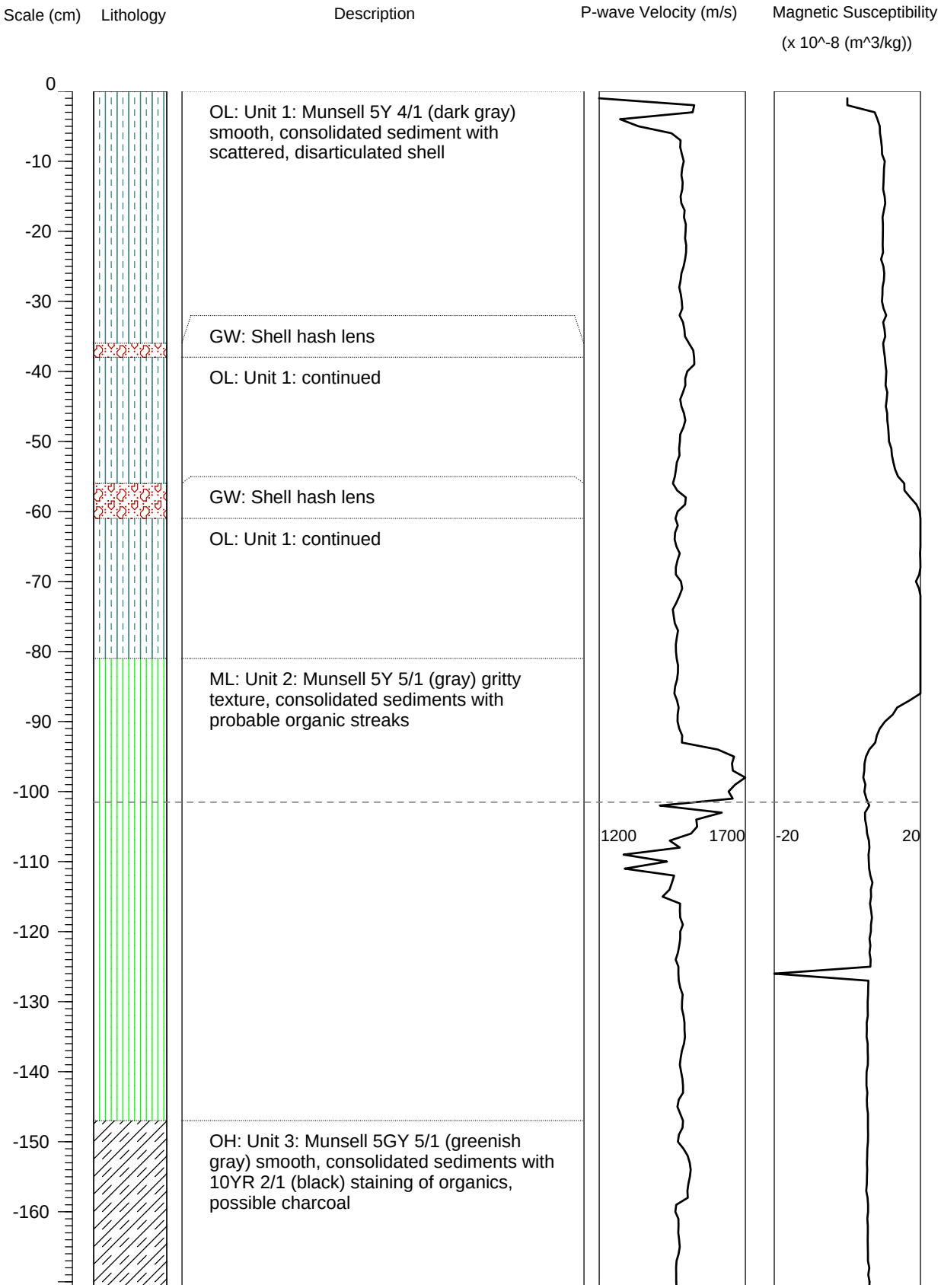

Site No. GA426 **Collection Date** 1 July 2009

Core No. 10

Water Depth 30.9 m BSL

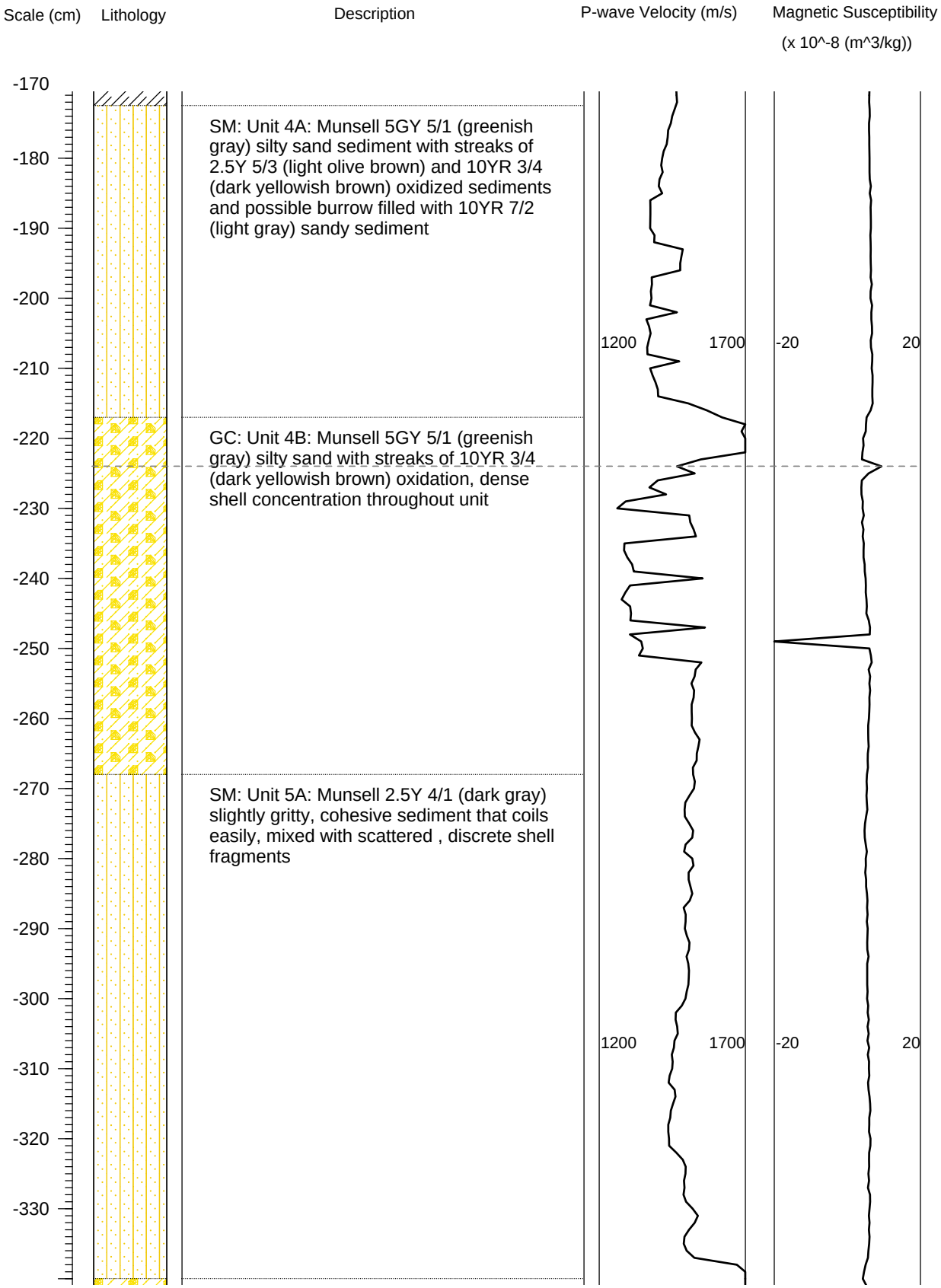

Site No. GA426 **Collection Date** 1 July 2009

Core No. 10

Water Depth 30.9 m BSL

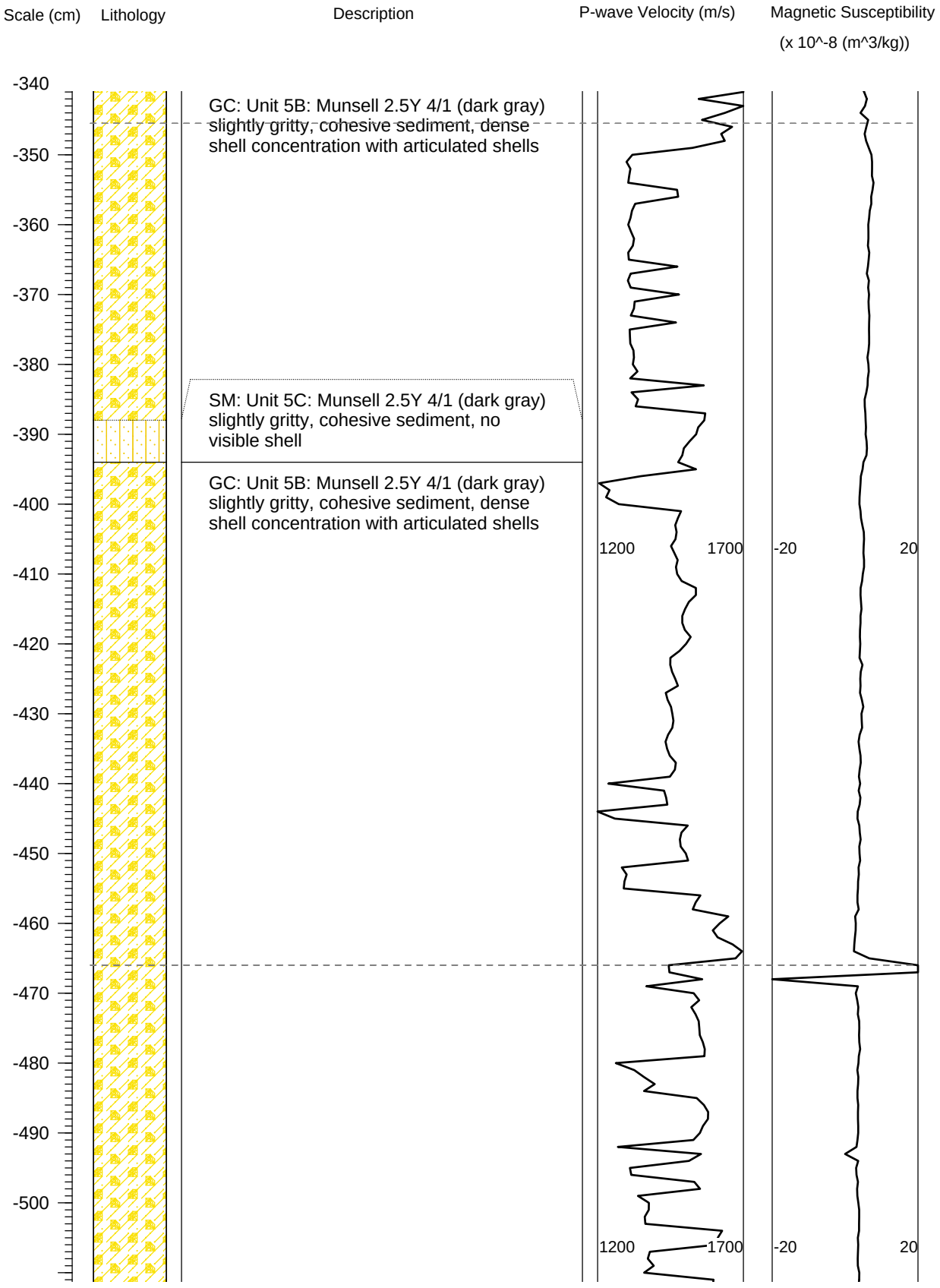

Site No. GA426 **Collection Date** 1 July 2009

Core No. 10

Water Depth 30.9 m BSL

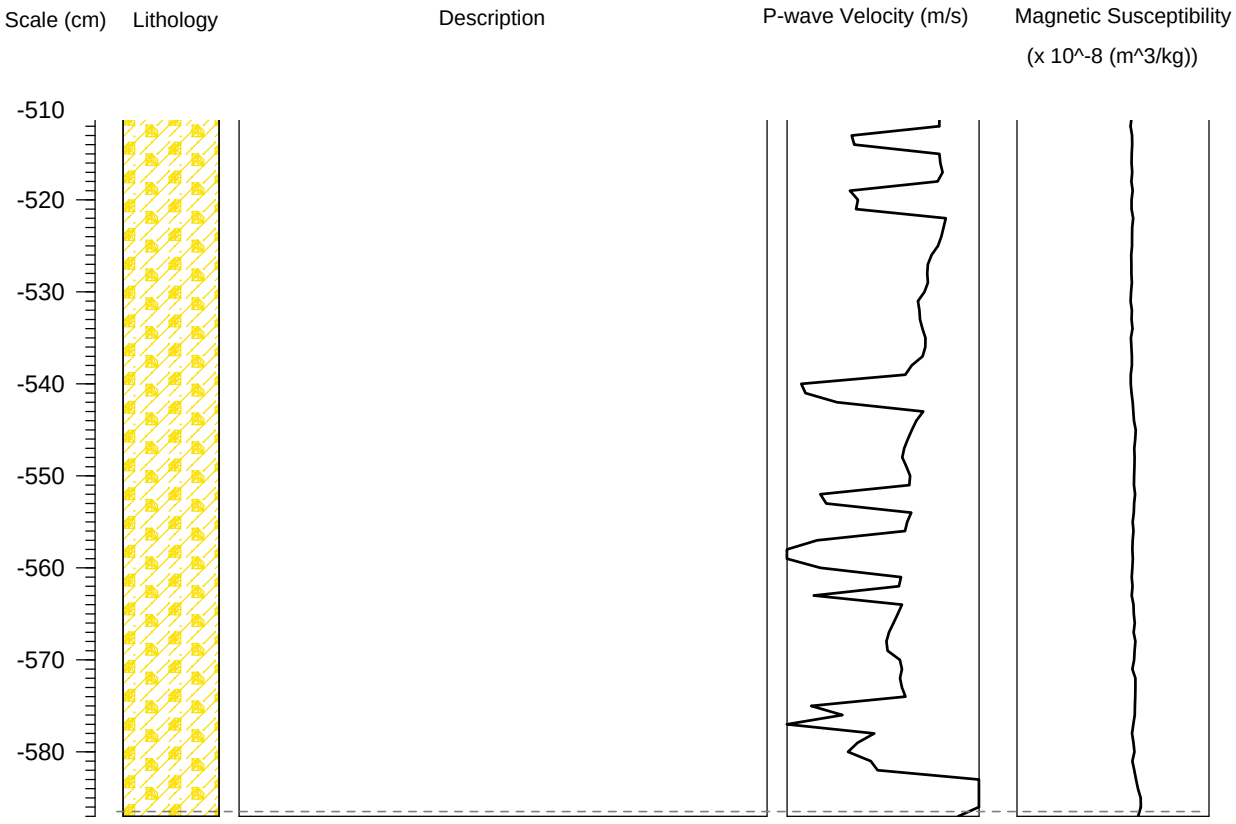

Site No. GA426 **Collection Date** 1 July 2009

Core No. 11

Water Depth 30.9 m BSL

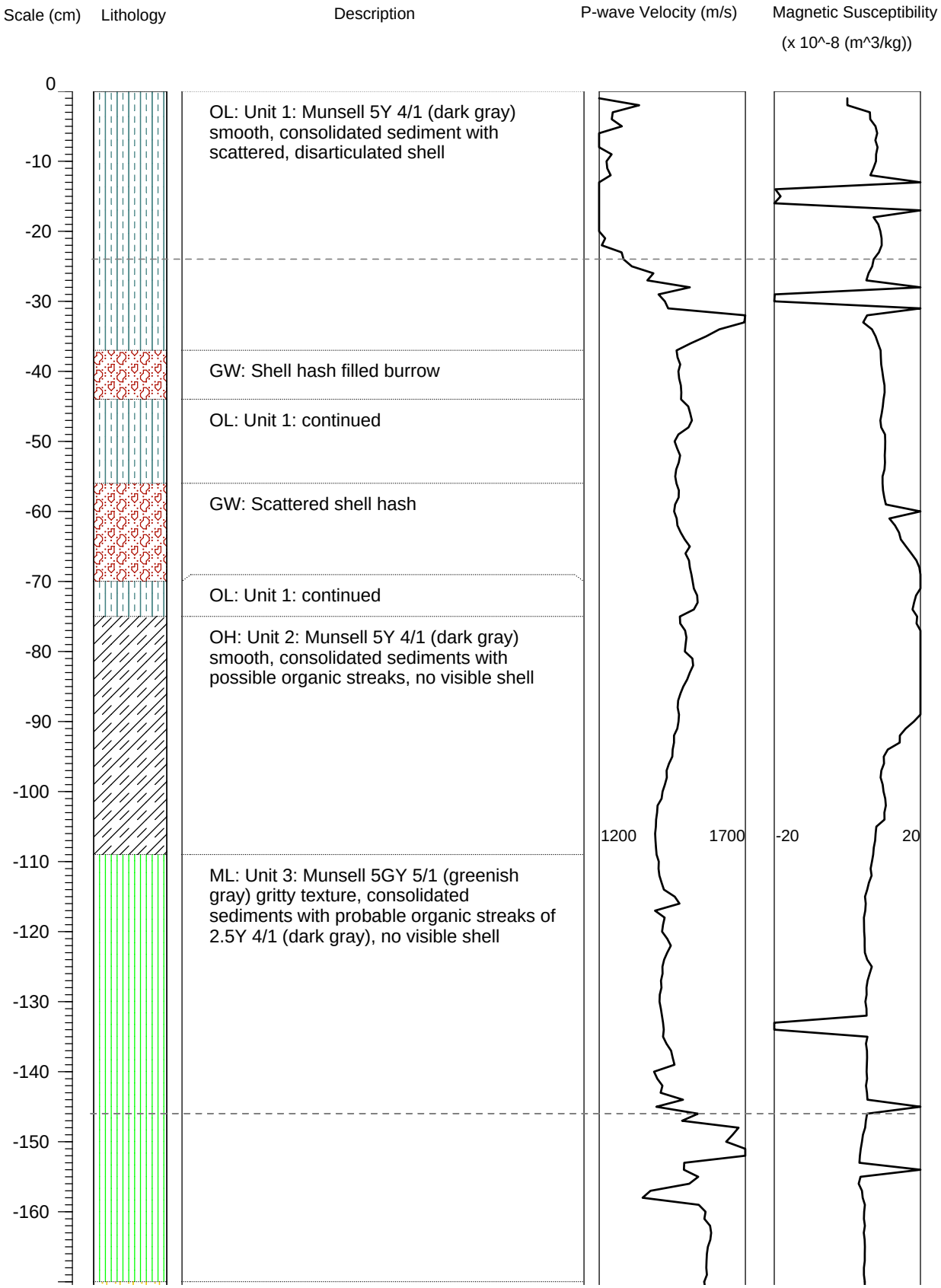

Site No. GA426 **Collection Date** 1 July 2009

Core No. 11

Water Depth 30.9 m BSL

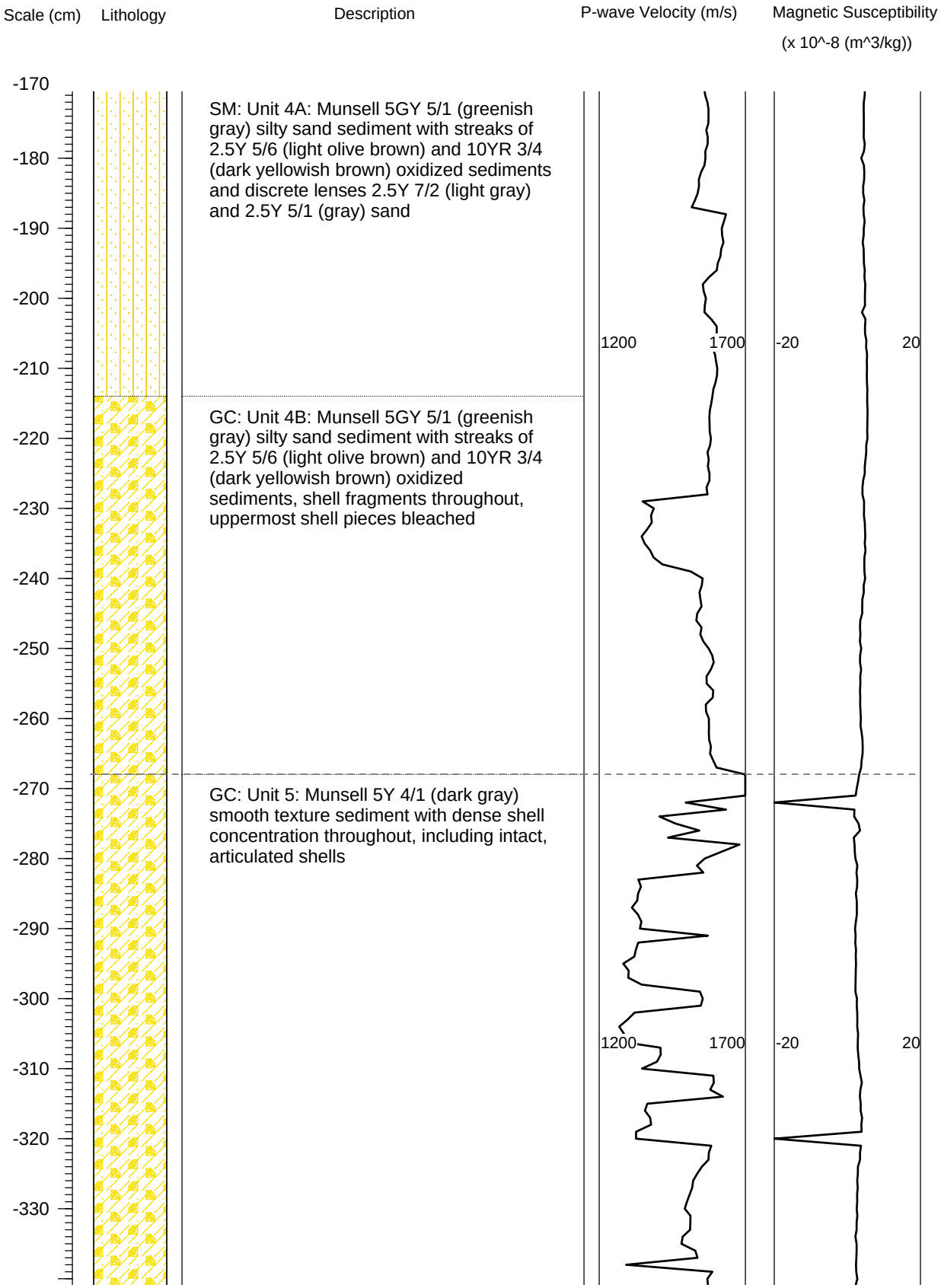

Site No. GA426 **Collection Date** 1 July 2009

Core No. 11

Water Depth 30.9 m BSL

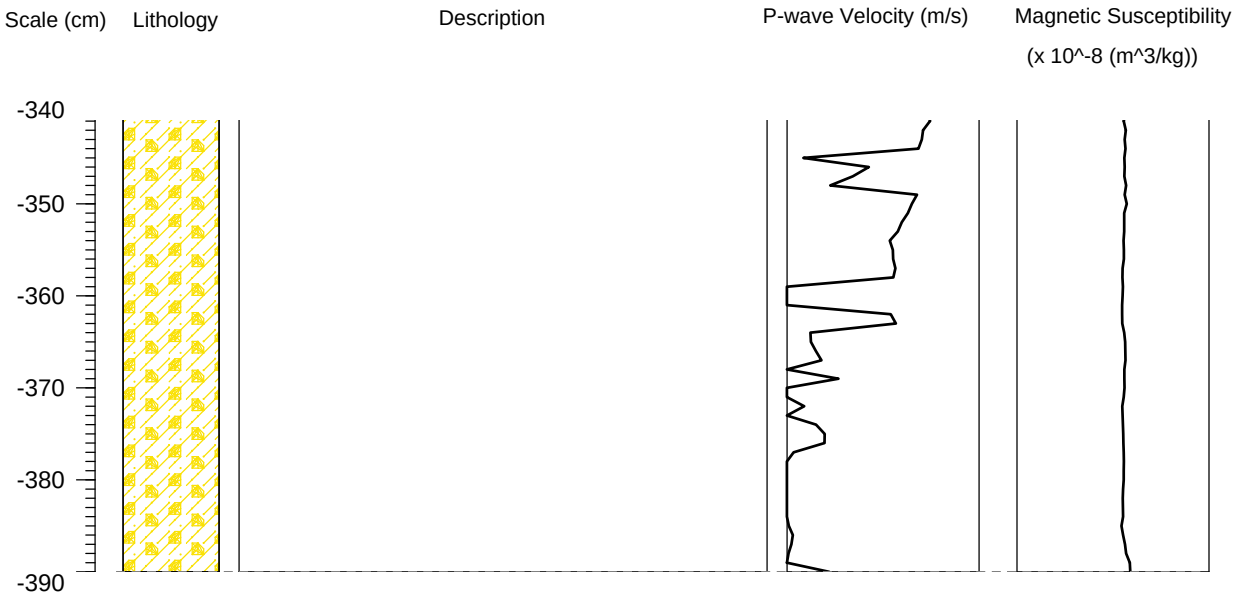

APPENDIX C. SUPPLEMENTAL REPORTS

POLLEN AND ORGANIC RESIDUE (FTIR) ANALYSIS OF SAMPLES FROM SITES GA426 AND HI178, TEXAS GULF COAST

By

Linda Scott Cummings
and
Melissa K. Logan

With Assistance from
R.A. Varney
and
Mikaela Murphy

PaleoResearch Institute
Golden, Colorado

PaleoResearch Institute Technical Report 10-119

Prepared For

Louisiana State University
Baton Rouge, Louisiana

January 2011

INTRODUCTION

Three core samples recovered from two underwater sites (GA426 and HI178) on the outer continental shelf off the Texas coast in the Gulf of Mexico were submitted for pollen and organic residue analysis. Two of the samples were examined for organic residues using Fourier Transform Infrared Spectroscopy (FTIR), and two were examined for pollen. Pollen and organic residue analysis will be used to determine if the core samples represent sites on land or deposition of floral remains blown to sea.

METHODS

Pollen

A chemical extraction technique based on flotation is the standard preparation technique used in this laboratory for the removal of the pollen from the large volume of sand, silt, and clay with which they were mixed. This particular process was developed for extraction of pollen from soils where preservation has been less than ideal and pollen density is lower than in peat. It is important to recognize that it is not the repetition of specific and individual steps in the laboratory, but rather mastery of the concepts of extraction and how the desired result is best achieved, given different sediment matrices, that results in successful recovery of pollen for analysis.

Hydrochloric acid (10%) was used to remove calcium carbonates present in the soil, after which the samples were screened through 250 micron mesh. The samples were rinsed until neutral by adding water, letting the samples stand for 2 hours, then pouring off the supernatant. A small quantity of sodium hexametaphosphate was added to each sample once it reached neutrality, then the samples were allowed to settle according to Stoke's Law in settling columns. This process was repeated with ethylenediaminetetraacetic acid (EDTA). These steps remove clay prior to heavy liquid separation. The samples then were freeze dried. Sodium polytungstate (SPT), with a density 1.8, was used for the flotation process. The samples were mixed with SPT and centrifuged at 1500 rpm for 10 minutes to separate organic from inorganic remains. The supernatant containing pollen and organic remains was decanted. Sodium polytungstate again was added to the inorganic fraction to repeat the separation process. The supernatant was decanted into the same tube as the supernatant from the first separation. This supernatant was then centrifuged at 1500 rpm for 10 minutes to allow any silica remaining to be separated from the organics. Following this, the supernatant was decanted into a 50 ml conical tube and diluted with distilled water. These samples were centrifuged at 3000 rpm to concentrate the organic fraction in the bottom of the tube. After rinsing the pollen-rich organic fraction obtained by this separation, all samples receive a short (20-30 minute) treatment in hot hydrofluoric acid to remove any remaining inorganic particles. The samples then were acetolated for 3-5 minutes to remove any extraneous organic matter.

A light microscope was used to count pollen at a magnification of 500x. Pollen preservation in these samples varied from good to poor. Comparative reference material collected at the Intermountain Herbarium at Utah State University and the University of Colorado Herbarium was used to identify the pollen to the family, genus, and species level, where possible.

Pollen aggregates were recorded during identification of the pollen. Aggregates are clumps of a single type of pollen and may be interpreted to represent pollen dispersal over short distances or the introduction of portions of the plant represented into an archaeological setting. Aggregates were included in the pollen counts as single grains, as is customary. The presence of aggregates is noted by an "A" next to the pollen frequency on the pollen diagram. Pollen diagrams are produced using Tilia 2.0 and TGView 2.0.2. Total pollen concentrations are calculated in Tilia using the quantity of sample processed in cubic centimeters (cc), the quantity of exotics (spores) added to the sample, the quantity of exotics counted, and the total pollen counted and expressed as pollen per cc of sediment.

Indeterminate pollen includes pollen grains that are folded, mutilated, and otherwise distorted beyond recognition. These grains are included in the total pollen count since they are part of the pollen record. The microscopic charcoal frequency registers the relationship between pollen and charcoal. The total number of microscopic charcoal fragments was divided by the pollen sum, resulting in a charcoal frequency that reflects the quantity of microscopic charcoal fragments observed, normalized per 100 pollen grains.

Pollen analysis also includes examination for and identification of algal bodies and foraminifera tests, when present.

FTIR (Fourier Transform Infrared Spectroscopy)

A mixture of chloroform and methanol (CHM) was used as a solvent to remove lipids and other organic substances that had soaked into the sediment. This mixture is represented in the FTIR graphics as CHM. The CHM solvent and sample were placed in a glass container, and allowed to sit, covered, for several hours. After this period of time, the solvent was pipetted into an aluminum evaporation dish, where the CHM was allowed to evaporate. This process leaves the residue of any absorbed chemicals in the aluminum dishes. The residue remaining in the aluminum dishes was then placed on the FTIR crystal and the spectra were collected. The aluminum dishes were tilted during the process of evaporation to separate the lighter from the heavier fraction of the residue. The lighter and heavier fractions are designated upper (lighter fraction) and lower (heavier fraction) respectively in the subsequent analysis.

FTIR is performed using a Nicolet 6700 optical bench with an ATR and a diamond crystal. The sample is placed in the path of a specially encoded infrared beam, which passes through the sample and produces a signal called an “inferogram.” The inferogram contains information about the frequencies of infrared that are absorbed and the strength of the absorptions, which is determined by the sample’s chemical make-up. A computer reads the inferogram and uses Fourier transformation to decode the intensity information for each frequency (wave numbers) and presents a spectrum.

FTIR (FOURIER TRANSFORM INFRARED SPECTROSCOPY) REVIEW

Infrared spectroscopy (IR) is the study of how molecules absorb infrared radiation and ultimately convert it to heat, revealing how the infrared energy is absorbed, as well as the

structure of specific organic molecules. Infrared spectroscopy has been experiencing a renaissance for identifying organic substances during the past few decades. It is currently considered one of the more powerful tools in organic and analytical chemistry. One of the primary advantages to the FTIR is that it measures all wave lengths simultaneously. It has a relatively high signal-to-noise ratio and a short measurement time. Each peak in the spectrum represents either a chemical bond or a functional group.

Since molecular structures absorb the vibrational frequencies or wavelengths of infrared radiation, the bands of absorbance can then be used to identify the composition of the materials under study. In the case of the current research, the portion of the electromagnetic spectrum between 4000-400 wave numbers is used for identifying organic materials. Carbohydrates, lipids, proteins, and other organic molecules are associated with specific wave number bands (Isaksson 1999:36-39).

The infrared spectrum can be divided into two regions--the functional group region and the fingerprint region. These two groups are recognized by the effect that infrared radiation has on the respective molecules of these groups. The functional group region is located between 4000 and approximately 1500 wave numbers. The molecular bonds display specific characteristic vibrations that identify fats, lipids, waxes, lignins, proteins, carbohydrates, etc. The fingerprint region, located below 1500 wave numbers, is influenced by bending motions, which further identify the molecules present.

Using the FTIR, it is possible to identify different types of organic compounds and eventually recognize different types of materials such as plant or animal fats or lipids, plant waxes, esters, proteins, carbohydrates, and more. Specific regions of the spectrum are important in identifying these compounds.

The results of the identification of specific wavelengths can be compared with commercial or laboratory-created analytical standards to identify the specific types of bonds present in different materials. By combining the results of the analysis of individual samples with all of the reference materials in the PaleoResearch Institute (PRI) library, the percent match with individual reference items can be displayed. For instance, plant lipids or fats are identifiable between 3000-2800 wave numbers. A match might be obtained on this portion of the spectrum with nuts such as hickory, walnut, or acorn, or with animal fats or corn oil. Recovery of high level matches with several types of nuts (in this example) indicates that nuts were processed. If the match with the PRI library is with meats, then the fats matched are more consistent with those produced by meat than plant parts, such as nuts.

Samples containing many compounds are more difficult to identify – and many archaeological samples are complex mixtures. Multi-purpose artifacts, such as groundstone, which could have been used to crush or grind a variety of foodstuffs, or ceramic cooking vessels, which are expected to have been used to cook many different foods, might present a mixture problem. Mixtures sometimes have many absorption bands that overlap, yielding only broad envelopes of absorption and few distinctive features. FTIR analysis is expected to be particularly valuable in examining fire-cracked rock (FCR), for which few other means of analysis exist, since the fats, lipids, waxes, and other organic molecules contained in liquids that seep out of the food being processed become deposited on the rocks during the baking process. Once again, these rocks might have been present in more than one cooking episode, thus having the potential to yield a complex signature. The PRI extraction method gently

removes these organic molecules from the groundstone, ceramics, and/or rocks so that they can be measured with the FTIR and subsequently identified.

Organic molecules from sediments can be extracted and the sediments then characterized. This has the potential to be very useful in identifying signatures of the remains responsible for a dark horizon. For instance, if the dark horizons are the result of decaying organic matter (plant or animal), the FTIR will yield a signature of decaying organic remains. If the dark horizons are the result of blowing ash from cultural features, the FTIR signature will be considerably different. This is an affordable technique for making distinctions between horizons and identifying cultural horizons.

Carbohydrates

Carbohydrates are a product of photosynthesis in green plants. This group of compounds is the most abundant found on earth. Carbohydrates is a term that encompasses three main groups of compounds: 1) sugars, 2) starches, and 3) fibers. To elaborate, sugars include the simple carbohydrates found in table sugar, honey, natural fruit sugars, and molasses. Starches and complex carbohydrates are present in legumes, grains, vegetables, and fruits. Fibers, including cellulose, hemicellulose, and pectin, are present in whole grains, legumes, vegetables, and fruits (Garrison and Somer 1985:13). Dietary carbohydrates provide energy for bodily functions, including our ability to digest and absorb other foods. They are the body's preferred source of energy, although proteins and lipids also may be converted to energy. Carbohydrates are so important that an inadequate intake may result in nutritional deficiencies such as ketosis, energy loss, depression, and even loss of essential body protein. On the other hand, excess intake of carbohydrates causes obesity and dental decay.

To understand carbohydrates and their detection with the FTIR, it is important to know that they are formed of carbon atoms coupled to "hyrates," such as water, resulting in empirical formulas of $C_nH_{2n}O_n$ where "n" represents the number of atoms for C, H, and O, respectively. "Biochemically, carbohydrates are polyhydroxy alcohols with aldehyde or ketone groups that are potentially active" (Garrison and Somer 1985:13). Since carbohydrates are classified according to their structure and the FTIR detects the bonds between molecules, we will review the simple sugars (monosaccharides), multiple sugars (oligosaccharides), and complex molecules (polysaccharides) that are made up of simple sugars.

Polysaccharides

These complex starchy compounds follow the empirical formula: $C_6H_{10}O_5$. They are not sweet, do not crystallize, and are not water soluble. Simply defined, polysaccharides are complex carbohydrates found in plants as starch and cellulose, and in animals as glycogen. Because the FTIR detects the bonds between atoms in molecules, it is important to know that polysaccharides are formed of repeating units of mono- or disaccharides that are joined together by glycosidic bonds. Polysaccharides are often heterogeneous. The slight modifications of the repeating unit results in slightly different wave number signatures on the FTIR. Types of polysaccharides are descriptive and include storage (starches and glycogen), structural (cellulose and chitin), acidic (containing carboxyl groups, phosphate groups, and/or sulfuric ester groups), neutral (presumably without the acid features), bacterial

(macromolecules that include peptidoglycan, lipipolysaccharides, capsules and exopolysaccharides), and more. The study of polysaccharides is an ever growing field and industry, since polysaccharides are important to proper immune function, bowel health, and a host of other factors that are important in human health. At present there is no comprehensive study of which plants and animal parts contain which polysaccharides. Research into this field is currently growing at a rapid pace. Some highlights for the purpose of our discussions are presented below.

Storage Polysaccharides

Storage polysaccharides are digestible polysaccharides. Starch and glycogen are the two primary groups of these polysaccharides (Wardlaw and Insel 1996:80-81).

Starch

Starch is the primary digestible polysaccharide in the human diet, and the most important carbohydrate food source (Murray, et al. 2000:155; Wardlaw and Insel 1996:80). Starch is composed of long chains of glucose units. "Cooking increases the digestibility of...starches...making them more soluble in water and thus more available for attack by digestive enzymes" (Wardlaw and Insel 1996:80). Amorphous starch granules encased in cell walls burst free when cooked because the granules absorb water and expand. The two primary constituents of starch are amylose and amylopectin, both of which are a source of energy for plants and animals (Murray, et al. 2000:155; Wardlaw and Insel 1996:80). When the glucose chains are long and straight, the starch is labeled amylose. If the chains are short and branched, they are amylopectin. Shorter chains of glucose (dextrin) are the intermediate product of the hydrolysis of starch. Glucan, which is often found in association with pectin, resides in the cell walls of plants and trees and many forms of bacteria and fungi (Stephen 2006). Most people are familiar with beta glucans, which are a diverse group of molecules that occur commonly in the cellulose of plants, bran of cereals, cell walls of baker's yeast, and certain fungi, mushrooms, and bacteria. Some beta glucans may be useful as texturing agents and soluble fiber supplements. Beta glucans derived from yeast and medicinal mushrooms have been used for their ability to modulate the immune system.

Structural Polysaccharides

Structural polysaccharides, which are also known as dietary fiber, are indigestible by humans and other animals. Structural polysaccharides are primarily composed of cellulose, hemicellulose, pectin, gum, and mucilage (Wardlaw and Insel 1996:82). "The only noncarbohydrate components of dietary fiber are lignins, which are complex alcohol derivatives" (Wardlaw and Insel 1996:82). Lignins are complex alcohol derivatives that make up the non-carbohydrate components of insoluble plant fibers (Wardlaw and Insel 1996:82). As such, they cannot be digested by the enzymes animals produce (Carlile 1994). Lignin is found in all plants and is an important component of the secondary cell walls (Lebo, et al. 2001; Martone 2009; Wardlaw and Insel 1996:82). One of the important functions of lignin is to provide support through strengthening of the xylem cells of wood in trees (Arms 1995; Esau 1977; Wardrop 1969). In linking plant polysaccharides, lignin provides strength to the cell walls and by extension to the entire plant (Chabannes, et al. 2001). Because cellulose and chitin provide structural support to plants and animals they are not water soluble. Cellulose, hemicellulose,

and pectin are all comprised of simple sugars, and their differences are defined by the various inclusions, exclusions, and combinations of these sugars, as well as how the sugars are bonded, and the molecular structure of the sugars of these polysaccharides.

Cellulose

Cellulose is comprised of a long linear chain of glucose, whereas hemicellulose consists of shorter branched chains of simple sugars in addition to glucose, including especially xylose, but also mannose, galactose, rhamnose, and arabinose (Crawford 1981; Updegraff 1969). Pectin, however, may be found in either a linear or branched form of simple sugars that is primarily composed of rhamnose.

Hemicellulose

Hemicellulose resides in the cell wall structures of many plants, particularly grain and vegetable plants, and is a component of both insoluble and soluble fibers (Wardlaw and Insel 1996:82). Some specific hemicelluloses include galactan, galactoglucomannan, glucomannan, glucuronoxylan (GX), and xyloglucan (Walker 2006; Wilkie 1985).

Galactoglucomannan. Galactoglucomannan is a primary component of the woody tissue of coniferous plants (Gymnosperms) (Bochicchio and Reicher 2003).

Pectin, Gums, and Mucilages

Pectin, gums, and mucilages are soluble fibers found inside and around plant cells that help "glue" them together (Wardlaw and Insel 1996:82). Pectin is a structural heteropolysaccharide and common substance found in many plants (apples, plums, gooseberries, and citrus) often used for its gelling or thickening action. Plant derived gums and mucilages such as gum arabic, guar gum, and locus bean gum are also used for this same purpose. Arabinan, arabinogalactan, arabinoglucuronoxylan, and rhamnogalacturonan are some examples of these types of polysaccharides (Wilkie 1985).

Arabinan. In plants, arabinan is essential for the function of guard cells, which "play a key role in the ability of plants to survive on dry land, because their movements regulate the exchange of gases and water vapor between the external environment and the interior of the plant" (Jones, et al. 2003:11783).

Arabinogalactan. Arabinogalactan is a sugar found in plant carbohydrate structures, particularly gums and hemicelluloses. One of arabinogalactan's many functions is to bond with proteins to repair damage when it occurs to a plant or its parts (Nothnagel 2000).

Esters

Esters are an important functional group because they are present as flavoring agents in food and are components of biological compounds such as fats, oils, and lipids. In an ester, the basic unit of the molecule is known as a carbonyl. The presence of the double peak

between 3000 and 2800 wave numbers identifies the presence of the aldehyde functional group, which is present in fats, oils, lipids, and waxes.

There are two important groups of esters, saturated esters and aromatic esters. Aromatic esters take their name from their ability to produce distinctive odors and are present as flavoring agents in food. In contrast, saturated esters do not produce distinctive odors. Esters are expressed in the FTIR spectrum by three distinct peaks ("the rule of three") located at approximately 1700, 1200, and 1100 wave numbers, and a fourth peak in the region between 750 and 700 wave numbers, which represents the CH_2 bend associated with aromatic esters. The first peak for saturated esters falls in the 1750-1735 range, the second peak lies between 1210 and 1160, and the third peak sits between 1100 and 1030. Saturated esters have a unique peak to acetates at 1240. This band can be very strong in the signature. The first peak for aromatic esters falls in the range between 1730 and 1715, the second peak between 1310 and 1250, and the third peak between 1130 and 1100 (Smith 1999:110-112). Distinguishing between saturated and aromatic esters, which are both components of foods, is easy if all three bands are present, since they occupy different wave number regions.

Lipids

Lipids that are solid at room temperature are called "fats," and those that are liquid at room temperature are referred to as "oils" (Wardlaw and Insel 1996:108). Both forms of lipids can be detrimental, as well as beneficial, to human health. Consumption of certain animal fats rich in saturated fatty acids can lead to heart disease, while ingesting omega-3 fatty acids such as EPA (eicosapentaenoic acid) and DHA (docosahexaenoic acid) found in fish and other plant sources are essential to good health.

Fatty Acids

Fatty acids are found in most lipids in the human and animal body, as well as in the lipids in foods (Wardlaw and Insel 1996:108). Long chains of carbons bonded together which are then bonded to hydrogens define the structure of fatty acids (Wardlaw and Insel 1996:109). A fatty acid is considered saturated if the carbons are connected by single bonds. Saturated fatty acids are high in animal fats. If the carbon chain has one double bond between two of the carbons, then the fatty acid is monounsaturated. If there are two or more double bonds between carbons, then the fatty acid is polyunsaturated.

Essential Fatty Acids

Essential fatty acids, are those lipids critical to human health, such as omega-3 and omega-6 fatty acids, alpha-lineolic acid, and linoleic acid, that cannot be created within the body and must be obtained from dietary sources (Wardlaw and Insel 1996:110-111). These essential fatty acids are part of "vital body structures, perform vital roles in immune system function and vision, help form cell membranes, and produce hormone like compounds," and are necessary to maintain good health (Wardlaw and Insel 1996:111). Diets high in essential fatty acids, like omega-3 and omega-6, reduce the risk of heart attacks because they minimize the tendency for blood to clot (Wardlaw and Insel 1996:112). Fish oils contain high concentrations of omega-3 and omega-6 fatty acids and may be administered as a dietary supplement.

Proteins

The human body uses protein from dietary plant and animal sources to form body structures and other constituents (Wardlaw and Insel 1996:152). "Proteins contribute to key body functions, including blood clotting, fluid balance, production of hormones and enzymes, vision, and cell growth and repair" (Wardlaw and Insel 1996:152). This constant regulation and maintenance of the body requires thousands of different types of proteins that are not all available within the body (Wardlaw and Insel 1996:152). The majority of the building blocks for these proteins, which are also known as amino acids, are produced by plants.

Amino Acids

Within the body, amino acids are linked to form the necessary proteins, making them not only essential for life, but key to nutrition. Amino acids can be combined in a multitude of ways to create a vast variety of proteins. Differences between these proteins are distinguished by the unique arrangements of amino acids. Proteins are created through a process called translation, in which amino acids are added, one-by-one, to form short polymer chains called peptides, or longer chains called polypeptides or proteins (Rodnina 2007). The order in which the amino acids are added is determined by the genetic code of the mRNA template, which is a copy of an organism's genes (Creighton 1993). Amino acids are divided into standard and non-standard types.

Standard Amino Acids

There are twenty (20) naturally occurring amino acids on earth called standard amino acids (Creighton 1993). These amino acids are encoded by the standard genetic code and are found in all forms of life (Creighton 1993). The standard amino acids are broken down into two different types, essential and nonessential.

Essential Amino Acids

Eight of the standard amino acids are considered "essential amino acids" because they are necessary for normal human growth and cannot be synthesized by the human body (Young 1994). Essential amino acids must be obtained from food sources, and include histidine, isoleucine, leucine, lysine, methionine, phenylalanine, threonine, tryptophan, and valine (Furst and Stehle 2004; Reeds 2000; Wardlaw and Insel 1996:154).

Leucine. Leucine is used in the liver, adipose tissue, and muscle tissue. In adipose and muscle tissue, leucine aids in the formation of sterols, and slows the degradation of muscle tissue by increasing the synthesis of muscle proteins (Combaret, et al. 2005; Rosenthal, et al. 1974). Common sources of leucine in the diet include beef, fish, shellfish, nuts and seeds, eggs, and legumes.

Lysine. Lysine is important for calcium absorption, building muscle, recovering from injuries or illnesses, and the production of hormones, enzymes, and antibodies (Nelson and Cox 2005). Plants that contain significant amounts of lysine include legumes, gourds/squash, spinach, amaranth, quinoa, and buckwheat (Wardlaw and Insel 1996:158). Other dietary sources of lysine include beef, poultry, pork, fish, eggs, and dairy.

Nonessential Amino Acids

The majority of the standard amino acids are considered "nonessential," meaning that under normal circumstances these amino acids can be manufactured by the human body and are not required in the diet. However, some amino acids that are normally nonessential may become an essential part of the diet for a person whose health has been compromised (Wardlaw and Insel 1996:155). Nonessential amino acids include alanine, arginine, asparagine, aspartate (aspartic acid), cysteine, glutamate (glutamic acid), glutamine, glycine, proline, serine, and tyrosine (Furst and Stehle 2004; Reeds 2000)(Wardlaw and Insel 1996:154).

Glutamate. Glutamate, or glutamic acid, is an important molecule in cellular metabolism. It is the most abundant excitatory neurotransmitter in the nervous system of mammals (Nelson and Cox 2005). Glutamate is found in dairy products, eggs, and all meats, such as beef, pork, poultry, wild meats, and fish (Reeds, et al. 2000).

Glutamine. Glutamine is the most abundant and naturally occurring, non-essential amino acid in the human body. It is one of the few amino acids which directly crosses the blood-brain barrier (Lee, et al. 1998). The blood-brain barrier is a collection of high density cells joined with almost impenetrable connections that protect the brain from being exposed to all elements in the blood, particularly bacteria (Lee, et al. 1998). Unlike many other substances, such as solutes, which are redistricted from making this passage, glutamine in the blood can easily pass through these junctions (Lee, et al. 1998). Glutamine is not only found circulating in the blood, but is also stored in the skeletal muscles (Lee, et al. 1998). At times of illness or injury, glutamine can be considered a conditionally essential amino acid that must be obtained temporarily from the diet because the body is unable to synthesize it on its own (Lee, et al. 1998). Glutamine is also beneficial in healing the cells of the gastrointestinal tract by stimulating regeneration and promoting new cellular growth. Common sources of glutamine in the diet include beef, chicken, fish, eggs, dairy, legumes, cabbage, beets, spinach, and parsley.

Nonstandard Amino Acids

Nonstandard amino acids are amino acids that are chemically altered after they have been incorporated into a protein and/or amino acids that exist in living organisms but are not found in proteins (Driscoll 2003).

Nucleic Acids

Millions of proteins exist in all living organisms to assist with the daily functions of these complex systems. Proteins are produced and assembled locally to exact specifications, and a large amount of information is necessary to properly manage the system. This information is stored in a set of molecules called nucleic acids. Nucleic acids not only contain the genetic instructions for the proper development and functioning of living organisms, but also play a role in copying genetic information to protein (Saenger 1984). The most common examples of nucleic acids are DNA (deoxyribonucleic acid) and RNA (ribonucleic acid).

DISCUSSION

The underwater sites GA426 and HI178 are located on the outer continental shelf off the Texas coast in the Gulf of Mexico. Both sites were exposed as dry land during the last glacial maximum, and due to the difference in elevation, were inundated at slightly different time intervals due to rising sea levels. Although the cultural affiliation of these sites is unknown, radiocarbon dating of core sediments suggests an early Archaic, or possibly a Paleoindian association when correlated to terrestrial archaeological sites in Texas and Louisiana. Three core samples from these sites were examined for pollen and organic residues (Table 1). Samples were tested for organic residues using Fourier Transform Infrared Spectroscopy (FTIR). Pollen and organic residue analysis are used to determine if the core samples represent sites on land or deposition of floral remains blown to sea. Results from these analyses will be discussed below by site.

GA426

Site GA426 is located approximately thirty-one miles off the Texas coast 102 feet below modern sea level. Although exposed during the last glacial maximum, the area was probably inundated between 7,700 and 10,900 BP, depending on the sea-level curve used. Subaerially exposed surface located near entrenched river channels would have transitioned to low energy estuarine zones prior to being inundated. A core sample (GA426-9-G) collected between 399 to 400 centimeters below the sea floor was examined for pollen and organic residues. The unit from which this sample was recovered is described as a very dark brown smooth textured clayey sediment. A single isolated shell was observed in this unit. Radiocarbon dates obtained from sediment above this unit at approximately 105 centimeters below the sea floor were dated to 9,980 ± 50 BP (Amanda Evans, personal communication, September 28, 2010). Sediments at the depth (390 centimeters below the sea floor) from which sample GA426-9-G was recovered were reported as greater than 43,500 BP, so are considered too old to be reliably radiocarbon dated.

The pollen record for sample GA426-9-G was dominated by *Quercus* pollen, representing local growth of oak trees (Figure 1, Table 2). In addition, small quantities of *Betula*, *Carya*, *Pinus*, and *Ulmus* pollen were recorded, indicating a mixture of hickory, pine, and elm trees growing with the oaks. A small quantity of diploxylon *Pinus* pollen, representing red, rather than white, pine, was noted. A very large quantity of Poaceae pollen was noted in this sample, suggesting a dense population of grasses. Phytolith analysis of these sediments would document the types of grasses growing in the area. The Cheno-am pollen frequency was moderately large, suggesting local growth of saltbush, goosefoot, or a similar plant. Smaller quantities of Low-spine Asteraceae, High-spine Asteraceae, Cyperaceae, *Eriogonum*, *Phlox*, Rosaceae, and Rosaceae striate pollen represent various members of the marshelder and rabbitbrush/sunflower portions of the sunflower family, sedges, wild buckwheat, phlox, and two members of the rose family. Striate Rosaceae pollen may represent any of several genera, although the most likely is *Prunus* (chokecherry). Members of the Low-spine Asteraceae group, such as marshelder, are expected as part of wetland communities, as are Cyperaceae and some of the Cheno-ams.

Organic residue analysis of the core sample (GA426-9-G) yielded peaks representing major categories (functional groups) of compounds (4000-1500 wave number), as well as specific compounds noted in the fingerprint region (1500-400 wave numbers) of the spectrum. The functional group peaks indicate the presence of absorbed water and fats/oils/lipids and/or plant waxes (Table 3). Peaks within the fingerprint region represent the presence of aromatic and saturated esters; proteins including nucleic acids; the amino acids lysine, glutamine, and leucine; pectin; humates; and the polysaccharides arabinan and arabinogalactan.

Matches for these peaks include *Achillea* (yarrow) stems, *Schoenoplectus* (bulrush) stems, *Cicuta* (hemlock) stems, *Helianthus* (sunflower) seed shells, ground Cheno-am seeds, dried, ground *Thalia dealbata* (alligator flag) seeds, dried *Cylindropuntia* (cholla cactus) buds, and wet *Sambucus* (elderberry) (Table 4) probably represent elements of the local vegetation community. Several of these plants are expected to grow in the vicinity of river channels and estuarine zones. They include members of the sunflower family that might have been confused with yarrow, bulrush, hemlock, and alligator flag.

Arabinan identified in the sample suggests the presence of terrestrial plant materials in the sample representing the core sediments. This compound is unique to land plants because it is essential for the function of guard cells. These cells “play a key role in the ability of plants to survive on dry land, because their movements regulate the exchange of gases and water vapor between the external environment and the interior of the plant” (Jones, et al. 2003:11783).

The presence of the polysaccharide arabinogalactan suggests plant gums and hemicelluoses are contributing to the signature; however, due to the ubiquitous nature of this compound in the plant kingdom specific plants cannot be identified.

Other matches were made with crickets and turtle blood. Although matches with crickets are being detected, it is the protein, and not the chitin, that was identified and matched. Therefore, matches with crickets probably indicate the presence of insect protein in the sample, and not chitin as a proxy for shellfish. Recovery of a match to turtle blood is indicative of blood, but not necessarily only turtle blood. FTIR distinctions of blood between the major categories of reptiles/amphibians, land mammals, birds, and fish are considered to be reliable, although protein residue analysis, based on immunological principles provides more specific identifications.

Peaks representing the amino acids lysine, glutamate, and leucine suggest the presence of fish remains in the samples, which is expected for sediments deposited below the sea floor. These amino acids also are found in crickets and reptiles, and probably are reflecting compounds present in these matched references, as well. It is possible that organic residues from fish were integrated into the inundated sediments.

HI178

Site HI178 is located approximately twenty-one miles off the shore of Texas at a depth of about 52 feet below modern sea level. This location probably was inundated between 7,000 and 9,200 BP, depending on the sea-level curve used. Two core samples (HI178-1-B and

HI178-1-C) were recovered from a unit described as black sediment with discrete lenses of dark gray material. Sample HI178-1-B, collected between 120.5 to 121.5 centimeters below the sea floor, was examined for organic residues using FTIR. Pollen analysis was performed on sample HI178-1-C, collected from approximately 123 to 124 centimeters below the sea floor. Charcoal was visible in this unit as a discrete lens at about 122 centimeters below the sea floor and continued as scattered fragments to a maximum depth of 142.5 centimeters below the sea floor. Radiocarbon dating of sediments above and below these samples yielded an uncalibrated age range of 7,420-8,530 BP suggesting this sample also falls within this time frame (Amanda Evans, personal communication, September 28, 2010).

Pollen analysis of sample HI178-1-C exhibits a different pollen signature, indicating a different assemblage of vegetation in this area. Probable *Thalictrum* pollen dominated the record, indicating that local vegetation was typical of a meadow. Poaceae pollen was sub-dominant, representing a large local grass population, which is consistent with this interpretation. Further clarification of the grass population is possible with phytolith analysis. Moderate quantities of *Quercus* and Cheno-am pollen represent oak and members of the Cheno-am group that might include goosefoot, saltbush, or others. Recovery of *Alnus*, *Juglans*, and *Pinus* pollen indicates that alder grew in wetlands and that walnut and pines were part of the local woodland. Once again, a few diploxylon *Pinus* pollen were observed, representing red pines. Recovery of smaller quantities of *Artemisia*, Low-spine Asteraceae, High-spine Asteraceae, *Allium*-type, Boraginaceae, Cyperaceae, Fabaceae, *Plantago*, and Rosaceae pollen represents sagebrush or wormwood, marshelder or similar plants, other members of the sunflower family, wild onion or a similar plant, members of the borage, sedge, and legume families, plantain, and a member of the rose family. Most of this assemblage of plants is compatible with an interpretation of meadow vegetation. *Globerigina* tests were slightly more abundant than pollen in this sample. *Globerigina* are a type of foraminifera with a calcium carbonate outer test. During normal pollen sample extraction calcium carbonates are removed through the use of hydrochloric (HCl) acid. Foraminifera also have an inner organic form that survives pollen extraction. It is this portion that was recovered in this sample. *Globerigina* are temperature sensitive, although finding published documentation that they represent cooler sea temperatures has proven extremely difficult. They are commonly reported as forming an “oozy” deposit on the ocean bottom. Recovery of *Globerigina* in this sample, which is close to the level that was radiocarbon dated, points to the possibility of contamination of a total soil organic date by the organic portion of the interior test. The calcium carbonate outer test should have been dissolved in the chemical pre-treatment routinely practiced by all radiocarbon labs. The reported observation of charcoal as a discrete lens in this core and the recovery of a large quantity (more than 40 times as abundant as pollen) of microscopic charcoal particles in this sample point to the opportunity to extract this microscopic charcoal and clean it chemically. Because even microscopic charcoal fragments can be cleaned more effectively of microscopic organisms such as bacteria and Foraminifera inner tests than sediment, it is possible that dating microscopic charcoal from this lens will yield a date more reflective of the time period represented by that charcoal.

FTIR analysis of the core sample (HI178-1-B) yielded peaks representing functional group compounds including absorbed water and fats/oils/lipids and/or plant waxes. Other peaks identified in the fingerprint range indicate the presence aromatic and saturated esters; protein; the amino acid glutamate; pectin; starch; cellulose and carbohydrates; and the polysaccharide galactoglucomannan.

The local vegetation community is represented by matches with *Achillea* (yarrow, a member of the High-spine Asteraceae group) stems, *Cicuta* (hemlock) stems, Poaceae (grass family) stems and joints, *Helianthus* (sunflower) seed shells, *Prunus* (choke cherry) and *Ribes* (currant) fruit. Most of these plants might be found growing in meadows, although the *Prunus* is more likely to grow in drainages.

The presence of the polysaccharide galactoglucomannan suggests woody and fibrous tissues from coniferous plants (Gymnosperms) are contributing to the signature. This compound might reflect pines, noted in the pollen record, growing in the area.

Peaks representing the amino acid glutamate indicate fish in the sample, which is expected for sediment deposits below the sea floor.

SUMMARY AND CONCLUSIONS

Pollen and FTIR analysis of organic residues of samples from GA426 and HI178 provide a record of probable vegetation for both locations. The pollen record indicates that site GA426 was located closer to an open wooded area that included at least oak and probably also birch, hickory, pine, and elm, with an understory of grasses. Vegetation also included various members of the sunflower family, sedges, wild buckwheat, mallow, phlox, and members of the rose family. FTIR analysis confirms a signature of land plants. Pollen analysis of a sediment sample from HI178 suggests the presence of a meadow at this location. FTIR analysis is consistent with this interpretation. Pollen and FTIR analyses combine to indicate that these sediments were part of the exposed land surface, rather than part of the inundated sea bed, at the point of sediment deposition. Recovery of large quantities of *Globerigina* inner tests from sediments at HI178 points to the possibility that the radiocarbon date for that location is too young.

TABLE 1
PROVENIENCE DATA FOR SAMPLES FROM SITES GA426 AND HI178,
TEXAS GULF COAST

Site	Sample Number	Depth (cmbs)	Provenience/Description	Radiocarbon Dates	Analysis
HI178	HI178-1-B	120.5 - 121.5	Core sample: charcoal from discrete lens beginning at 122cmbs, decreasing to scattered fragments until 142.5cmbs	7420-8530 BP	FTIR
	HI178-1-C	123 - 124	Core sample: charcoal from discrete lens beginning at 122cmbs, decreasing to scatter fragments until 142.5cmbs	7420-8530 BP	Pollen
GA426	GA426-9-G	399 - 400	Core sample: sediment	> 43900 BP	Pollen FTIR

cmbs = centimeters below sea floor
FTIR = Fourier Transform Infrared Spectrometry

TABLE 2
POLLEN TYPES OBSERVED IN SAMPLES FROM SITES GA426 AND HI178,
TEXAS GULF COAST

Scientific Name	Common Name
ARBOREAL POLLEN:	
Alnus	Alder
Betula	Birch
Carya	Hickory, Pecan
Juglans	Walnut
Pinus	Pine
Quercus	Oak
Ulmus	American Elm or, White Elm, Water Elm
NON-ARBOREAL POLLEN:	
Allium-type	Wild onion
Asteraceae:	Sunflower family
Artemisia	Sagebrush
Low-spine	Includes ragweed, cocklebur, sumpweed
High-spine	Includes aster, rabbitbrush, snakeweed, sunflower, etc.
Boraginaceae	Borage family
cf. *Thalictrum*	Meadow rue
Cheno-am	Includes the goosefoot family and amaranth
Cyperaceae	Sedge family
Eriogonum	Wild buckwheat
Fabaceae	Bean or Legume family
Phlox	Phlox
Plantago	Plantain
Poaceae	Grass family
Rosaceae:	Rose family
Rosaceae - striate (includes *Purshia*, *Prunus*, *Coleogyne*, *Crataegus*, *Malus*, and *Pyrus*)	Rose family - includes bitterbrush, chokecherry, cherry, plum, peach/nectarine, apricot, almond, blackbrush, hawthorn, apple, and pear

TABLE 2 (Continued)

Scientific Name	Common Name
Indeterminate	Too badly deteriorated to identify
OTHER:	
Forams:	
Foraminifera Inner Test	Tests
Globergina Inner Test	Tests
Charcoal	Microscopic charcoal
Total pollen concentration	Quantity of pollen per cubic centimeter (cc) of sediment

TABLE 3
FTIR PEAK SUMMARY TABLE FOR SAMPLES FROM SITES GA426 AND HI178,
TEXAS GULF COAST

Peak Range	Represents	GA426-9-G Core sediment	H178-1-B Core sediment
3600-3200	Absorbed Water (O-H Stretch)	3396,3357, 3283	3324,3303 3293,3284, 3278
3000-2800	Aldehydes: fats, oils, lipids, waxes	2917,2916, 2849	2918/17/16, 2850,2849
1730-1705	Aromatic esters (C=O Stretch)	1708,1707	1710, 1707/08
1700-1500	Protein, incl. 1650 protein	1655/54, 1637,1617, 1545,1511	1648, 1597,1560, 1546,1542, 1508/07
1653	Proteins (Amide bands, 80% C=O Stretch, 10% C-N Stretch, 10% N-H Bend)	1654	
1680-1600, 1260, 955	Pectin	1655/54, 1637,1617	1648
1660-1655	Proteins, Nucleic acids	1655	
1640-1610, 1550-1485	Lysine (amino acid) NH_3^+ bending	1637,1617	
1615	Proteins (Glutamine, NH_2 Bend)	1617	
1560	Glutamate (amino acid) CO_2^- asymmetric stretching		1560
1500-1400	Protein	1464, 1413	1463/62/61, 1459,1420
1465-1455	Protein/lipids	1464	1463/62/61
1490-1350	Protein	1464, 1413, 1376	1463/62/61, 1459,1420, 1364
1377	Fats, oils, lipids, humates (CH_3 symmetric bend)	1376	
1375	Leucine (amino acid) CH_3 symmetric bending	1376	
1375	CH_3 Umbrella mode	1376	
1170	Lipids	1171,1170	

TABLE 3 (Continued)

Peak Range	Represents	GA426-9-G Core sediment	H178-1-B Core sediment
1170-1150, 1050, 1030	Cellulose		1163 ,1128
1162	Cellulose		1163
1130-1100	Aromatic esters		1128/27/26/25
1100-1030	Saturated esters	1040,1039	1081
1028-1000	Cellulose Carbohydrates		1015
1082	Starch		1081
1040	Arabinogalactan (Type II)	1040	
1039	Arabinan	1039	
934	Galactoglucomannan		935
931	Starch		931
930	Cellulose		930
918	Arabinan	920	
889	C-CH_2-O Symmetric stretch		888
830	Symmetric C-C-O stretch		831
750-700	Aromatic esters	719	719
722-719	CH_2 Rock (methylene)	719	719

TABLE 4
MATCHES SUMMARY TABLE FOR FTIR RESULTS FROM SITE GA426 AND HI178,
TEXAS GULF COAST

Match (Scientific Name)	Match (Common Name)	Part	GA426-9-G Core sediment (Range)	HI178-1-B Core sediment (Range)
Achillea	Yarrow	Stem	1183-1153	1476-1443 738-690
Cheno-am	Goosefoot family and amaranth	Seed (ground)	1479-1434	
Cicuta	Hemlock	Stem	1476-1428 1183-1153	1616-1574
Cylindropuntia	Cholla cactus	Bud (baked/dried)	1392-1356 1183-1153	
Helianthus	Sunflower seed	Shell	1476-1428 735-711	1616-1574 1481-1440 1174-1150 735-708
Poaceae	Grass family	Joints		1514-1490 1481-1440 735-708
		Stem		1481-1440 735-708
Prunus	Choke cherry	Fruit		1616-1574 735-708
Ribes	Currant	Fruit		1481-1440
Sambucus	Elderberry	Fruit (boiled/wet)	1479-1434 738-705	
Schoenoplectus	Bulrush	Stem (raw)	1392-1356 735-711	
Thalia dealbata	Alligator flag	Seed (baked/dried, ground)	1183-1144 735-711	
	Cricket	Whole	1476-1428 1392-1356 735-711	
	Turtle	Blood	1392-1356 1183-1153	

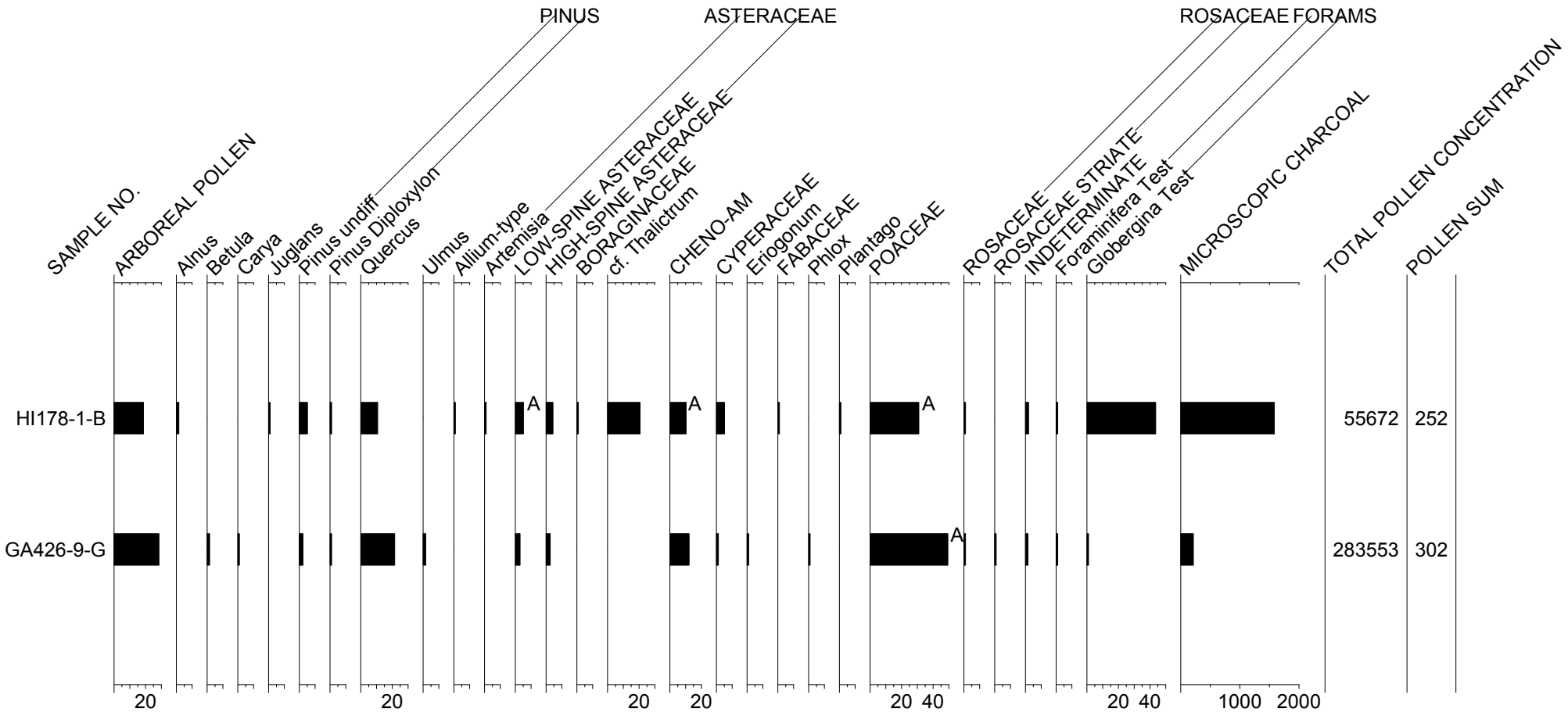

FIGURE 1. POLLEN DIAGRAM FOR TWO OFFSHORE CORE SAMPLES, GULF COAST, TEXAS

REFERENCES CITED

Arms, Karen and Pamela S. Camp
1995 *Biology*. Saunders College Publishing, Fort Worth.

Bochicchio, R. and F. Reicher
2003 Are Hemicelluloses from Podocarpus Lambertii Typical of Gymnosperms? *Carbohydrate Polymers* 53(2):127-136.

Carlile, Michael J. and Sarah C. Watkinson
1994 *The Fungi*. Academic Press, San Diego.

Chabannes, Matthieu, Katia Ruel, Arata Yoshinaga, Brigitte Chabbert, Alain Jauneau, Jean-Paul Joseleau and Alain-Michel Boudet
2001 In Situ Analysis of Lignins in Transgenic Tobacco Reveals a Differential Impact of Individual Transformations on the Spatial Patterns of Lignin Deposition at the Cellular and Subcellular Levels. *The Plant Journal* 28:271-282.

Combaret, Lydie, Dominique Dardevet, Isabelle Rieu, Marie-Noelle Pouch, Daniel Bechet, Daniel Taillandier, Jean Grizard and Didier Attaix
2005 A Leucine-supplemented Diet Restores the Defective Postprandial Inhibition of Proteasome-dependent Proteolysis in Aged Rat Skeletal Muscle. *Journal of Physiology* 569(2):489-499.

Crawford, R. L.
1981 *Lignin Biodegradation and Transformation*. John Wiley and Sons, New York.

Creighton, Thomas E.
1993 *Proteins: Structures and Molecular Properties*. 2nd ed. W. H. Freeman and Company, Ltd., San Francisco.

Driscoll, D. and P. Copeland
2003 Mechanism and Regulation of Selenoprotein Synthesis. *Annual Review of Nutrition* 23:17-40.

Esau, Katherine
1977 *Anatomy of Seed Plants*. John Wiley and Sons, New York.

Furst, P and P. Stehle
2004 What are the Essential Elements Needed for the Determination of Amino Acid Requirements in Humans? *Journal of Nutrition* 134(6):1558S-1565S.

Garrison, Robert, Jr. and Elizabeth Somer
1985 *The Nutrition Desk Reference*. Keats Publishing, Inc., New Canaan.

Isaksson, Sven
1999 Guided By Light: The Swift Characterization of Ancient Organic Matter by FTIR, IR-Fingerprinting and Hierarchical Cluster Analysis. *Laborativ Arkeologi* 12:35-43.

Jones, Louise, Jennifer L. Milne, David Ashford and Simon J. McQueen-Mason
2003 Cell Wall Arabinan is Essential for Guard Cell Function. *Proceedings of the National Academy of Sciences of the United States of America* 100(20):11783-11788.

Lebo, Stuart E., Jr., Jerry D. Gargulak and Timothy J. McNally
2001 Lignin. In *Encyclopedia of Chemical Technology*. 4th ed. John Wiley and Sons, Inc.

Lee, Wha-Joon, Richard A. Hawkins, Juan R. Vina and Darryl R. Peterson
1998 Glutamine Transport by the Blood-Brain Barrier: A Possible Mechanism for Nitrogen Removal. *American Journal of Physiology Cell Physiology* 274(4):C1101-C1107.

Martone, Patrick T., Jose M. Estevez, Fachuang Lu, Katia Ruel, Mark W. Denny, Chris Somerville, and John Ralph
2009 Discovery of Lignin in Seaweed Reveals Convergent Evolution of Cell-Wall Architecture. *Current Biology* 19(2).

Murray, Robert K., Daryl K. Granner, Peter A. Mayes and Victor W. Rodwell
2000 *Harper's Biochemistry*. 25th Edition ed. McGraw-Hill, New York.

Nelson, D. L. and M. M. Cox
2005 *Lehninger Principles of Biochemistry*. 4th ed. W. H. Freeman and Company, New York.

Nothnagel, Eugene A., Antony Bacic, and Adrienne E. Clarke
2000 *Cell and Developmental Biology of Arabinogalactan-proteins*. Kluwer Academic, New York.

Reeds, P. J.
2000 Dispensable and Indespensable Amino Acids for Humans. *Journal of Nutrition* 130(7):1835S-1840S.

Reeds, Peter J., Douglas G. Burrin, Barbara Stoll and Farook Jahoor
2000 Intestinal Glutamate Metabolism. *Journal of Nutrition* 130(4):978S-982S.

Rodnina, M. V., M. Beringer, and W. Wintermeyer
2007 How Ribosomes Make Peptide Bonds. *Trends in Biochemical Sciences* 32(1):20-26.

Rosenthal, J., A. Angel and J. Farkas
1974 Metabolic Fate of Leucine: A Significant Sterol Precursor in Adipose Tissue and Muscle. *American Journal of Physiology* 226(2):411-418.

Saenger, Wolfram
1984 *Principles of Nucleic Acid Structure.* Springer, New York.

Smith, Brian
1999 *Infrared Spectral Interpretation, A Systematic Approach*. CRC Press, New York.

Stephen, Alistair M., Glyn O. Phillips, and Peter A. Williams
2006 *Food Polysaccharides and Their Applications*. Taylor & Francis, Boca Raton.

Updegraff, D. M.
1969 Semimicro Determination of Cellulose in Biological Materials. *Analytical Biochemistry* 32:420-424.

Walker, J. C. F.
2006 *Primary Wood Processing: Principles and Practice*. Springer, Dordrecht, The Netherlands.

Wardlaw, Gordon M., Ph.D., R.D., L.D. and Paul M. Insel, Ph.D.
1996 *Perspectives in Nutrition*. Mosby-Year Book, Inc., St. Louis, Missouri.

Wardrop, A. B.
1969 The Structure of the Cell Wall in Lignifies Collenchyma of Eryngium sp. (Umbelliferae). *Australian Journal of Botany* 17:229-240.

Wilkie, K. C. B.
1985 New Perspectives on Non-Cellulosic Cell-Wall Polysaccharides (Hemicellulose and Pectic Substances) of Land Plants. In *Biochemistry of Plant Cell Walls*, edited by C. T. Brett and J. R. Hillman. Cambridge University Press, Cambridge.

Young, V. R.
1994 Adult Amino Acid Requirements: The Case for a Major Revision in Current Recommendations. *Journal of Nutrition* 124(8):1517S-1523S.

POLLEN ANALYSIS OF CORES FROM SITE GA426, OFFSHORE NEAR GALVESTON, TEXAS

By

Linda Scott Cummings
and
R. A. Varney

PaleoResearch Institute
Golden, Colorado

PaleoResearch Institute Technical Report 11-079

Prepared for

Louisiana State University
Baton Rouge, Louisiana

November 2011

INTRODUCTION

Five sediment samples from two cores collected at site GA426, located approximately 31 miles offshore near Galveston, Texas, were examined for pollen. The site is on an old river terrace that is now submerged in an estuary or back bay. The site is a possible Paleoindian site that is expected to date to between approximately 9,000 and 10,000 BP. The area was above water during the last glacial maximum and was subsequently submerged in the range of 8,400 to 10,000 BP (Patrick Hesp, personal communication, June 7, 2011). Pollen analysis of these samples provides information about the past vegetation growing in the area and also may be used to describe the paleoenvironment.

METHODS

Pollen

A chemical extraction technique based on flotation is the standard preparation technique used in this laboratory for the removal of the pollen from the large volume of sand, silt, and clay with which it is mixed. This particular process was developed for the extraction of pollen from soils where preservation has been less than ideal and the pollen density is lower than in peat. It is important to recognize that it is not the repetition of specific and individual steps in the laboratory, but rather mastery of the concepts of extraction and how the desired result is best achieved, given different sediment matrices, that results in successful recovery of pollen for analysis.

Hydrochloric acid (10%) was used to remove calcium carbonates present in the soil, after which the samples were screened through 250-micron mesh. The samples were rinsed until neutral by adding water, letting the samples stand for 2 hours, then pouring off the supernatant. A small quantity of sodium hexametaphosphate was added to each sample once it reached neutrality; then the samples were allowed to settle according to Stoke's Law in settling columns. This process was repeated with ethylenediaminetetraacetic acid (EDTA). These steps remove clay prior to heavy liquid separation. The samples then were freeze dried. Sodium polytungstate (SPT), with a density 1.8, was used for the flotation process. The samples were mixed with SPT and centrifuged at 1500 rpm for 10 minutes to separate organic from inorganic remains. The supernatant containing pollen and organic remains was decanted. SPT again was added to the inorganic fraction to repeat the separation process. The supernatant was decanted into the same tube as the supernatant from the first separation. This supernatant was then centrifuged at 1500 rpm for 10 minutes to allow any silica remaining to be separated from the organics. Following this, the supernatant was decanted into a 50-ml conical tube and diluted with distilled water. These samples were centrifuged at 3000 rpm to concentrate the organic fraction in the bottom of the tube. After rinsing the pollen-rich organic fraction obtained by this separation, all samples receive a short (20–30 minute) treatment in hot hydrofluoric acid to remove any remaining inorganic particles. The samples then were acetylated for 3–5 minutes to remove any extraneous organic matter.

A light microscope was used to count pollen at a magnification of 500x. The pollen preservation in these samples varied from good to poor. Comparative reference material collected at the Intermountain Herbarium at Utah State University and the University of

Colorado Herbarium was used to identify the pollen to the family, genus, and species level, where possible.

Pollen aggregates were recorded during identification of the pollen. Aggregates are clumps of a single type of pollen and may be interpreted to represent pollen dispersal over short distances or the introduction of portions of the plant represented into an archaeological setting. Aggregates were included in the pollen counts as single grains, as is customary. The presence of aggregates is noted by an "A" next to the pollen frequency on the pollen diagram. Pollen diagrams are produced using Tilia 2.0 and TGView 2.0.2. Total pollen concentrations are calculated in Tilia using the quantity of sample processed in cubic centimeters (cc), the quantity of exotics (spores) added to the sample, the quantity of exotics counted, and the total pollen counted and expressed as pollen per cc of sediment.

Indeterminate pollen includes pollen grains that are folded, mutilated, or otherwise distorted beyond recognition. These grains are included in the total pollen count since they are part of the pollen record. The microscopic charcoal frequency registers the relationship between pollen and charcoal. The total number of microscopic charcoal fragments was divided by the pollen sum, resulting in a charcoal frequency that reflects the quantity of microscopic charcoal fragments observed, normalized per 100 pollen grains.

DISCUSSION

This site is located approximately 31 miles offshore on the outer continental shelf. The current water depth is 101' BSL. Although this area is currently underwater, it was exposed as dry land during the last glacial maximum and probably was inundated between approximately 8,400 and 10,000 BP, depending on which sea level curve is selected. Two cores were collected on the topographic rise between two entrenched river channels. One speculation is that this area could have been a low-energy estuarine zone. Small charcoal flecks and/or organic staining were present in the unit that was cored.

Core 2

The pollen record in Core 2, designated GA-426-2, displays evidence of vegetation change through time. The samples were collected at depths between 137 and 103 cm below the sediment surface (Table 1) at this location. The lowest sample was collected at a depth of 136 to 137 cm below the sediment surface. This sample was co-dominated by High-spine Asteraceae and Cheno-am pollen (Figure 1, Table 2) and also exhibited moderate quantities of *Pinus* and Poaceae pollen. This pollen record suggests an open area that supported various members of the sunflower family, plants in the Cheno-am group, and grasses. Pine trees probably grew at some distance from this location on more elevated ground. Small quantities of *Carya*, *Quercus*, and *Ulmus* pollen indicate that hickory, oak, and elm trees also grew in the area. Recovery of small quantities of *Artemisia*, Low-spine Asteraceae, *Corylus*, and *Persicaria* pollen indicate that sagebrush, marsh elder or similar plants, hazel, and smartweed also grew as part of the local vegetation community. The presence of *Corylus* and *Persicaria* pollen in this sample suggests proximity to a wetland. The remainder of the pollen record, however, is more typical of a meadow. A moderate quantity of microscopic charcoal was observed that might

represent cultural activity or natural fires in this area. Recovery of foraminifera in this sample might reflect later inundation of the sediments. The total pollen concentration is calculated at approximately 9500 pollen per cubic centimeter (cc) of sediment.

The local plant community appears to have changed rapidly, as is recorded in the sample collected at a depth of 132 cm. This sample records a dramatic increase in *Quercus* pollen, indicating an encroachment of oaks. The recovery of small quantities of *Alnus*, *Juniperus*, and *Abies* pollen indicates local growth of alder, as well as the inclusion of juniper and fir into stands of conifers that were probably growing at a greater distance from this location. The presence of Apiaceae suggests growth of members of the umbel family in the immediate vicinity of the area sampled, or possibly their use or processing by people working in this area if the charcoal is interpreted to represent a cultural activity area. The dramatic reduction in High-spine Asteraceae pollen reflects a decrease in the local growth of plants in the sunflower family. A gradual increase in Low-spine Asteraceae pollen frequencies suggests an increase in the marshelder (and similar plant) population. This sample is the first to contain small quantities of Cyperaceae and Rosaceae pollen, and monolete fern spores, reflecting the local growth of sedges, a member of the rose family, and ferns. The quantity of microscopic charcoal remains unchanged. The total pollen concentration, however, has increased from less than 10,000 pollen per cc of sediment to more than 47,000 pollen per cc of sediment. This increase in total pollen concentration is consistent with the presence of a stable surface.

The sample collected at a depth of 103-105 cm below the surface is noteworthy because of an increase in *Pinus* pollen. This change might reflect either an increase in the quantity of pine trees growing in the area or a decrease in local vegetation that results in an over-representation of pollen present through long distance transport. The latter is a possibility, since this sample exhibited a much larger quantity of microscopic charcoal than did the lower samples. If a fire was responsible for reducing local vegetation, then there would be little input from local plants and most of the pollen record would consist of pollen transported on the wind. Increases in *Pinus* pollen would be expected since it is readily transported over long distances. The total pollen concentration is more than 20,000 pollen per cc of sediment, slightly less than half that observed in sample 132. This reduction is not sufficient to warrant an interpretation of a massive fire that denuded the landscape of vegetation. Therefore, the most reasonable interpretation is that the quantity of pine trees growing in the region increased. It is also likely that this sample represents a surface that experienced very slow aggradation through time. The gradual increase in Low-spine Asteraceae pollen noted in sample 132 continues in this sample, suggesting local growth of marsh elder-type plants in moderately wet sediments. *Persicaria* pollen has dropped out of the record, indicating that the moist ground that supported this type of knotweed probably did not exist at the time represented by this sample. Other pollen taxa recovered from this sample are similar to those noted in the underlying sample, sample 132. The recovery of *Alnus* and *Corylus* pollen represents alder trees and hazel shrubs growing along the local drainage. Plants that are expected to grow along the margins of wetlands are represented by Apiaceae and Cyperaceae pollen, representing a member of the umbel family and sedges.

The pollen record for Core 2 indicates moderate sediment aggradation in the lower (earliest) sample, then surface stabilization in the middle sample, followed by a resumption of slow sediment aggregation in the uppermost sample. A general increase in dryness is suggested through time, with pines becoming more abundant on the landscape in the upper sample. These changes in the pollen record are consistent with vegetational succession as

communities mature. Evidence for the continuation of wetland communities in the vicinity of the area sampled continues.

Core 10

Core 10 from site G8 426 was sampled at depths of 104-106 cm and 85-87 cm below the surface. The sample collected from a depth of 104-106 centimeters was similar in pollen content to the lowest sample examined from Core 2. This sample also was dominated by Cheno-am pollen, and the quantity of High-spine Asteraceae pollen was larger in this sample than the sample above it. The quantities of *Pinus* and *Quercus* pollen also were lower in this sample than in the sample above it, indicating that while pine and oak trees grew in the area, they were not particularly abundant. The Poaceae pollen frequency was moderately high, indicating that grasses were an important part of the plant cover. Pollen recovered from this sample representing trees growing in the area also includes *Alnus*, *Carya*, *Juglans*, and *Juniperus*, representing alder, hickory, walnut, and juniper. Although they were noted in small quantities, recovery of these pollen documents local growth of these trees. Pollen representing herbaceous or shrubby plants growing in the area (and not mentioned earlier) includes Apiaceae, *Artemisia*, Low-spine Asteraceae, Caryophyllaceae, Cyperaceae, *Plantago*, Rosaceae, *Salix*, and *Typha*, indicating that a member of the umbel family, sagebrush, members of the sunflower family, a member of the pink family, sedges, plantain, a member of the rose family, willow, and cattails grew locally. This sample displays a moderately large quantity of microscopic charcoal, which is consistent with the presence of a cultural layer at this depth. The total pollen concentration was more than 18,000 pollen per cc of sediment, suggesting a moderately stable surface.

The upper sample, collected at 86-87 cm, displays slightly elevated *Carya*, *Juniperus*, *Pinus*, and *Quercus* pollen frequencies compared to the lower sample, indicating increases in quantities of hickory, juniper, pine, and oak trees. Recovery of small quantities of *Alnus*, *Elaeagnus*, and *Tsuga* pollen indicate that alder, silverberry, and hemlock trees also grew in the area. The herbaceous and shrubby portion of this record is dominated by Poaceae pollen, which has increased slightly over the quantity observed in the lower sample. Once again, it is likely that forested areas were interspersed with grassy meadows on the landscape. Recovery of small quantities of Apiaceae, *Artemisia*, Low-spine Asteraceae, High-spine Asteraceae, Cheno-am, *Corylus*, Cyperaceae, *Eriogonum*, Fabaceae, Rosaceae, *Salix*, and *Typha* pollen indicate that the local vegetation also included a member of the umbel family, sagebrush, members of the sunflower family, Cheno-am, hazel, sedges, wild buckwheat, legumes, a member of the rose family, willow, and cattail. It is likely that plants growing in a wetland community included plants in the umbel family, marsh elder, hazel, sedges, willow, cattails, and alder. The quantity of microscopic charcoal was severely reduced in this sample when compared with the lower samples from this core. The total pollen concentration also was reduced to approximately 10,000 pollen per cc of sediment. This is consistent with a moderately stable surface.

The pollen record from Core 10 also exhibits evidence of drying through time and vegetation succession with maturation of woodland communities, expressed as increases in *Carya*, *Pinus*, and *Quercus* pollen. Grassy or meadow communities either shrink in size or are filled in with trees. The lowest sample represents a period of slow sediment aggradation and a

relatively stable land surface, while the upper sample represents an increase in sediment aggradation.

SUMMARY AND CONCLUSIONS

The pollen records from Cores 2 and 10 exhibit similar signals representing local vegetation communities. The total pollen concentration indicates periods of changing sediment aggregation. Core 2 sediments aggraded most rapidly in the lower portion that was examined (sample 137). Sediment aggradation slowed dramatically and a relatively stable surface is reflected in sample 132. Slow aggradation is indicated in sample 105. A more open vegetation, possibly wet riparian vegetation community is represented in the lowest sample (137) of this core, suggesting a disturbed landscape and moderate sediment aggradation. It is likely that the large quantities of High-spine Asteraceae (sunflower family) and Cheno-am (goosefoot and related plants) pollen represent vegetation response to this disturbance. The increase in Poaceae pollen in sample 132 probably represents replacement of many of the plants in the sunflower family by grasses as the disturbance abates and the surface becomes more stable. The Cheno-am frequency declines only slightly at this point. Increases in *Pinus* and *Quercus* pollen indicate that woodlands including pine and oak as the dominant trees increased in density and/or proximity. This vegetation pattern continues into the uppermost sample (105) as the woodland vegetation communities mature. The uppermost sample, exhibiting the largest quantity of microscopic charcoal, represents a relatively mature woodland interspersed with openings that experienced only slow sediment aggradation.

This general pattern of vegetation succession is also noted in the Core 10 samples, with the lowest sample containing the largest High-spine Asteraceae and Cheno-am pollen frequencies and smallest quantities of pollen representing trees. It is interesting that this signature is observed in a sample that registers slow sediment aggradation rather than rapid aggradation. As sediment aggradation increases, grasses replace members of the sunflower family and Cheno-ams, and pine and oak trees become slightly more abundant, which suggests that the rate of vegetation community maturation was greater than the disturbance caused by the aggradation of sediments. These records are not exactly the same, but both indicate proximity to wet riparian communities and exhibit signatures that indicate they represent riparian meadows at some point. Natural fires or cultural activity is evident in both cores with increases in microscopic charcoal. General drying through time and woodland community maturation is indicated in the pollen records from both cores.

TABLE 1
PROVENIENCE DATA FOR SAMPLES FROM SITE GA-426,
OFFSHORE NEAR GALVESTON, TEXAS

Sample No.	Core	Depth (cmbs)	Provenience/Description	Analysis
GA-426-10-A-87	10	86-87	River terrace fill	Pollen
GA-426-10-B-106	10	104-106	River terrace fill	Pollen
GA-426-2-B-105	2	103-105	River terrace fill	Pollen
GA-426-2-B-132	2	130-132	River terrace fill	Pollen
GA-426-2-B-137	2	136-137	River terrace fill	Pollen

TABLE 2
POLLEN TYPES OBSERVED IN SAMPLES FROM SITE GA426,
OFFSHORE NEAR GALVESTON, TEXAS

Scientific Name	Common Name
ARBOREAL POLLEN:	
Alnus	Alder
Carya	Hickory, Pecan
Elaeagnus	Russian olive
Juglans	Walnut
Juniperus	Juniper
Pinaceae:	Pine family
Abies	Fir
Pinus	Pine
Quercus	Oak
Tsuga	Hemlock
Ulmus	American Elm or, White Elm, Water Elm
NON-ARBOREAL POLLEN:	
Apiaceae	Umbel family
Asteraceae:	Sunflower family
Artemisia	Sagebrush
Low-spine	Includes ragweed, cocklebur, sumpweed
High-spine	Includes aster, rabbitbrush, snakeweed, sunflower, etc.
Caryophyllaceae	Pink family
Cheno-am	Includes the goosefoot family and amaranth
Corylus	Hazel
Cyperaceae	Sedge family
Fabaceae	Bean or Legume family
Plantago	Plantain
Poaceae	Grass family
Polygonaceae:	Knotweed/Smartweed family

TABLE 2 (Continued)

Scientific Name	Common Name
Eriogonum	Wild buckwheat
Persicaria	Smartweed, Persicaria, Pinkweed
Rosaceae	Rose family
Salix	Willow
Typha latifolia	Cattail
Indeterminate	Too badly deteriorated to identify
FERNS:	
Monolete Smooth	Fern
Trilete Smooth	Fern
OTHER:	
Foraminifera	A group of plankton species
Hystrichosphere	Geologic plankton
Charcoal	Microscopic charcoal
Total pollen concentration	Quantity of pollen per cubic centimeter (cc) of sediment

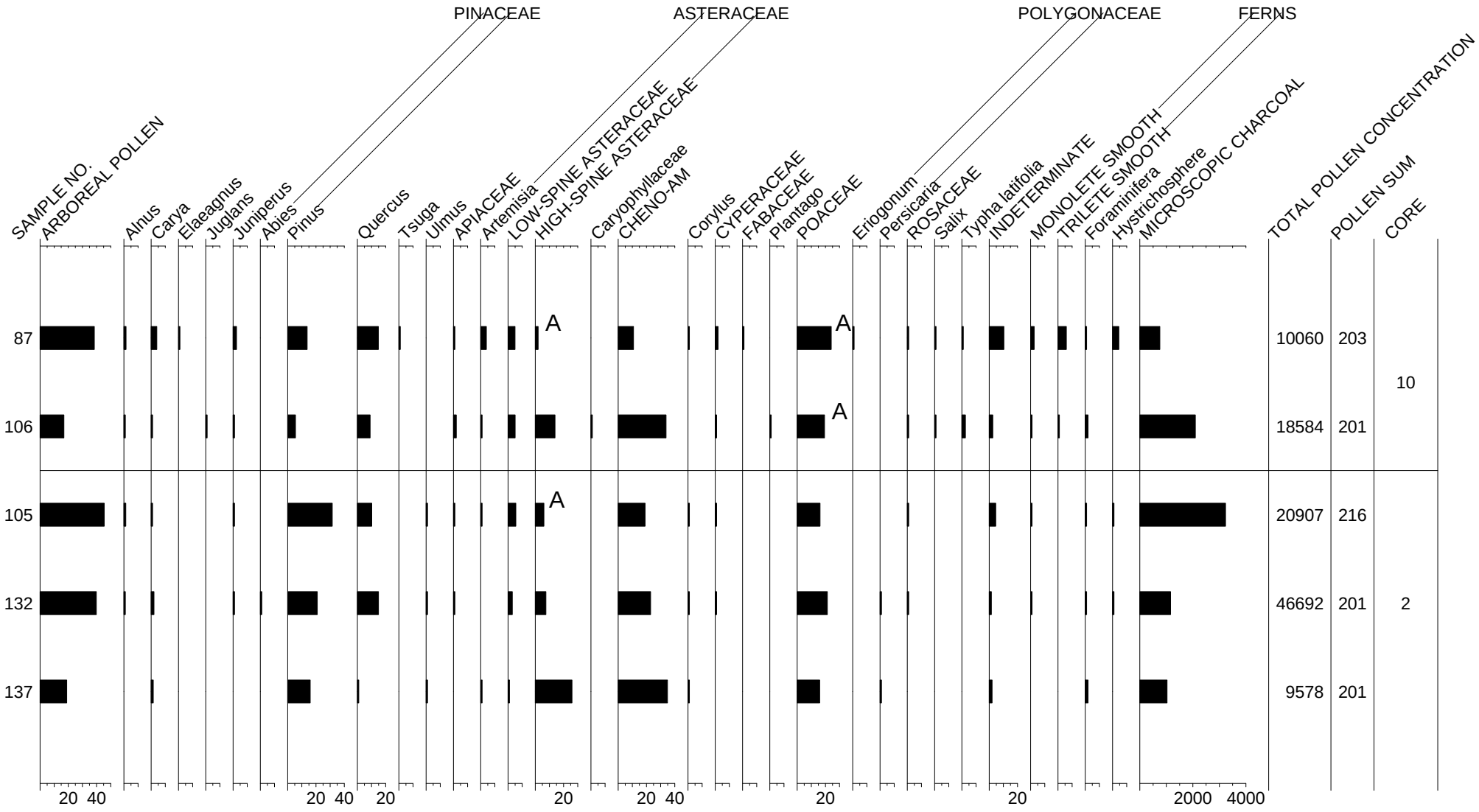

FIGURE 1. POLLEN DIAGRAM FOR TWO CORES FROM SITE GA426, OFFSHORE GALVESTON, TEXAS.

VITA

Amanda M. Evans was born in Indianapolis, Indiana, and earned her Bachelor's degree in Anthropology with a History minor from Indiana University in 1998. She received her Master's degree in Anthropology with a History minor from Florida State University in 2005. She has conducted field work in the Gulf of Mexico region, as well as Indiana, Florida, Louisiana, the Bahamas, Belize, the Cayman Islands, and Dominican Republic. Her research interests are focused on underwater archaeology, especially the use of geophysics in archaeology, site formation processes, and the relationship between cultural ecology and maritime culture. Amanda is active in public outreach and legislative issues related to the protection of the underwater cultural heritage. She has delivered papers at professional conferences for organizations including, but not limited to, the Society for Historical Archaeology, Society for American Archaeology, and Geological Society of America, and has published articles in the *Journal of Maritime Archaeology* and *Conservation and Management of Archaeological Sites*. Amanda currently serves as an elected board member and officer for the Advisory Council on Underwater Archaeology and the Register of Professional Archaeologists, and is the Chair of the Society for Historical Archaeology UNESCO Committee. She has been employed with Tesla Offshore, LLC since 2005 and currently serves as Senior Marine Archaeologist.